VISCOSITY OF SILICATE MELTS

by

Hejiu Hui

A dissertation submitted in partial fulfillment
of the requirements for the degree of
Doctor of Philosophy
(Geology)
in The University of Michigan
2008

Doctoral Committee:

Professor Youxue Zhang, Chair
Professor Eric J. Essene
Professor John Kieffer
Professor Rebecca A. Lange
Professor Lars P. Stixrude

2008

To
Xiaoqing and our families

ACKNOWLEDGEMENTS

I would first of all like to thank my dissertation advisor, Dr. Youxue Zhang, who offered me this great opportunity to be a scientist and guided my academic development with patience. I have great respect and admiration of his enthusiasm in science, critical thinking and hard work. I would like to thank other members in my dissertation committee: Drs. Eric Essene, Becky Lange, Lars Stixrude and John Kieffer. Special thanks go to Dr. Eric Essene for his advice and encouragements along my study. I benefited a lot from his wealth of knowledge and directness during my study here. My sincere thanks go to Dr. Becky Lange. I learned a lot on the melt not only in her igneous petrology class, but also in her group meeting. I would like to thank Dr. Lars Stixrude. I benefited a lot from his scientific thoughts and insightful comments on this dissertation. Finally, I would like to thank my cognate, Dr. John Kieffer. He provided helpful comments and fresh perspectives from the outside of geology.

I would also like to thank all other people who have contributed to my dissertation in various ways. My sincere thanks go to Zhengjiu Xu, who taught me a lot of things in the lab, Dr. Harald Behrens at University of Hannover, who provided advice on various aspects of the research in this disseration and his hospitality during my stay in Hannover. Perio Del Gaudio, Francesco Vetere, Jan Schüβler, Otto Diedrich and other people in Hannover, who gave me a lot of help during this visit. Tony Withers provided a lot of instructions from temperature recording system of piston cylinder to salt cell.

Yang Liu taught me a lot to do experiments. Yang Chen provided help in glass composition analysis with EMPA. Wenjun Yong and Lixing Jin helped me with XRD. Huaiwei Ni helped in pressure calibration.

I would like to express my gratitude to my fellow students for their friendship and support, including: Yang Liu, Daming Wang, Maodu Yan, Kate Kenedi, Zeb Page, Qiong Liu, Matt Mannon, Yang Chen, Huaiwei Ni, Wenjun Yong, Xiqiao Xu, Ni Sun, Steven Ownby, Lixing Jin, Lin Ma, and Tie Sun. I also would like to express my special thanks to my friend and former landlord, Bob Trees, for his support and help during my hard time at Ann Arbor.

My deepest gratitude goes to my wife, Xiaoqing, and our families. Their love and support are critically important for me to accomplish this work.

TABLE OF CONTENTS

LIST OF FIGURES

Figure

LIST OF TABLES

Table

LIST OF APPENDICES

Appendix

CHAPTER 1

INTRODUCTION

Knowledge of viscosity of silicate melts is necessary in order to quantitatively model volcanic and magmatic processes and in turn to provide insights into the structure and dynamics of silicate melts. A mechanistic study of xenolith dissolution may aid in understanding the diagenesis of magmatic system (e.g., Morgan et al., 2006; Shaw, 2006). A numerical model of bubble growth may advance in predicting the mode of volcanic eruption (e.g., Proussevitch and Sahagian, 1998; Liu and Zhang, 2000). The success of these models in accurately predicting kinetic and dynamic processes in igneous systems is critically dependent on the quality of viscosity data of silicate melts. Laboratory viscosity measurements are performed to better understand detailed physicochemical behaviors and the results of these studies are then used to understand the behavior of the melts in nature (e.g., Scaillet et al., 1996). Because the conditions that pertained in laboratory experiments cannot always be identical to those occurring in nature, it is also important to have means of interpolating or extrapolating laboratory results to different (T, P, X) conditions. In this study, one of the primary aims is to establish a general viscosity model to estimate viscosity of silicate melts at ambient pressure. Furthermore, hydrous species reaction viscometer based on the kinetics of hydrous species reaction in the rhyolitic melts at high pressure is used to infer viscosity

of hydrous rhyolitic melts at pressure up to 2.83 GPa, and parallel-plate creep viscometer in an internally-heated pressure vessel is employed to measure natural rhyolitic melts at pressure up to 0.4 GPa, and the pressure effect on the viscosity of rhyolitic melts is examined.

Chapter II presents a new and empirical viscosity equation of anhydrous and hydrous natural silicate melts. The compositional dependence of viscosity of silicate melts is of fundamental importance to understand the evolution of magmatic systems (e.g., Marsh, 2006). However, previous viscosity models can only provide viscosity prediction of silicate melts either in a limited composition range over a large temperature range (e.g., Hess and Dingwell, 1996; Zhang et al., 2003), or in a limited temperature range in a large compositional range (e.g., Shaw, 1972). This chapter provides a general viscosity model of silicate melts, which can be used to calculate viscosity of all natural silicate melts in a large temperature range. Natural and nearly natural melt compositions covered in this model include: anhydrous peridotite to rhyolite, anhydrous peralkaline to peraluminous melts, hydrous basalt to rhyolite, hydrous peralkaline to peraluminous melts. This model can also be used to estimate the glass transition temperatures and cooling rate of natural silicate melts. The results of this study have been published in *Geochimica et Cosmochimica Acta* (Hui and Zhang, 2007).

Chapter III is an experimental study of the speciation of dissolved water in rhyolitic melts at pressure up to 2.83 GPa. This study is prerequisite for inferring viscosity of hydrous rhyolitic melts using the hydrous species reaction viscometer (Dingwell and Webb, 1990; Zhang et al., 2003) at high pressure (Chapter IV). Furthermore, the quantification of hydrous speciation in the rhyolitic melts under high

pressure can be applied to model H_2O diffusion and understand the structure of hydrous melts at high pressure. In addition, information from this study is also useful in future models of thermodynamic properties of hydrous silicate melts. Chapter III addresses the first systematic experimental study of H_2O speciation in rhyolitic melts containing 0.8 – 4 wt% water at high pressure, 0.94 – 2.83 GPa. A speciation model accommodating temperature, pressure and water content dependence of hydrous species in rhyolitic melts is also presented in this chapter. The results from this study have been submitted to *Geochimica et Cosmochimica Acta* (Hui et al., 2008).

Chapter IV contains the first experimental study of viscosity of any melts at pressure up to 2.83 GPa in the high viscosity range. It extends a newly developed method (hydrous species reaction viscometer, Zhang et al., 2003) to high pressures. This new development represents the only method capable of extracting viscosity data of melts in the high viscosity range at pressures above 1 GPa. Previously, high-pressure (≥ 1 GPa) viscosity data were obtained by the falling-sphere technique in high-pressure apparatus, which can be applied only in the low viscosity range. Hence, all previous viscosity data at high pressure (≥ 1GPa) fall in the high temperature range (i.e., low viscosity range). No viscosity data in the low temperature range at high pressure ((≥ 1GPa) have been published. This study is the first to infer viscosity of hydrous rhyolitic melts containing 0.8 – 4 wt% water using the hydrous species reaction viscometer (Dingwell and Webb, 1990; Zhang et al., 2003) at high pressures. The viscosity of natural rhyolitic melts containing 0.13 and 0.8 wt% water at pressures up to 0.4 GPa also has been measured using a parallel plate creep viscometer. A viscosity model of rhyolitic melts in the high viscosity range accounting for the dependence on pressure, temperature and water content

is also presented in this chapter. The results from this chapter have been submitted to *Geochimica et Cosmochimica Acta* (Hui et al., 2008).

REFERENCES

Dingwell, D.B., Webb, S.L. (1990) Relaxation in silicate melts. *Eur. J. Mineral.* **2**, 427-449.

Hess, K.-U., Dingwell, D.B. (1996) Viscosities of hydrous leucogranitic melts: A non-Arrhenian model. *Am. Mineral.* **81**, 1297-1300.

Hui, H., Zhang, Y. (2007) Toward a general viscosity equation of natural anhydrous and hydrous silicate melts. *Geochim. Cosmochim. Acta* **71**, 403-416.

Hui, H., Zhang, Y., Xu, Z., Behrens, H. (2008) Pressure dependence of the speciation of dissolved water in rhyolitic melts. *Geochim. Cosmochim. Acta*. In revision.

Hui, H., Zhang, Y., Xu, Z., Del Gaudio, P., Behrens, H. (2008) Pressure dependence of viscosity of rhyolitic melts. *Geochim. Cosmochim. Acta*. Submitted.

Liu, Y., Zhang, Y. (2000) Bubble growth in rhyolitic melt. *Earth Planet. Sci. Lett.* **181**, 251-264.

Marsh, B.D. (2006) Dynamics of magmatic systems. *Elements* **2**, 287-292.

Morgan, Z., Liang, Y., Hess, P. (2006) An experimental study of anorthosite dissolution in lunar picritic magmas: Implications for assimilation processes. *Geochim. Cosmochim. Acta* **70**, 3477-3491.

Proussevitch, A.A., Sahagian, D.L. (1998) Dynamics and energetics of bubble growth in magmas: analytical formulation and numerical modeling. *J. Geophys. Res.* **103**, 18223-18251.

Scaillet, B., Holtz, F., Pichavant, M., Schmidt, M. (1996) Viscosity of Himalayan leucogranites: Implications for mechanisms of granitic magma ascent. *J. Geophys. Res.* **101**, 27691-27699.

Shaw, C.S.J. (2006) Effects of melt viscosity and silica activity on the rate and mechanism of quartz dissolution in melts of the CMAS and CAS systems. *Contrib. Mineral. Petrol.* **151**, 665-680.

Zhang, Y., Xu., Z., and Liu, Y. (2003) Viscosity of hydrous rhyolitic melts inferred from kinetic experiments, and a new viscosity model. *Am. Mineral.* **88**, 1741-1752.

CHAPTER II

TOWARD A GENERAL VISCOSITY EQUATION OF NATURAL ANHYDROUS AND HYDROUS SILICATE MELTS

ABSTRACT

A new and empirical viscosity equation for anhydrous and hydrous natural silicate melts has been developed using the following formulation:

$$\log \eta = A + \frac{B}{T} + \exp\left(C + \frac{D}{T}\right),$$

where η is viscosity in Pa·s, T is temperature in K, and A, B, C, and D are linear functions of mole fractions of oxide components except for H_2O. The formulation is applied successfully to fit the temperature and compositional dependence of viscosity for some binary systems. Furthermore, the new model with eight parameters fits the compositional and temperature dependence of the viscosity data of anhydrous natural silicate melts better than the ten-parameter model in the literature. The main purpose of this work is to fit the entire high- and low-temperature viscosity database (1451 data points) of all "natural" silicate melts using this empirical formulation. The general viscosity equation has 37 parameters and is as follows:

$$\log\eta = \left[-6.83X_{SiO_2} - 170.79X_{TiO_2} - 14.71X_{Al_2O_{3ex}} - 18.01X_{MgO} - 19.76X_{CaO}\right.$$
$$\left.+34.31X_{(Na,\,K)_2O_{ex}} - 140.38Z + 159.26X_{H_2O} - 8.43X_{(Na,\,K)AlO_2}\right]$$
$$+\left[18.14X_{SiO_2} + 248.93X_{TiO_2} + 32.61X_{Al_2O_{3ex}} + 25.96X_{MgO} + 22.64X_{CaO}\right.$$
$$\left.-68.29X_{(Na,\,K)_2O_{ex}} + 38.84Z - 48.55X_{H_2O} + 16.12X_{(Na,\,K)AlO_2}\right]1000/T +$$
$$\exp\left\{\left[21.73X_{Al_2O_{3ex}} - 61.98X_{(Fe,\,Mn)O} - 105.53X_{MgO} - 69.92X_{CaO}\right.\right.$$
$$\left.-85.67X_{(Na,\,K)_2O_{ex}} + 332.01Z - 432.22X_{H_2O} - 3.16X_{(Na,\,K)AlO_2}\right]$$
$$+\left[2.16X_{SiO_2} - 143.05X_{TiO_2} - 22.10X_{Al_2O_{3ex}} + 38.56X_{(Fe,\,Mn)O} + 110.83X_{MgO} + 67.12X_{CaO}\right.$$
$$\left.\left.+58.01X_{(Na,\,K)_2O_{ex}} + 384.77X_{P_2O_5} - 404.97Z + 513.75X_{H_2O}\right]1000/T\right\}, \quad (1)$$

where η is viscosity in Pa·s, T is temperature in K, X_i means mole fraction of oxide component i, and $Z=(X_{H2O})^{1/[1+(185.797/T)]}$. Al_2O_{3ex} or $(Na, K)_2O_{ex}$ mean excess oxides after forming $(Na, K)AlO_2$. The 2σ deviation of the fit is 0.61 logη units. This general model is recommended for viscosity calculations in modeling magma chamber processes and volcanic eruptions.

1. INTRODUCTION

Knowledge of the viscosity of silicate melts is critical to the understanding of igneous processes, such as melt segregation and migration in source regions, magma recharge, magma mixing, differentiation by crystal fractionation, convection in magma chambers, dynamics and style of eruptions, and magma fragmentation. Numerous measurements have been made on the viscosity of various silicate melts, from felsic (e.g., rhyolitic melt, Neuville et al., 1993) to ultramafic composition (e.g., peridotite liquid, Dingwell et al., 2004), from anhydrous (e.g., Neuville et al., 1993) to hydrous ones (e.g., Whittington et al., 2000), and from high temperature to low temperature. A number of authors have made efforts to model the viscosity data for the purpose of interpolation and extrapolation. Bottinga and Weill (1972) and Shaw (1972) were pioneers in developing

viscosity models for natural silicate melts. Because of the extreme difficulty in calibrating a better viscosity model, these models were the only ones available for over twenty years (Lange, 1994). More advanced models and relationships have been developed for specific melt compositions such as rhyolitic melts (e.g., Hess and Dingwell, 1996; Zhang et al., 2003). For melt compositions from rhyolite to peridotite, Persikov (1998) developed a viscosity model for anhydrous and hydrous silicate melts at high temperatures (for viscosity below 10^5 Pa·s), and Giordano and Dingwell (2003a) developed new models for anhydrous silicate melts applicable to a larger temperature range, 700 – 1600ºC.

In spite of recent advances in viscosity models, there is still a need for a general model that would apply to all natural silicate melts, all accessible temperature ranges, and especially including the effect of H_2O content. The model of Giordano and Dingwell (2003a) is noteworthy in this connection. In the modeled temperature range (700-1600°C) for anhydrous melts, it has a 2σ uncertainty of 0.78 in $\log\eta$. However, the model is limited to anhydrous melts, and cannot be applied to estimate viscosity at lower temperatures. For example, the model predicts $\log\eta$ of 16.9 for a phonolite at 614.7°C, while the experimentally determined $\log\eta$ is 11.63 (Giordano et al., 2000). Viscosity at < 700°C is critical for understanding magma fragmentation and welding in tuffs. The purpose of this work is to develop a practical viscosity model for natural silicate melts that is applicable to both anhydrous and hydrous natural melts and to the entire temperature range in which experimental data are available.

2. TEMPERATURE DEPENDENCE OF VISCOSITY

The temperature dependence of viscosity of silicate melts has been extensively studied from a theoretical point of view or through empirical fitting of viscosity data. For a narrow temperature range, usually for viscosities between 0.1 to 10^4 Pa·s, the dependence of viscosity on temperature is well described by the Arrhenius equation (e.g., Bottinga and Weill, 1972; Shaw, 1972). When the temperature range is large enough, most silicate melts exhibit a non-Arrhenian relationship between viscosity and temperature (e.g., Neuville et al., 1993; Hess and Dingwell, 1996; Whittington et al., 2000). It is possible that the isostructural viscosity variation is Arrhenian (Scherer, 1984), but viscosity variation due to temperature-induced structure change is the origin of the non-Arrhenian behavior. Many equations have been proposed to explain or fit the temperature dependence of viscosity (e.g., Brush, 1962).

One thermodynamic description of the temperature dependence of viscosity of silicate melts is the Adam-Gibbs equation (e.g., Adam and Gibbs, 1965; Richet, 1984):

$$\eta = A_e \exp\left[B_e/(TS_{conf})\right], \quad (1)$$

where η is viscosity, A_e is the pre-exponential factor independent of temperature, B_e is an energy term, T is temperature in K, and S_{conf} is the configurational entropy of the melt. For compositions corresponding to a pure stable crystalline phase (such as diopside), the configurational entropy as a function of temperature can be determined from appropriate heat capacity measurements of liquids, and crystals and glasses down to zero K (Richet et al., 1986). However, for a multicomponent melt system in which oxide concentrations are variable, the configurational entropy as a function of temperature and composition cannot be evaluated independently. The above equation becomes a fitting equation with many

parameters, which loses its theoretical appeal. Hence this model is not used often to fit viscosity-temperature relationship of silicate melts.

The most often used empirical description for the temperature dependence of viscosity is the VFT (Vogel-Fulcher-Tammann) equation (e.g., Fulcher, 1925; Tammann and Hesse, 1926):

$$\log \eta = A + \frac{B}{T - T_0}, \tag{2}$$

where A, B and T_0 are fitting parameters. Another model related to the fragility of the melt has also been used (e.g., Avramov, 1998; Zhang et al., 2003).

$$\log \eta = A + \left(\frac{B}{T}\right)^{\alpha}, \tag{3}$$

where α is fragility parameter and depends on heat capacity. For a restricted compositional range α is found to depend linearly on chemical composition, as illustrated by data in sodium or lead silicates (Avramov, 1998).

Both Eqns. 2 and 3 are three-parameter equations with no explicit consideration of melt composition, which is the least number of parameters to fit the non-Arrhenian behavior. Eqns. 2 and 3 were extended to multicomponent melts by allowing the three parameters to vary with composition, but no working scheme was found to fit the viscosity data (2σ uncertainty in $\log\eta$ is too large, > 0.9 log unit). With many trials, the following empirical relation was found to be extendable to multicomponent melts:

$$\log \eta = A + \frac{B}{T} + \exp\left(C + \frac{D}{T}\right), \tag{4}$$

where A, B, C, and D are fitting parameters and are allowed to vary linearly with mole fraction of oxide components in melts. This equation would imply that the activation

energy for viscous relaxation depends on temperature exponentially: $E_a = d(\ln\eta)/d(1/T) = 2.303[B + D\exp(C+D/T)]$, consistent with the activation energy of viscous flow derived from Eqn. 1 in Richet et al. (1986). It is not clear whether there is theoretical basis for Eqn. 4, but it works empirically to fit viscosity data of multicomponent silicate melts.

Although the above four-parameter equation can also fit viscosity data of a single composition, not all four parameters are necessary, and a three-parameter equation, either Eqn. 2 or 3 would be more advisable. Nonetheless, letting $C = 0$ reduces Eqn. 4 to a three-parameter equation, which may fit viscosity data of a single composition:

$$\log\eta = A + \frac{B}{T} + \exp\left(\frac{D}{T}\right). \qquad (4a)$$

Fig. 2.1 compares fits of viscosity data using Eqns. 2, 3, and 4a on anhydrous trachyte melt (AMS_D1, Romano et al., 2003) and tephrite melt (Whittington et al., 2000). As shown in Fig. 2.1, these three equations all fit viscosity data well for a given anhydrous melt.

The primary purpose of proposing Eqn. 4 is to fit viscosity data of multicomponent silicate melts by making the four parameters linearly dependent on composition. Below, first the compositional dependence of viscosity in binary melts is discussed, then Eqn. 4 is applied to fit viscosity of anhydrous natural silicate melts, and finally the entire viscosity database on "natural" anhydrous and hydrous silicate melts.

3. VISCOSITY OF BINARY MELTS

At low temperatures the viscosity of melts in simple binary systems often shows minima at intermediate compositions. This minimum diminishes with increasing

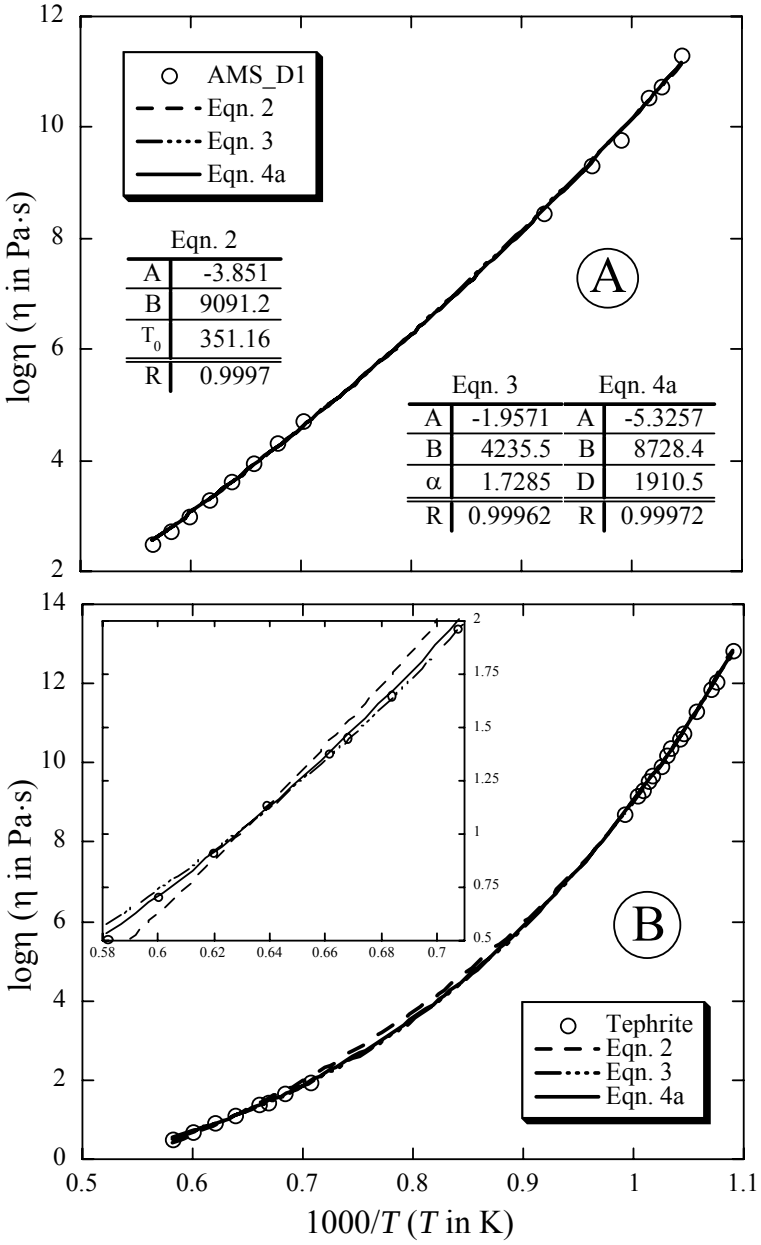

Fig. 2.1 Comparisons of fitting results using Eqns. 2, 3, and 4a for viscosity data of (a) AMS_D1 trachyte (Romano et al., 2003) and (b) tephrite (Whittington et al., 2000).

temperature, and eventually disappears at high enough temperature (Neuville and Richet, 1991). The minimum of viscosity data in a binary system can be explained by a combination of the Adam-Gibbs model and mixing law of configurational entropy of two end-members (Neuville and Richet, 1991). However, in this strategy, many fitting parameters are needed to account for the viscosity dependence on composition and temperature. For example, Neuville and Richet (1991) used a fifteen-parameter equation to fit the viscosity data of $Ca_3Al_2Si_3O_{12}$-$Mg_3Al_2Si_3O_{12}$ binary system. Moreover, asymmetry of viscosity as a function of composition, such as in the $Na_2Si_3O_7$-$K_2Si_3O_7$ binary system, can make it even more difficult for the Adam-Gibbs model to fit the viscosity data in the binary system (Richet, 1984).

On the other hand, assuming that each of the four parameters is a linear function of composition, Eqn. 4 becomes an eight-parameter equation to fit the temperature and compositional dependence of viscosity of a binary system:

$$\log\eta = \left(a_1X_1 + a_2X_2\right) + \frac{\left(b_1X_1 + b_2X_2\right)}{T} + \exp\left(\left(c_1X_1 + c_2X_2\right) + \frac{\left(d_1X_1 + d_2X_2\right)}{T}\right), \quad (5)$$

where *a*, *b*, *c* and *d* with subscript 1 and 2 are fitting parameters, *X* is mole fraction of two end-members in the system. Compared to the fifteen-parameter equation of Neuville and Richet (1991), the number of fitting parameters is almost halved although the physical meaning of each parameter is less clear in Eqn. 5.

Fits using Eqn. 5 and all fits below are carried out using the commercially available program MatLab or Stata, which employs nonlinear least square regression to minimize $\chi^2 = \sum(\log\eta_{calc,i}-\log\eta_{obs,i})^2$. The fitting errors on all parameters are obtained by the program Stata. When the standard error of a parameter is larger than the absolute

value of the parameter, the parameter is removed and a new fit with one less fitting parameter is carried out.

Figure 2.2 shows fits of viscosity data of four binary systems: $MgSiO_3$-$CaSiO_3$ (Urbain et al., 1982; Scarfe and Cronin, 1986; Neuville and Richet, 1991), $Mg_3Al_2Si_3O_{12}$-$Ca_3Al_2Si_3O_{12}$, pyrope-grossular (Neuville and Richet, 1991), $NaAlSi_3O_8$-$CaAl_2Si_2O_8$, albite-anorthite (Kozu and Kani, 1944; Urbain et al., 1982; Hummel and Arndt, 1985), and NS_3-KS_3, $Na_2Si_3O_7$-$K_2Si_3O_7$ (Taylor and Dear, 1937; Lillie, 1939; Taylor and Doran, 1941; Poole, 1948; Shartsis et al., 1952; Bockris et al., 1955; Mackenzie, 1957; Taylor and Rindone, 1970; Ammar et al., 1977). The viscosities of partially crystallized samples during measurement are not used in the fitting. The fitting parameters are shown in Table 2.1. The 2σ deviations in terms of $\log\eta$ for $CaSiO_3$-$MgSiO_3$, garnet, plagioclase and NS_3-KS_3 systems are 0.39, 0.25, 0.29 and 0.30 respectively. There is a minimum viscosity at intermediate compositions in all four binary systems at low temperatures, such as $CaSiO_3$-$MgSiO_3$ and garnet at 1050 K (Fig. 2.3A), plagioclase at 1123 K (Fig. 2.3B) and NS_3-KS_3 at 715 K (Fig. 2.3C).

The compositional location of viscosity minimum varies with temperature. This can be seen from the viscosity data of plagioclase (albite-anorthite) binary system (Hummel and Arndt, 1985). As shown in Fig. 2.3B, the viscosity minimum of albite-anorthite system is located at around 40 mole% of anorthite in the composition range at 1123 K, but the minimum is at a greater anorthite content at higher temperatures. This variation has been explained by Richet (1984) to be due to the mixing of configurational entropies of anorthite and albite melts, which increase at considerably different rates with increasing temperature. The magnitude of the viscosity minimum diminishes with

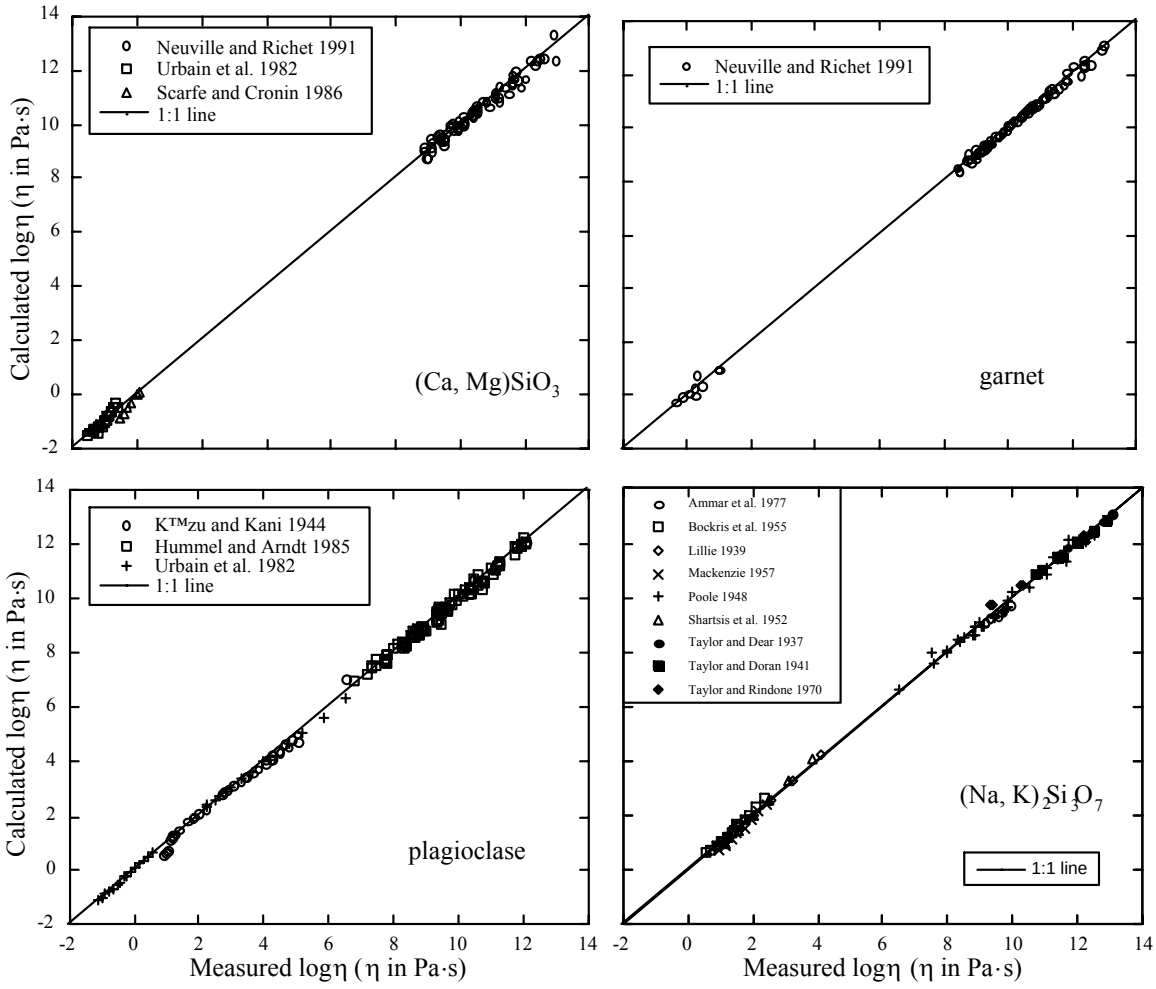

Fig. 2.2 Comparisons of experimental viscosity data with calculated values using Eqn. 5 with fitting parameters in Table 2.1. The data sources are as follows: $CaSiO_3$-$MgSiO_3$ (Urbain et al., 1982; Scarfe and Cronin, 1986; Neuville and Richet, 1991); $Ca_3Al_2Si_3O_{12}$-$Mg_3Al_2Si_3O_{12}$ garnets (Neuville and Richet, 1991); $CaAl_2Si_2O_8$-$NaAlSi_3O_8$ plagioclases (Kozu and Kani, 1944; Urbain et al., 1982; Hummel and Arndt, 1985); NS_3-KS_3 ($Na_2Si_3O_7$-$K_2Si_3O_7$) (Taylor and Dear, 1937; Lillie, 1939; Taylor and Doran, 1941; Poole, 1948; Shartsis et al., 1952; Bockris et al., 1955; Mackenzie, 1957; Taylor and Rindone, 1970; Ammar et al., 1977).

Table 2.1 Fitting parameters of Eqn. 5 in the binary systems of $CaSiO_3$-$MgSiO_3$, garnet, plagioclase and NS_3-KS_3.

parameter	$CaSiO_3$-$MgSiO_3$	garnet	plagioclase	NS_3-KS_3
a_1	-3.1287 (0.4255)	2.3593 (1.1691)	-4.5179 (1.0170)	-3.2839 (0.5488)
a_2	-9.4323 (0.4710)	-4.3178 (0.1053)	-6.3903 (0.6947)	-6.1410 (0.7446)
b_1		-21260.4 (1635.9)	5940.2 (3446.3)	4770.6 (2081.4)
b_2	17903.8 (952.7)		16551.2 (1944.6)	11821.8 (1348.6)
c_1	-1.2322 (0.3808)	0.8438 (0.1057)	-2.0844 (0.9118)	-1.1788 (0.9117)
c_2	-5.9221 (0.9186)		-3.1234 (1.5216)	-5.1302 (3.2636)
d_1	4071.6 (371.3)	2704.9 (115.7)	5061.4 (831.2)	2464.7 (478.4)
d_2	7465.5 (863.6)	2878.9 (8.8)	4690.9 (1299.1)	4295.5 (2.0116)

Note: Numbers in parentheses are 2 times the standard errors (2σ) of the fitting respective parameters. For $CaSiO_3$-$MgSiO_3$, 1=$CaSiO_3$, 2=$MgSiO_3$; for garnet, 1=$Ca_3Al_2Si_3O_{12}$ (grossular), 2=$Mg_3Al_2Si_3O_{12}$ (pyrope); for plagioclase, 1=$CaAl_2Si_2O_8$ (anorthite), 2=$NaAlSi_3O_8$ (albite); for NS3-KS3, 1=$Na_2Si_3O_7$, 2=$K_2Si_3O_7$.

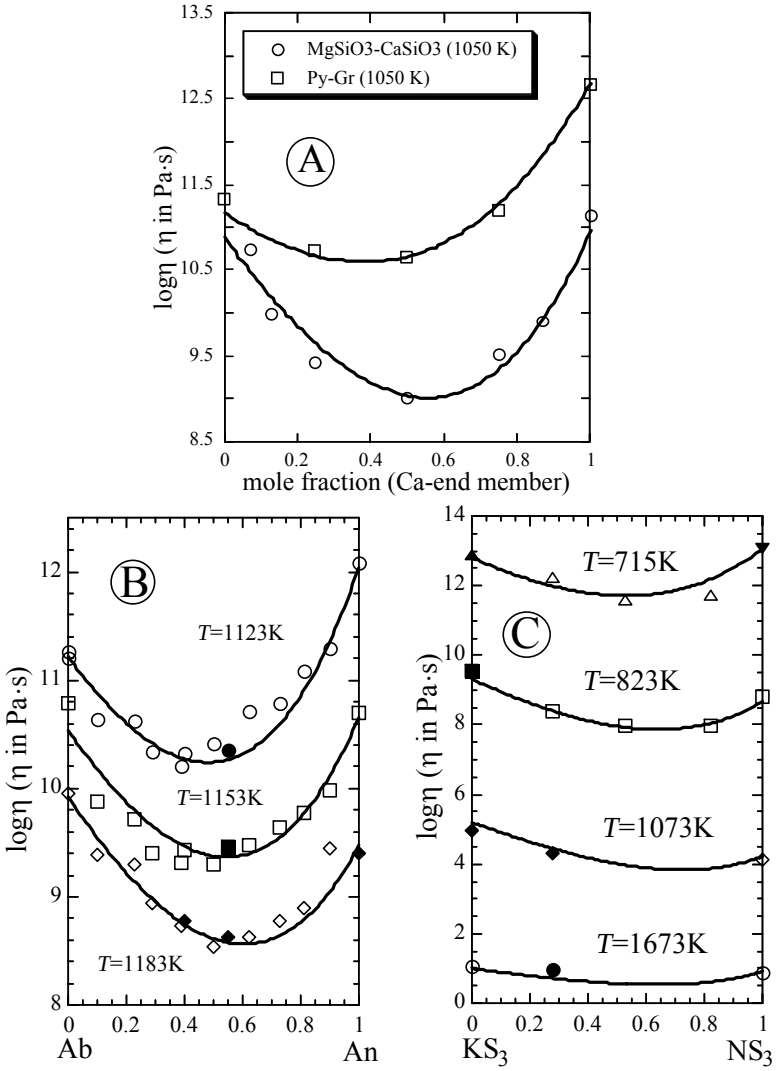

Fig. 2.3 Viscosity as a function of composition in four binary systems: (A) $CaSiO_3$-$MgSiO_3$ and garnet, (B) plagioclase and (C) NS_3-KS_3 ($Na_2Si_3O_7$-$K_2Si_3O_7$). The solid curves are calculated from Eqn. 5 with fitting parameters in Table 2.1. The sources of viscosity data are as follows: (A) interpolated from Neuville and Richet (1991) using Arrhenius relationship of viscosity and temperature (narrow temperature range) with the same compositions. (B) open symbols: Hummel and Arndt, 1985; solid symbols: interpolated data from Hummel and Arndt (1985) using Arrhenius relationship of viscosity and temperature (narrow temperature range). (C) data are from Taylor and Dear, 1937; Lillie, 1939; Taylor and Doran, 1941; Poole, 1948; Bockris et al., 1955; Mackenzie, 1957; Ammar et al., 1977; interpolated data from Taylor and Doran (1941), Poole (1948), Shartsis et al. (1952), Bockris et al. (1955), and Ammar et al. (1977); and Poole (1948) and Mackenzie (1957) using VFT equation for the same compositions.

increasing temperature, as inferred by Neuville and Richet (1991). As shown in Fig. 2.3C, the viscosity minimum in NS_3-KS_3 system is less pronounced at 1673K than the one at 715K.

4. VISCOSITY MODELS FOR NATURAL ANHYDROUS AND HYDROUS SILICATE MELTS

The main purpose of this work is to present a working model for calculation of the viscosity of all natural anhydrous and hydrous silicate melts covering the entire experimental temperature range. The equation used to fit the viscosity data is Eqn. 4, with each of *A*, *B*, *C*, and *D* as a linear function of the compositional parameters. For example, for an N-component system, the parameter *A* may be written as:

$$A = \sum_{i=1}^{N} a_i X_i , \tag{6a}$$

Or $$A = a_0 + \sum_{i=1}^{N-1} a_i X_i \tag{6b}$$

where a_0, and a_i are fitting parameters, with *i* being the *i*th oxide in the anhydrous melts. This formulation requires many fitting parameters. In order to avoid the impression that the model works only because of many parameters, first an effort to use formulation of Eqn. 4 to fit a smaller data set that has been modeled recently by Giordano and Dingwell (2003a) is presented to show that the new model can fit the same data using a smaller number of parameters than that of Giordano and Dingwell (2003a).

4.1. A SIMPLE MODEL FOR NATURAL ANHYDROUS MELTS

For multicomponent silicate melts, the dependence of viscosity on melt composition is complicated. In the quest of seeking simpler equations with a smaller number of fitting parameters, various parameters such as NBO/T (e.g., Giordano and Dingwell, 2003a) and SM (SM = $\sum$ (Na_2O+K_2O+CaO+MgO+MnO+FeO_{tot}/2)) (Giordano and Dingwell, 2003a) have been used in modeling melt viscosity. Various parameters were explored to simplify the compositional dependence. After a number of trials, using the sum of network formers, SiO_2, Al_2O_3 and P_2O_5 as one single parameter is found to work well in the context of Eqn. 6b. Hence this parameter is defined as:

$$\mathrm{SAP} = X_{\mathrm{SiO_2}} + X_{\mathrm{Al_2O_3}} + X_{\mathrm{P_2O_5}}, \tag{7}$$

where X_i is mole fraction of oxide i in the melt. Based on the above considerations, the following equation to relate viscosity, temperature and melt composition is used:

$$\log\eta = (a_0 + a_1 X) + \frac{(b_0 + b_1 X)}{T} + \exp\left((c_0 + c_1 X) + \frac{(d_0 + d_1 X)}{T}\right), \tag{8}$$

where $X = \mathrm{SAP}$; a, b, c, and d with subscript 0 or 1 are fitting parameters.

Giordano and Dingwell (2003a) presented two models for the viscosity of anhydrous silicate melts. The data set contained 314 viscosity data points. Their preferred model using the parameter SM contained 10 fitting parameters. Although their database contained viscosity data below 700°C, they only modeled the data in the temperature range of 700-1600°C. With 10 parameters, the 2σ deviation of their preferred model is 0.78 logη units at 700-1600°C.

The purpose of using Eqn. 8 to fit viscosity data is to compare with previous fits. Hence fitting the same viscosity database of the anhydrous natural silicate melts as used

by Giordano and Dingwell (2003a) is the ideal solution. All the viscosity data used by them plus the data at temperatures below 700°C are used to carry out the nonlinear fit and the new model is as follows:

$$\log \eta = (-21.3517 + 12.7366X) + \frac{29300.3 - 9757.4X}{T} + \exp\left((29.9791 - 32.4047X) + \frac{-58868.8 + 65081.8X}{T}\right). \quad (9)$$

The standard errors for the fitting parameters are shown in Table 2.2. Applying the above equation to viscosity data at 700-1600°C, the 2σ deviation is 0.63 logη units (Fig. 2.4A). That is, with a smaller number of fitting parameters (8 versus 10), the formulation of Eqn. 4 is able to fit anhydrous melt viscosity data to a slightly better precision at this temperature range than the model of Giordano and Dingwell (2003a).

Another measure of a successful model is applicability to a wide range of conditions. For example, Hess and Dingwell (1996) compared their viscosity model for hydrous rhyolite at both high and low temperatures to the model of Shaw (1972) although his model was for all anhydrous and hydrous silicate melts but at high temperatures only, and showed that their model is superior to that of Shaw (1972) at low temperatures. The eight-parameter model is able to fit low-temperature viscosity data (i.e., data at ≤ 700°C, Fig. 2.4B). For the whole temperature range, Eqn. 9 reproduces the experimental data with a 2σ standard uncertainty of 0.77 (Fig. 2.4). The model of Giordano and Dingwell (2003a), on the other hand, did not include data at ≤ 700°C in the fit and hence did not predict the data well. Although Giordano and Dingwell's model is not designed for application below 700°C, the applicability of this eight-parameter model to the full temperature range of viscosity data demonstrates its superiority. Viscosity data at ≤700°C are of importance in processes such as magma fragmentation and welding in tuffs.

Table 2.2 Fitting parameters for Eqn. 8.

	a	*b*	*c*	*d*
0	-21.3517	29300.3	29.9791	-58868.8
	(2.1976)	(2159.0)	(14.7288)	(27112.4)
1	12.7366	-9757.4	-32.4047	65081.8
	(3.8896)	(3708.8)	(16.8378)	(30272.4)

Note: Numbers in parentheses are 2σ errors of fitting coefficients respectively.

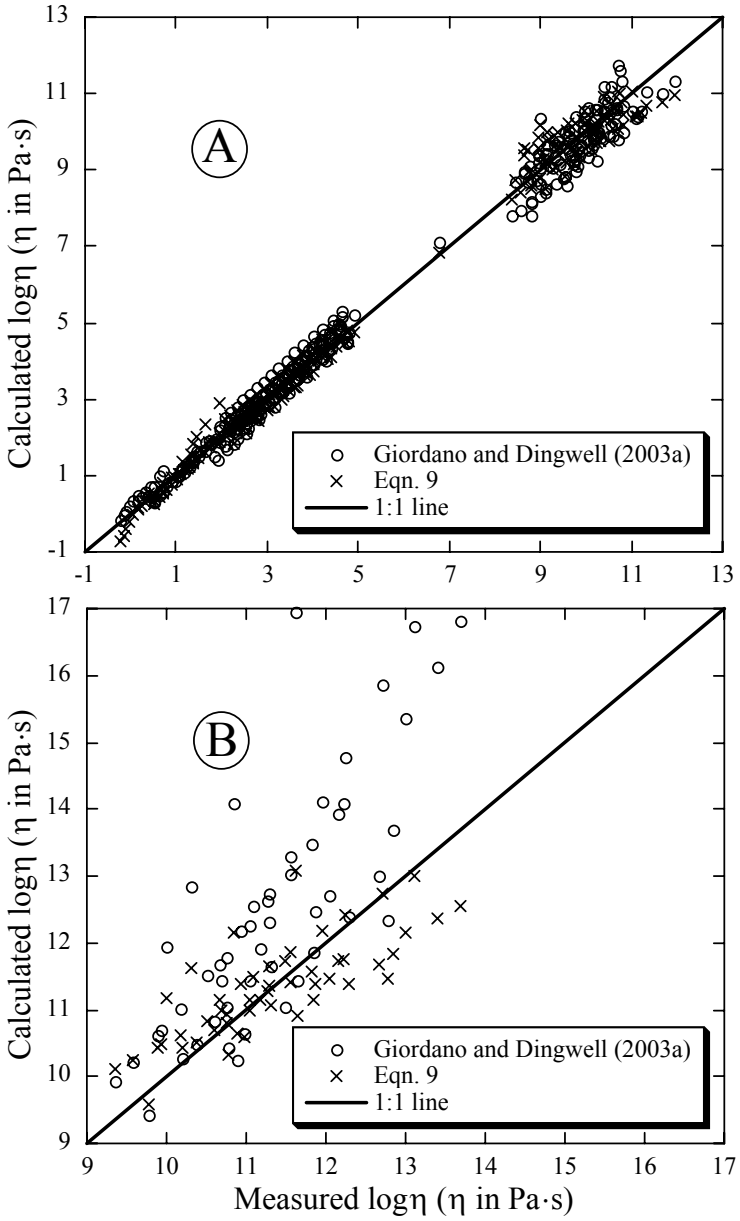

Fig. 2.4 Comparison of experimental viscosity data with calculated values (A) in the temperature range from 700 to 1600°C (which is the temperature range that Giordano and Dingwell (2003a) recommended for their model); and (B) below 700°C.

In summary, with a smaller number of fitting parameters, the new model does a better job than the most recent viscosity models (Giordano and Dingwell, 2003a). This verifies that Eqn. 4 provides a practical way to describe the compositional and temperature dependences of the viscosity of natural silicate melts, and the success of the model below is not purely because of the many parameters involved.

4.2. VISCOSITY DATA

The primary motivation of this work is to develop a practical viscosity model for natural anhydrous and hydrous silicate melts. Viscosity data for the development of new viscosity model come from literature. The compositional range is limited to "natural" silicate melts (including Fe-free haplogranitic, haploandesitic, haplobasanitic, haplotephritic, haplophonolitic and haplotrachytic melts). The compositions range from peridotite to rhyolite, from peralkaline to peraluminous silicate melts, and from anhydrous to hydrous melts. Simple synthetic melts, such as Li_2O-SiO_2, Na_2O-SiO_2, K_2O-SiO_2, $CaSiO_3$-$MgSiO_3$, feldspar systems, are not included, but synthetic melts intended to approximate natural silicate melt are included. Simple synthetic melts are excluded from the new model because there is still more work needed in developing a completely general compositional model for the viscosity of all silicate melts. For example, including simple melts such as Na_2O-SiO_2 would expand the compositional space to pure Na_2O melt, which may require parameters *A*, *B*, *C*, and *D* in Eqn. 4 to vary as a nonlinear function of oxide mole fractions. This limitation was also encountered in literature when other silicate liquid properties are modeled: (1) The density model of liquids is developed only for natural silicate liquids, excluding simple synthetic melts

(Lange and Carmichael, 1987; Lange, 1997), (2) The thermodynamic model of silicate melts is also developed only for natural silicate liquids, excluding simple synthetic melts (Ghiorso et al., 1983, 2002).

The compositions of "natural" silicate melts for which viscosity data are available are listed in Table 2.3 on an anhydrous basis. The references are also given in Table 2.3. There are 1451 viscosity measurements. Natural melt compositions covered in the database are presented in Fig. 2.5 on an anhydrous basis. The compositions covered by the data include: anhydrous peridotite to rhyolite, anhydrous peralkaline to peraluminous melts, hydrous basalt to rhyolite, hydrous peralkaline to peraluminous melts. The FeO-free melts include haplogranitic melts (H1-26), haploandesite (A2 and A4), haplobasanite (Bn3), haplotephrite (Te2), haplophonolite (Ph4) and haplotrachyte (Tr6) as shown in Table 2.3. Some samples with the same or similar sample names (such as two HPG8, and one HPG08) but different chemical compositions are treated as different samples with different chemical compositions (that is, all compositions were treated to be different and the chemical analyses were not averaged). The viscosity ranges from 0.1 to 10^{15} Pa·s. The temperature ranges from 573 to 1977.9 K. The H_2O concentration is ≤12.3 wt% for rhyolitic melt, and below 5 wt% for other melts.

Viscosity data from partially crystallized melt (such as andesite ME113e, Richet et al, 1996) are not used. Viscosity data of phonolite melt with 0.88 wt% water in Whittington et al. (2001) are shown by these authors to be outliers, and are hence not included. The viscosities of Sample A (LGB rhyolite) in Neuville et al. (1993) are not used because these authors suspected the quality of the viscosity data. Data on rhyolite shown to be outliers by Zhang et al. (2003) are not included. The data of

Table 2.3 Melt composition on anhydrous basis (on wt% basis)

Composition	SiO_2	TiO_2	Al_2O_3	FeO	MnO	MgO	CaO	Na_2O	K_2O	P_2O_5	total	ID	ref
Basanite (EIF)	41.15	2.74	12.10	10.11	0.00	11.24	15.66	2.76	3.04	1.02	99.82	Bn1	19
Basanite (EIF)	41.22	2.74	12.12	10.03	0.00	11.26	15.69	2.76	3.05	1.02	99.89	Bn2	17
Basanite (NIQ)	43.57	2.97	10.18	0.00	0.00	9.17	26.07	7.59	0.96	0.00	100.51	Bn3	1
Peridotite	45.83	0.18	4.87	8.63	0.00	31.63	6.37	0.32	0.00	0.00	97.83	Pr	27
Basalt (ETN)	47.03	1.61	16.28	10.88	0.20	5.17	10.47	3.75	1.94	0.59	97.92	Bl1	25
Basalt (ETN)	47.81	1.94	17.91	10.90	0.19	4.75	9.96	3.94	2.11	0.48	99.99	Bl2	17
Basalt	48.21	1.25	15.50	10.64	0.00	9.08	11.92	2.40	0.08	0.14	99.22	Bl3	21
Tephrite (Ves_G_tot)	49.20	0.83	16.40	7.20	0.13	5.10	10.20	2.70	6.50	0.72	98.98	Te1	19
Basalt (MTV9)	49.61	4.27	11.01	14.73	0.00	4.46	10.04	2.81	0.47	2.51	99.91	Bl5	28
Basalt (Kilauea 1921)	50.01	2.60	12.56	10.79	0.24	9.39	10.88	2.33	0.48	0.00	99.37	Bl7	29
Tephrite	50.56	2.35	14.03	0.00	0.00	8.79	15.00	7.04	3.01	0.00	100.78	Te2	1
Basalt (MTV4)	50.66	3.95	11.35	13.90	0.00	3.94	9.60	2.98	0.51	2.40	99.29	Bl6	28
Basalt (MTV6)	50.84	4.26	11.38	15.05	0.00	4.42	10.18	3.01	0.55	0.04	99.73	Bl8	28
Basalt (MTV2)	50.87	4.05	11.36	14.20	0.00	4.23	9.62	3.06	0.52	0.09	98.00	Bl9	28
Phonolite (Ves_W_tot)	51.20	0.67	18.60	6.10	0.13	2.50	7.30	3.75	7.90	0.40	98.55	Ph1	19
Phonolite (V_1631_G)	53.14	0.59	19.84	4.72	0.13	1.77	6.75	4.77	8.28	0.00	99.99	Ph2	23
Phonolite (V_1631_W)	53.52	0.60	19.84	4.80	0.14	1.76	6.76	4.66	7.91	0.00	99.99	Ph3	23
Basalt	53.54	1.05	17.29	7.82	0.00	5.46	8.32	3.59	1.64	0.20	98.91	Bl4	21
Andesite	58.56	0.64	18.98	7.45	0.00	3.48	6.17	3.24	0.92	0.00	99.44	A1	21
Andesite	58.69	0.01	21.57	0.02	0.02	5.38	9.49	3.30	1.57	0.00	100.05	A2	26
Phonolite	58.82	0.79	19.42	0.00	0.00	1.87	2.35	9.31	7.44	0.00	100.00	Ph4	2
Andesite (Crater Lake)	59.46	0.73	17.90	5.18	0.10	3.71	6.45	4.23	1.47	0.00	99.26	A5	29
Phonolite (ATN)	59.70	0.46	18.52	3.60	0.17	0.65	2.80	3.89	8.45	0.15	98.39	Ph5	19
Phonolite (Td_ph)	60.46	0.56	18.81	3.31	0.20	0.36	0.67	9.76	5.45	0.06	99.64	Ph6	22
Trachyte (IGC)	60.74	0.27	19.22	3.37	0.18	0.28	2.11	5.28	6.32	0.06	97.83	Tr1	20
Trachyte (AMS_D1)	60.86	0.39	18.27	3.88	0.12	0.90	2.96	4.12	8.50	0.00	100.00	Tr2	23
Andesite	61.17	0.84	17.29	5.39	0.00	3.35	5.83	3.85	1.39	0.00	99.11	A3	11
Trachyte (AMS_B1)	61.26	0.38	18.38	3.50	0.14	0.74	2.97	4.58	8.04	0.00	99.99	Tr3	23
Andesite (Crater Lake)	62.15	0.76	16.80	4.96	0.25	3.26	5.08	5.02	1.72	0.00	100.00	A6	32
Andesite	62.40	0.55	20.01	0.03	0.02	3.22	9.08	3.52	0.93	0.12	99.88	A4	8
Trachyte (MNV)	63.88	0.31	17.10	2.90	0.13	0.24	1.82	5.67	6.82	0.05	98.92	Tr4	20
Trachyte (PVC)	63.99	0.45	16.96	2.55	0.14	0.32	0.83	6.33	6.37	0.09	98.03	Tr5	19
Trachyte	64.45	0.50	16.71	0.00	0.00	2.92	5.36	6.70	3.37	0.00	100.01	Tr6	2
Dacite	65.28	0.59	17.05	4.02	0.08	1.82	4.70	4.34	1.29	0.13	99.30	D1	30
Dacite (UNZ)	66.00	0.36	15.23	4.08	0.10	2.21	5.01	3.84	2.16	0.14	99.13	D2	24
Granite (263-2)	66.77	0.39	20.15	4.31	0.01	0.72	3.64	1.37	2.17	0.00	99.53	R1	16
Trachyte (570-2)	66.95	0.87	21.24	2.57	0.06	0.01	1.63	1.83	4.55	0.00	99.71	Tr7	16
Plagioliparite (851-2)	67.16	0.01	21.65	2.81	0.01	0.73	2.65	2.85	1.82	0.00	99.69	R2	16
Trachyte (570-3)	68.71	0.90	19.28	2.59	0.06	0.00	1.65	1.87	4.66	0.00	99.72	Tr8	16
Trachyte (570-1)	70.16	0.92	17.18	2.74	0.06	0.00	1.70	2.07	4.88	0.00	99.71	Tr9	16
Plagioliparite (851-1)	71.22	0.24	16.80	2.91	0.06	0.80	2.62	3.09	1.94	0.00	99.68	R3	16
Granite (130)	71.42	0.01	16.10	4.58	0.01	1.57	0.94	1.94	2.92	0.00	99.49	R4	16
Granite (Barlak)	73.12	0.19	13.56	3.19	0.00	0.18	1.68	3.86	4.20	0.00	99.98	R33	31
Rhyolite	73.23	0.19	13.60	2.78	0.00	0.17	1.69	3.78	4.11	0.13	99.68	R5	21

Trachyte (570-4)	73.35	0.90	14.83	2.38	0.07	0.00	1.64	1.87	4.70	0.00	99.74	Tr10	16
HPG05	73.49	0.00	13.26	0.00	0.00	0.00	0.00	2.40	8.98	0.00	98.13	H21	38
HPG8An10	73.60	0.00	15.60	0.00	0.00	0.00	2.10	4.40	3.80	0.00	99.50	H4	33
Rhyolite	73.79	0.05	15.11	0.42	0.05	0.07	0.97	4.71	4.02	0.01	99.20	R6	9
Rhyolite (GB4)	73.89	0.06	15.77	0.75	0.00	0.14	0.58	4.62	4.19	0.00	100.00	R34	34
HPG8Na5	74.10	0.00	11.70	0.00	0.00	0.00	0.00	9.00	4.40	0.00	99.20	H5	4,35
HPG8Ca5 (Ca5)	74.10	0.00	12.20	0.00	0.00	0.00	5.20	4.40	4.00	0.00	99.90	H6	36
HPG8K5	74.60	0.00	11.80	0.00	0.00	0.00	0.00	4.40	9.20	0.00	100.00	H7	4
Rhyolite (M981023)	74.70	0.08	13.28	1.65	0.00	0.00	0.77	4.30	5.22	0.00	100.00	R7	18
HPG04	74.90	0.00	13.52	0.00	0.00	0.00	0.00	3.64	7.22	0.00	99.28	H22	38
Rhyolite (P3RR)	75.37	0.07	12.84	1.57	0.07	0.04	0.72	4.19	5.13	0.00	100.00	R8	17
HPG8Al5 (Al05)	75.40	0.00	16.10	0.00	0.00	0.00	0.00	4.70	4.30	0.00	100.50	H8	37
HPG03	75.52	0.00	13.90	0.00	0.00	0.00	0.00	4.77	5.53	0.00	99.72	H23	38
HPG8Mg5 (Mg5)	75.60	0.00	12.00	0.00	0.00	4.90	0.00	4.50	4.00	0.00	101.00	H9	36
Rhyolite	76.03	0.06	11.48	1.05	0.06	0.36	3.21	2.42	4.60	0.00	99.27	R9	13
HPG02	76.08	0.00	13.89	0.00	0.00	0.00	0.00	5.96	3.84	0.00	99.77	H24	38
AOQ	76.12	0.00	13.53	0.00	0.00	0.00	0.00	4.65	5.68	0.00	99.98	H1	6
Rhyolite	76.38	0.06	11.59	1.03	0.05	0.36	3.25	2.44	4.66	0.00	99.82	R10	13
HPG01	76.52	0.00	14.05	0.00	0.00	0.00	0.00	7.14	2.19	0.00	99.90	H25	38
Rhyolite	76.57	0.06	11.65	1.04	0.07	0.36	3.23	2.46	4.62	0.00	100.06	R11	13
Rhyolite (MCR)	76.59	0.08	12.67	1.00	0.00	0.03	0.52	3.98	4.88	0.00	99.75	R12	14
Rhyolite	76.60	0.10	12.70	1.17	0.00	0.02	0.31	4.10	4.60	0.00	99.60	R13	15
HPG09	76.88	0.00	11.45	0.00	0.00	0.00	0.00	3.60	5.60	0.00	97.53	H10	38
Rhyolite (LGB)	76.92	0.10	12.92	0.89	0.05	0.11	0.86	3.89	4.25	0.03	100.02	R14	10
Rhyolite (RH)	76.99	0.03	13.02	0.71	0.10	0.04	0.48	4.31	4.31	0.00	99.99	R15	10
Rhyolite	77.00	0.06	11.77	1.00	0.06	0.36	3.29	2.48	4.68	0.00	100.70	R16	13
Rhyolite (RH-r)	77.01	0.03	13.14	0.71	0.10	0.04	0.51	4.28	4.18	0.00	100.00	R17	10
Rhyolite	77.07	0.06	11.67	0.99	0.07	0.35	3.28	2.42	4.62	0.00	100.53	R18	13
Rhyolite (SH-r)	77.08	0.09	12.44	1.30	0.02	0.02	0.36	4.49	4.20	0.00	100.00	R19	10
Rhyolite (EDFmr)	77.15	0.09	12.82	0.56	0.07	0.07	0.52	4.11	4.61	0.01	100.01	R20	12
Rhyolite (SH)	77.17	0.08	12.40	1.30	0.02	0.01	0.35	4.50	4.20	0.00	100.03	R21	10
Rhyolite (EDF)	77.18	0.09	12.91	0.61	0.07	0.07	0.51	4.05	4.52	0.01	100.02	R22	12
HPG8Al2 (Al02)	77.20	0.00	13.90	0.00	0.00	0.00	0.00	4.50	4.30	0.00	99.90	H11	37
Rhyolite	77.27	0.03	11.75	1.05	0.05	0.36	3.31	2.43	4.73	0.00	100.98	R23	13
Rhyolite	77.38	0.05	11.70	1.03	0.05	0.36	3.24	2.44	4.80	0.00	101.05	R24	13
Rhyolite	77.46	0.05	11.64	1.04	0.07	0.35	3.23	2.45	4.70	0.00	100.99	R25	13
Rhyolite (BL6)	77.48	0.17	12.20	1.30	0.05	0.17	1.14	3.90	3.60	0.00	100.01	R26	10
Rhyolite (BL6-r)	77.53	0.17	12.17	1.30	0.05	0.17	1.13	3.89	3.60	0.00	100.01	R27	10
Rhyolite (LGB-r)	77.88	0.07	12.73	0.76	0.04	0.06	0.50	3.93	4.03	0.01	100.01	R28	10
Rhyolite (BL3)	77.88	0.16	12.03	1.19	0.05	0.05	1.06	3.64	3.88	0.01	99.95	R29	12
HPG8	77.90	0.00	11.89	0.00	0.00	0.00	0.00	4.53	4.17	0.00	98.49	H2	5
Rhyolite	77.90	0.07	12.05	0.76	0.00	0.05	0.52	4.01	4.06	0.00	99.42	R30	11
Rhyolite (EDF-1)	78.00	0.09	12.15	0.54	0.07	0.06	0.50	4.08	4.48	0.02	99.99	R31	10
Rhyolite (EDF-2)	78.00	0.09	12.15	0.54	0.07	0.07	0.50	4.08	4.48	0.00	99.98	R32	10
HPG11	78.14	0.00	11.64	0.00	0.00	0.00	0.00	1.26	9.11	0.00	100.15	H12	38
HPG10	78.21	0.00	11.69	0.00	0.00	0.00	0.00	2.41	7.43	0.00	99.74	H13	38
HPG07	78.28	0.00	11.92	0.00	0.00	0.00	0.00	5.91	2.23	0.00	98.34	H14	38

HPG8	78.60	0.00	12.50	0.00	0.00	0.00	0.00	4.60	4.20	0.00	99.90	H3	3,4,7
HPG08	78.60	0.00	11.99	0.00	0.00	0.00	0.00	4.57	4.20	0.00	99.36	H15	38
HPG06	78.98	0.00	12.11	0.00	0.00	0.00	0.00	7.04	0.62	0.00	98.75	H26	38
HPG16	81.03	0.00	9.91	0.00	0.00	0.00	0.00	1.24	7.39	0.00	99.57	H16	38
HPG15	81.74	0.00	10.03	0.00	0.00	0.00	0.00	2.47	5.66	0.00	99.90	H17	38
HPG14	82.22	0.00	10.17	0.00	0.00	0.00	0.00	3.66	3.89	0.00	99.94	H18	38
HPG12	82.31	0.00	10.16	0.00	0.00	0.00	0.00	5.89	0.70	0.00	99.06	H19	38
HPG13	82.94	0.00	10.30	0.00	0.00	0.00	0.00	4.68	2.41	0.00	100.33	H20	38

The melt compositions are listed according to SiO_2 content. References: 1, Whittington et al. (2000); 2, Whittington et al. (2001); 3, Dorfman et al. (1996); 4, Hess et al. (1995); 5, Dingwell et al. (1992); 6, Schulze et al. (1996); 7, Dingwell et al. (1996); 8, Richet et al. (1996); 9, Burnham (1964); 10, Stevenson et al. (1998); 11, Neuville et al. (1993); 12, Stevenson et al. (1996); 13, Goto et al. (2005); 14, Zhang et al. (2003); 15, Shaw (1963); 16, Goto et al. (1997); 17, Gottsmann et al (2002); 18, Stein and Spera (1993); 19, Giordano and Dingwell (2003a); 20, Giordano et al. (2004); 21, Persikov (1991); 22, Giordano et al. (2000); 23, Romano et al. (2003); 24, Giordano et al. (2005); 25, Giordano and Dingwell (2003b); 26, Liebskie et al. (2003); 27, Dingwell et al. (2004); 28, Toplis et al. (1994); 29, Kushiro et al. (1976); 30, Alidibirov et al. (1997); 31, Persikov et al. (1986); 32, Dunn and Scarfe (1986); 33, Dingwell et al. (2000); 34, Scaillet et al. (1996); 35, Dingwell et al. (1998a); 36, Hess et al. (1996); 37, Dingwell et al. (1998b); 38, Hess et al. (2001).

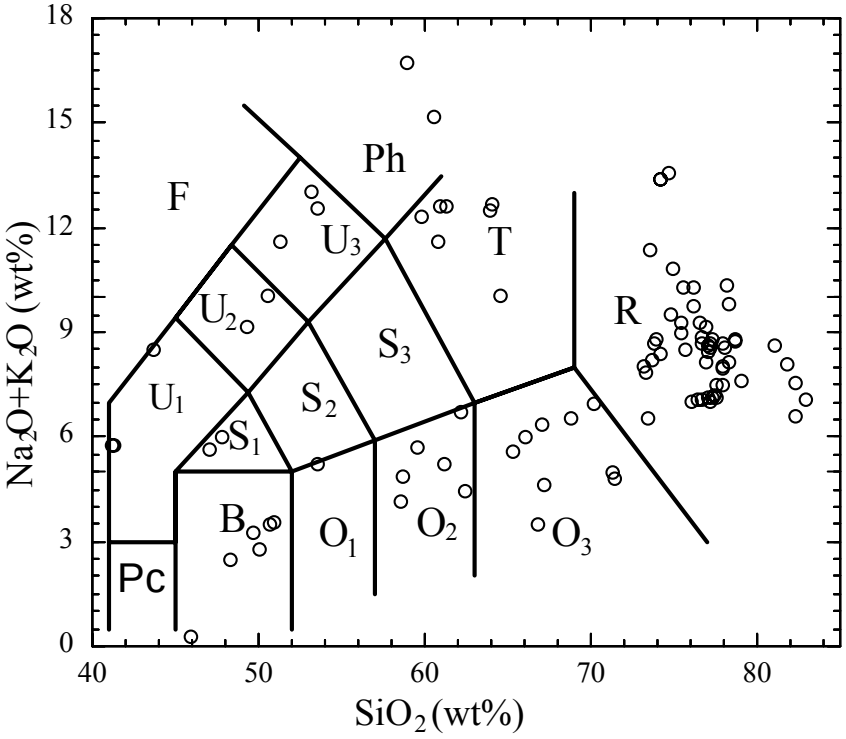

Fig. 2.5 Total alkalis versus SiO_2 diagram (Le Bas et al., 1986) showing the compositions of samples modeled in this work. Pc: picrobasalt; B: basalt; O_1: basaltic andesite; O_2: andesite; O_3: dacite; R: rhyolite; S_1: trachybasalt; S_2: basaltic trachyandesite; S_3: trachyandesite; T: trachyte or trachydacite; U_1: basanite or tephrite; U_2: phonotephrite; U_3: tephriphonolite; Ph: phonolite; F: foidite.

Friedman (1963) are not used due to their large uncertainty. Some viscosity data of identical composition, experimental temperature and viscosity value were reported in two or more publications and it is not clear to us whether or not they mean the same measurements. Such data are counted only once in the database and in the regression, such as viscosity data of EIF basanite (Gottsmann et al., 2002; Giordano and Dingwell, 2003a). All the viscosity data used in the following fit are listed in Appendix A.

Most viscosity data in the database are at 1 bar, and some are at pressures up to 5 kbars. The pressure effect is ignored as it has been shown that the effect is negligible for pressures up to 5 kbars (Persikov, 1998; Zhang et al., 2003).

4.3. THE PREFERRED MODEL

The eight-parameter model (Eqn. 9) grouped the effects of SiO_2, Al_2O_3 and P_2O_5 on viscosity. The model, although appealing because of its simplicity, still does not reproduce experimental viscosity data well. Furthermore, it does not apply to hydrous melts. In order to produce a model that can be used to calculate viscosity to better precision, more compositional parameters are necessary. In the preferred model in this section, the goal is to fit the entire viscosity database on "natural" silicate melts as accurately as possible. Although using the least number of parameters to fit is also a goal, it is subordinate to the goal of fitting the viscosity data as accurately as possible.

In the preferred model, parameters *A*, *B*, *C*, and *D* in Eqn. 4 are assumed to be linear functions of oxide mole fractions because the assumption is simple and because it considers different effects of the different oxide components to the viscosity. Fe in the natural silicate melts has two oxidation states: ferric and ferrous. The two behave

differently in the structure of the silicate melts. Although the oxidation state of Fe has been found to affect melt viscosity significantly, especially at low temperatures (Dingwell and Virgo, 1987; Liebske et al., 2003), often there is not enough information to calculate the ferric to ferrous ratio of the experimental melts at low temperatures. Hence all iron is considered as FeO.

Previous studies (e.g., Riebling, 1966; Bruckner, 1983) show that aluminum-saturated melts [Na/Al (molar) = 1] have higher viscosities than either aluminum-oversaturated (peraluminous) or aluminum-undersaturated (alkaline to peralkaline) melts. Hence, $NaAlO_2$ and $KAlO_2$ would be reasonable end members in this multicomponent system. Al_2O_3 in the melt is considered to combine with alkalis to form (Na, K)AlO_2. After forming (Na, K)AlO_2, either excess alkalis or excess aluminum are left as a component in the melts.

For hydrous melts, H_2O content plays a major role and the effect is not linear. Viscosity decreases rapidly with the first small amount of total dissolved water, and then not so rapidly at higher H_2O contents (Lange, 1994; Dingwell et al., 1996). Water is present in the silicate melts as at least two species: molecular H_2O and hydroxyl group (Stolper, 1982). The exact role of OH and molecular H_2O on affecting melt viscosity is not known. H_2O content raised to some power as an additional parameter is used as shown in Zhang et al. (2003). After many trials, the following parameter seems useful in fitting viscosity data of hydrous melts:

$$Z = (X_{H_2O})^{\frac{1}{1+(e_1/T)}}, \tag{10}$$

where e_1 is constant, T is temperature in K, and X_{H_2O} is oxide mole fraction of total dissolved H_2O. Combining Eqns. 4, 6a and 10, the following model is used to fit all the viscosity data in the database:

$$\log \eta = \left(\sum_i a_i X_i \right) + \frac{\left(\sum_i b_i X_i \right)}{T} + \exp\left(\left(\sum_i c_i X_i \right) + \frac{\left(\sum_i d_i X_i \right)}{T} \right), \quad (11)$$

where X_i is the mole fraction of SiO_2, TiO_2, $Al_2O_{3_{ex}}$, FeO_T, MnO, MgO, CaO, (Na, K)$_2O_{ex}$, P_2O_5, H_2O, (Na, K)AlO_2, plus another term related to H_2O, $(X_{H_2O})^{1/[1+(e_1/T)]}$, because a simple linear term with H_2O is not enough to account for the dependence of viscosity on H_2O content. The values of a_i, b_i, c_i, d_i, and e_1 with standard errors obtained from the fit are listed in Table 2.4. In the process of fitting, some parameters turned out to be unnecessary and some could be combined. These simplifications were made to reduce the number of parameters. The final fit contains 37 fitting parameters. As shown in Table 2.4, all the fitting parameters are statistically significant. This model can reproduce all the viscosity data (in the electronic annex) with a 2σ deviation of 0.61 logη units in the available temperature and compositional range of natural silicate melts. Fig. 2.6 shows comparison between measured viscosity values of all the melts in the database, including hydrous and anhydrous natural melts, and those calculated from Eqn. 11. Because this is the preferred model, the full equation is written down as follows:

Table 2.4 Fitting parameters for Eqn. 11.

	a	$b10^3$	c	$d10^3$
SiO_2	-6.83	18.14		2.16
	(0.47)	(0.47)		(0.16)
TiO_2	-170.79	248.93		-143.05
	(20.98)	(33.12)		(26.57)
Al_2O_{3ex}	-14.71	32.61	21.73	-22.10
	(4.32)	(4.70)	(10.75)	(11.27)
(Fe, Mn)O			-61.98	38.56
			(25.91)	(26.81)
MgO	-18.01	25.96	-105.53	110.83
	(2.78)	(4.16)	(19.50)	(19.95)
CaO	-19.76	22.64	-69.92	67.12
	(3.27)	(3.65)	(11.23)	(11.26)
$(Na, K)_2Oex$	34.31	-68.29	-85.67	58.01
	(9.60)	(7.96)	(50.49)	(46.09)
P_2O_5				384.77
				(118.21)
Z	-140.38	38.84	332.01	-404.97
	(78.46)	(27.10)	(189.53)	(237.47)
H_2O	159.26	-48.55	-432.22	513.75
	(79.94)	(29.76)	(207.27)	(260.04)
$(Na, K)AlO_2$	-8.43	16.12	-3.16	
	(1.70)	(1.68)	(0.83)	
e_1	185.797			
	(91.556)			

Note: Numbers in parentheses are 2σ errors of fitting coefficients respectively.

$$
\begin{aligned}
\log\eta = &\left[-6.83X_{SiO_2} - 170.79X_{TiO_2} - 14.71X_{Al_2O_{3ex}} - 18.01X_{MgO} - 19.76X_{CaO}\right.\\
&\left.+34.31X_{(Na,\,K)_2O_{ex}} - 140.38Z + 159.26X_{H_2O} - 8.43X_{(Na,\,K)AlO_2}\right]\\
&+\left[18.14X_{SiO_2} + 248.93X_{TiO_2} + 32.61X_{Al_2O_{3ex}} + 25.96X_{MgO} + 22.64X_{CaO}\right.\\
&\left.-68.29X_{(Na,\,K)_2O_{ex}} + 38.84Z - 48.55X_{H_2O} + 16.12X_{(Na,\,K)AlO_2}\right]1000/T +\\
&\exp\left\{\left[21.73X_{Al_2O_{3ex}} - 61.98X_{(Fe,\,Mn)O} - 105.53X_{MgO} - 69.92X_{CaO}\right.\right.\\
&\left.-85.67X_{(Na,\,K)_2O_{ex}} + 332.01Z - 432.22X_{H_2O} - 3.16X_{(Na,\,K)AlO_2}\right]\\
&+\left[2.16X_{SiO_2} - 143.05X_{TiO_2} - 22.10X_{Al_2O_{3ex}} + 38.56X_{(Fe,\,Mn)O} + 110.83X_{MgO} + 67.12X_{CaO}\right.\\
&\left.\left.+58.01X_{(Na,\,K)_2O_{ex}} + 384.77X_{P_2O_5} - 404.97Z + 513.75X_{H_2O}\right]1000/T\right\}
\end{aligned}
\quad , \qquad (12)
$$

where $Z=(X_{H_2O})^{1/[1+(185.797/T)]}$, and all mole fractions (including H_2O) add up to 1.

Examples of calculation are given in Table 2.5.

Fig. 2.6 compares calculated viscosity with experimental viscosity for all data in the database and shows that there is no systematic misfit. The behavior of Eqn. (12) was examined by varying temperature and various oxide concentrations. The calculated viscosity varies smoothly and monotonically with these parameters with no up and down fluctuations. Furthermore, in order to investigate whether some melts are systematically misfit or are not fit as well as other melts, $\Delta\pm2\sigma$ for each melt composition is listed in Table 2.6, where Δ is the average difference between the experimental $\log\eta$ and calculated $\log\eta$, and σ is the standard deviation. The value of Δ characterizes systematic misfit and 2σ is a measure of data scatter. As shown in Table 2.6, all rock groups of melts have small Δ values; but Δ values for subgroups vary from 0 up to 0.30 and most subgroups still have small Δ values. There is no correlation between the Δ values and compositions of the melts. On 2σ values, there are some variations, but no group is obviously misfit. There is no correlation between the reproducibility and the degree of polymerization.

Two sets of viscosity data on hydrous leucogranite (Whittington et al., 2004) and

Table 2.5 Examples of calculation using Eqn. 12.

composition	wt%	composition	mole fraction	T (K)	calculated logη (Pas)
SiO_2	53.52	SiO_2	0.5336	753.75	9.47
TiO_2	0.60	TiO_2	0.0045	748.75	9.60
Al_2O_3	19.84	Al_2O_{3ex}	0.0212	727.75	10.15
FeO_t	4.80	(Fe, Mn)O	0.0412	717.65	10.42
MnO	0.14	MgO	0.0262	704.35	10.80
MgO	1.76	CaO	0.0722		
CaO	6.76	$(Na, K)_2O_{ex}$	0.0000		
Na_2O	4.66	P_2O_5	0.0000		
K_2O	7.91	H_2O	0.1104		
P_2O_5	0.00	$(Na, K)AlO_2$	0.1907		
H_2O	3.32				

Note: The melt is hydrous phonolite from Romano et al. (2003).

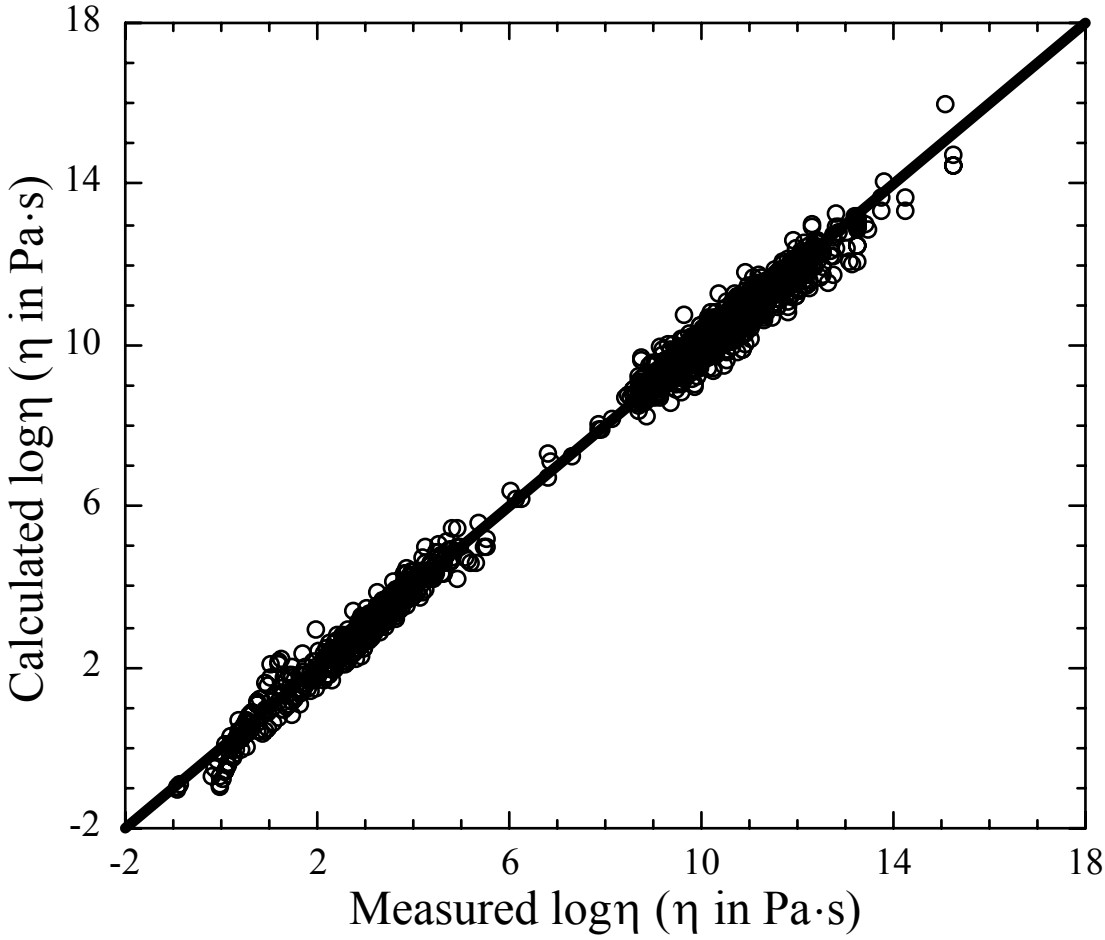

Fig. 2.6 Comparison of experimental viscosity values with calculated values using Eqn. 12.

Table 2.6 The 2σ deviations and data points of sub-groups in the viscosity database.

Composition			Δ±2σ	number of data points	Δ±2σ (rock group)
basanite (Bn1-3)		anhydrous	-0.21±0.56	33	-0.10 ±0.55
		hydrous	0.01±0.45	33	
tephrite (Te1-2)		anhydrous	0.23±0.73	38	0.13 ±0.75
		hydrous	0.01±0.72	33	
phonolite	Ph1-3	anhydrous	-0.04±0.54	40	-0.05 ±0.63
		hydrous	0.30±0.38	25	
	Ph4-6	anhydrous	-0.15±0.57	59	
		hydrous	-0.13±0.63	40	
Trachyte	Tr1-3	anhydrous	-0.04±0.71	43	0.04±0.53
		hydrous	-0.01±0.39	56	
	Tr4-6	anhydrous	0.11±0.52	68	
		hydroous	0.13±0.43	55	
	Tr7-10	anhydrous	-0.12±0.41	31	
Andesite	A1-2, A5	anhydrous	-0.05±0.40	27	-0.01 ±0.43
		hydrous	-0.02±0.37	42	
	A3-4, A6	anhydrous	-0.03±0.40	52	
		hydrous	0.06±0.52	45	
Rhyolite	R1-4	anhydrous	0.05±0.45	25	-0.00±0.54
	R5-8, R33-34	anhydrous	0.02±0.13	7	
		hydrous	0.13±0.51	40	
	R9-32	anhydrous	0.04±0.43	83	
		hydrous	-0.06±0.58	197	
dacite (D1-2)		anhydrous	0.20±0.37	32	0.14 ±0.47
		hydrous	-0.09±0.53	9	
Basalt	Bl1-3, Bl5	anhydrous	-0.11±1.05	20	0.01 ±0.92
		hydrous	0.07±0.51	21	
	Bl4, Bl6-9	anhydrous	0.06±1.09	28	
		hydrous	0.03±0.74	6	
periodite (Pr)		anhydrous	-0.07±0.55	8	-0.07±0.55
haplogranitic melt (H1-26)		anhydrous	-0.01±0.78	161	0.03 ±0.72
		hydrous	0.09±0.61	94	
leucogranite*		hydrous	-0.15±0.51	14	
HPG8An10*		anhydrous	-0.02±0.22	8	

* the melt used to test the model.

anhydrous HPG8An10 (Dingwell et al., 2000) are not included in the fit, but are chosen to test whether this preferred model can predict data not included in the fit. Because water content in the "anhydrous" melt of Whittington et al. (2004) is not determined, the viscosity data of anhydrous melt are not used due to large effect of a small amount of water on viscosity (Lange, 1994; Zhang et al., 2003). As shown in Fig. 2.7, this new model has the capability to predict the viscosity at low temperature with a 2σ deviation of 0.61.

There are many viscosity models for specific compositions, and many of them have better accuracy than the 37-parameter general model. For example, the viscosity model for hydrous and anhydrous rhyolitic melt by Zhang et al. (2003) has a 2σ uncertainty of 0.36 $\log\eta$ units; specific models for five individual anhydrous and hydrous melt compositions by Giordano et al. (2005) have very low 2σ uncertainties. Therefore, although the use of this grand model is recommended, some specific models have better accuracy and should be used when appropriate.

One unattractive feature of the preferred model is the large number of parameters used. This means the fitting parameters themselves are not well resolved. However, it does not affect the accuracy of the calculation of viscosities as long as no extrapolation is attempted. That is, the model should not be extrapolated to binary systems, nor to viscosities above 10^{15} Pa·s, nor to temperature below 573 K, nor to H_2O content above 5 wt% for melts other than rhyolite. (For rhyolite, the highest H_2O content in the viscosity database is 12.3 wt%.) As mentioned earlier, Eqn. 12 predicts smooth and monotonic variations of $\log\eta$ with mole fraction of oxides or temperature. Although it is desirable to develop a model with a smaller number of fitting parameters, the drawback of many

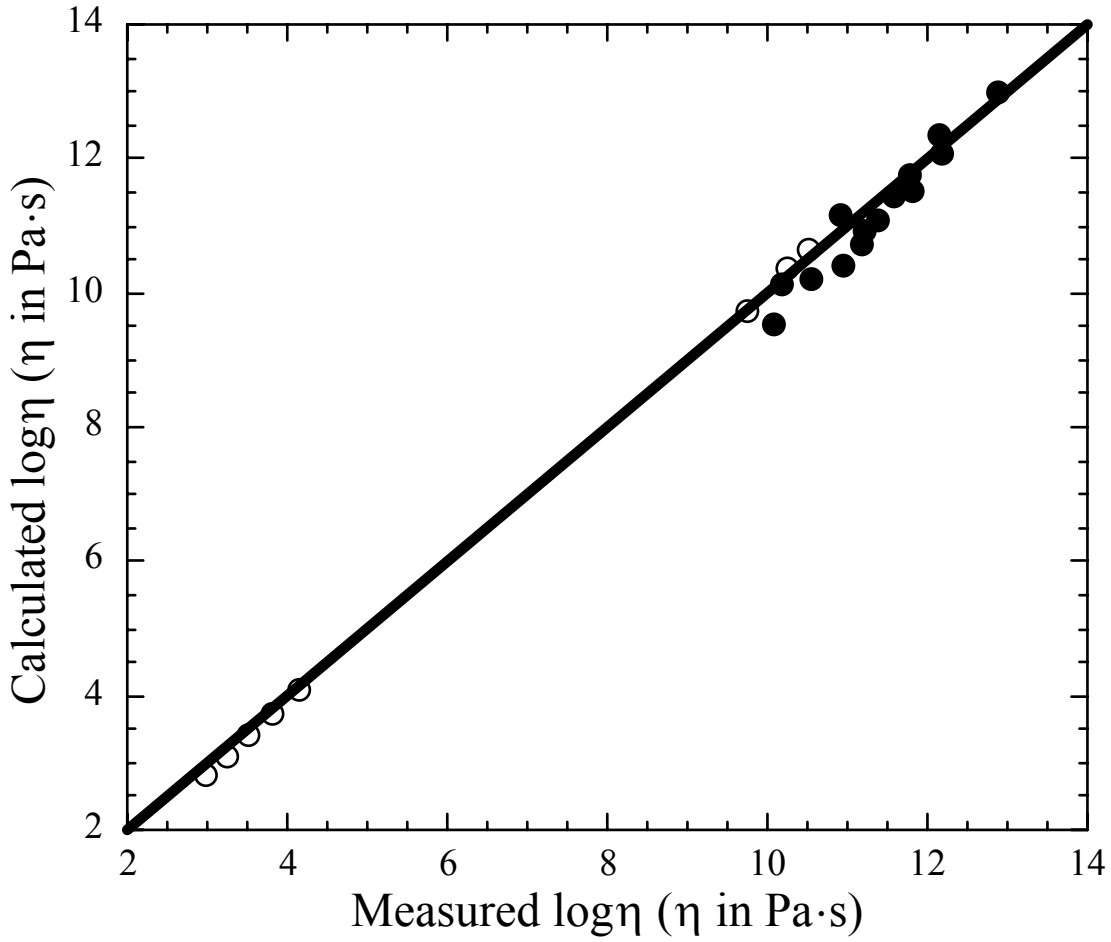

Fig. 2.7 The predictions of Eqn. 12. Data sources: filled symbols: Whittington et al. (2004); open symbols: Dingwell et al. (2000).

fitting parameters should not prevent the use of Eqn. 12 in calculating viscosity of natural silicate melts in a wide range of applications such as volcanic eruption dynamics, as well as other magmatic processes. For example, the viscosity model of Bottinga and Weill (1972) has 285 fitting parameters for anhydrous melts at high temperatures and it was widely applied. Eqn. 12 is easy to include in a software program or in a spreadsheet program. Using it to calculate viscosities of all natural silicate melts is recommended. Other applications of the viscosity model include: (1) estimation of glass transition temperature of any natural silicate melt given cooling rate (Dingwell and Webb, 1990; Dingwell et al., 2004; Giordano et al., 2005), and (2) estimation of cooling rate of any natural hydrous silicate glass based on apparent equilibrium temperature from H_2O speciation (Dingwell and Webb, 1990; Zhang, 1994; Zhang et al., 2000, 2003).

Even though this viscosity model can reproduce the entire viscosity database to a better accuracy and for a greater range of compositions than previous models, the uncertainty in reproducing the viscosity data is still larger than the experimental data uncertainty, which is usually 0.1 logη units or less. Hence there is still much room for improvement. The most important improvement might come from the development of a better functional equation to describe viscosity dependence on temperature, pressure and composition. For example, new models adopted a different functional form of viscosity. A second improvement might derive from consideration of the effect of ferric and ferrous iron, which requires knowledge of experimental conditions under which the glasses were prepared for the low-temperature viscosity measurements. A third improvement might arise from improved quantification of the effect of H_2O on viscosity, both in terms of accurate determination of H_2O for reported viscosity data and in terms of the functional

form used to handle the dependence of viscosity on H_2O content. Specifically, in the future every viscosity data should be accompanied by H_2O content and other concentrations; simply describing a melt as dry is not good enough. A fourth improvement might originate from the incorporation of the effect of CO_2 and other volatile components in the melt. So far, the effect of CO_2 on the viscosity of silicate melts has only been carried out in several synthetic melts (Lange, 1994; Bourgue and Richet, 2001). A fifth improvement might stem from the incorporation of the pressure effect (Persikov, 1998). New experimental viscosity data are needed especially at high pressures, at low temperatures, for melts with well-characterized ferric/ferrous ratios, and for melts with various and well-characterized volatile (H_2O and CO_2) concentrations.

REFERENCES

Adam G. and Gibbs J.H. (1965) On the temperature dependence of cooperative relaxation properties in glass-forming liquids. *J. Chem. Phys.* **43**, 139-146.

Alidibirov M., Dingwell D.B., Stevenson R.J., Hess K.-U., Webb S.L. and Zinke J. (1997) Physical properties of the 1980 Mount St. Helens cryptodome magma. *Bull. Volcanol.* **59**, 103-111.

Ammar M.M., El-Badry Kh. and Gharib S. (1977) Viscous properties of some alkali silicate glasses in the annealing range. *Egypt. J. Phys.* **8**, 1-8.

Avramov I. (1998) Viscosity of glassforming melts. *Glastech. Ber.* **71C**, 198-203.

Bockris J. O'M., Mackenzie J.D. and Kitchener J.A. (1955) Viscous flow in silica and binary liquid silicates. *Trans. Faraday Soc.* **51**, 1734-1748.

Bottinga Y. and Weill D.F. (1972) The viscosity of magmatic silicate liquids: a model for calculation. *Am. J. Sci.* **272**, 438-475.

Bourgue E. and Richet P. (2001) The effects of dissolved CO_2 on the density and viscosity of silicate melts: a preliminary study. *Earth Planet. Sci. Lett.* **193**, 57-68.

Bruckner R. (1983) Structure and properties of silicate melts. *Bull. Minéral.* **106**, 9-22.

Brush S.G. (1962) Theories of liquid viscosity. *Chem. Rev.* **62**, 513-548.

Burnham C.W. (1964) Viscosity of a H_2O rich pegmatite melt at high pressure (abstract). *Geol. Soc. Am. Special Paper* **76**, 26.

Dingwell D.B. and Virgo D. (1987) The effect of oxidation state on the viscosity of melts in the system Na_2O-FeO-Fe_2O_3-SiO_2. *Geochim. Cosmochim. Acta* **51**, 195-205.

Dingwell D. B. and Webb S.L. (1990) Relaxation in silicate melts. *Eur. J. Mineral.* **2**, 427-449.

Dingwell D.B., Courtial P., Giordano D. and Nichols A.R.L. (2004) Viscosity of peridotite liquid. *Earth Planet. Sci. Lett.* **226**, 127-138.

Dingwell D.B., Hess K.-U. and Romano C. (1998a) Extremely fluid behavior of hydrous peralkaline rhyolites. *Earth Planet. Sci. Lett.* **158**, 31-38.

Dingwell D.B., Hess K.-U. and Romano C. (1998b) Viscosity data for hydrous peraluminous granitic melts: Comparison with a metaluminous model. *Am. Mineral.* **83**, 236-239.

Dinwell D.B., Hess K.-U. and Romano C. (2000) Viscosities of granitic (sensu lato) melts: Influence of the anorthite component. *Am. Mineral.* **85**, 1342-1348.

Dingwell D.B., Knoche R. and Webb S.L. (1992) The effect of B_2O_3 on the viscosity of haplogranitic liquids. *Am. Mineral.* **77**, 457-461.

Dingwell D.B., Romano C. and Hess K.-U. (1996) The effect of water on the viscosity of a haplogranitic melt under *P-T-X* conditions relevant to volcanism. *Contrib. Mineral. Petrol.* **124**, 19-28.

Dorfman A., Hess K.-U. and Dingwell D. (1996) Centrifuge-assisted falling-sphere viscometry. *Eur. J. Mineral.* **8**, 507-514.

Dunn T. and Scarfe C.M. (1986) Variation of the chemical diffusivity of oxygen and viscosity of an andesite melt with pressure at constant temperature. *Chem. Geol.* **54**, 203-215.

Friedman I., Long W. and Smith R.L. (1963) Viscosity and water content of rhyolitic glass. *J. Geophys. Res.* **68**, 6523-6535.

Fulcher G.S. (1925) Analysis of recent measurements of the viscosity of glasses. *J. Am. Ceram. Soc.* **8**, 339-355.

Ghiorso M.S., Carmichael I.S.E., Rivers M.L. and Sack R.O. (1983) The Gibbs free energy of mixing of natural silicate liquids: an expanded regular solution approximation for the calculation of magmatic intensive variables. *Contrib. Mineral. Petrol.* **84**, 107-145.

Ghiorso M.S., Hirschmann M.M., Reiners P.W. and Kress V.C. III (2002) The pMELTS: A revision of MELTS for improved calculation of phase relations and major element partitioning related to partial melting of the mantle to 3 GPa. *Geochem. Geophys. Geosys.* **3**, 10.1029/2001GC000217.

Giordano D. and Dingwell D.B. (2003a) Non-Arrhenian multicomponent melt viscosity: a model. *Earth Planet. Sci. Lett.* **208**, 337-349.

Giordano D. and Dingwell D.B. (2003b) Viscosity of hydrous Etna basalt: implications for Plinian-style basaltic eruptions. *Bull. Volcanol.* **65**, 8-14.

Giordano D., Dingwell D.B. and Romano C. (2000) Viscosity of a Teide phonolite in the welding interval. *J. Volcanol. Geotherm. Res.* **103**, 239-245.

Giordano D., Nichols A.R.L. and Dingwell D.B. (2005) Glass transition temperatures of natural hydrous melts: a relationship with shear viscosity and implications for the welding process. *J. Volcanol. Geotherm. Res.* **142**, 105-118.

Giordano D., Romano C., Papale P. and Dingwell D.B. (2004) The viscosity of trachytes, and comparison with basalts, phonolites, and rhyolites. *Chem. Geol.* **213**, 49-61.

Goto A., Oshima H. and Nishida Y. (1997) Empirical method of calculating the viscosity of peraluminous silicate melts at high temperatures. *J. Volcanol. Geotherm. Res.* **76**, 319-327.

Goto A., Taniguchi H. and Kitakaze A. (2005) Viscosity measurements of hydrous rhyolitic melts using the fiber elongation method. *Bull. Volcanol.* **67**, 590-596.

Gottsmann J., Giordano D. and Dingwell D.B. (2002) Predicting shear viscosity during volcanic processes at the glass transition: a calorimetric calibration. *Earth Planet. Sci. Lett.* **198**, 417-427.

Hess K.-U. and Dingwell D.B. (1996) Viscosities of hydrous leucogranitic melts: A non-Arrhenian model. *Am. Mineral.* **81**, 1297-1300.

Hess K.-U., Dingwell D.B., Gennaro C. and Mincione V. (2001) Viscosity-temperature behavior of dry melts in the Qz-Ab-Or system. *Chem. Geol.* **174**, 133-142.

Hess K.-U., Dingwell D.B. and Webb S.L. (1995) The influence of excess alkalis on the viscosity of a haplogranitic melt. *Am. Mineral.* **80**, 297-304.

Hess K.U., Dingwell D.B. and Webb S.L. (1996) The influence of alkaline-earth oxides (BeO, MgO, CaO, SrO, BaO) on the viscosity of a haplogranitic melt: systematics of non-Arrhenian behaviour. *Eur. J. Mineral.* **8**, 371-381.

Hummel W. and Arndt J. (1985) Variation of viscosity with temperature and composition in the plagioclase system. *Contrib. Mineral. Petrol.* **90**, 83-92.

Kozu S. and Kani K. (1944) Viscosity measurements of the ternary system diopside-albite-anorthite at high temperatures. *Bull. Am. Ceram. Soc.* **23**, 377-378.

Kushiro I., Yoder H.S.Jr. and Mysen B.O. (1976) Viscosities of basalt and andesite melts at high pressures. *J. Geophys. Res.* **81**, 6351-6356.

Lange R.A. (1994) The effect of H_2O, CO_2, and F on the density and viscosity of silicate melts. *Rev. Mineral.* **30**, 331-360.

Lange R.A. (1997) A revised model for the density and thermal expansivity of K_2O-Na_2O-CaO-MgO-Al_2O_3-SiO_2 liquids from 700 to 1900 K: extension to crustal magmatic temperatures. *Contrib. Mineral. Petrol.* **130**, 1-11.

Lange R.A. and Carmichael I.S.E. (1987) Densities of Na_2O-K_2O-CaO-MgO-FeO-Fe_2O_3-Al_2O_3-TiO_2-SiO_2 liquids: new measurements and derived partial molar properties. *Geochim. Cosmochim. Acta* **53**, 2195-2204.

Le Bas M.J., Le Maitre R.W., Streckeisen A. and Zanettin B. (1986) A chemical classification of volcanic rocks based on the total alkali-silica diagram. *J. Petrol.* **27**, 745-750.

Liebske C., Behrens H., Holtz F. and Lange R.A. (2003) The influence of pressure and composition on the viscosity of andesitic melts. *Geochim. Cosmochim. Acta* **67**, 473-485.

Lillie H.R. (1939) High-temperature viscosities of soda-silica glasses. *J. Am. Ceram. Soc.* **22**, 367-374.

Mackenzie J.D. (1957) The discrete ion theory and viscous flow in liquid silicates. *Trans. Faraday Soc.* **53**, 1488-1493.

Neuville D.R. and Richet P. (1991) Viscosity and mixing in molten (Ca, Mg) pyroxenes and garnets. *Geochim. Cosmochim. Acta* **55**, 1011-1019.

Neuville D.R., Courtial P., Dingwell D.B. and Richet P. (1993) Thermodynamic and rheological properties of rhyolite and andesite melts. *Contrib. Mineral. Petrol.* **113**, 572-581.

Persikov E.S., Epel'baum M.B. and Bukhtiyarov P.G. (1986) The viscosity of a granite magma interacting with an aqueous chloride fluid. *Geochem. Intern.* **23**, 21-30.

Persikov E.S. (1991) The viscosity of magmatic liquids: Experiment, generalized patterns; a model for calculation and prediction; application. *Adv. Phys. Geochem.* **9**, 1-40.

Persikov E.S. (1998) Viscosities of model and magmatic melts at the pressures and temperatures of the Earth's crust and upper mantle. *Russian Geol. Geophys*. **39**, 1780-1792.

Poole J.P. (1948) Viscosité a basse température des verres alcalino-silicatés. *Verres Réfract*. **2**, 222-228.

Richet P. (1984) Viscosity and configurational entropy of silicate melts. *Geochim. Cosmochim. Acta* **48**, 471-483.

Richet P., Lejeune A.-M., Holtz F. and Roux J. (1996) Water and the viscosity of andesite melts. *Chem. Geol.* **128**, 185-197.

Richet P., Robie R.A. and Hemingway B.S. (1986) Low-temperature heat capacity of diopside glass ($CaMgSi_2O_6$): a calorimetric test of the configurational-entropy theory applied to the viscosity of liquid silicates. *Geochim. Cosmochim. Acta* **50**, 1521-1533.

Riebling E.F. (1966) Structure of sodium aluminosilicate melts containing at least 50 mole% SiO_2 at 1500 ˚C. *J. Chem. Phys.* **44**, 2857-2865.

Romano C., Giordano D., Papale P., Mincione V., Dingwell D.B. and Rosi M. (2003) The dry and hydrous viscosities of alkaline melts from Vesuvius and Phlegrean Fields. *Chem. Geol.* **202**, 23-38.

Scaillet B., Holtz F., Pichavant M. and Schmidt M. (1996) Viscosity of Himalayan leucogranites: Implication for mechanisms of granitic magma ascent. *J. Geophys. Res.* **101**, 27691-27699.

Scarfe C.M. and Cronin D.J. (1986) Viscosity-temperature relationships at 1 atm in the system diopside-albite. *Am. Mineral.* **71**, 767-771.

Scherer G.W. (1984) Use of the Adam-Gibbs equation in the analysis of structural relaxation. *J. Am. Ceram. Soc.* **67**, 504-511.

Schulze F., Behrens H., Holtz F., Roux J. and Johannes W. (1996) The influence of H_2O on the viscosity of a haplogranitic melt. *Am. Mineral.* **81**, 1155-1165.

Shartsis L., Spinner S. and Capps W. (1952) Density, expansivity, and viscosity of molten alkali silicates. *J. Am. Ceram. Soc.* **35**, 155-160.

Shaw H.R. (1963) Obsidian-H_2O viscosities at 1000 and 2000 bars in the temperature range 700° to 900°C. *J. Geophys. Res.* **68**, 1512-1520.

Shaw H.R. (1972) Viscosities of magmatic silicate liquids: an empirical method of prediction. *Am. J. Sci.* **272**, 870-893.

Stein D.J. and Spera F.J. (1993) Experimental rheometry of melts and supercolled liquids in the system $NaAlSiO_4$-SiO_2: Implications for structure and dynamics. *Am. Mineral.* **78**, 710-723.

Stein D.J. and Spera F.J. (2002) Shear viscosity of rhyolite-vaporemulsions at magmatic temperatures by concentric cylinder rheometry. *J. Volcanol. Geotherm. Res.* **113**, 243-258.

Stevenson R.J., Bagdassarov N.S. and Dingwell D.B. (1998) The influence of trace amounts of water on the viscosity of rhyolites. *Bull. Volcanol.* **60**, 89-97.

Stevenson R.J., Dingwell D.B., Webb S.L. and Sharp T.G. (1996) Viscosity of microlite-bearing rhyolitic obsidians: an experimental study. *Bull. Volcanol.* **58**, 298-309.

Stolper E. (1982) The speciation of water in silicate melts. *Geochim. Cosmochim. Acta* **46**, 2609-2620.

Tammann G. and Hesse W. (1926) Die abhängigkeit der viscosität von der temperatur bei unterkühlten flüssigkeiten. *Z. Anorg. Allg. Chem.* **156**, 245-257.

Taylor N.W. and Dear P.S. (1937) Elastic and viscous properties of several soda-silica glasses in the annealing range of temperature. *J. Am. Ceram. Soc.* **20**, 296-304.

Taylor N.W. and Doran R.F. (1941) Elastic and viscous properties of several potash-silica glasses in the annealing range of temperature. *J. Am. Ceram. Soc*. **24**, 103-109.

Taylor T.D. and Rindone G.E. (1970) Properties of soda aluminosilicate glasses: V, low-temperature viscosities. *J. Am. Ceram. Soc*. **53**, 692-695.

Toplis M.J., Dingwell D.B. and Libourel G. (1994) The effect of phosphorus on the iron redox ratio, viscosity, and density of an envolved ferro-basalt. *Contrib. Mineral. Petrol.* **117**, 293-304.

Urbain G., Bottinga Y. and Richet P. (1982) Viscosity of liquid silica, silicates and alumino-silicates. *Geochim. Cosmochim. Acta* **46**, 1061-1072.

Whittington A., Richet P. and Holtz F. (2000) Water and the viscosity of depolymerized aluminosilicate melts. *Geochim. Cosmochim. Acta* **64**, 3725-3736.

Whittington A., Richet P. and Holtz F. (2001) The viscosity of hydrous phonolites and trachytes. *Chem. Geol.* **174**, 209-223.

Whittington A., Richet P., Behrens H., Holtz F. and Scaillet B. (2004) Experimental temperature-X(H_2O)-viscosity relationship for leucogranites and comparison with synthetic silicic liquids. *Tran. Royal Soc. Edinburgh: Earth Sci.* **95**, 59-71.

Zhang Y. (1994) Reaction kinetics, geospeedometry, and relaxation theory. *Earth Planet. Sci. Lett.* **122**, 373-391.

Zhang Y., Xu Z. and Behrens H. (2000) Hydrous species geospeedometer in rhyolite: improved calibration and application. *Geochim. Cosmochim. Acta* **64**, 3347-3355.

Zhang Y., Xu Z. and Liu Y. (2003) Viscosity of hydrous rhyolitic melts inferred from kinetic experiments, and a new viscosity model. *Am. Mineral.* **88**, 1741-1752.

CHAPTER III

PRESSURE DEPENDENCE OF THE SPECIATION OF DISSOLVED WATER IN RHYOLITIC MELTS

ABSTRACT

Water speciation in rhyolitic melts with dissolved water ranging from 0.8 to 4 wt% under high pressure was investigated. Samples were heated in a piston-cylinder apparatus at 624-1027 K and 0.94-2.83 GPa for sufficient time to equilibrate hydrous species (molecular H_2O and hydroxyl group, $H_2O_m + O = 2OH$) in the melts and then quenched roughly isobarically. Concentrations of two hydrous species in the quenched glasses were measured with Fourier transform infrared (FTIR) spectroscopy. For samples with total water content less than 2.7 wt%, the equilibrium constant is independent of total H_2O concentration. Incorporating samples with higher water contents, the equilibrium constant depends on total H_2O content, and a regular solution model is used to describe the dependence. The equilibrium constant changes nonlinearly with pressure for samples with a given water content at a given temperature. The equilibrium constant does not change much from ambient pressure to 1 GPa, but it increases significantly from 1 to 3 GPa. In other words, more molecular H_2O reacts to form hydroxyl groups as pressure increases from 1 GPa, which is consistent with breakage of tetrahedral aluminosilicate units due to compression of the melt induced by high pressure. The effect

of 1.9 GPa (from 0.94 to 2.83 GPa) on the equilibrium constant at 873 K is equivalent to a temperature effect of 51 K (from 873 K to 924 K) at 0.94 GPa. The results can be used to evaluate the role of speciation in water diffusion, to estimate the apparent equilibrium temperature, and to infer the viscosity of hydrous rhyolitic melts under high pressure.

1. INTRODUCTION

The nature of dissolved water in silicate melt has received considerable attention (e.g., Goranson, 1938; Wasserburg, 1957; Shaw, 1964; Burnham, 1975; Stolper, 1982a,b; McMillan, 1994; Zhang, 1999; Zhang et al., 2007). As the most abundant volatile component dissolved in terrestrial silicate melts, dissolved water in melts plays an important role in igneous processes. Water can alter the structure of silicate melts, hence significantly change their physical and chemical properties, such as solidus/liquidus temperatures (e.g., Tuttle and Bowen, 1958), viscosity (e.g., Shaw, 1972; Hui and Zhang, 2007), crystal nucleation rates (e.g., Davis et al., 1997), chemical diffusion (e.g., Watson, 1991; Behrens and Zhang, 2001) and oxygen "self" diffusion (e.g., Zhang et al., 1991a; Behrens et al., 2007). Some of these effects are related to the speciation reaction below (Stolper, 1982a,b),

$$H_2O_m + O = 2OH, \quad (1)$$

where H_2O_m denotes dissolved H_2O molecules, O denotes anhydrous oxygen, and OH denotes hydroxyl groups in silicate melts. Total H_2O content will be denoted as H_2O_t. The equilibrium and kinetics of the above speciation reaction in rhyolitic melt has been extensively studied (Stolper, 1982a, b; Zhang et al., 1991a, 1995, 1997b, 2003; Ihinger et al., 1999; Nowak and Behrens, 2001). Two debates have occurred about speciation

studies (see reviews by Zhang, 1999; Behrens and Nowak, 2003; Zhang et al., 2007). The early debate on whether species concentrations can be quenched from high temperature (such as 1100 K) has been settled and the conclusion is that species concentrations will be altered during quench if the initial temperature is above the glass transition temperature for the given quench rate (Dingwell and Webb, 1990). The later debate on quenched versus *in situ* speciation studies has also been resolved, and the conclusion is that species concentrations can be preserved by rapid quench from intermediate experimental temperatures (such as 800 K, depending on H_2O_t and quench rate) below the glass transition temperature for the given quench rate (Withers et al., 1999; Nowak and Behrens, 2001). The speciation data not only provide an understanding of the detailed dissolution mechanism of H_2O in melts, but also can be applied to understand H_2O solubility and diffusivity in silicate melts and to infer viscosity of hydrous melts.

Previous experimental studies mostly investigated H_2O speciation at pressures below 1 GPa. This paper extends the experimental range to higher pressures. The new data reported here span 0.94-2.83 GPa, 624-1027 K and 0.8-4.0 wt% H_2O_t. Combining these data with previous results (Ihinger et al., 1999), a regular solution model is developed to fit H_2O speciation data from low to high pressures.

2. EXPERIMENTAL METHODS

In this study, hydrous rhyolitic glasses were held under a constant temperature (623-1023 K, nominal temperature) and pressure (1-3 GPa, nominal pressure) in a piston cylinder apparatus for sufficient duration (96 s to 3 days) for the two hydrous species in the melt to reach equilibrium, but short enough to avoid significant crystallization. The

samples were then quenched to room temperature roughly isobarically. Species concentrations were measured by Fourier transform infrared (FTIR) spectroscopy at ambient environment on the quenched glasses. Based on various assessments (see Introduction and Discussion), the quenched species concentrations reflect those at high temperature and pressure.

Starting materials include both natural hydrous rhyolitic glass (KS) and synthetic hydrous rhyolitic glass prepared by hydration of natural rhyolitic glasses. Sample KS is from Mono Crater, California. Samples GMR+2 and GMR+4 were synthesized by adding water to obsidian from Glass Mountain, California. The chemical compositions of these two natural rhyolitic obsidians are listed in Table 3.1. Hydration of rhyolitic glasses was implemented at 0.5 GPa by re-melting glass powders with added H_2O at University of Hannover, Germany. The obsidian glass powder and water were sealed in Au-Pd capsules. The capsules were placed in an internally heated pressure vessel (IHPV), and heated to 1473 K at 0.5 GPa for overnight. Sample assemblages were under H_2O-undersaturated running conditions during heating so that the loaded water was completely dissolved in the melts. Samples were then quenched isobarically. The hydrated glasses were crystal-free and bubble-free.

The equilibrium experiments were performed in a piston cylinder apparatus at the University of Michigan. Glass fragments were prepared into cylinders with diameters of about 2 mm and heights of about 2 mm. Then a glass cylinder was placed into a graphite capsule, which was enclosed in crushable MgO as the inner pressure medium, with graphite heater outside and then $BaCO_3$ cell as outer pressure medium. The lid of the graphite capsule was thin (about 0.5 mm thickness) to minimize the distance between the

Table 3.1 Chemical compositions (oxide wt%) of KS and GMR rhyolite on an anhydrous basis

	KS	GMR
SiO_2	75.94	73.22
TiO_2	0.09	0.31
Al_2O_3	12.98	14.08
FeO	0.98	1.45
MnO	0.05	0.05
MgO	0.03	0.26
CaO	0.56	1.31
Na_2O	4.01	4.06
K_2O	4.71	4.32
P_2O_5	0.29	0.07
H_2O_t	0.76-0.90	1.89-2.23 in GMR+2 3.38-4.17 in GMR+4
Total	99.63	99.13

Glass analyses were carried out with a CAMECA 5X-100 electron microprobe using a defocused beam (10 μm) with 1 nA current at the University of Michigan. The oxide wt% on an anhydrous basis is calculated by dividing the electron microprobe measured oxide concentration by 1-*C* where *C* is weight percent of H_2O_t obtained by infrared spectroscopy.

thermocouple tip and the sample. The glass cylinder was placed in the center of the graphite heater. The running temperature was measured with a type-S thermocouple (Pt90Rh10-Pt) or type-D thermocouple (Re3W97-Re25W75). The distance between thermocouple tip and the center of the sample was typically about 1.3 mm after experiments.

A "piston-out" procedure was used to bring the assemblage to the final pressure at 373 K or 473 K. The sample assemblage was relaxed at this temperature and at the desired experimental pressure for at least 2 hours to close the gaps in the sample assemblage. After relaxation of the sample assemblage under pressure, temperature was increased at a rate of 200 K per minute to the designated temperature. The sample stayed at the desired temperature for sufficient time to ensure equilibrium for the interconversion reaction between the two hydrous species in the sample but not too long enough for appreciable crystallization. No temperature overshoot occurred and temperature fluctuation was ≤ 2 K. The sample was quenched roughly isobarically by turning off the power and manually pumping to keep up the pressure. The cooling rate is estimated to be ~ 100 K/s (Zhang et al., 2000).

The thermal gradient in the piston cylinder was calibrated using water speciation in rhyolitic glass (Zhang et al., 1997a; Ihinger et al., 1999). Five experiments at 0.5 GPa were carried out to calibrate the temperature distribution along the central axis of the graphite heater. The temperature distribution along the distance from the center of the charge is shown in Fig. 3.1. The equation for the temperature correction is:

$$\Delta T \approx 2.21(T/600)x^2, \quad (2)$$

where x is the distance between the thermocouple tip and the center of the charge in mm,

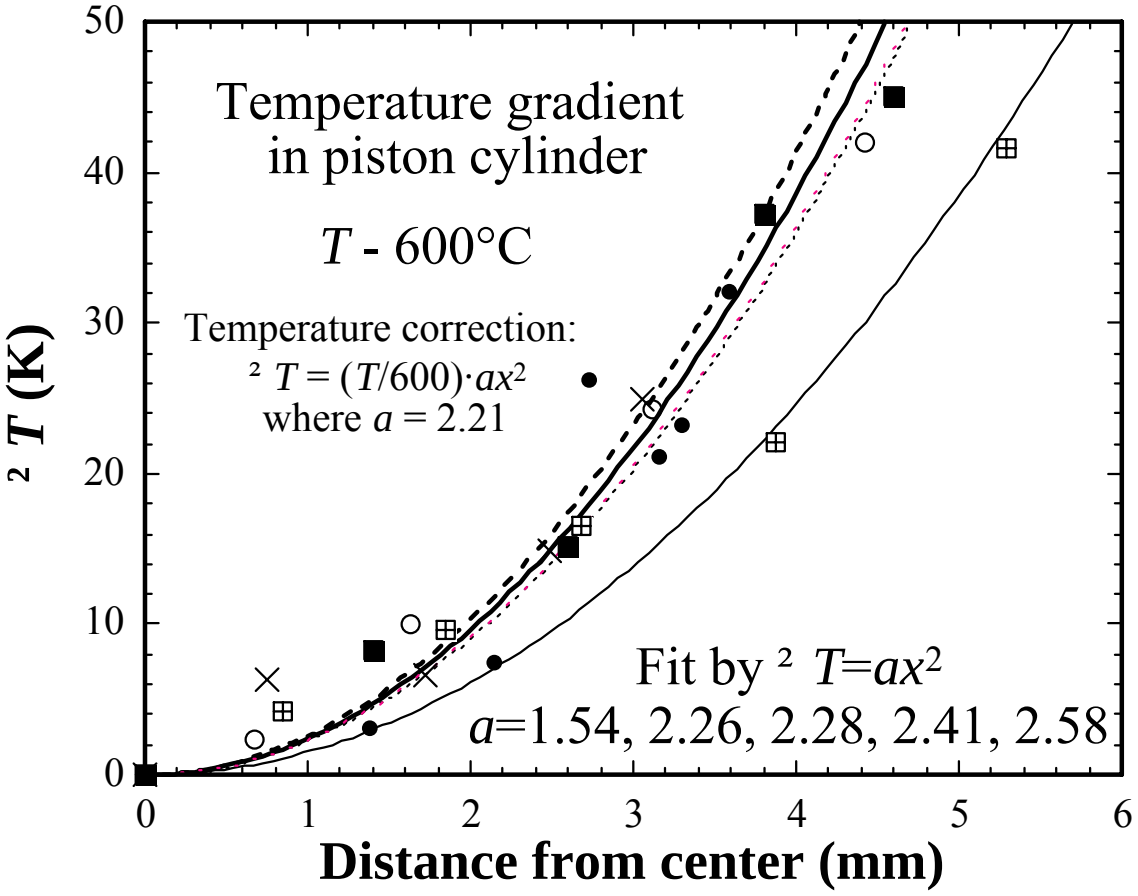

Fig. 3.1 Experimental results for temperature distribution in piston cylinder 2 at the University of Michigan laboratory, calibrated using hydrous species equilibrium in rhyolite based on the speciation model of Zhang et al. (1997a). Curves are best fittings of the different set of experimental data with different *a* values shown in the figure using Eqn. 2.

T is the temperature reading of the thermocouple in ˚C, ΔT is the temperature difference between the center and the thermocouple tip in ˚C, and the constant 2.21 is the average of 5 experiments. Therefore $T+\Delta T$ is the temperature at the center of sample. Depending on the IR measurement position on the glass chip, a correction of up to 6˚C was added to the nominal temperature recorded by the thermocouple. The pressure effect on emf of different thermocouples results only in a small effect on temperature at ≤ 3 GPa (Li et al., 2003) and is ignored. Overall, the temperature uncertainty (2σ) for the series of experiments in this study is estimated to be about 6 K.

Pressure calibration of the piston-cylinder apparatus (Piston-cylinder 2 in the laboratory) was conducted using two types of experiments: the melting point of gold (Akella and Kennedy, 1971) at ≤ 1.0 GPa, and the quartz-coesite transition (e.g., Boyd and England, 1960; Kitahara and Kennedy, 1964; Akella, 1979; Mirwald and Massonne, 1980; Bohlen and Boettcher, 1982; Bose and Ganguly, 1995) at 1073 K. In the calibration using gold melting temperature, a gold wire connected the two legs of a type-D thermocouple in a piston-cylinder. At a well-maintained nominal pressure, the assemblage was gradually heated until melting of the Au wire (at which the thermocouple signal was lost). The experiments show that the actual pressure is similar to the nominal pressure within several percent. Quartz-coesite reversal experiments at 1073 K were also carried out with a starting material of a mixture of quartz (50 wt%) and coesite (50 wt%) powder, moistened to accelerate the reaction and sealed in Au capsule. Here the experimental procedure of Bose and Ganguly (1995) was followed. The run product of each experiment consists of only one pure crystalline phase as verified by X-ray diffraction. The experimental results are listed in Table 3.2a. The calculated quartz-

coesite phase transition pressures at 1073 K from the literature are given in Table 3.2b. The literature data vary by 0.24 GPa reflecting difficulties in the experimental calibrations. Because these results do not completely agree with each other, the most recent experimental calibration (Bose and Ganguly, 1995) was adopted to correct the pressure in the piston cylinder apparatus by -6% (i.e., dividing the nominal pressure by 1.06). Some experiments were carried out using another piston cylinder, for which the correction is 5% based on another series of experiments to be reported in Ni and Zhang (2008).

In order to further extend the pressure range some speciation experiments at 4-6 GPa were carried out in a multi-anvil apparatus at the University of Michigan. However, except for one, these charges crystallized extensively. Because of the extreme difficulty in quenching liquid to glass, equilibrium speciation experiments were not continued at 4-6 GPa.

3. ANALYTICAL PROCEDURES

After quench, each charge was embedded in epoxy resin. Then, it was polished on both sides into a thin section along the cylindrical axis. The thickness of the layer polished away on each side of the charge was at least twice of the water diffusion distance estimated using the diffusivity of Zhang and Behrens (2000). All run products were analyzed for concentrations of H_2O_m and OH expressed in terms of H_2O using an FTIR Perkin-Elmer GX spectrometer at the University of Michigan. An aperture of 0.1 mm in diameter was used to delimit the infrared beam size. This aperture size allows acquisition of high-quality IR spectra and evaluation of sample heterogeneity. The

Table 3.2a Experimental results for pressure calibration using quartz-coesite transition at 1073 K

Nominal *P* (GPa)	*t* (h)	Result
28.96	72	quartz
29.65	70	quartz
30.34	70	quartz
31.03	66	quartz
31.37	70	coesite
31.72	67	coesite
33.78	66	coesite

Table 3.2b Literature data on quartz-coesite transition pressure at 1073 K

P (GPa)	Reference
28.46	Boyd & England (1960)
29.08	Kitahara & Kennedy (1964)
30.30	Akella (1979)
29.20	Akella (1979)
28.62	Mirwald & Massonne (1980)
27.92	Bohlen & Boettcher (1982)
29.35	Bose & Ganguly (1995)

intensities (peak heights) of the absorption bands at 5230 cm^{-1} (A_{523}) and 4520 cm^{-1} (A_{452}) were measured. The baseline was fit by flexicurve as shown in Zhang et al. (1997a).

Species (OH and H_2O_m) concentrations in terms of H_2O were obtained from IR band intensities according to Beer's law. Extensive effort has been made to calibrate the IR method on hydrous rhyolitic glasses (e.g., Newman et al., 1986; Zhang et al., 1997a; Withers and Behrens, 1999). The calibrations of Newman et al. (1986) and Withers and Behrens (1999) assumed constant molar absorptivities, whereas Zhang et al. (1997a) considered the variability of the molar absorptivities. With the calibration of Zhang et al. (1997a), the H_2O_t content is highly reproducible for the same sample but with different cooling rates, but less so with other calibrations. Furthermore, the calibration of Zhang et al. (1997a) results in concentration-independent equilibrium constants of reaction (1) at $H_2O_t \leq 2.7$ wt%. However, the calibration of Zhang et al. (1997a) becomes increasingly less accurate as H_2O_t increases, with error of 0.17 wt % at 3.8 wt%, 0.39 wt% at 5.6 wt%, and 1.1 wt% at 7.7 wt% (Zhang and Behrens, 2000). Because H_2O_t in this work is less than 4.2 wt%, and for consistency with the low-pressure speciation data of Ihinger et al. (1999), the molar absorptivities of Zhang et al. (1997a) were adopted. If a different calibration is used, there would be significant and systematic differences in species concentrations and *K*. Nonetheless, the trends of how *K* depends on temperature and pressure stay the same. Furthermore, as long as self-consistency is maintained, the equilibrium temperature (or the apparent equilibrium temperature) can be retrieved from species concentrations accurately.

Whether or not equilibrium is reached for reaction (1) in a particular experiment, the parameter

$$Q \equiv \frac{(X_{\mathrm{OH}}^{\mathrm{glass}})^2}{X_{\mathrm{H_2O_m}}^{\mathrm{glass}} X_{\mathrm{O}}^{\mathrm{glass}}}$$

is used to monitor the change of proportions of OH and H_2O_m in a sample, where X_i^{glass} is the measured mole fraction of species *i* in the quenched glass on a single oxygen basis (Stolper, 1982a, b), and O denotes an anhydrous oxygen. When the reaction duration is long enough for the interconversion of these two hydrous species in the melt to reach equilibrium, and furthermore if this equilibrium state is retained in the quench process, *Q* will be equal to the equilibrium constant *K*.

4. RESULTS AND DISCUSSION

4.1. SPECIES CONCENTRATIONS AND EQUILIBRIUM CONSTANTS

The concentrations of H_2O_m and OH in all quenched glasses calculated using the calibration of Zhang et al. (1997a) are listed in Table 3.3. The actual IR absorbance data are also reported because there may be further improvement in the IR calibration. The equilibrium constants are listed in Table 3.3 and plotted as a function of 1000/*T* in Fig. 3.2.

The uncertainty in each IR band intensity is about 1% relative, leading to an error of 0.022 in ln*K*, not accounting for systematic uncertainty of the calibration. The uncertainty in thickness measurement is about 2 μm, which results in a negligible increase in the overall uncertainty of ln*K*. For high-pressure data, there are additional

Table 3.3 The equilibrium speciation of water in rhyolitic melts under various pressures.

Measurement[#]	$T^{\$}$	$P^{\$}$	Time	Abs.	Abs.	Thickness	H_2O_t	H_2O_m	OH	$X(H_2O_t)$	$X(H_2O_m)$	X(OH)	$1000/T$	ln$K$
	K	GPa	s	5200	4500	mm	wt%	wt%	wt%				K^{-1}	
KS-1-2.1	927	0.94	600	0.0270	0.1034	0.717	0.844	0.160	0.684	0.0151	0.0029	0.0245	1.07873	-1.538
KS-1-2.2	926	0.94	600	0.0278	0.1028	0.713	0.849	0.166	0.683	0.0152	0.0030	0.0245	1.08043	-1.573
KS-1-2.3	926	0.94	600	0.0255	0.0998	0.708	0.819	0.153	0.666	0.0147	0.0027	0.0239	1.07938	-1.545
KS-1-3.1	879	0.94	14400	0.0593	0.1999	1.415	0.845	0.178	0.666	0.0151	0.0032	0.0239	1.13736	-1.695
KS-1-3.2	877	0.94	14400	0.0589	0.1989	1.407	0.845	0.178	0.667	0.0151	0.0032	0.0239	1.14041	-1.693
KS-1-3.3	878	0.94	14400	0.0627	0.2065	1.431	0.869	0.186	0.683	0.0156	0.0033	0.0245	1.13925	-1.691
KS-1-4.1	819	0.94	187200	0.0676	0.1833	1.321	0.868	0.218	0.650	0.0155	0.0039	0.0233	1.22117	-1.945
KS-1-4.2	817	0.94	187200	0.0673	0.1805	1.311	0.863	0.218	0.644	0.0155	0.0039	0.0231	1.22410	-1.966
KS-1-4.3	818	0.94	187200	0.0694	0.1857	1.326	0.880	0.223	0.657	0.0158	0.0040	0.0235	1.22228	-1.946
GMR+2-1-1.1	828	0.94	600	0.1862	0.2472	1.038	1.964	0.772	1.192	0.0349	0.0137	0.0423	1.20769	-1.977
GMR+2-1-1.2	827	0.94	600	0.1892	0.2480	1.041	1.974	0.782	1.192	0.0350	0.0139	0.0423	1.20907	-1.991
GMR+2-1-1.3	826	0.94	600	0.1808	0.2449	1.033	1.940	0.753	1.187	0.0344	0.0134	0.0422	1.21022	-1.960
GMR+2-1-2.1	777	0.94	600	0.2150	0.2467	1.063	2.014	0.870	1.144	0.0357	0.0154	0.0406	1.28775	-2.180
GMR+2-1-2.2	778	0.94	600	0.2114	0.2467	1.059	2.010	0.859	1.151	0.0357	0.0152	0.0408	1.28497	-2.155
GMR+2-1-2.3	778	0.94	600	0.2099	0.2451	1.058	1.997	0.854	1.143	0.0354	0.0152	0.0406	1.28515	-2.163
GMR+2-1-3.1	725	0.94	183600	0.1824	0.1848	0.885	1.886	0.886	1.000	0.0335	0.0157	0.0355	1.37978	-2.469
GMR+2-1-3.2	727	0.94	183600	0.1841	0.1873	0.888	1.904	0.891	1.012	0.0338	0.0158	0.0360	1.37634	-2.452
GMR+2-1-3.3	726	0.94	183600	0.1868	0.1892	0.888	1.929	0.905	1.024	0.0343	0.0161	0.0364	1.37800	-2.443
GMR+2-1-R1.1*	776	0.94	720	0.1756	0.1913	0.782	2.180	0.968	1.212	0.0386	0.0172	0.0430	1.28916	-2.166
GMR+2-1-R1.2*	775	0.94	720	0.1742	0.1870	0.773	2.167	0.972	1.195	0.0384	0.0172	0.0424	1.29036	-2.199
GMR+2-1-R1.3*	776	0.94	720	0.1746	0.1903	0.789	2.146	0.954	1.193	0.0381	0.0169	0.0423	1.28916	-2.186
GMR+4-1-2.1	726	0.94	10800	0.1375	0.0780	0.243	4.010	2.485	1.525	0.0701	0.0434	0.0533	1.37751	-2.626
GMR+4-1-2.2	725	0.94	10800	0.1396	0.0807	0.256	3.893	2.392	1.501	0.0681	0.0418	0.0525	1.37846	-2.621
GMR+4-1-2.3	725	0.94	10800	0.1315	0.0745	0.236	3.944	2.447	1.497	0.0689	0.0428	0.0523	1.37928	-2.648
GMR+4-1-3.1	676	0.94	46800	0.2577	0.1364	0.490	3.575	2.300	1.276	0.0627	0.0403	0.0447	1.47921	-2.914
GMR+4-1-3.2	675	0.94	46800	0.2586	0.1344	0.482	3.621	2.348	1.273	0.0635	0.0411	0.0446	1.48152	-2.938
GMR+4-1-3.3	676	0.94	46800	0.2581	0.1368	0.499	3.515	2.261	1.255	0.0617	0.0397	0.0440	1.47982	-2.931
GMR+4-1-4.1	626	0.94	261360	0.3017	0.1423	0.573	3.394	2.298	1.096	0.0596	0.0404	0.0385	1.59840	-3.224
GMR+4-1-4.2	624	0.94	261360	0.3013	0.1414	0.574	3.375	2.291	1.084	0.0593	0.0402	0.0381	1.60157	-3.242

GMR+4-1-4.3	625	0.94	261360	0.3012	0.1408	0.568	3.406	2.315	1.091	0.0598	0.0406	0.0383	1.59905	-3.240
KS-2-1.1	926	1.89	600	0.0476	0.1838	1.209	0.894	0.168	0.727	0.0160	0.0030	0.0260	1.07938	-1.459
KS-2-1.2	926	1.89	600	0.0475	0.1828	1.208	0.891	0.167	0.723	0.0159	0.0030	0.0259	1.08049	-1.469
KS-2-1.3	926	1.89	600	0.0463	0.1806	1.203	0.880	0.164	0.716	0.0158	0.0029	0.0257	1.07968	-1.466
KS-2-2.1	877	1.89	14400	0.0699	0.2340	1.561	0.904	0.191	0.713	0.0162	0.0034	0.0255	1.14018	-1.625
KS-2-2.2	876	1.89	14400	0.0653	0.2264	1.562	0.864	0.178	0.687	0.0155	0.0032	0.0246	1.14156	-1.633
KS-2-2.3	876	1.89	14400	0.0649	0.2264	1.560	0.865	0.177	0.688	0.0155	0.0032	0.0246	1.14176	-1.625
KS-2-4.1	960	1.89	600	0.0419	0.1795	1.189	0.872	0.150	0.722	0.0156	0.0027	0.0259	1.04195	-1.360
KS-2-4.2	959	1.89	600	0.0419	0.1795	1.196	0.866	0.149	0.717	0.0155	0.0027	0.0257	1.04320	-1.368
KS-2-4.3	962	1.89	600	0.0415	0.1795	1.198	0.863	0.147	0.716	0.0155	0.0026	0.0256	1.03982	-1.362
GMR+2-2-1.1	825	1.89	7200	0.1032	0.1397	0.538	2.153	0.827	1.325	0.0382	0.0147	0.0470	1.21199	-1.829
GMR+2-2-1.2	826	1.89	7200	0.0992	0.1378	0.536	2.109	0.797	1.312	0.0374	0.0141	0.0465	1.21006	-1.814
GMR+2-2-1.3	825	1.89	7200	0.0962	0.1329	0.524	2.080	0.790	1.289	0.0369	0.0140	0.0457	1.21179	-1.841
GMR+2-2-2.1	777	1.89	86400	0.1633	0.2049	0.850	2.032	0.827	1.205	0.0361	0.0147	0.0428	1.28756	-2.023
GMR+2-2-2.2	776	1.89	86400	0.1618	0.2020	0.852	1.998	0.817	1.181	0.0355	0.0145	0.0419	1.28904	-2.053
GMR+2-2-2.3	776	1.89	86400	0.1607	0.2027	0.852	1.998	0.812	1.187	0.0355	0.0144	0.0421	1.28904	-2.036
GMR+2-2-4.1	856	1.89	600	0.1450	0.2017	0.757	2.196	0.826	1.370	0.0389	0.0146	0.0486	1.16794	-1.760
GMR+2-2-4.2	856	1.89	600	0.1461	0.2051	0.759	2.225	0.830	1.395	0.0394	0.0147	0.0494	1.16807	-1.729
GMR+2-2-4.3	855	1.89	600	0.1468	0.2042	0.759	2.221	0.834	1.387	0.0394	0.0148	0.0491	1.16954	-1.746
GMR+4-2-1.1	757	1.89	1260	0.2299	0.1444	0.414	4.165	2.444	1.721	0.0727	0.0426	0.0601	1.32182	-2.361
GMR+4-2-1.2	756	1.89	1260	0.2228	0.1393	0.403	4.132	2.432	1.701	0.0721	0.0424	0.0594	1.32305	-2.381
GMR+4-2-1.3	756	1.89	1260	0.2359	0.1500	0.432	4.117	2.401	1.716	0.0719	0.0419	0.0599	1.32297	-2.351
GMR+4-2-2.1	726	1.89	14400	0.2950	0.1847	0.575	3.809	2.249	1.560	0.0667	0.0394	0.0546	1.37766	-2.482
GMR+4-2-2.2	725	1.89	14400	0.2949	0.1838	0.574	3.804	2.253	1.552	0.0666	0.0394	0.0543	1.37956	-2.494
GMR+4-2-2.3	726	1.89	14400	0.2918	0.1833	0.578	3.749	2.212	1.537	0.0656	0.0387	0.0538	1.37788	-2.496
GMR+4-2-3.1	676	1.89	172800	0.4221	0.2261	0.741	3.920	2.500	1.420	0.0685	0.0437	0.0496	1.48015	-2.778
GMR+4-2-3.2	675	1.89	172800	0.4178	0.2246	0.737	3.907	2.488	1.419	0.0683	0.0435	0.0496	1.48155	-2.773
GMR+4-2-3.3	675	1.89	172800	0.4296	0.2279	0.745	3.953	2.532	1.421	0.0691	0.0443	0.0497	1.48070	-2.788
KS-3-1.1	876	2.86	7200	0.0622	0.2310	1.566	0.870	0.169	0.701	0.0156	0.0030	0.0251	1.14211	-1.539
KS-3-1.2	875	2.86	7200	0.0614	0.2297	1.568	0.863	0.166	0.696	0.0154	0.0030	0.0249	1.14288	-1.540
KS-3-1.3	875	2.86	7200	0.0631	0.2318	1.564	0.877	0.172	0.705	0.0157	0.0031	0.0253	1.14248	-1.543
KS-3-R1.1*	877	2.83	14400	0.0349	0.1493	1.117	0.760	0.133	0.627	0.0136	0.0024	0.0225	1.14045	-1.524
KS-3-R1.2*	878	2.83	14400	0.0353	0.1499	1.121	0.762	0.134	0.628	0.0137	0.0024	0.0225	1.13841	-1.532

KS-3-R1.3*	877	2.83	14400	0.0357	0.1501	1.118	0.766	0.136	0.630	0.0137	0.0024	0.0226	1.14035	-1.536
KS-3-2.1	977	2.86	600	0.0352	0.1785	1.248	0.799	0.120	0.680	0.0143	0.0021	0.0244	1.02327	-1.259
KS-3-2.2	977	2.86	600	0.0355	0.1788	1.248	0.802	0.121	0.681	0.0144	0.0022	0.0244	1.02372	-1.264
KS-3-2.3	977	2.86	600	0.0355	0.1785	1.248	0.800	0.121	0.679	0.0143	0.0022	0.0244	1.02347	-1.269
KS-3-2.4	975	2.86	600	0.0348	0.1761	1.251	0.786	0.118	0.667	0.0141	0.0021	0.0239	1.02525	-1.283
KS-3-3.1	926	2.86	600	0.0435	0.1998	1.438	0.785	0.128	0.657	0.0141	0.0023	0.0235	1.08042	-1.399
KS-3-3.2	927	2.86	600	0.0431	0.1987	1.439	0.779	0.127	0.652	0.0140	0.0023	0.0234	1.07927	-1.404
KS-3-3.3	926	2.86	600	0.0435	0.2005	1.439	0.787	0.128	0.659	0.0141	0.0023	0.0236	1.07982	-1.391
KS-3-4.1	1027	2.86	96	0.0372	0.2101	1.489	0.776	0.106	0.670	0.0139	0.0019	0.0240	0.97390	-1.168
KS-3-4.2	1026	2.86	96	0.0376	0.2105	1.489	0.779	0.107	0.671	0.0140	0.0019	0.0241	0.97456	-1.174
KS-3-4.3	1026	2.86	96	0.0369	0.2093	1.489	0.772	0.105	0.667	0.0138	0.0019	0.0239	0.97456	-1.168
KS-3-4.4	1026	2.86	96	0.0365	0.2082	1.489	0.767	0.104	0.663	0.0138	0.0019	0.0238	0.97490	-1.170
GMR+2-3-1.1	876	2.83	600	0.1364	0.2250	0.837	2.102	0.702	1.400	0.0373	0.0124	0.0497	1.14103	-1.554
GMR+2-3-1.2	875	2.83	600	0.1377	0.2250	0.836	2.111	0.709	1.402	0.0374	0.0126	0.0497	1.14243	-1.563
GMR+2-3-1.3	876	2.83	600	0.1326	0.2220	0.831	2.078	0.687	1.391	0.0369	0.0122	0.0493	1.14191	-1.547
GMR+2-3-2.1	825	2.83	7200	0.1509	0.2250	0.845	2.145	0.769	1.376	0.0380	0.0136	0.0488	1.21184	-1.682
GMR+2-3-2.2	825	2.83	7200	0.2077	0.3063	1.159	2.134	0.772	1.362	0.0378	0.0137	0.0483	1.21149	-1.706
GMR+2-3-2.3	825	2.83	7200	0.2067	0.3075	1.162	2.131	0.766	1.365	0.0378	0.0136	0.0484	1.21149	-1.694
GMR+2-3-3.1	777	2.83	172800	0.2163	0.2836	1.081	2.202	0.863	1.339	0.0390	0.0153	0.0475	1.28707	-1.851
GMR+2-3-3.2	777	2.83	172800	0.2174	0.2826	1.082	2.197	0.866	1.331	0.0389	0.0153	0.0472	1.28745	-1.867
GMR+2-3-3.3	775	2.83	172800	0.2199	0.2841	1.080	2.220	0.878	1.342	0.0393	0.0156	0.0476	1.28972	-1.864
GMR+4-3-1.1	776	2.83	960	0.2616	0.2005	0.563	3.871	2.039	1.833	0.0677	0.0357	0.0641	1.28814	-2.055
GMR+4-3-1.2	775	2.83	960	0.2644	0.2014	0.564	3.894	2.057	1.837	0.0681	0.0360	0.0643	1.29041	-2.059
GMR+4-3-1.3	776	2.83	960	0.2598	0.1991	0.561	3.857	2.031	1.825	0.0675	0.0355	0.0639	1.28818	-2.060
GMR+4-3-3.1	726	2.83	21600	0.2769	0.1951	0.580	3.777	2.092	1.685	0.0661	0.0366	0.0590	1.37668	-2.253
GMR+4-3-3.2	726	2.83	21600	0.2748	0.1930	0.579	3.745	2.079	1.666	0.0656	0.0364	0.0583	1.37835	-2.271
GMR+4-3-3.3	726	2.83	21600	0.2763	0.1959	0.589	3.718	2.054	1.664	0.0651	0.0360	0.0583	1.37770	-2.261
GMR+4-3-4.1	676	2.83	259200	0.3326	0.1961	0.601	3.999	2.431	1.568	0.0699	0.0425	0.0548	1.47929	-2.547
GMR+4-3-4.2	675	2.83	259200	0.3337	0.1972	0.602	4.012	2.435	1.577	0.0701	0.0426	0.0551	1.48109	-2.538
GMR+4-3-4.3	675	2.83	259200	0.3297	0.1955	0.598	3.995	2.422	1.574	0.0698	0.0423	0.0550	1.48041	-2.536
KS-1b-1.1	973	0.0001	600	0.0191	0.0907	0.611	0.842	0.133	0.709	0.0151	0.0024	0.0254	1.02759	-1.276
KS-1b-1.2	973	0.0001	600	0.0194	0.0907	0.608	0.849	0.136	0.713	0.0152	0.0024	0.0256	1.02759	-1.287
KS-1b-1.3	973	0.0001	600	0.0190	0.0898	0.606	0.841	0.134	0.708	0.0151	0.0024	0.0253	1.02759	-1.286

KS-1b-2.1	923	0.0001	600	0.0214	0.0959	0.691	0.787	0.131	0.655	0.0141	0.0024	0.0235	1.08325	-1.425
KS-1b-2.2	923	0.0001	600	0.0206	0.0938	0.685	0.774	0.128	0.646	0.0139	0.0023	0.0231	1.08325	-1.430
KS-1b-2.3	923	0.0001	600	0.0219	0.0966	0.688	0.800	0.135	0.664	0.0143	0.0024	0.0238	1.08325	-1.427
KS-1b-R1.1*	923	0.0001	7200	0.0402	0.1796	1.292	0.789	0.132	0.657	0.0141	0.0024	0.0235	1.08325	-1.426
KS-1b-R1.2*	923	0.0001	7200	0.0400	0.1794	1.291	0.788	0.132	0.657	0.0141	0.0024	0.0235	1.08325	-1.423
KS-1b-R1.3*	923	0.0001	7200	0.0402	0.1797	1.292	0.789	0.132	0.657	0.0141	0.0024	0.0236	1.08325	-1.424
KS-1b-R2.1*	923	0.0001	2400	0.0685	0.2875	1.975	0.839	0.147	0.692	0.0150	0.0026	0.0248	1.08325	-1.430
KS-1b-R2.2*	923	0.0001	2400	0.0685	0.2870	1.976	0.838	0.147	0.690	0.0150	0.0026	0.0247	1.08325	-1.435
KS-1b-R2.3*	923	0.0001	2400	0.0675	0.2846	1.973	0.830	0.145	0.685	0.0149	0.0026	0.0245	1.08325	-1.438
KS-1b-3.1	873	0.0001	21600	0.0501	0.1763	1.231	0.851	0.173	0.678	0.0152	0.0031	0.0243	1.14528	-1.632
KS-1b-3.2	873	0.0001	21600	0.0501	0.1766	1.231	0.852	0.173	0.679	0.0153	0.0031	0.0243	1.14528	-1.628
KS-1b-3.3	873	0.0001	21600	0.0498	0.1757	1.230	0.848	0.172	0.676	0.0152	0.0031	0.0242	1.14528	-1.633

Note: $ *T* has been corrected using Eqn. (2). *P* has been corrected based on pressure calibration. .

Three or four points were measured by IR for each experimental sample; they are listed as xxx.1, .2, .3 or .4.

* These experiments are reversal runs (Fig. 3.3).

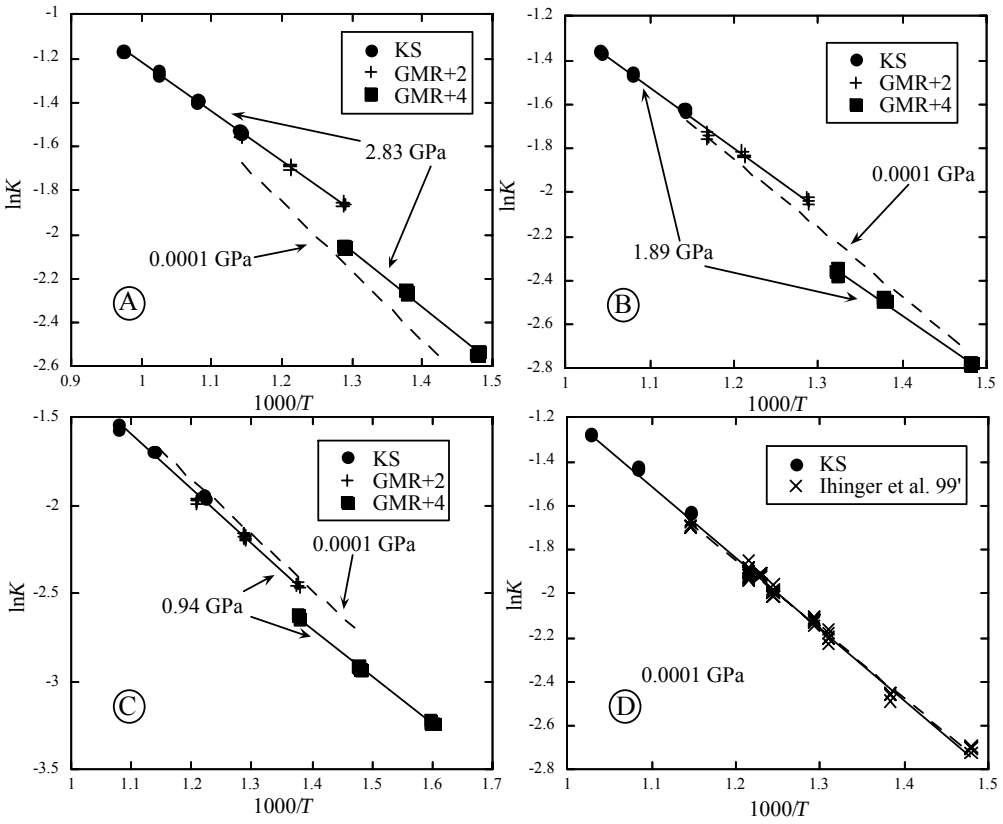

Fig. 3.2 The temperature dependence of ln$K$ at some pressures. Water concentrations for samples KS (0.76-0.90 wt%) and GMR+2 (1.89-2.23 wt%) are less than 2.7 wt% and speciation data on them overlap, indicating that K is independent of H_2O_t when water content is less than 2.7 wt%. The dashed reference line is the ideal mixing model for water content less than 2.7 wt% at ambient pressure from Ihinger et al. (1999). The solid lines are the best-fit linear regression results for the data, showing that ideal solution model (Eqn. 3) works well for < 2.7 wt% H_2O_t (KS and GMR+2), The regression for GMR+4 was separated from that for other compositions and is different.

errors in estimating the species concentrations such as density variation with pressure. Hence the uncertainty from the IR measurement in ln$K$ is estimated to be0.03.

4.2. ATTAINMENT AND RETENTION OF EQUILIBRIUM

In this section, the attainment of equilibrium at the experimental temperature and the retention during quench are examined. In either of the following two scenarios, the measured species concentrations would not reflect those at equilibrium, in other words, $Q \neq K$: (1) the duration for the reaction at the experimental temperature is not long enough for it to reach equilibrium (attainment of equilibrium), or (2) species concentrations in the melt are changed during isobarically quenching to room temperature (retention of equilibrium).

To demonstrate the attainment of equilibrium, reversal experiments have been carried out under two sets of conditions (a. GMR+2-1-R1, 776 K, 0.94 GPa, and 2.16 wt% H_2O_t; b. KS-3-R1, 877 K, 2.83 GPa, and 0.76 wt% H_2O_t; Table 3.3). One experiment in each reversal pair was first relaxed at a temperature above the reversal experimental temperature and one below to obtain different Q values. Hence, each set of the reversal experiments approached the same final value of Q from initially higher or lower Q values (Fig. 3.3). This final Q value is the equilibrium constant K. These experiments are informative for constraining the duration required for a sample to reach equilibrium at this set of conditions. Durations for all other experiments were estimated from these experiments and from kinetic experiments under ambient pressure (Zhang et al., 1995, 1997b, 2000); the actual experimental duration was longer than that estimated for reaching equilibrium at specific running condition.

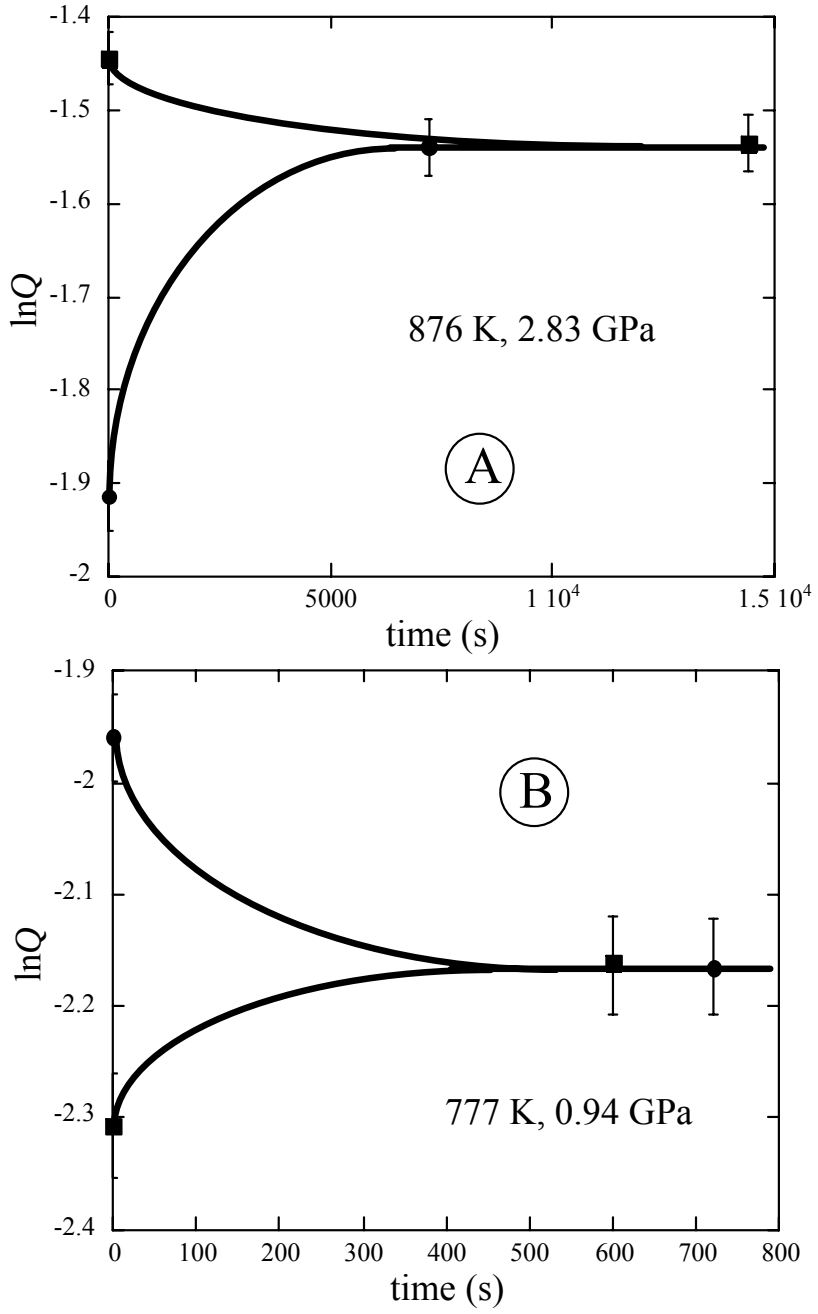

Fig. 3.3 Two sets of reversal experiments to examine the duration required to reach equilibrium. Solid curves are schematic illustrations of *Q* evolution in different experiments. (A), KS sample; (B), GMR+2 sample. The relaxation might be much faster than illustrated by the curves.

The issue of whether or not the equilibrium state can be retained during quench has received considerable attention during the last two decades (e.g., Dingwell and Webb, 1990; Zhang et al., 1991b, 1995; Ihinger et al., 1999; Withers et al., 1999; Zhang, 1999; Nowak and Behrens, 2001; Xu and Zhang, 2002; Behrens and Nowak, 2003). As reviewed in the Introduction, the different sides have worked together and resolved the debates: the consensus is that species concentrations can be retained by quench if the experimental temperature is not too high (such as ≤850 K, depending on H_2O_t, see Table 3.3), so that it is below the glass transition temperature for the given quench rate and pressure (Withers et al., 1999; Behrens and Nowak, 2003).

In summary, for attainment of equilibrium, the experimental temperature must be high enough (such as 673 K, depending on H_2O_t and pressure, see Table 3.3). For retention of equilibrium species concentrations through quench, the experimental temperature must be low enough. In other words, the experimental temperature must satisfy the conditions that for the time scale of the isothermal experiments, the sample is in the liquid state; whereas for the time scale of quenching, the sample is in the glass state. Hence there is a limited temperature window for a given H_2O_t and pressure, at which equilibrium speciation can be obtained from quench experiments.

4.3. EQUILIBRIUM CONSTANT AS A FUNCTION OF TEMPERATURE, H_2O_t AND PRESSURE

Equilibrium speciation data are listed in Table 3.3 and results are plotted in Fig. 3.2 as ln$K$ versus 1000/T. As shown in Figs. 3.2a, 3.2b and 3.2c, K is independent of water content when H_2O_t in the sample is less than 2.7 wt%, consistent with Zhang et al.

(1997a). Some new experimental data at ambient pressure are also reported here to extend the temperature coverage of Ihinger et al. (1999). Other speciation data have been obtained on rhyolitic or quasi-rhyolitic melts (e.g., Sowerby and Keppler, 1999; Nowak and Behrens, 2001; Behrens and Nowak, 2003), but they are based on different IR calibrations (different molar absorptivities) and cannot be directly compared with the new data. The new 1-bar data are consistent with those of Ihinger et al. (1999) as shown in Fig. 3.2d. A simple ideal solution model (Eqn. 3) can be used to describe speciation in the rhyolitic melts with low water content (up to 2.7 wt% H_2O) at any given pressure.

$$\ln K = A + \frac{1000}{T} B, \tag{3}$$

where A and B are fitting parameters independent of chemical composition. The fitting results are shown in Figs. 3.2 and 3.4a and fitting parameters at each pressure are listed in Table 3.4. The high-pressure experiments show an increase of ln$K$ with increasing pressure systematically. As shown in Fig. 3.4a, the effect of 1.89 GPa (from 0.94 to 2.83 GPa) on the equilibrium constant of the speciation reaction at 773 K is equivalent to that of 67 K (from 773 K to 840 K) on the equilibrium constant at 0.94 GPa. The enthalpy of reaction (1) at a given pressure can be inferred from the slopes of the best-fitting lines in Fig. 3.4a, i.e., from fitting parameter B. As shown in Fig. 3.4b, enthalpy of reaction (1) decreases nonlinearly with pressure from 27.02 kJ/mol under ambient pressure to 18.53 kJ/mol at 2.83 GPa (Fig. 3.4b).

Although K for reaction (1) does not depend on H_2O_t concentration for water content less than 2.7 wt%, at higher water content (here ~ 4 wt% H_2O_t) it depends on H_2O_t content. This result indicates either mixing between H_2O_m, OH and O in reaction

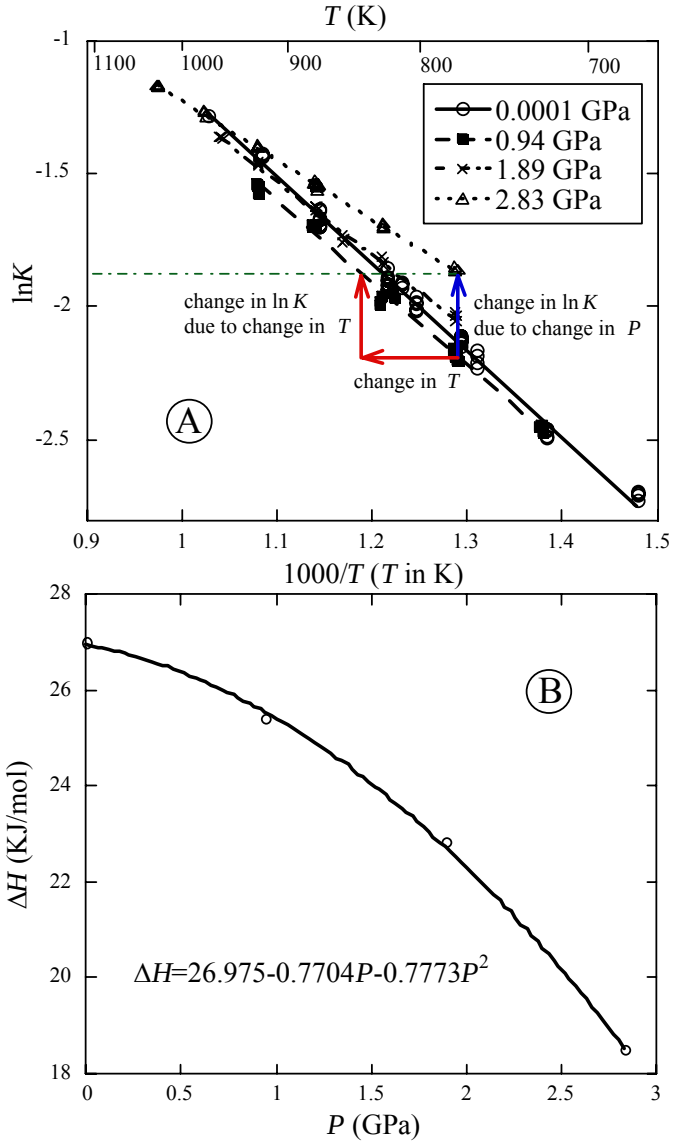

Fig. 3.4 (A) The dependence of K on temperature for samples with H_2O_t <2.7 wt% at various pressures. Data for 0.0001 GPa are from Ihinger et al. (1999) and this work. The curves are the best-fit linear regression results using Eqn. 3. The arrow lines indicate changes in ln$K$ and T respectively. (B) The pressure dependence of enthalpy of reaction (1) for samples with H_2O_t <2.7 wt%. The solid line is the best-fit regression result with equation shown in the figure.

(1) is non-ideal, or the already complicated calibration of Zhang et al. (1997a) to convert IR band intensities to species concentrations is imperfect (Ihinger et al., 1999).

In the absence of an unambiguous calibration of the molar absorptivities of two hydrous species in high-water-content samples, the simplest approximation beyond ideal mixing of H_2O_m, OH and O in hydrous silicate melt is a regular solution model. Silver and Stolper (1989) illustrated a way to extend the simple ideal mixing model to a regular solution model, adapted also by Silver et al. (1990), Zhang et al. (1991b), and Ihinger et al. (1999). The same formulation is adapted here:

$$\ln K = \ln\left(\frac{X_{\mathrm{OH}}^2}{X_{\mathrm{H_2O_m}} X_{\mathrm{O}}}\right) = A' + \frac{1000}{T}\left(B' + C' X_{\mathrm{H_2O_m}} + D' X_{\mathrm{OH}}\right), \tag{4}$$

where A', B', C' and D' are fitting parameters independent of H_2O_t and their physical meanings are shown in Silver and Stolper (1989). Values of these fitting parameters at each pressure are listed in Table 3.4. The maximum differences for these equations to reproduce experimental equilibrium temperature are also listed in Table 3.4 and they are within 10 K at high pressures.

Eqn. 4 could be expanded to accommodate the dependence of K on temperature, pressure and water content if the fitting parameters A, B, C and D in Eqn. 4 are assumed to be functions of pressure. As discussed above, the dependence on pressure is not linear. After some trials, the following formulation is found to fit all speciation data in rhyolitic melt well:

$$\begin{aligned}\ln K = \left(A_0' + A_{\mathrm{P}}' P\right) + \frac{1000}{T}\Bigg(& (B_0' + B_{\mathrm{P}}' P + B_{\mathrm{P}^{3/2}}' P^{\frac{3}{2}}) + \\ & (C_0' + C_{\mathrm{P}}' P + C_{\mathrm{P}^{3/2}}' P^{\frac{3}{2}}) X_{\mathrm{H_2O_m}} + (D_0' + D_{\mathrm{P}}' P + D_{\mathrm{P}^{3/2}}' P^{\frac{3}{2}}) X_{\mathrm{OH}}\Bigg),\end{aligned} \tag{5}$$

Table 3.4. Fitting parameters for Eqns. 3, 4 and 6.

	ln*K*							ln*K'*				
	ideal mixing[#]		regular solution model					regular solution model				
	A	*B*	*A*'	*B*'	*C*'	*D*'	ΔT (K)[$]	*A*''	*B*''	*C*''	*D*''	ΔT (K)[$]
0.0001 GPa *	2.0616	-3.2495	1.8120	-3.0830	-7.4203	3.0437	18.3	2.7524	-2.8404		-1.2945	18.9
0.94 GPa	1.7636	-3.0599	1.3264	-2.6529	-5.3362	0.1706	7.9	2.2910	-2.4292	0.1720	-1.7996	7.7
1.89 GPa	1.4995	-2.7503	1.0359	-2.3199	-7.1853	0.9728	7.3	1.8976	-2.0068		-1.6630	8.6
2.83 GPa	1.0053	-2.2285	0.7611	-2.0211	-7.5335	1.8349	9.0	1.6609	-1.7348		-1.5492	10.2

Note: # Water content is less than 2.2 wt%.

$ Maximum temperature difference between experimental temperature and model predicted temperature.

* New data reported here and literature data from Ihinger et al. (1999), which include some speciation data at $P \leq 100$ MPa.

where P is pressure in GPa, T is temperature in K and X is mole fraction of species H_2O_m or OH. This formulation could reproduce all experimental data with a 2σ uncertainty of 0.058 in ln$K$. The best-fit parameters in Eqn. 5 with 2σ errors are: $A'_0 = 1.8120 \pm 0.1044$, $A'_P = -0.3832 \pm 0.0418$, $B'_0 = -3.0830 \pm 0.0796$, $B'_P = 0.2999 \pm 0.0638$, $B'_{P^{3/2}} = 0.0507 \pm 0.0386$, $C'_0 = -7.4203 \pm 1.4953$, $C'_P = 5.0262 \pm 1.4040$, $C'_{P^{3/2}} = -3.1271 \pm 0.9076$, $D'_0 = 3.0437 \pm 1.3731$, $D'_P = -5.4527 \pm 1.9763$, $D'_{P^{3/2}} = 3.0464 \pm 1.2441$. The reproducibility of experimental equilibrium temperature by Eqn. 5 is shown in a histogram (Fig. 3.5), which is approximately a Gaussian distribution. Fig. 3.6 further shows how well K at some water contents can be reproduced.

4.4. RELATING ABSORBANCES DIRECTLY TO TEMPERATURE AND PRESSURE

Estimating the apparent equilibrium temperature of hydrous rhyolite of a given cooling rate for inferring viscosity is one of the most important applications of this work (Zhang et al., 2003; Zhang and Xu, 2007). Owing to possible future improvement of molar absorptivities of two hydrous species, it is useful to recast speciation data directly in terms of IR band intensities (Ihinger et al., 1999; Liu et al., 2004a), so that equilibrium temperature or the apparent equilibrium temperature can be directly estimated from infrared data. Following Zhang et al. (2000), K' is defined below:

$$K' = \left(\overline{A}_{452}\right)^2 \Big/ \overline{A}_{523} .$$

where $\overline{A}$ is absorbance per mm sample thickness. By analogy with the regular solution model (Eqn. 4), the following equation is used to relate K' and $\overline{A}$,

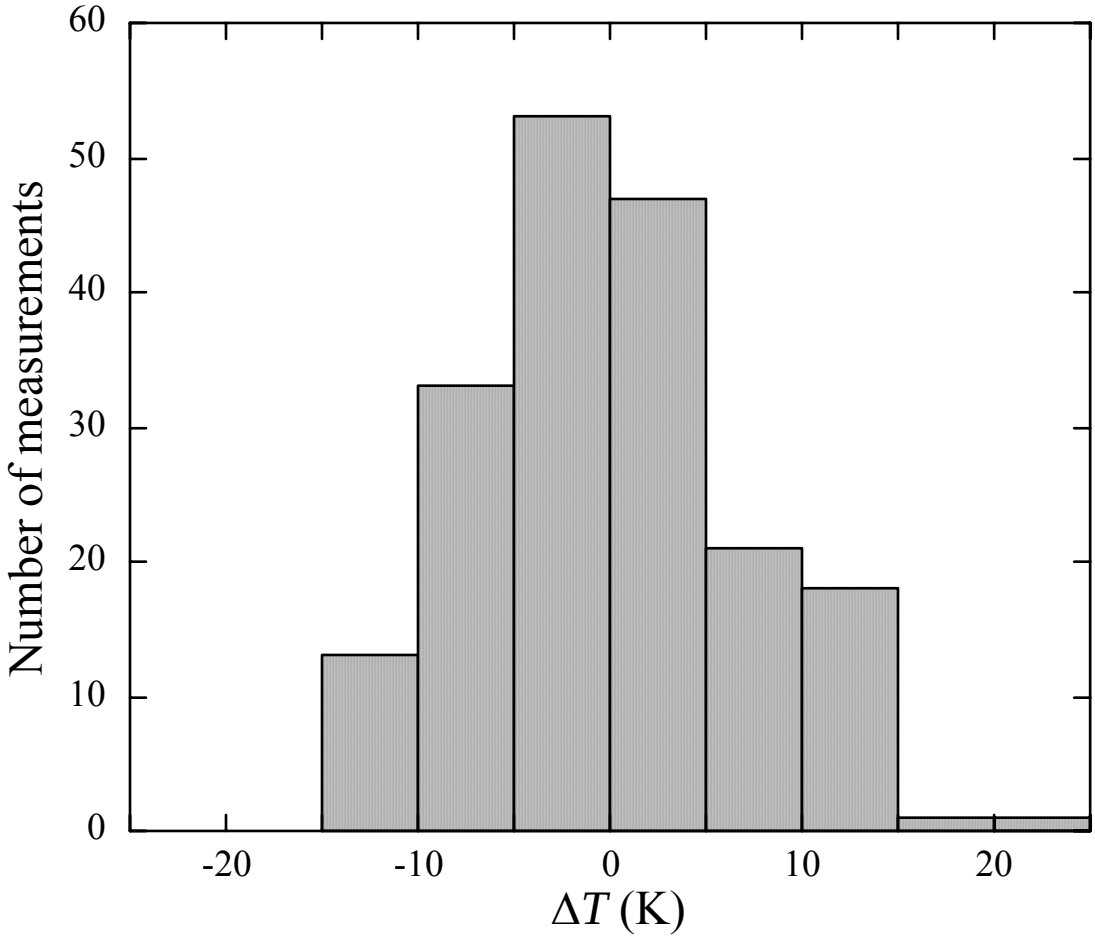

Fig. 3.5 Histogram showing the distribution of differences between the experimental equilibrium temperature and predicted temperature by Eqn. 5. Sources of data include Ihinger et al. (1999) and this work.

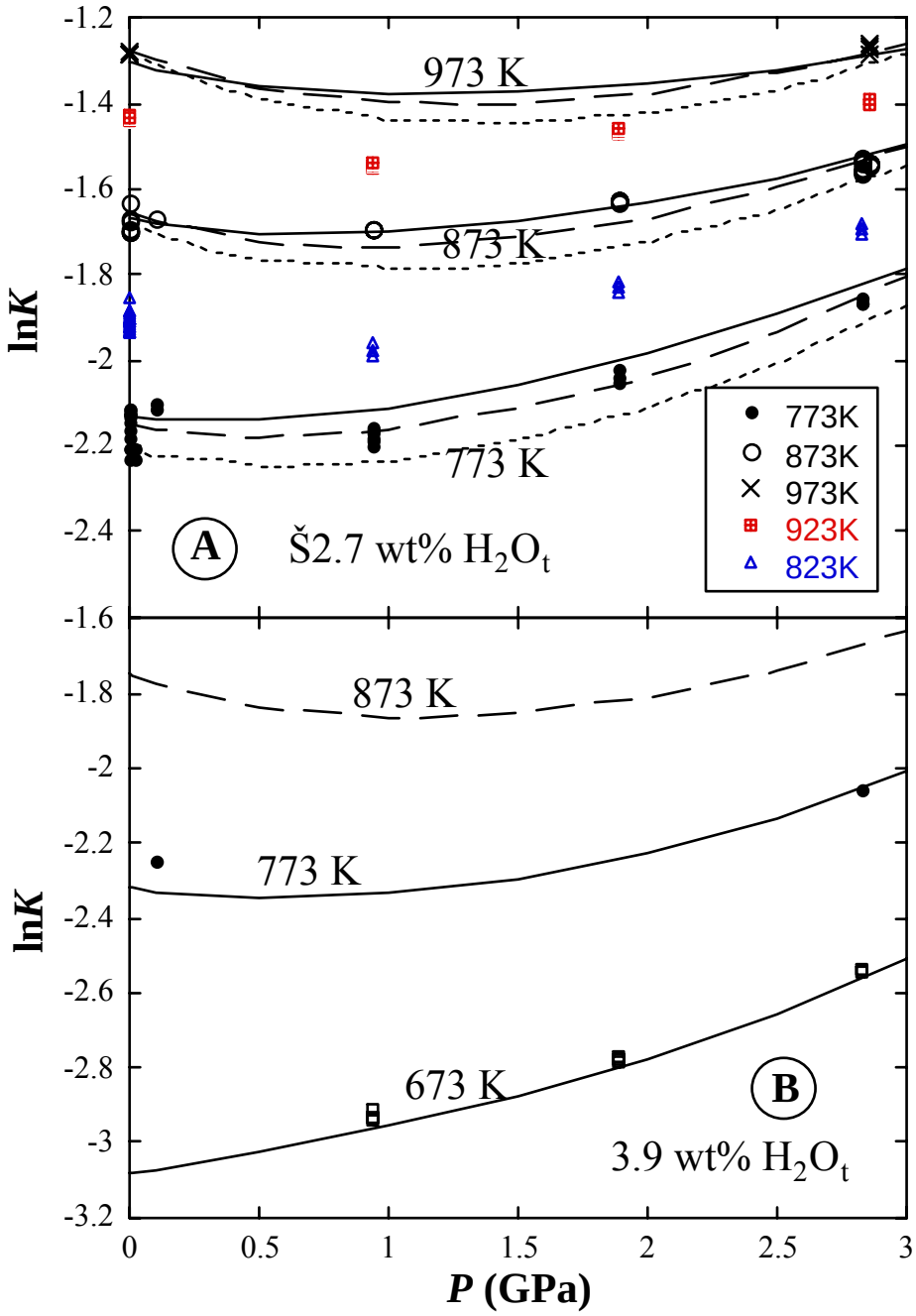

Fig. 3.6 Pressure effect on ln$K$ at some temperatures and water concentrations. The curves are calculated from Eqn. 5. Points are experimental data. In (A), three curves are calculated at each temperature for H_2O_t of 0.7, 1.7 and 2.7 wt% from top to bottom at each temperature. In (B), the dashed curve means temperature is above the experimental temperature.

$$\ln K' = \ln \frac{\left(\overline{A}_{452}\right)^2}{\overline{A}_{523}} = A'' + \frac{1000}{T}\left(B'' + C''\overline{A}_{523} + D''\overline{A}_{452}\right). \quad (6)$$

The best-fit parameters for four different pressures are listed in Table 3.4. The differences between experimental and predicted temperatures using Eqn. 6 are also listed in Table 3.4, which are not much different from the regular solution model using species concentrations (Eqn. 4). A model was developed to directly relate K', $\overline{A}$, T and P, analogous to Eqn. 5, as follows:

$$\ln K = \left(A_0'' + A_P'' P\right) + \frac{1000}{T}\left((B_0'' + B_P'' P + B_{P^{3/2}}'' P^{\frac{3}{2}}) + (C_0'' + C_P'' P + C_{P^{3/2}}'' P^{\frac{3}{2}})\overline{A}_{523} + (D_0'' + D_P'' P + D_{P^{3/2}}'' P^{\frac{3}{2}})\overline{A}_{452} \right), \quad (7)$$

where P is pressure in GPa, T is temperature in K and $\overline{A}$ is absorbance per mm sample thickness for species H_2O_m or OH. This formulation reproduces all of the data with a 2σ uncertainty of 0.059 in lnK'. The best-fit parameters in Eqn. 7 with 2σ errors are: A''_0 = 2.7524 ± 0.0944, A''_P = -0.3890 ± 0.0395, B''_0 = -2.8404 ± 0.0809, B''_P = 0.3053 ± 0.0697, $B''_{P^{3/2}}$ = 0.0531 ± 0.0433, C''_P = 0.3768 ± 0.1301, $C''_{P^{3/2}}$ = -0.2261 ± 0.0836, D''_0 = -1.2945 ± 0.0893, D''_P = -0.9499 ± 0.4076, $D''_{P^{3/2}}$ = 0.5121 ± 0.2573. Because Eqn. 7 is independent of molar absorptivity, future improvement in molar absorptivities of these bands will not affect the reproducibility of Eqn. 7. It can reproduce experimental temperature with a 2σ uncertainty of 13 K (similar to the reproducibility of Eqn. 5 shown in Fig. 3.5) directly from measured absorbances.

4.5. APPLICATIONS

Speciation plays an important role in H_2O solubility (e.g., Silver et al., 1990; Blank et al., 1993; Zhang, 1999), as well as diffusion (e.g., Zhang et al., 1991a,b; Zhang and Behrens, 2000; Liu et al., 2004b; Zhang et al., 2007) and crystal nucleation (e.g., Davis et al., 1997). Several models (Eqns. 3-5) are provided to determine H_2O_m and OH concentrations as functions of pressure, temperature and H_2O_t in rhyolitic melts. Hence the new results can be applied to model H_2O diffusion, quantify the dependence of molecular H_2O diffusivity on pressure, and quantitatively understand the effect of dissolved H_2O_t on the nucleation and crystal growth in hydrous melts under high pressure. Furthermore, information from this work may be useful in future models of thermodynamic properties of hydrous silicate melts.

Another application of the new results is to predict apparent equilibrium temperature, T_{ae} (Zhang, 1994). As discussed by Zhang (1994), T_{ae} is one of the well-defined parameters in measurements for any given cooling history and can be a good indicator of cooling rate. Because of negligible dependence of K on pressure when the pressure is < 1 GPa, and because natural rhyolitic glasses general cool at nearly surface pressures, for naturally cooled hydrous rhyolitic glasses, the equation at ambient pressure (e.g., Eqn. 7 in Ihinger et al., 1999) is applicable to calculate apparent equilibrium temperature. For experimental glasses cooled at high pressures such as 2 GPa, the pressure effect must be considered. Knowledge of T_{ae} is critical to inferring viscosity based on kinetic experiments of the hydrous species reaction (Zhang et al., 2003; Zhang and Xu, 2007), since it is assumed that the viscosity at the apparent equilibrium temperature is inversely proportional to the cooling rate (Dingwell and Webb, 1990,

Zhang et al., 2003). Hence, by conducting a controlled cooling rate experiment of a hydrous rhyolitic melt under pressure, after calculating T_{ae}, the viscosity at this temperature (and pressure) can be estimated. At present, this is the only method to estimate viscosity at $P > 1$ GPa in the viscosity range of 10^9-10^{14} Pa·s. The application for inferring viscosity is the main motivation for us to conduct this research. Results from this work are applied to infer viscosity at high pressure in Chapter IV.

5. CONCLUSIONS

The equilibrium of the interconversion reaction between two dissolved water species (H_2O_m and OH) was experimentally investigated as a function of pressure (0.0001, 0.94, 1.89 and 2.83 GPa), temperature (624-1027 K), and H_2O concentrations (0.8% to 4.2 wt%). The speciation data at total H_2O content ≤ 2.7% can be described by an ideal mixing model, consistent with previous results. With inclusion of speciation data at higher water contents, one way to describe the speciation data is a regular solution model. The general speciation model (Eqn. 5) constructed to accommodate the dependence of H_2O speciation in the rhyolitic melts on *T*-*P*-*X* can be used to predict species concentrations at P ≤ 2.83 GPa, total H_2O content ≤ 4.2 wt%, and temperature of 624-1027 K. Furthermore, it can be used to calculate apparent equilibrium temperature, which can then be used to infer viscosity of hydrous rhyolitic melts under high pressure.

REFERENCES

Akella J. (1979) Quartz ⇔ coesite transition and the comparative friction measurements in piston-cylinder apparatus using talc-alsimag-glass (TAG) and NaCl high-pressure cells. *N. Jb. Miner. Mh.* **H.5**, 217-224.

Akella J. and Kennedy G.C. (1971) Melting of gold, silver, and copper – proposal for a new high-pressure calibration scale. *J. Geophys. Res.* **76**, 4969-4977.

Behrens H. and Nowak M. (2003) Quantification of H_2O speciation in silicate glasses and melts by IR spectroscopy – *in situ* versus quench techniques. *Phase Trans.* **76**, 45-61.

Behrens H. and Zhang Y. (2001) Ar diffusion in hydrous silicic melts: implications for volatile diffusion mechanisms and fractionation. *Earth Planet. Sci. Lett.* **192**, 363-376.

Behrens H., Zhang Y., Leschik M., Wiedenbeck M., Heide G., and Frischat G.H. (2007) Molecular H_2O as carrier for oxygen diffusion in hydrous silicate melts. *Earth Planet. Sci. Lett.* **254**, 69-76.

Blank J.G., Stolper E.M., and Carroll M.R. (1993) Solubilities of carbon dioxide and water in rhyolitic melt at 850 ºC and 750 bars. *Earth Planet. Sci. Lett.* **119**, 27-36.

Bohlen S.R. and Boettcher A.L. (1982) The quartz ⇔ coesite transformation: a precise determination and the effects of other components. *J. Geophys. Res.* **87**, 7073-7078.

Bose K. and Ganguly J. (1995) Quartz-coesite transition revisited: reversed experimental determination at 500-1200 ˚C and retrieved thermochemical properties. *Am. Mineral.* **80**, 231-238.

Boyd F.R. and England J.L. (1960) The quartz-coesite transition. *J. Geophys. Res.* **65**, 749-756.

Burnham C.W. (1975) Water and magmas: a mixing model. *Geochim. Cosmochim. Acta* **39**, 1077-1084.

Davis M.J., Ihinger P.D., and Lasaga A.C. (1997) The influence of water on nucleation kinetics in silicate melt. *J. Non-Cryst. Solids* **219**, 62-69.

Dingwell D.B. and Webb S.L. (1990) Relaxation in silicate melts. *Eur. J. Mineral.* **2**, 427-449.

Goranson R.W. (1938) Silicate-water systems: phase equilibria in the $NaAlSi_3O_8$-H_2O and $KAlSi_3O_8$-H_2O systems at high temperatures and pressures. *Am. J. Sci.* **35-A**, 71-91.

Hui H. and Zhang Y. (2007) Toward a general viscosity equation for natural anhydrous and hydrous silicate melts. *Geochim. Cosmochim. Acta* **71**, 403-416.

Ihinger P.D., Zhang Y., and Stolper E.M. (1999) The speciation of dissolved water in rhyolitic melt. *Geochim. Cosmochim. Acta* **63**, 3567-3578.

Kitahara S. and Kennedy G.C. (1964) The quartz-coesite transition. *J. Geophys. Res.* **69**, 5395-5400.

Li J., Hadidiacos C., Mao H., Fei Y., and Hemley R.J. (2003) Behavior of thermocouples under high pressure in a multi-anvil apparatus. *High Pressure Res.* **23**, 389-401.

Liu Y., Behrens H., and Zhang Y. (2004a) The speciation of dissolved H_2O in dacitic melt. *Am. Mineral.* **89**, 277-284.

Liu Y., Zhang Y., and Behrens H. (2004b) H_2O diffusion in dacitic melts. *Chem. Geol.* **209**, 327-340.

McMillan P.F. (1994) Water solubility and speciation models. *Rev. Mineral.* **30**, 131-156.

Mirwald P.W. and Massonne H.-J. (1980) The low-high quartz and quartz-coesite transition to 40 kbar between 600˚ and 1600˚C and some reconnaissance data on the effect of $NaAlO_2$ compoenent on the low quartz-coesite transition. *J. Geophys. Res.* **85**, 6983-6990.

Newman S., Stolper E.M., and Epstein S. (1986) Measurement of water in rhyolitic glasses: calibration of an infrared spectroscopic technique. *Am. Mineral.* **71**, 1527-1541.

Ni H. and Zhang Y. (2008) H_2O diffusion models in rhyolitic melt with new high pressure data. *Chem. Geol.* Revised.

Nowak M. and Behrens H. (2001) Water in rhyolitic magmas: getting a grip on a slippery problem. *Earth Planet. Sci. Lett.* **184**, 515-522.

Shaw H.R. (1964) Theoretical solubility of H_2O in silicate melts: quasi-crystalline models. *J. Geol.* **72**, 601-617.

Shaw H.R. (1972) Viscosities of magmatic silicate liquids: an empirical method of prediction. *Am. J. Sci.* **272**, 870-893.

Silver L.A. and Stolper E. (1989) Water in albitic glasses. *J. Petrol.* **30**, 667-709.

Silver L.A., Ihinger P.D., and Stolper E. (1990) The influence of bulk composition on the speciation of water in silicate glasses. *Contrib. Mineral. Petrol.* **104**, 142-162.

Sowerby J.R. and Keppler H. (1999) Water speciation in rhyolitic melt determined by in situ infrared spectroscopy. *Am. Mineral.* **84**, 1843-1849.

Stolper E.M. (1982a) The speciation of water in silicate melts. *Geochim. Cosmochim. Acta* **46**, 2609-2620.

Stolper E.M. (1982b) Water in silicate glasses: an infrared spectroscopic study. *Contrib. Mineral. Petrol.* **81**, 1-17.

Tuttle O.F. and Bowen N.L. (1958) Origin of granite in the light of experimental studies in the system $NaAlSi_3O_8$- $KAlSi_3O_8$- SiO_2-H_2O. *Geol. Soc. Am. Memoir* **74**, 1-153.

Wasserburg G.J. (1957) The effects of H_2O in silicate systems. *J. Geol.* **65**, 15-23.

Watson E.B. (1991) Diffusion of dissolved CO_2 and Cl in hydrous silicic to intermediate magmas. *Geochim. Cosmochim. Acta* **55**, 1897-1902.

Withers A.C. and Behrens H. (1999) Temperature-induced changes in the NIR spectra of hydrous albitic and rhyolitic glasses between 300 and 100 K. *Phys. Chem. Minerals* **27**, 119-132.

Withers A.C., Zhang Y., and Behrens H. (1999) Reconciliation of experimental results on H_2O speciation in rhyolitic glass using *in situ* and quenching techniques. *Earth Planet. Sci. Lett.* **173**, 343-349.

Xu Z. and Zhang Y. (2002) Quench rates in air, water, and liquid nitrogen, and inference of temperature in volcanic eruption columns. *Earth Planet. Sci. Lett.* **200**, 315-330.

Zhang Y. (1994) Reaction kinetics, geospeedometry, and relaxation theory. *Earth Planet. Sci. Lett.* **122**, 373-391.

Zhang Y. (1999) H_2O in rhyolitic glasses and melts: measurement, speciation, solubility, and diffusion. *Rev. Geophys.* **37**, 493-516.

Zhang Y. and Behrens H. (2000) H_2O diffusion in rhyolitic melts and glasses. *Chem. Geol.* **169**, 243-262.

Zhang Y., Belcher R., Ihinger P.D., Wang L., Xu Z., and Newman S. (1997a) New calibration of infrared measurement of dissolved water in rhyolitic glasses. *Geochim. Cosmochim. Acta* **61**, 3089-3100.

Zhang Y., Jenkins J., and Xu Z. (1997b) Kinetics of the reaction $H_2O + O = 2OH$ in rhyolitic glasses upon cooling: geospeedometry and comparison with glass transition. *Geochim. Cosmochim. Acta* **61**, 2167-2173.

Zhang Y., Solper E.M., and Ihinger P.D. (1995) Kinetics of reaction $H_2O + O = 2OH$ in rhyolitic glasses: preliminary results. *Am. Mineral.* **80**, 593-612.

Zhang Y., Stolper E.M., and Wasserburg G.J. (1991a) Diffusion of a multi-species component and its role in oxygen and water transport in silicates. *Earth Planet. Sci. Lett.* **103**, 228-240.

Zhang Y., Stolper E.M., and Wasserburg G.J. (1991b) Diffusion of water in rhyolitic glasses. *Geochim. Cosmochim. Acta* **55**, 441-456.

Zhang Y., Xu Z., and Behrens H. (2000) Hydrous species geospeedometer in rhyolite: Improved calibration and application. *Geochim. Cosmochim. Acta* **64**, 3347-3355.

Zhang Y., Xu Z., and Liu Y. (2003) Viscosity of hydrous rhyolitic melts inferred from kinetic experiments, and a new viscosity model. *Am. Mineral.* **88**, 1741-1752.

Zhang Y., Xu Z., Zhu M., and Wang H. (2007) Silicate melt properties and volcanic eruptions. *Rev. Geophys.* doi:10.1029/2006RG000216.

CHAPTER IV

PRESSURE DEPENDENCE OF VISCOSITY OF RHYOLITIC MELTS

ABSTRACT

Viscosity of silicate melts is a critical property for understanding volcanic and igneous processes in the Earth. Two methods were used to study the pressure effect on the viscosity of rhyolitic melts: hydrous species reaction viscometer in a piston cylinder and parallel plate creep viscometer in an internally-heated pressure vessel (IHPV). With the hydrous species reaction viscometer, viscosities of hydrous rhyolitic melts were inferred based on the kinetics of hydrous species reaction in the melt upon cooling (i.e., the equivalence of rheologically defined glass transition temperature and chemically defined apparent equilibrium temperature). The cooling experiments were carried out in a piston cylinder apparatus using hydrous rhyolitic samples with 0.8 to 4 wt% water at pressures up to 2.83 GPa. Cooling rates of the experiments varied from 0.1 K/s to 100 K/s; hence the range of viscosity inferred from this method is 3 orders of magnitude. The data from this method show that viscosity increases with increasing pressure from 1 GPa to 3 GPa for hydrous rhyolitic melts with water content ≥ 0.8 wt%. Viscosity of rhyolitic melt with 0.13 wt% water was also measured using parallel plate viscometer at pressures

0.2 and 0.4 GPa in an IHPV. The data show that viscosity of rhyolitic melt with 0.13 wt% water decreaseswith increasing pressure. Combining new data with literature data, a viscosity model of rhyolitic melts in the high viscosity range as a function of temperature, pressure and water content is developed.

1. INTRODUCTION

Viscosity of silicate melts is a property of fundamental importance in Earth sciences. Viscosities of silicate melts under ambient pressure have been studied extensively (e.g., Shaw, 1972; Hui and Zhang, 2007). Several experimental techniques are available to measure viscosity directly: (1) in the low viscosity range (0.1 to 10^5 Pa·s), concentric cylinder viscometer (e.g., Dingwell, 1986) and falling sphere technique (e.g., Shaw, 1963); (2) in the high viscosity range (10^8 to 10^{14} Pa·s), micropenetration method (e.g., Hummel and Arndt, 1985), parallel plate creep viscometer (e.g., Neuville and Richet, 1991) and fiber elongation method (e.g., Lillie, 1931). Few viscosity data are in the intermediate viscosity range of 10^5 to 10^8 Pa·s (Dorfman et al., 1996, 1997) because (1) the methods applicable to low viscosity cannot be used because rotation rate or falling rate would be too slow; (2) the methods applicable to high viscosities cannot be used because the melt would flow too easily; and (3) many silicate melts crystallize rapidly in this viscosity range. In most cases, geologists interpolated viscosity from models constructed using experimental data in the high and low viscosity ranges (e.g., Rust and Cashman, 2007).

Some of these viscometers have been adapted to high-pressure apparatus (Dingwell, 1998). In the low viscosity range, viscosity data at high pressure (≥ 1 GPa) are

obtainable with the falling sphere technique (e.g., Kushiro et al., 1976; Liebske et al., 2005). For example, *in situ* falling sphere technique in the high-pressure apparatus, such as multi-anvil, with assistance of synchrotron, can reach pressures up to 13 GPa (e.g., Reid et al., 2003; Liebske et al., 2005). On the other hand, in the high viscosity range, no viscosity data exist at pressures ≥ 1 GPa. The practical reason is the limit of the current experimental methods. For example, the maximum pressure that traditional viscometers could reach is 0.4 GPa (e.g., Behrens and Schulze, 2003). Based on the equivalence of enthalpy relaxation and viscous relaxation, Rosenhauer et al. (1979) used high-pressure differential thermal analysis experiments in an internally-heated pressure vessel (IHPV) to infer viscosities of diopside, albite and trisilicate at glass transition temperatures at elevated pressures up to 0.7 GPa.

Many geologic processes related to silicate melts deal with elevated pressures. The pressure scales of these processes may vary from 0-200 MPa for volcanic eruptions, to a couple of GPa for crustal anatexis and mantle melting, to hundreds of GPa for core-mantle segregation. This extreme range of magnitudes requires the experimental approach of studying melt viscosities to explore a very broad spectrum of measurement principles and technologies. In this report, the hydrous species viscometer is developed for high-pressure viscosity determination.

Rosenhauer et al. (1979) assumed the equivalence of enthalpy relaxation and viscous relaxation to infer viscosity. Dingwell and Webb (1990) assumed the equivalence between viscous relaxation and hydrous species equilibration (see below). Dingwell (1998) discussed the inference of viscosity at high pressures from glass transition based on volume relaxation, enthalpy relaxation, spectroscopic measurements (applied in this

study) and called them as “one of the most important breakthroughs for the prospect of obtaining high pressure viscosity data”. Zhang et al. (2003) and Zhang and Xu (2007) applied the hydrous species viscometer (see section 2.1) to infer viscosity of hydrous silicate melts at the glass transition temperature range. This method has several advantages and disadvantages. The most important advantage here is that this method can be adapted to high-pressure apparatus, such as piston cylinder, as far as glass can be obtained by quench. Because the method relies on the measurement of hydrous species concentrations, it is only applicable to hydrous silicate melts with ≥ 0.5 wt% total H_2O, but not to melts with less H_2O. With this method, viscosity is inferred but not obtained from direct measurement.

In this study, the hydrous species reaction viscometer was applied in a piston cylinder to investigate viscosity of hydrous rhyolitic melts with water content from 0.8 to 4 wt% at pressures up to 2.83 GPa. This pressure range is aimed to cover rhyolitic (granitic) melt generated at depth from field observations (e.g., Sylvester, 1999) and experimental studies (e.g., Rapp and Watson, 1995). Furthermore, as will be shown later, increasing pressure seems to have a significant effect on crystallization rate in rhyolitic melts, which seems to indicate that viscosity decreases significantly with increasing pressure. The large pressure coverage allows the evaluation of whether this is true.

In addition to this new method, the parallel-plate viscometer in an IHPV was also used to directly measure viscosity of natural rhyolite from 0.2 GPa to 0.4 GPa. Combining the literature data at pressure ≤0.5 GPa, a viscosity model is developed accommodating the dependence of viscosity of rhyolitic melts on temperature, pressure and water content in the high viscosity range.

2. EXPERIMENTAL AND ANALYTICAL METHODS

The pressure effect on melt viscosity was studied on rhyolitic melts with different water content. The concentrations of total water and hydrous species in the samples were determined by FTIR (Fourier transform infrared spectroscopy) at the University of Michigan following the procedure shown in Zhang et al. (1997a). There are a few other calibration methods in the literature (e.g., Newman et al., 1986; Withers and Behrens, 1999). The reason to use the calibration of Zhang et al. (1997a) here is to be consistent with the speciation study in Hui et al. (2008) because their study is used to calculate the apparent equilibrium temperature from concentrations of hydrous species retained in the quenched glass.

Starting materials include both natural rhyolitic glasses (EDF and KS) and synthetic hydrous rhyolitic glasses prepared by hydration of natural rhyolitic glass (GMR). Sample EDF is from Erevan Dry Fountain, Armenia. Sample KS is from Mono Crater, California. Samples GMR+2 and GMR+4 were synthesized by adding water to a natural obsidian (GMR) from Glass Mountain, California. The chemical compositions of the samples are listed in Table 4.1. Hydration of rhyolitic glasses was implemented at 1473 K, 0.5 GPa by re-melting glass powder with added H_2O at University of Hannover (Hui et al., 2008). The hydrated glasses are crystal free and bubble free.

2.1. HYDROUS SPECIES REACTION VISCOMETER

It is well known that water is present in the silicate melts as at least two species: molecular H_2O (H_2O_m) and hydroxyl group (OH) (Stolper, 1982a,b). The species reaction in the melts is

Table 4.1 Chemical compositions (oxide wt%) of KS, GMR and EDF rhyolite on anhydrous basis

	KS	GMR	EDF
SiO_2	75.94	73.22	76.78
TiO_2	0.09	0.31	0.10
Al_2O_3	12.98	14.08	12.77
FeO	0.98	1.45	0.52
MnO	0.05	0.05	0.09
MgO	0.03	0.26	0.07
CaO	0.56	1.31	0.56
Na_2O	4.01	4.06	4.08
K_2O	4.71	4.32	4.55
P_2O_5	0.29	0.07	-
Total	99.63	99.13	99.67
H_2O	0.75-0.90	1.89-2.16 in GMR+2; 3.54-4.20 in GMR+4	0.13
ref.		1	2

1. Hui et al., 2008; 2. Behrens et al., 2007.

$$H_2O_m + O = 2OH, \quad (1)$$

where O is anhydrous bridging oxygen in the melt. Total H_2O content is denoted as H_2O_t. The equilibrium constant K of Reaction (1) is defined as

$$K = \frac{X_{OH}^2}{X_{H_2O_m} X_O}, \quad (2)$$

where X means activity approximated by mole fraction. The relationship between equilibrium constant K and temperature (equilibrium line in Fig. 4.1) can be expressed by a regular solution model as (Silver et al., 1990; Ihinger et al., 1999):

$$\ln K = A + \frac{1000}{T}\left(B + CX_{H_2O_m} + DX_{OH}\right), \quad (3)$$

where T is temperature in K, and A, B, C and D are fitting parameters. Hui et al. (2008) estimated these parameters for rhyolitic melts at high pressures. During cooling, at a certain low temperature, the concentrations of these two hydrous species in the melt start to deviate from the equilibrium state; In Fig. 4.1, this is shown as curves off the straight line (the equilibrium line). When temperature becomes too low to change species concentrations, water speciation is frozen in the melt as indicated by the horizontal segments in Fig. 4.1. The intersection of each horizontal line, which is calculated from the hydrous species concentrations retained in the quenched glass, with the equilibrium line defines the apparent equilibrium temperature (Zhang, 1994). An equilibrated melt at this temperature has the same water speciation as observed in the quenched glass at room temperature. This apparent equilibrium temperature depends on the cooling rate shown in Fig. 4.1. A higher apparent equilibrium temperature indicates a faster cooling rate.

Glass transition temperature is defined rheologically as the temperature at which viscosity is equal to 10^{12} Pa·s for a cooling rate of the order 10 K/min. As the cooling rate

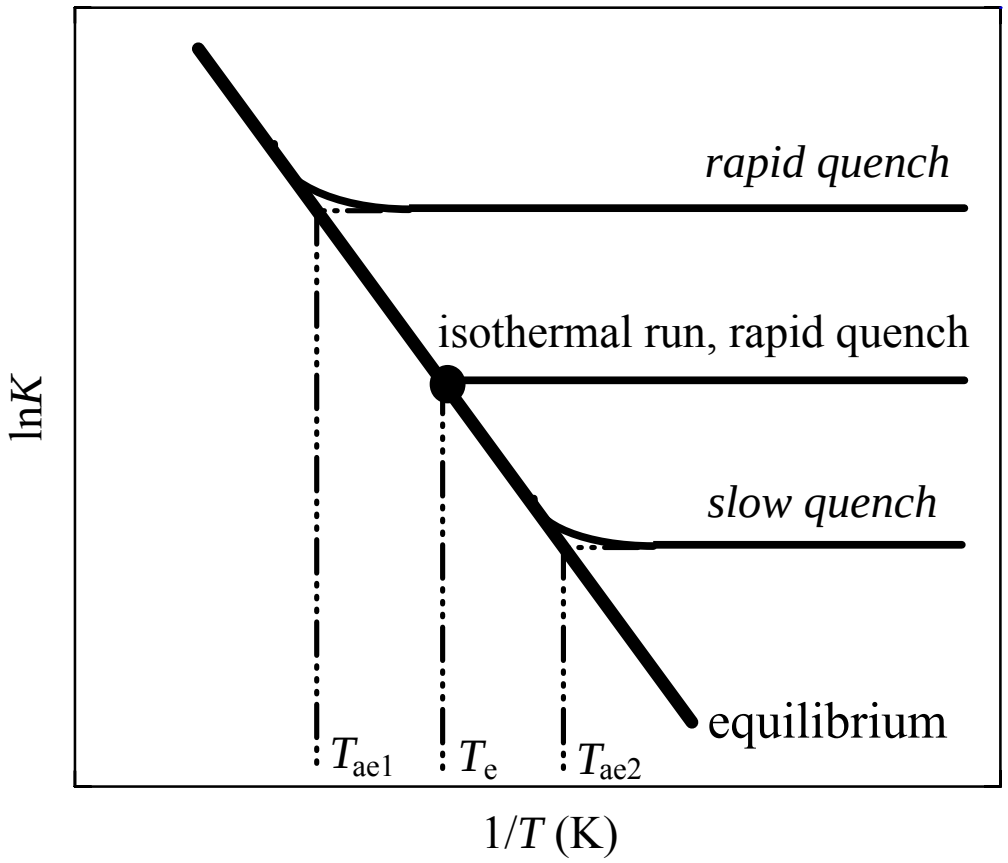

Fig. 4.1 Sketch of kinetics of Reaction (1) during cooling (Behrens and Nowak, 2003). T_{ae} is apparent equilibrium temperature, which depends on the cooling rate. T_e is equilibrium temperature.

varies, the glass transition temperature also changes. Based on theoretical considerations and experimental results, Moynihan et al. (1976) showed the formula of dependence of the glass transition temperature on the cooling rate:

$$\frac{d\log q}{d(1/T_g)} = -\frac{\Delta H}{R}, \tag{4}$$

where q is quench rate in K/s, T_g is glass transition temperature in K, R is the gas constant, and ΔH is the activation enthalpy for the relaxation times controlling the structural enthalpy or volume relaxation, which is also equal to the activation enthalpy of the shear viscosity within experimental error. Scherer (1984) generalized that viscosity is reciprocal to the quench rate at the glass transition temperature. Dingwell and Webb (1990) advanced it further to infer viscosity from kinetics of hydrous species reaction (i.e., Reaction 1) in the rhyolitic melt assuming the equivalence of the apparent equilibrium temperature and glass transition temperature (i.e., time scale of Reaction 1 in rhyolitic melt is the same as the structural relaxation time scale of rhyolitic melt because both involve bridging oxygen in the melt structure of rhyolite.). By comparing kinetic data on Reaction (1) and viscosity data obtained by other methods (including from bubble growth data of Liu et al., 2000), Zhang et al. (2003) formulated the equation below to infer viscosity at the glass transition temperature (i.e., apparent equilibrium temperature) for hydrous rhyolitic melts:

$$\log \eta_{T_g} = \log \eta_{T_{ae}} = 11.45 - \log q, \tag{5}$$

where η is viscosity in Pa·s, q is quench rate in K/s and 11.45 is a constant. Other experimental studies have verified the equivalence of relaxation at the glass transition temperature on viscosity, volume and heat capacity (e.g., Sipp et al., 1999; Toplis et al.,

2000). So, the key in this method is to calculate the apparent equilibrium temperature for a cooling experiment with known quench rate, whereas viscosity at this temperature is calculated from Eq. (5).

All the cooling experiments were conducted in a piston cylinder. A glass cylinder with a diameter of about 2 mm and a height of about 2 mm was placed into a graphite capsule, which was enclosed in crushable MgO as the inner pressure medium, with graphite heater outside and then $BaCO_3$ cell as outer pressure medium. The charge was heated to a high temperature for melt relaxation and for hydrous species in the melt to reach equilibrium. Then, the sample was isobarically cooled at a desired cooling rate to room temperature. The temperature was measured with a type-S ($Pt_{90}Rh_{10}$-Pt) or type-D ($W_{97}Re_3$-$W_{75}Re_{25}$) thermocouple. The temperature history was recorded either by computer or manually. Pressure in the piston cylinder was calibrated using quartz-coesite phase transition and melting of a gold wire (Hui et al., 2008). The pressure of cooling experiments ranges from 0.94 GPa (nominal pressure of 1 GPa) to 2.83 GPa (nominal pressure of 3 GPa). Infrared spectra of the quenched glass were obtained using a Perkin-Elmer FTIR spectrometer. The baseline of IR spectra was fit by a flexicurve (Newman et al., 1986). The concentrations of hydrous species and total water content were obtained using the calibration of Zhang et al. (1997a). The apparent equilibrium temperature was calculated from the hydrous species concentrations measured in the quenched glass using Eqs. (2) and (3) with parameters listed in Hui et al. (2008). With the recorded cooling rate, viscosity was inferred from Eq. (5) at the apparent equilibrium temperature. The 2σ error for viscosity inferred from this method is estimated to be 0.2 in terms of $\log\eta$ (Zhang et al., 2003).

In addition to the experiments in piston-cylinders at pressures below 3 GPa, some experiments at pressures above 3 GPa were also carried out in a multi-anvil device at the University of Michigan. But these experimental charges crystallized.

2.2. PARALLEL-PLATE VISCOMETER

The parallel-plate creep viscometer in an IHPV was also used to measure viscosity of rhyolitic melts near glass transition temperature. Melt viscosity was derived from the rate of deformation of a cylindrical sample with a diameter of 3.8 mm and a height of 10 mm as a function of a constant vertically applied stress. The design, operation and calibration of this viscometer are described in detail by Schulze et al. (1999). The detailed experimental procedure is explained in Behrens and Schulze (2003). This technique can measure viscosity of the same cylinder in high viscosity range covering three orders of magnitude from $10^{8.5}$ to $10^{11.5}$ Pa·s at pressures up to 0.4 GPa by pumping in Ar (pressure media) or releasing it. Effect of dehydration of the sample on the viscosity measurements was monitored by repeated viscosity measurements at the same *P-T* conditions during the whole experimental course; and water content in the sample was also checked after the experiment by infrared spectroscopy.

To mitigate the effect of dehydration of the samples during measurement, only the samples with low water content was used in this method, including sample EDF with 0.13 wt% H_2O_t, and sample KS with 0.79 wt% H_2O_t. For sample EDF, viscosity was measured at different pressures in the order of 0.2, 0.4, and 0.2 GPa. As shown in Table 4.2 and Fig. 4.2, the viscosity values at the first and last 0.2 GPa are in good agreement with difference within ±0.1 log units, indicating that there was no significant water loss

or gain during viscosity measurement. Temperature was corrected based on the melting point of aluminum at 0.2 GPa (Lees and Williamson, 1965). For sample KS, dehydration was discovered in a test run. Hence, only viscosity at 0.4 GPa was measured without cycling back and forth to minimize the duration of the sample at high temperatures. Temperature in this measurement was corrected based on the melting point of zinc at 0.4 GPa (Akella et al., 1973). Both samples were checked for water content by FTIR after isobaric quench of the experimental charge. Water loss or gain was negligible in both viscosity measurement courses. After experiments, both samples were still in good cylinder shapes, indicating negligible temperature gradient and regular deformation during creep experiments. The reproducibility of viscosities is always within ±0.15 log units (Behrens and Schulze, 2003). However, within one series of experiments, the precision is much better (within ±0.1 log units in this study).

3. EXPERIMENTAL RESULTS

Experimental results from the hydrous species reaction viscometer are summarized in Table 4.3. Original IR absorbance peak heights are also reported because there may be further improvement in the IR calibration. Viscosity is plotted as a function of 1000/T at different pressures in Fig. 4.2. Within the small temperature range of viscosity measurements, temperature dependence of viscosity of rhyolitic melts at each pressure can be described by the Arrhenius relationship:

$$\eta = \eta_0 \cdot \exp\left(\frac{E_a}{RT}\right), \tag{6}$$

where η_0 is the pre-exponential factor and E_a is the activation energy for viscous flow,

Table 4.2 Results of parallel plate creep viscometer with sample EDF at pressures of 0.2 and 0.4 GPa and sample KS at 0.4 GPa.

EDF						KS		
0.2 GPa			0.4 GPa			0.4 GPa		
T K	logη Pa·s	exp.#	*T* K	logη Pa·s	exp.#	*T* K	logη Pa·s	exp.#
1038.15	11.42	12	1028.15	11.19	11	848.15	11.51	1
1048.15	11.28	1	1038.15	11.03	6	856.15	11.35	6
1048.15	11.21	13	1038.15	11.01	10	867.15	11.14	5
1067.15	10.83	2	1058.15	10.78	7	886.15	10.60	2
1067.15	10.74	5	1088.15	10.25	8	907.15	10.30	3
1088.15	10.52	14	1118.15	9.80	9	925.15	10.02	4
1087.15	10.47	3						
1118.15	9.97	4						

Note: # means the chronological order of the measurements.

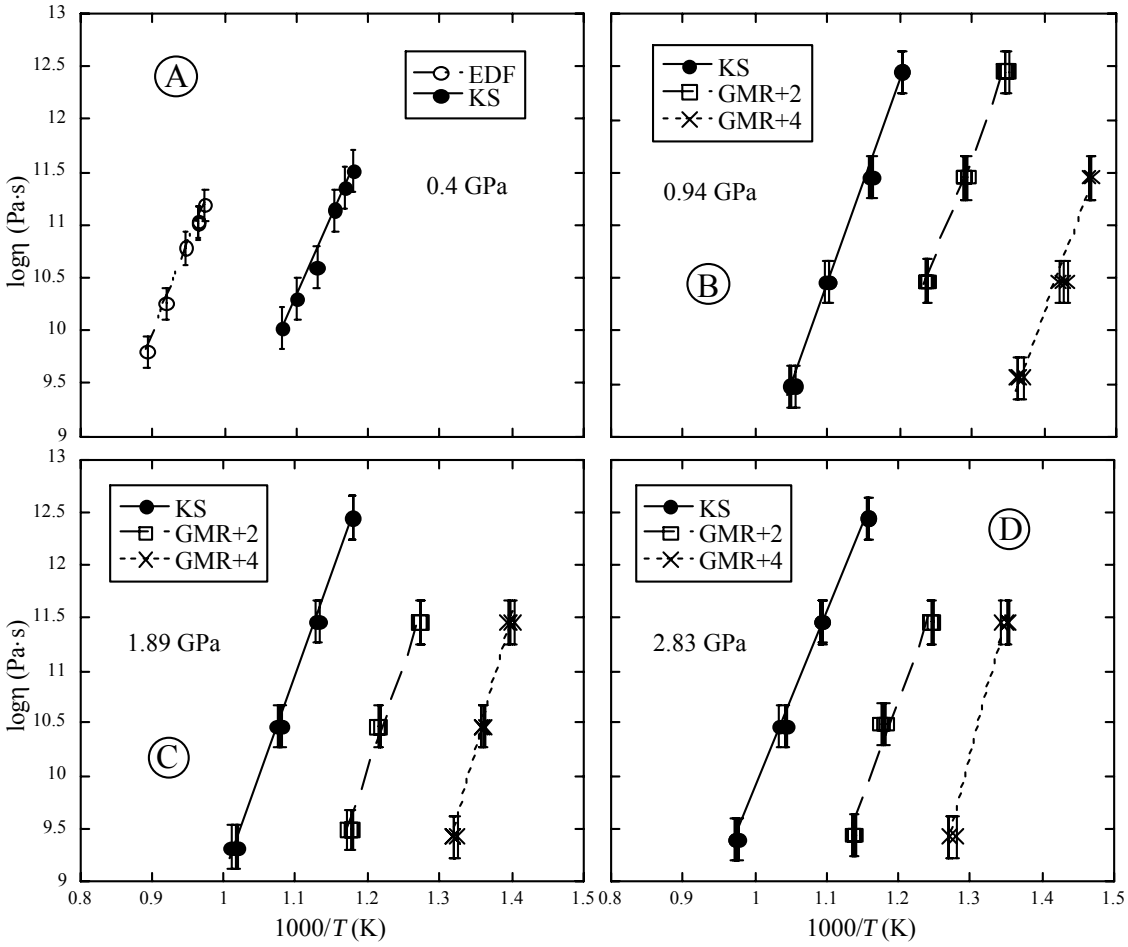

Fig. 4.2 Dependence of viscosities of rhyolitic melts (EDF, KS, GMR+2 and GMR+4) on temperature at pressures of 0.4, 0.94, 1.89 and 2.83 GPa. All the data are from this study: A is for parallel plate creep viscometer, and B-D are from hydrous species reaction viscometer. Straight lines are fit of the data by Arrhenius equation (i.e., Eq. 6).

Table 4.3 Viscosity of hydrous rhyolitic melts at various pressures inferred from hydrous species reactions.

Measurement[#]	$P^{\$}$	q^*	Abs.	Abs.	Thickness	H_2O_t	H_2O_m	OH	$X(H_2O_t)$	$X(H_2O_m)$	X(OH)	T_{ae}	logη
	GPa	K/s	5200	4500	mm	wt%	wt%	wt%				K	Pa·s
KS-1-2.1	0.94	9.56	0.0448	0.1608	1.124	0.846	0.170	0.677	0.0152	0.0030	0.0242	906.03	10.47
KS-1-2.2	0.94	9.56	0.0447	0.1604	1.118	0.849	0.170	0.679	0.0152	0.0030	0.0243	907.11	10.47
KS-1-2.3	0.94	9.56	0.0441	0.1610	1.126	0.843	0.167	0.677	0.0151	0.0030	0.0242	911.23	10.47
KS-1-3.1	0.94	0.99	0.0557	0.1717	1.195	0.877	0.198	0.678	0.0157	0.0036	0.0243	862.61	11.45
KS-1-3.2	0.94	0.99	0.0539	0.1689	1.190	0.862	0.193	0.669	0.0154	0.0034	0.0240	863.08	11.45
KS-1-3.3	0.94	0.99	0.0585	0.1748	1.198	0.898	0.208	0.690	0.0161	0.0037	0.0247	859.79	11.45
KS-1-4.1	0.94	0.10	0.0649	0.1883	1.373	0.843	0.201	0.642	0.0151	0.0036	0.0230	829.61	12.45
KS-1-4.2	0.94	0.10	0.0626	0.1857	1.370	0.829	0.194	0.634	0.0148	0.0035	0.0227	831.31	12.45
KS-1-4.3	0.94	0.10	0.0646	0.1883	1.371	0.844	0.200	0.643	0.0151	0.0036	0.0231	831.40	12.45
KS-1-5.1	0.94	92.33	0.0432	0.1720	1.163	0.862	0.158	0.704	0.0154	0.0028	0.0252	954.99	9.48
KS-1-5.2	0.94	92.33	0.0432	0.1700	1.150	0.864	0.160	0.704	0.0155	0.0029	0.0252	951.13	9.48
KS-1-5.3	0.94	92.33	0.0435	0.1708	1.164	0.857	0.159	0.698	0.0153	0.0028	0.0250	946.06	9.48
GMR+2-1-1.1	0.94	9.50	0.1720	0.2272	0.990	1.886	0.747	1.140	0.0335	0.0133	0.0405	808.08	10.47
GMR+2-1-1.2	0.94	9.50	0.1709	0.2268	0.987	1.886	0.744	1.142	0.0335	0.0132	0.0406	809.82	10.47
GMR+2-1-1.3	0.94	9.50	0.1729	0.2275	0.991	1.890	0.750	1.140	0.0336	0.0133	0.0405	807.37	10.47
GMR+2-1-2.1	0.94	1.00	0.1729	0.2048	0.911	1.920	0.816	1.104	0.0341	0.0145	0.0392	774.82	11.45
GMR+2-1-2.2	0.94	1.00	0.1750	0.2064	0.910	1.942	0.827	1.115	0.0345	0.0147	0.0396	776.83	11.45
GMR+2-1-2.3	0.94	1.00	0.1712	0.2030	0.909	1.905	0.810	1.096	0.0338	0.0144	0.0389	773.10	11.45
GMR+2-1-3.1	0.94	0.10	0.1105	0.1131	0.502	2.041	0.947	1.094	0.0362	0.0168	0.0388	743.24	12.45
GMR+2-1-3.2	0.94	0.10	0.1089	0.1118	0.498	2.031	0.941	1.090	0.0360	0.0167	0.0387	742.89	12.45
GMR+2-1-3.3	0.94	0.10	0.1097	0.1123	0.504	2.017	0.937	1.080	0.0358	0.0166	0.0383	740.02	12.45
GMR+4-1-2.1	0.94	9.68	0.2159	0.1114	0.356	4.116	2.667	1.449	0.0719	0.0466	0.0506	701.15	10.46
GMR+4-1-2.2	0.94	9.68	0.2137	0.1107	0.351	4.141	2.678	1.462	0.0723	0.0467	0.0511	704.00	10.46
GMR+4-1-2.3	0.94	9.68	0.2152	0.1107	0.356	4.094	2.657	1.437	0.0715	0.0464	0.0502	698.69	10.46
GMR+4-1-3.1	0.94	76.87	0.1467	0.0859	0.268	3.937	2.403	1.534	0.0688	0.0420	0.0536	733.94	9.56
GMR+4-1-3.2	0.94	76.87	0.1540	0.0901	0.282	3.925	2.397	1.529	0.0686	0.0419	0.0534	733.01	9.56
GMR+4-1-3.3	0.94	76.87	0.1548	0.0885	0.276	3.989	2.463	1.526	0.0697	0.0430	0.0533	728.97	9.56
GMR+4-1-4.1	0.94	1.00	0.1509	0.0789	0.271	3.779	2.440	1.339	0.0661	0.0427	0.0469	684.09	11.45

GMR+4-1-4.2	0.94	1.00	0.1509	0.0779	0.267	3.815	2.477	1.338	0.0668	0.0433	0.0468	682.11	11.45
GMR+4-1-4.3	0.94	1.00	0.1498	0.0792	0.275	3.711	2.386	1.325	0.0650	0.0418	0.0464	682.96	11.45
KS-2-1.1	1.89	1.00	0.0111	0.0396	0.270	0.871	0.175	0.696	0.0156	0.0031	0.0249	883.40	11.45
KS-2-1.2	1.89	1.00	0.0106	0.0397	0.280	0.832	0.161	0.671	0.0149	0.0029	0.0240	885.52	11.45
KS-2-2.1	1.89	134.16	0.0431	0.1862	1.201	0.898	0.153	0.745	0.0161	0.0027	0.0267	984.15	9.32
KS-2-2.2	1.89	134.16	0.0381	0.1769	1.192	0.844	0.136	0.708	0.0151	0.0024	0.0254	989.96	9.32
KS-2-2.3	1.89	134.16	0.0428	0.1851	1.202	0.890	0.152	0.739	0.0159	0.0027	0.0265	979.76	9.32
KS-2-3.1	1.89	9.65	0.0496	0.1892	1.246	0.895	0.169	0.726	0.0160	0.0030	0.0260	923.76	10.47
KS-2-3.2	1.89	9.65	0.0462	0.1842	1.234	0.871	0.159	0.712	0.0156	0.0029	0.0255	931.37	10.47
KS-2-3.3	1.89	9.65	0.0466	0.1848	1.245	0.867	0.159	0.707	0.0155	0.0028	0.0253	927.31	10.47
KS-2-4.1	1.89	0.10	0.0384	0.1244	0.859	0.875	0.190	0.685	0.0157	0.0034	0.0246	847.43	12.45
KS-2-4.2	1.89	0.10	0.0368	0.1219	0.856	0.855	0.183	0.672	0.0153	0.0033	0.0241	847.46	12.45
KS-2-4.3	1.89	0.10	0.0360	0.1203	0.849	0.849	0.180	0.668	0.0152	0.0032	0.0239	847.82	12.45
GMR+2-2-2.1	1.89	9.50	0.1595	0.2196	0.870	2.071	0.789	1.282	0.0367	0.0140	0.0455	823.15	10.47
GMR+2-2-2.2	1.89	9.50	0.1579	0.2181	0.870	2.052	0.781	1.271	0.0364	0.0139	0.0451	820.82	10.47
GMR+2-2-2.3	1.89	9.50	0.1611	0.2184	0.860	2.097	0.807	1.290	0.0372	0.0143	0.0458	821.42	10.47
GMR+2-2-3.1	1.89	1.00	0.2053	0.2498	0.997	2.147	0.887	1.259	0.0381	0.0157	0.0447	786.31	11.45
GMR+2-2-3.2	1.89	1.00	0.2008	0.2459	0.989	2.123	0.875	1.248	0.0376	0.0155	0.0443	784.66	11.45
GMR+2-2-3.3	1.89	1.00	0.2032	0.2484	0.997	2.129	0.878	1.251	0.0378	0.0156	0.0444	785.17	11.45
GMR+2-2-5.1	1.89	90.72	0.1539	0.2177	0.831	2.142	0.798	1.343	0.0380	0.0142	0.0476	847.45	9.49
GMR+2-2-5.2	1.89	90.72	0.1526	0.2165	0.825	2.144	0.797	1.347	0.0380	0.0141	0.0478	849.47	9.49
GMR+2-2-5.3	1.89	90.72	0.1530	0.2180	0.825	2.158	0.799	1.359	0.0383	0.0142	0.0482	854.15	9.49
GMR+4-2-3.1	1.89	1.00	0.4415	0.2595	0.797	3.997	2.433	1.564	0.0698	0.0425	0.0546	716.58	11.45
GMR+4-2-3.2	1.89	1.00	0.4356	0.2573	0.796	3.954	2.402	1.552	0.0691	0.0420	0.0543	715.02	11.45
GMR+4-2-3.3	1.89	1.00	0.4453	0.2581	0.797	4.002	2.454	1.548	0.0699	0.0429	0.0541	711.81	11.45
GMR+4-2-4.1	1.89	107.00	0.2441	0.1593	0.465	4.004	2.306	1.698	0.0700	0.0403	0.0593	757.59	9.42
GMR+4-2-4.2	1.89	107.00	0.2370	0.1551	0.457	3.957	2.277	1.680	0.0692	0.0398	0.0587	754.55	9.42
GMR+4-2-4.3	1.89	107.00	0.2484	0.1621	0.473	4.005	2.307	1.698	0.0700	0.0403	0.0593	757.54	9.42
GMR+4-2-5.1	1.89	9.67	0.3797	0.2294	0.677	4.115	2.467	1.648	0.0718	0.0431	0.0576	736.32	10.46
GMR+4-2-5.2	1.89	9.67	0.3914	0.2307	0.677	4.195	2.545	1.650	0.0732	0.0444	0.0576	733.18	10.46
GMR+4-2-5.3	1.89	9.67	0.3914	0.2320	0.680	4.188	2.534	1.655	0.0731	0.0442	0.0577	734.81	10.46
KS-3-1.1	2.86	1.00	0.0491	0.2066	1.408	0.847	0.148	0.699	0.0152	0.0027	0.0250	916.18	11.45
KS-3-1.2	2.86	1.00	0.0493	0.2064	1.408	0.847	0.149	0.698	0.0152	0.0027	0.0250	913.16	11.45

KS-3-1.3	2.86	1.00	0.0489	0.2064	1.407	0.846	0.148	0.698	0.0152	0.0027	0.0250	916.67	11.45
KS-3-2.1	2.83	0.99	0.0534	0.2252	1.535	0.846	0.148	0.698	0.0152	0.0027	0.0250	916.66	11.45
KS-3-2.2	2.83	0.99	0.0538	0.2256	1.533	0.850	0.149	0.701	0.0152	0.0027	0.0251	915.89	11.45
KS-3-2.3	2.83	0.99	0.0563	0.2289	1.530	0.871	0.157	0.714	0.0156	0.0028	0.0256	912.06	11.45
KS-3-9.1	2.83	0.10	0.0479	0.1785	1.221	0.861	0.167	0.694	0.0154	0.0030	0.0249	865.65	12.45
KS-3-9.2	2.83	0.10	0.0490	0.1803	1.225	0.870	0.170	0.700	0.0156	0.0030	0.0251	864.01	12.45
KS-3-9.3	2.83	0.10	0.0472	0.1765	1.218	0.852	0.165	0.687	0.0153	0.0030	0.0246	862.42	12.45
KS-3-8.1	2.83	9.56	0.0546	0.2581	1.760	0.831	0.132	0.699	0.0149	0.0024	0.0251	968.21	10.47
KS-3-8.2	2.83	9.56	0.0638	0.2732	1.756	0.903	0.155	0.748	0.0162	0.0028	0.0268	957.34	10.47
KS-3-8.3	2.83	9.56	0.0628	0.2723	1.757	0.897	0.152	0.744	0.0161	0.0027	0.0267	960.32	10.47
KS-3-11.1	2.83	111.66	0.0332	0.1907	1.389	0.751	0.102	0.649	0.0135	0.0018	0.0233	1021.91	9.40
KS-3-11.2	2.83	111.66	0.0335	0.1925	1.395	0.755	0.102	0.653	0.0135	0.0018	0.0234	1026.81	9.40
KS-3-11.3	2.83	111.66	0.0335	0.1929	1.395	0.757	0.102	0.655	0.0136	0.0018	0.0235	1029.21	9.40
KS-3-11.4	2.83	111.66	0.0336	0.1925	1.392	0.757	0.103	0.655	0.0136	0.0018	0.0235	1026.15	9.40
GMR+2-3-2.1	2.83	9.07	0.1210	0.2070	0.823	1.925	0.632	1.293	0.0342	0.0112	0.0459	851.32	10.49
GMR+2-3-2.2	2.83	9.07	0.1260	0.2089	0.818	1.977	0.662	1.315	0.0351	0.0118	0.0467	848.23	10.49
GMR+2-3-2.3	2.83	9.07	0.1263	0.2093	0.823	1.968	0.660	1.308	0.0349	0.0117	0.0464	845.58	10.49
GMR+2-3-3.1	2.83	1.00	0.1726	0.2538	1.004	2.030	0.740	1.290	0.0360	0.0131	0.0458	802.91	11.45
GMR+2-3-3.2	2.83	1.00	0.1740	0.2539	1.004	2.035	0.746	1.289	0.0361	0.0132	0.0458	800.63	11.45
GMR+2-3-3.3	2.83	1.00	0.1664	0.2503	1.004	1.983	0.713	1.270	0.0352	0.0127	0.0451	803.50	11.45
GMR+2-3-4.1	2.83	104.30	0.0852	0.1523	0.594	1.944	0.617	1.327	0.0345	0.0110	0.0471	878.19	9.43
GMR+2-3-4.2	2.83	104.30	0.0849	0.1485	0.572	1.984	0.638	1.346	0.0352	0.0113	0.0478	876.98	9.43
GMR+2-3-4.3	2.83	104.30	0.0823	0.1449	0.558	1.981	0.634	1.347	0.0352	0.0113	0.0478	879.44	9.43
GMR+4-3-4.1	2.83	1.00	0.2215	0.1709	0.518	3.540	1.869	1.671	0.0621	0.0328	0.0586	739.53	11.45
GMR+4-3-4.2	2.83	1.00	0.2256	0.1729	0.516	3.614	1.913	1.702	0.0633	0.0335	0.0597	744.70	11.45
GMR+4-3-4.3	2.83	1.00	0.2210	0.1673	0.503	3.605	1.922	1.683	0.0632	0.0337	0.0590	738.43	11.45
GMR+4-3-5.1	2.83	107.00	0.1838	0.1477	0.417	3.766	1.931	1.835	0.0659	0.0338	0.0642	781.53	9.42
GMR+4-3-5.2	2.83	107.00	0.1812	0.1464	0.410	3.793	1.938	1.855	0.0664	0.0339	0.0649	786.93	9.42
GMR+4-3-5.3	2.83	107.00	0.1873	0.1509	0.422	3.803	1.946	1.857	0.0666	0.0341	0.0650	786.73	9.42

Note: # A few points (two to four) were measured by IR for each experimental sample; they are listed here as xxx.1, .2, .3 or .4.

$ *P* has been corrected based on pressure calibration.

* *q* was calculated from the thermal history recorded by computer or manually.

which depends on water content of the sample and experimental pressure. Viscosity of rhyolitic melts decreases with increasing water content systematically at a given pressure and temperature as shown in Fig. 4.2.

Viscosities of samples EDF and KS obtained from the parallel plate creep viscometer are listed in Table 4.2 including chronological order of measurements and shown in Figs. 4.3a and 4.3b. Temperature dependence of viscosity of each sample at each pressure can also be described by the Arrhenius relationship (i.e., Eq. 6) within the small temperature range of measurements.

The pressure dependence of viscosity is more complicated. For the "dry" sample (EDF), viscosity does not change significantly from 0.1 MPa to 0.2 GPa. From 0.2 to 0.4 GPa, the viscosity of sample EDF decreases by about 0.2 log units. For hydrous samples with 0.8 and 2 wt% H_2O_t (KS and GMR+2), viscosity increases monotonically by about 1 log unit as pressure increases from 0.1 MPa to 2.8 GPa. For hydrous sample with about 4 wt% H_2O_t (GMR+4), viscosity first decreases as pressure increases from 0.1 MPa to 0.9 GPa, and then increases from 0.9 to 2.8 GPa.

At the experimental petrology laboratory of the University of Michigan, a large database has been accumulated on successful versus failed experiments in the diffusion, reaction kinetics, and viscosity studies of silicate melts (Zhang et al., 1997b, 2000; Liu and Zhang, 2000; Zhang and Behrens, 2000; Behrens and Zhang, 2001; Xu and Zhang, 2002; Behrens et al., 2004; Liu et al., 2004a,b, 2005; Hui et al., 2008; Ni and Zhang, 2008). Most of the failed experiments crystallized significantly. Because these results may be relevant to the discussion of viscosity (see Discussion), they are summarized in Appendix D. The data show:

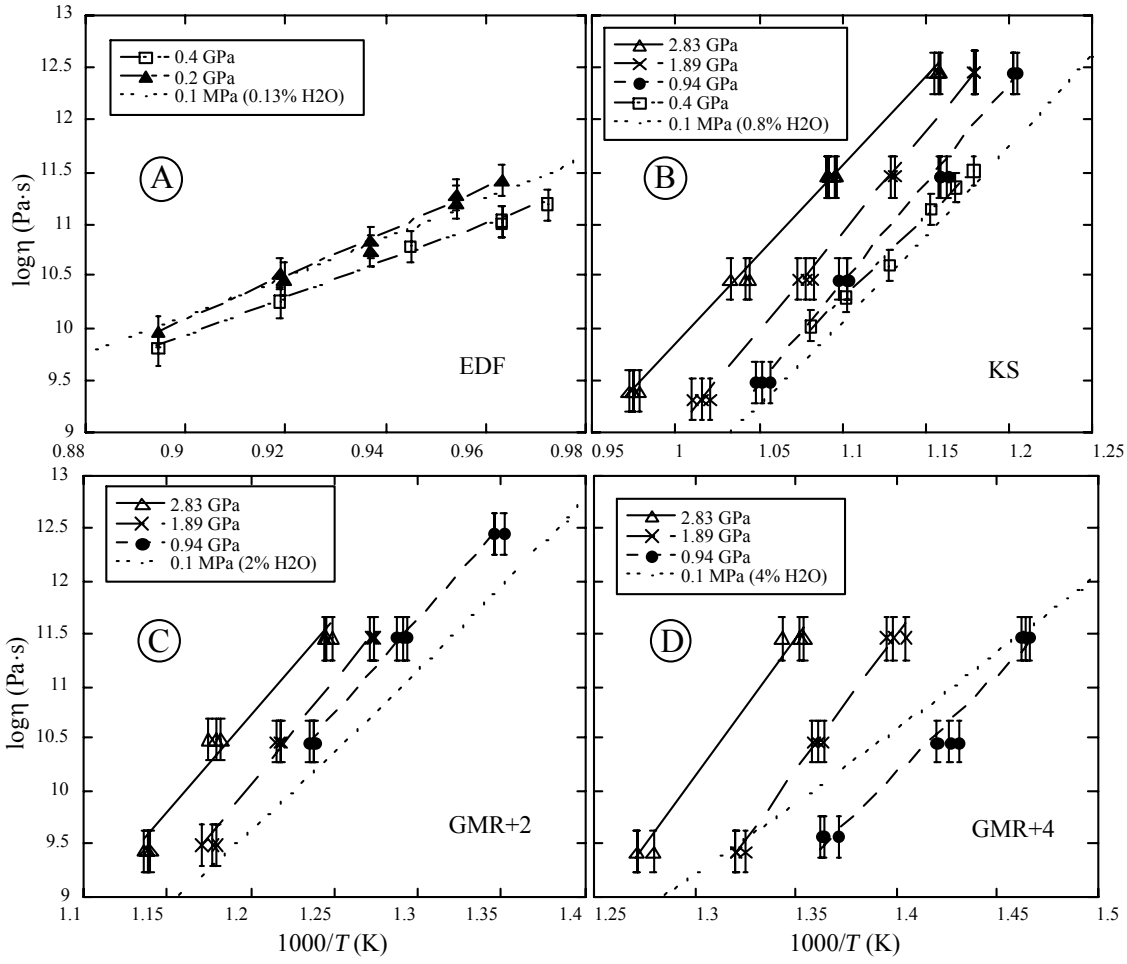

Fig. 4.3 Comparisons of viscosities of given rhyolitic melts (EDF, KS, GMR+2 and GMR+4) at various pressures. Data are from this study. Straight lines are fit of the data by Arrhenius equation (i.e., Eq. 6). Viscosities of various rhyolitic melts at 0.0001 GPa were calculated from Zhang et al. (2003) as references.

(1) It is more difficult to quench an overheated liquid into glass at high pressures than at low pressures because of crystallization during quench at high pressures. For example, a hydrous rhyolite melt containing 5.2 wt% H_2O_t quenched from 1873 K at 2 GPa (sample # 239 in Appendix D) did not crystallize, but a hydrous rhyolite sample containing only 0.9 wt% H_2O_t quenched from 1873 K at 4 GPa (sample # 240 in Appendix D) crystallized significantly.

(2) Melts in the isothermal experiments at a temperature below the liquidus often crystallize more easily at high pressures than at low pressures (Hui et al., 2008). For example, a hydrous rhyolitic glass (0.9 wt% H_2O_t) held at 823 K and 3 GPa for 10 days (sample # 56 in Appendix D) did not crystallize significantly, but a similar glass held at the same temperature but 4 GPa for only 3.1 hours (sample # 57 in Appendix D) crystallized. For another example, a hydrous rhyolitic glass with 0.77 wt% H_2O_t held at 1123 K and 6.1 MPa for 72 hours (sample # 172 in Appendix D) did not crystallize, but another sample with same amount of H_2O_t held at 1123 K and 3 GPa for only one minute (sample # 174 in Appendix D) crystallized significantly.

Fig. 4.4 shows some more trends. The findings indicate that crystallization rate increases significantly with increasing pressure, meaning crystal nucleation and/or growth rates in melts increase with increasing pressure in hydrous rhyolitic melts. The relationship with viscosity will be discussed in the next section.

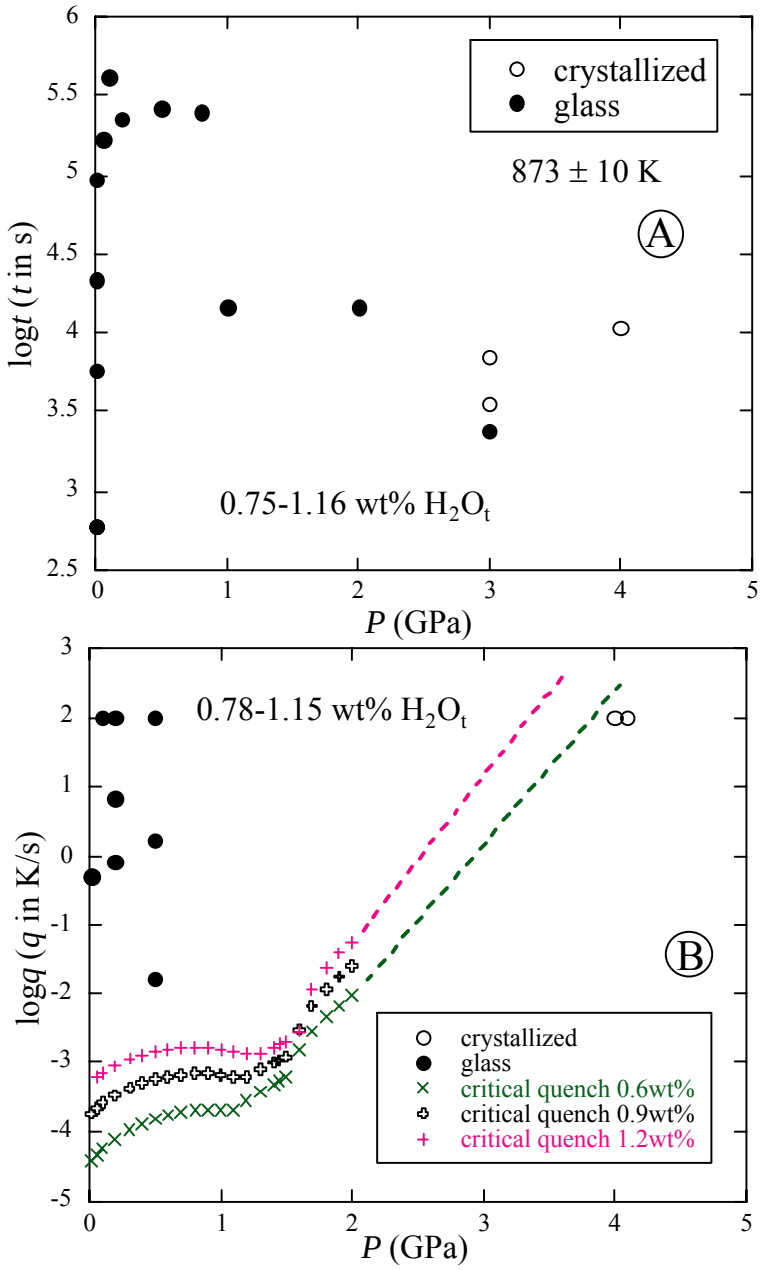

Fig. 4.4 The effect of pressure on crystallization kinetics in the rhyolitic melt for (A) isothermal experiments, and (B) controlled cooling rate experiments. In (B), critical quench rates for rhyolitic melt with water contents of 0.6, 0.9 and 1.2 wt% are calculated from Eqs. (8) and (9) (see text, Senkov, 2007) and the dashed lines are extrapolations to show the trends for 0.6 and 1.2 wt% water, respectively.

4. DISCUSSION

4.1. PRESSURE DEPENDENCE OF VISCOSITY

Viscosities of a variety of silicate liquids in the low viscosity range have been investigated using the falling sphere technique in high-pressure apparatus, demonstrating a complex pressure dependence of viscosities (Scarfe et al., 1987; Lange, 1994). Pressure-induced viscosity change has been related to the degree of polymerization of the melt in general (Scarfe et al., 1987). Viscosities of anhydrous rhyolite melt (e.g., Scarfe et al., 1987), jadeite melt (e.g., Kushiro, 1976), dacite melt (e.g., Tinker et al., 2004), andesite melt (e.g., Kushiro et al., 1976), and some basalt melts (e.g., Scarfe et al., 1987) decrease with increasing pressure in the first several GPa, whereas those of diopside melt (e.g., Scarfe et al., 1979) and peridotite melt (Liebske et al., 2005), both highly depolymerized, increase with increasing pressure.

Water dissolved in the silicate melt can depolymerize the melt by forming hydroxyl group (Reaction 1). The negative pressure dependence of viscosity of anhydrous melt may change to positive pressure dependence of viscosity after adding a certain amount of water, For example, viscosity of anhydrous andesite melt decreases with pressure (Kushiro et al., 1976), but viscosity of andesite with 3 wt% water increases with pressure (Kushiro, 1978). Also, the pressure dependence of viscosity of a given melt may change from positive to negative with further increase of pressure, such as periodite (Liebske et al., 2005), or from negative to positive, such as albite (Funakoshi, et al., 2002). In other words, there may be a viscosity maximum or minimum with increasing pressure.

In the high viscosity range, only a few studies have been conducted on the pressure dependence of viscosity of silicate melts in a pressure range up to 0.4 GPa previously. Viscosity of the albite-diopside binary system shows a change in the sign of the pressure dependence from negative for albite to positive for diopside (Schulze et al., 1999; Behrens and Schulze, 2003). The pressure dependence of viscosity of haploandesite in the high viscosity range changes from negative for anhydrous melt to positive for hydrous melt with 1.06 wt% water or up (Liebske et al., 2003). This is consistent with pressure dependence of viscosity of andesite in the low viscosity range in general (Kushiro et al., 1976; Kushiro, 1978). Moreover, pressure effect on viscosity becomes more pronounced with decreasing temperature.

Due to experimental limitations, viscosity of sample EDF, which contained minor amount of water, was measured at pressures $\leq$ 0.4 GPa. The viscosity decreases with increasing pressure as shown in Fig. 4.3a in this pressure range. That is, it behaves as a polymerized melt, as expected. But for the hydrous samples KS and GMR+2 as shown in Figs. 4.3b and 4.3c, the viscosity increases with increasing pressure based on the new data. As dissolved H_2O depolymerizes the melt, this trend is consistent with literature data (Kushiro et al., 1976; Kushiro, 1978; Liebske et al., 2003). The viscosities of the sample GMR+4, which contains about 4 wt% water, increase systematically from 1 GPa to 3 GPa as shown in Fig. 4.3d. The pressure dependence of viscosity from ambient pressure to 1 GPa is small and whether the dependence is positive or negative depends on the temperature.

4.2. MODELING THE P-T-X DEPENDENCE OF VISCOSITY

There are various models used to describe temperature dependence of viscosity of anhydrous and hydrous natural silicate melts (e.g., Shaw, 1972; Hui and Zhang, 2007). The pressure dependence of viscosity has been modeled for some anhydrous melts, such as peridotite liquid (Liebske et al., 2005), but has not been quantified for hydrous natural silicate melts because only limited data were available. For example, for hydrous rhyolitic melt, there are only two data points at pressure > 0.5 GPa (one data point of AOQ at 1173 K, 1 GPa; and another one at 1173 K, 0.75 GPa, Schulze et al., 1996) in the low viscosity range. These new data are the first viscosity data at pressures ≥ 1 GPa in the low-temperature (high viscosity) range. Because data on the pressure dependence of viscosity of rhyolitic melts in the high temperature range are limited (Schulze et al., 1996), only the data in the low temperature region are considered in constructing a model on the dependence of viscosity on temperature, pressure and water content. In this narrow temperature range, the Arrhenius relationship can describe the temperature dependence of viscosity. Hence, parameters η_0 and E_a in Eq. (6) are treated as functions of water content and pressure to construct a viscosity model. The data used for the model include viscosity data from this study and literature data in the high viscosity range (Neuville et al., 1993; Stevenson et al., 1995; Zhang et al., 2003; Zhang and Xu, 2007). Because the precision of the parallel plate viscometer is much higher, this data set was weighed 10 times more than other data in the regression. After some trials, the equation below is found to fit the data well:

$$\log\eta = \left(a_0 + a_P P^{\frac{1}{2}}\right) + \left(b_0 + b_P P^{\frac{1}{2}}\right)\left(1 - \exp\left(\left(c_0 + c_P P^{\frac{1}{2}}\right)X\right)\right) + \left(\left(d_0 + d_P P^{\frac{1}{2}}\right) + \left(e_0 + e_P P^{\frac{1}{2}}\right)\left(1 - \exp\left(\left(f_0 + f_P P^{\frac{1}{2}}\right)X\right)\right)\right)1000/T, \quad (7)$$

where P is pressure in GPa, and X is mole fraction of total water content in the melt on a single oxygen basis (Stolper, 1982b; Zhang, 1999). The best-fit parameters in Eq. (7) with 2σ errors are: a_0 = -7.8470 ± 0.4972, a_P = 1.1472 ± 0.5802, b_0 = -12.4257 ± 0.9940, b_P = 0.8080 ± 0.6278, c_0 = -3.6440 ± 1.6134, c_P = -10.1893 ± 1.7128, d_0 = 21.3531 ± 0.5706, d_P = -2.1722 ± 0.7371, e_0 = -5.8335 ± 0.7198, e_P = 4.0480 ± 0.6801, f_0 = -89.3887 ± 10.3647, and f_P = -30.5499 ± 15.2766. This equation can reproduce the whole database (206 data points) with 2σ of 0.38 in terms of logη. The dependence of viscosity as a function of OH and molecular H_2O concentrations was also examined at different pressures, but no simple relation emerged for a large range of water content. Hence, no species information is included in fitting how viscosity depends on water concentration. Fig. 4.5 shows a comparison between experimental viscosities and calculated values using Eq. (7). Although the fit is good, extrapolation of the model beyond experimental conditions is not recommended. That is, calculated viscosity at high pressures should be inside the range of 10^9 to 10^{12} Pa·s, and T-P-$X_{H_2O_t}$ conditions should be within conditions shown in Fig. 4.6. The calculated pressure dependence of viscosity of rhyolitic melts with different water contents is shown in Fig. 4.7 and it is in agreement with Figs. 4.3b, 4.3c and 4.3d.

Glass transition temperature is an important rheological parameter of glass and Eq. (7) can be used to estimate glass transition temperature of rhyolitic melt under high

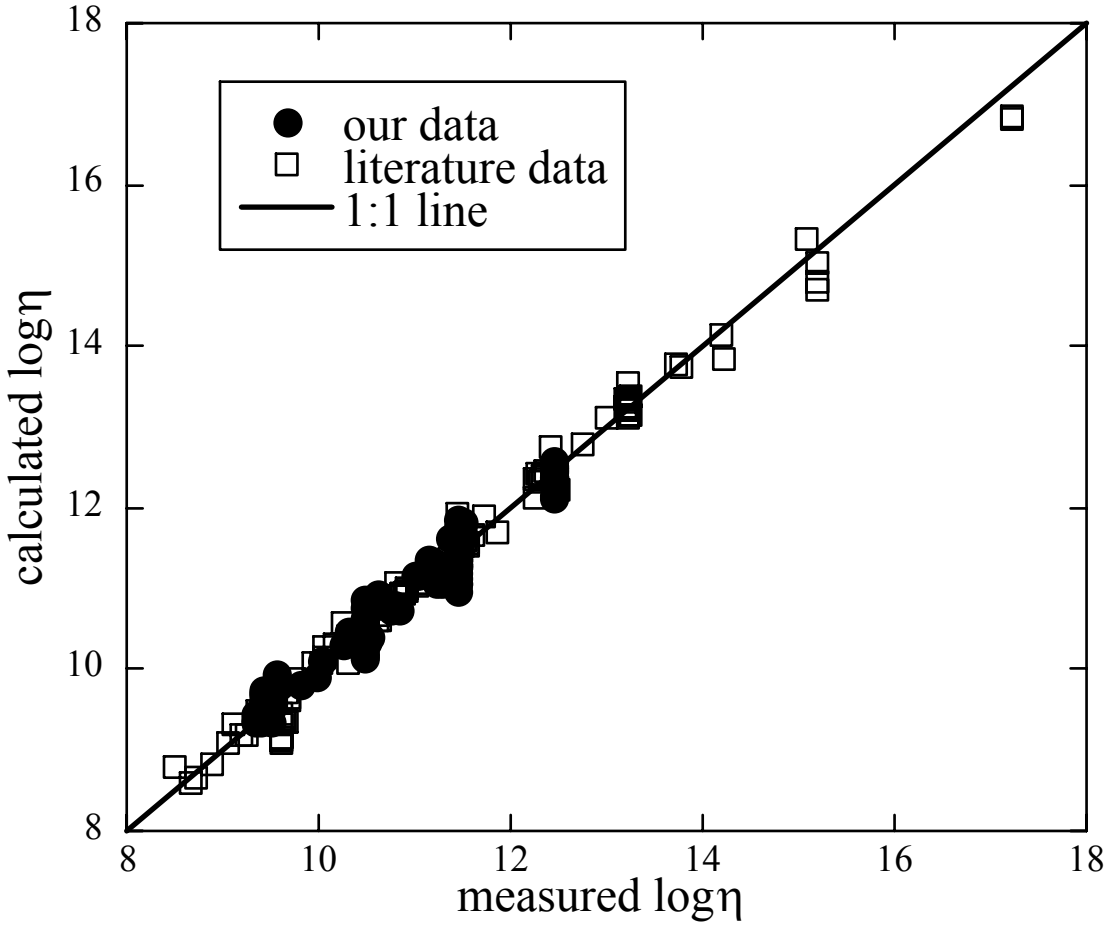

Fig. 4.5 Comparison of measured viscosity data of rhyolitic melts with those calculated from Eq. (7).

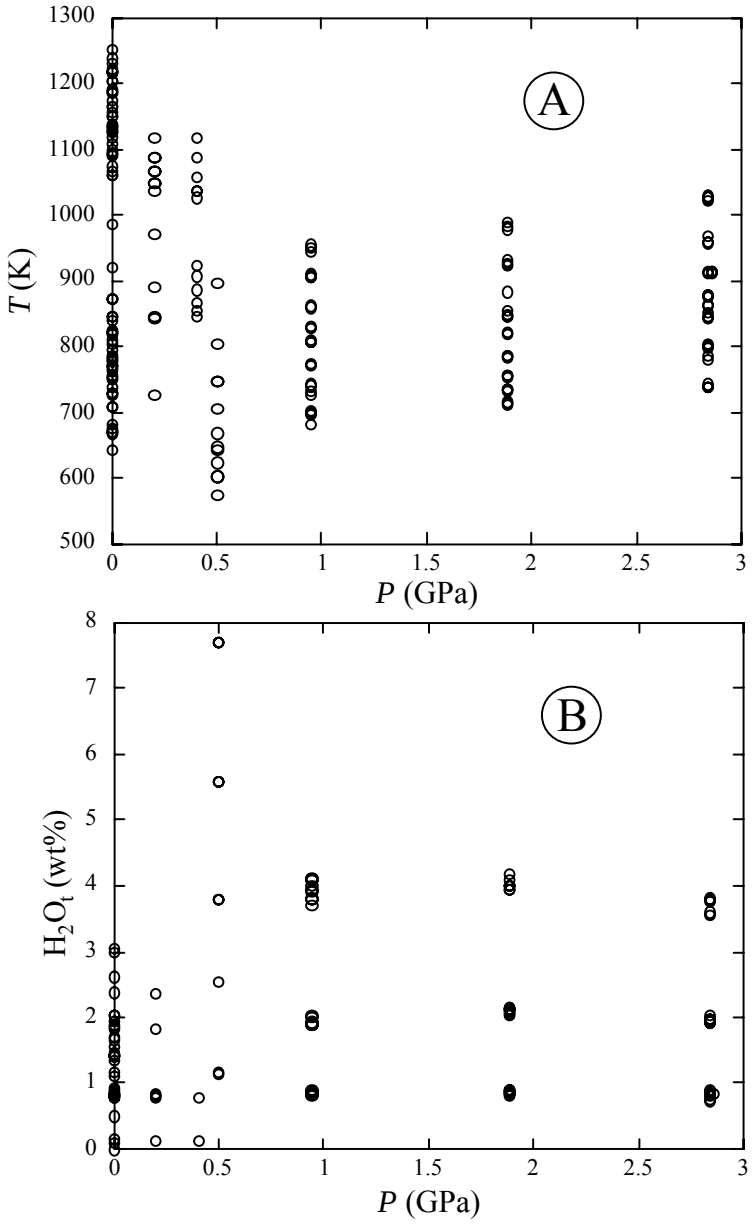

Fig. 4.6 P-T-$X_{H_2O_t}$ range of all experimental data of the model, i.e., Eq. (7).

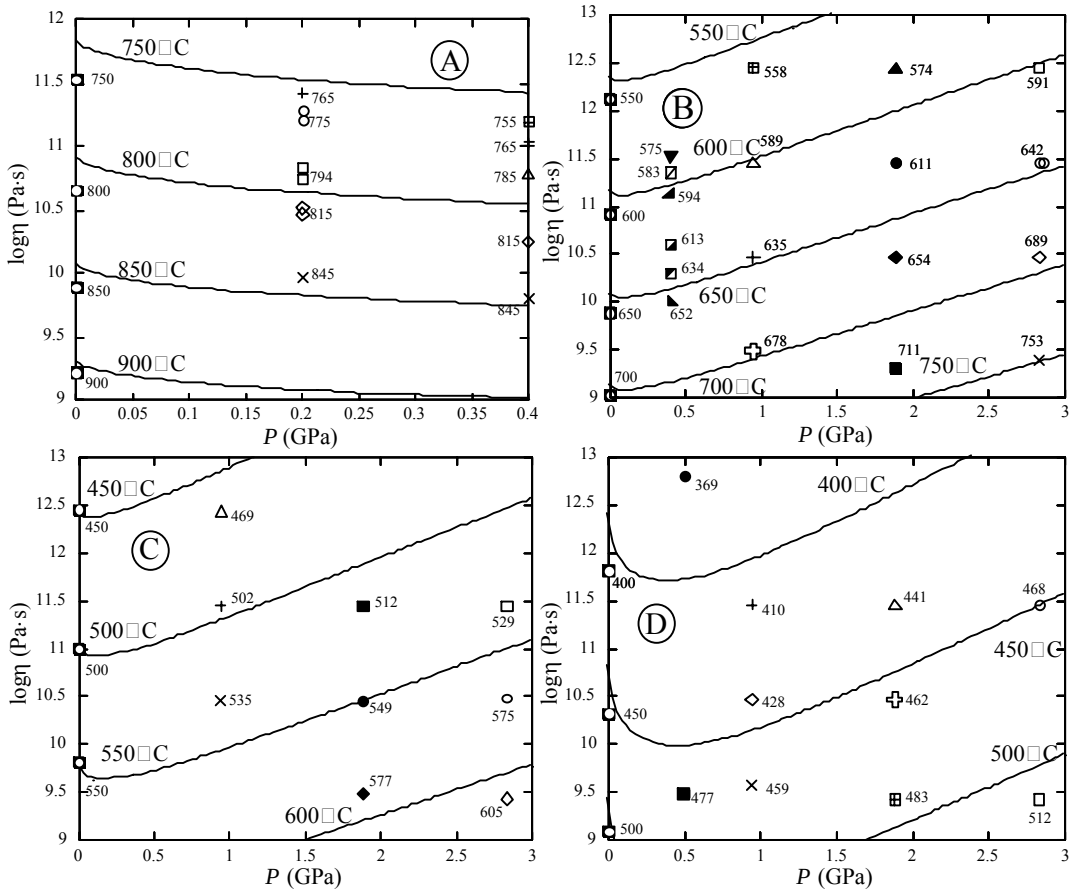

Fig. 4.7 Pressure effect on viscosity at some temperatures and water concentrations. The curves (with temperature indicated by large numbers) are calculated from Eq. (7) with different water concentrations: (A) 0.13 wt%, (B) 0.8 wt%, (C) 2 wt% and (D) 4 wt%. Points are experimental data at indicated temperatures (small numbers) and points at 0.1 MPa are calculated from the viscosity model of Zhang et al. (2003).

pressure. Fig. 4.8 shows pressure dependence of glass transition temperatures of hydrous rhyolitic melts containing different water contents calculated from Eq. (7) with a cooling rate of 0.28 K/s = 16.8 K/min (at $\eta = 10^{12}$ Pa·s). The trend of pressure dependence of the glass transition temperature (Fig. 4.8) is the same as that of viscosity (Fig. 4.7).

4.3. AN APPARENT PARADOX OF THE PRESSURE EFFECT ON VISCOSITY AND ON GLASS FORMATION

Appendix 4 lists the melt compositions, the experimental conditions and whether the sample charges crystallized significantly during experiments. Pressure facilitates crystallization in both isothermal experiments and cooling experiments based on the results in Appendix 4 as summarized in the Experimental results. That is, as pressure increases, crystallization is more rapid in isothermal experiments, and it is also more difficult to quench the same hydrous melt into glass from liquid. One might expect that the increased easiness of crystallization at high pressures were related to increasing diffusivity and hence decreasing viscosity with increasing pressure. However, new viscosity data show that viscosity of hydrous rhyolitic melt increases, rather than decreases, with increasing pressure. Hence, there is an apparent paradox of increasing viscosity as well as increased easiness of crystallization with increasing pressure.

Raising the pressure increases the density of the melt and changes the structure of the melt, which might facilitate crystallization. More importantly, increasing the pressure raises the liquidus of the melt. Hence, for a supercooled metastable liquid at a given temperature, the degree of undercooling is larger at higher pressure. That is, the Gibbs free energy difference between the melt and the crystals, $\Delta G_{m\text{-}c}$, increases with pressure.

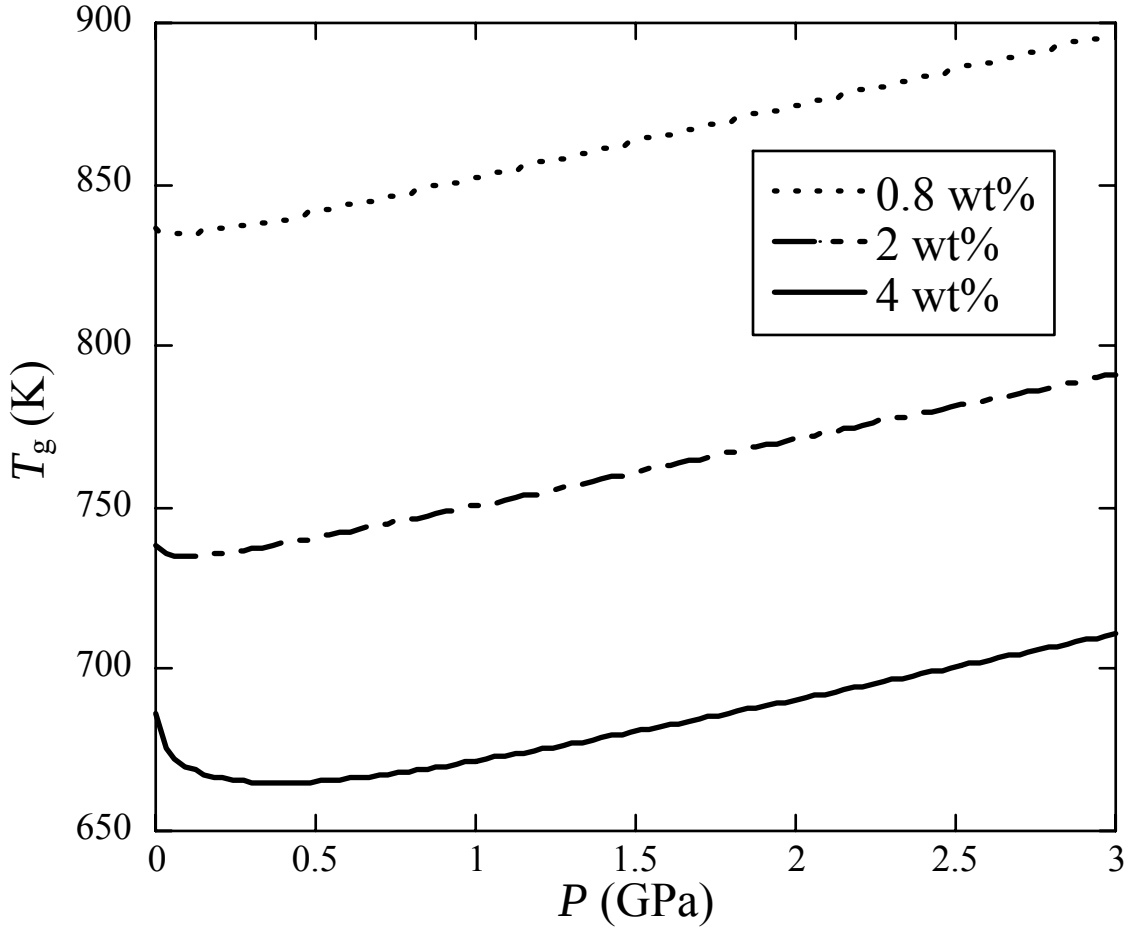

Fig. 4.8 Pressure dependence of glass transition temperatures of hydrous rhyolitic melts with different water contents (0.8, 2 and 4 wt% H_2O) calculated from Eq. (7) when $\eta = 10^{12}$ Pa·s (i.e., cooling rate is 0.28 K/s).

The increased easiness of crystallization at isothermal conditions may be partly attributed to greater $\Delta G_{m\text{-}c}$, although quantification is not available at the moment.

For cooling of a liquid from a temperature above the liquidus, as the pressure increases, the liquidus is crossed at a higher temperature. That is, crystallization starts at a higher temperature, where kinetics is more rapid. Furthermore, there is a larger temperature interval (and hence a larger time interval) for crystallization. Hence, more crystallization is expected. For this case, the glass-forming ability (that is, the degree of difficulty of crystallization) has been proposed recently using the concept of fragility (e.g., Martinez and Angell, 2001; Senkov, 2007). If the temperature dependence of viscosity is Arrhenian from low to high viscosity (0.01 to 10^{15} Pa·s), the liquid is said to be strong. If the temperature dependence of viscosity deviates from Arrhenian behavior more, the liquid is said to be more fragile. It is easier for strong liquids to quench to glass. Senkov (2007) defined a dimensionless glass forming ability (GFA) parameter F_1, which can be expressed as follows:

$$F_1 = \frac{2(T_g - T_0)}{2(T_g - T_0) + (T_L - T_g)}, \tag{8}$$

where T_L is the liquidus, T_g is the temperature at which the viscosity is 10^{12} Pa·s, and T_0 (related to fragility) is the temperature in the VFT equation of $\log\eta = A + B/(T\text{-}T_0)$. Senkov (2007) further related the critical cooling rate required for glass formation to the GFA parameter as follows:

$$q_c = 10^{(0.54\text{-}F_1)/0.047}. \tag{9}$$

If the cooling rate is above q_c, the liquid would be cooled into a glass. Otherwise, there would be significant crystallization. In order to apply the above approach, T_L as a

function of H_2O_t and P was estimated from the MELTS program (Ghiorso and Sack, 1995; Asimow and Ghiorso, 1998), and T_g from the viscosity model developed in this work (i.e., Eq. 7). For T_0 at low pressures, the viscosity model of Zhang et al. (2003) is used, which resulted in T_0 of 300±30 K for H_2O_t > 0.6 wt%. For viscosities of hydrous rhyolitic melt at high pressures, there are not enough data in the low-viscosity range to estimate T_0. Hence, a constant T_0 of 300 K was assumed to roughly estimate F_1 and q_c. The critical cooling rate as a function of pressure for a few H_2O_t contents is plotted in Fig. 4.4b. It can be seen that the limited experimental data are in agreement with this approach. Hence, it appears that the paradox of increased easiness of crystallization at high pressures and increasing viscosity with pressure can be reconciled by the GFA parameter of Senkov (2007).

5. CONCLUDING REMARKS

Viscosity of hydrous rhyolitic melts containing 0.8 to 4 wt% water was inferred using the hydrous species reaction viscometer at pressures up to 2.83 GPa. This represents the first viscosity data at low temperature (high viscosity) and pressures above 1 GPa. Viscosity of rhyolitic melts with 0.13 wt% and 0.8 wt% water was also measured using the parallel plate creep viscometer at pressures up to 0.4 GPa. No experimental method is available to determine viscosity of "dry" melt at higher pressures. Combining the data of this study with literature data, a viscosity model is constructed as a function of temperature, pressure, and water content in the high viscosity range. The model (i.e., Eq. 7) can be utilized for interpolation within the range of available data (Fig. 4.6), but is not recommended for extrapolation.

REFERENCES

Akella, J., Ganguly, J., Grover, R., and Kennedy, G. (1973) Melting of lead and zinc to 60 kbar. *J. Phys. Chem. Solids* **34**, 631-636.

Asimow, P.D. and Ghiorso, M.S. (1998) Algorithmic modifications extending MELTS to calculate subsolidus phase relations. *Am. Mineral.* **83**, 1127-1131.

Behrens, H. and Nowak, M. (2003) Quantification of H_2O speciation in silicate glasses and melts by IR spectroscopy – *in situ* versus quench techniques. *Phase Trans.* **76**, 45-61.

Behrens, H. and Schulze, F. (2003) Pressure dependence of melt viscosity in the system $NaAlSi_3O_8$-$CaMgSi_2O_6$. *Am. Mineral.* **88**, 1351-1363.

Behrens, H. and Zhang, Y. (2001) Ar diffusion in hydrous rhyolitic and albitic glasses/melts. *Earth Planet. Sci. Lett.* **192**, 363-376.

Behrens, H., Zhang, Y., and Xu, Z. (2004) H_2O diffusion in dacitic and andesitic melts. *Geochim. Cosmochim. Acta* **68**, 5139-5150.

Behrens, H., Zhang, Y., Leschik, M. Wiedenbeck, M., Heide, G., and Frischat, G.H. (2007) Molecular H_2O as carrier for oxygen diffusion in hydrous silicate melts. *Earth Planet. Sci. Lett.* **254**, 69-76.

Dingwell, D. (1986) Viscosity-temperature relationships in the system $Na_2Si_2O_5$-$Na_4Al_2O_5$. *Geochim. Cosmochim. Acta* **50**, 1261-1265.

Dingwell, D.B. (1998) Melt viscosity and diffusion under elevated pressures. *Rev. Mineral.* **37**, 397-422.

Dingwell, D.B. and Webb, S.L. (1990) Relaxation in silicate melts. *Eur. J. Mineral.* **2**, 427-449.

Dorfman, A., Dingwell, D.B., and Bagdassarov, N.S. (1997) A rotating autoclave for centrifuge studies: Falling sphere viscometry. *Eur. J. Mineral.* **9**, 345-350.

Dorfman, A., Hess, K.-U., and Dingwell, D.B. (1996) Centrifuge-assisted falling sphere viscometry. *Eur. J. Mineral.* **8**, 507-514.

Funakoshi, K.-i., Suzuki, A., and Terasaki, H. (2002) In situ viscosity measurements of albite melt under high pressure. *J. Phys. Condensed Matt.* **14**, 11343-11347.

Ghiorso, M.S. and Sack, R.O. (1995) Chemical mass transfer in magmatic processes. IV. A revised and internally consistent thermodynamic model for the interpolation and extrapolation of liquid-solid equilibria in magmatic systems at elevated temperatures and pressures. *Contrib. Mineral. Petrol.* **119**, 197-212.

Hui, H. and Zhang, Y. (2007) Toward a general viscosity equation for natural anhydrous and hydrous silicate melts. *Geochim. Cosmochim. Acta* **71**, 403-416.

Hui, H., Zhang, Y., Xu, Z., and Behrens, H. (2008) Pressure dependence of the speciation of dissolved water in rhyolitic melts. *Geochim. Cosmochim. Acta*. In revision.

Hummel, W. and Arndt, J. (1985) Variation of viscosity with temperature and composition in the plagioclase system. *Contrib. Mineral. Petrol.* **90**, 83-92.

Ihinger, P.D., Zhang, Y., and Stolper, E.M. (1999) The speciation of dissolved water in rhyolitic melt. *Geochim. Cosmochim. Acta* **63**, 3567-3578.

Kushiro, I. (1976) Changes in viscosity and structure of melt of $NaAlSi_2O_6$ composition at high pressures. *J. Geophys. Res.* **81**, 6347-6350.

Kushiro, I. (1978) Density and viscosity of hydrous calc-alkalic andesite magma at high pressures. *Carnegie Inst. Washington Year Book* **77**, 675-677.

Kushiro, I., Yoder, H.S. Jr., and Myson, B.O. (1976) Viscosities of basalt and andesite melts at high pressures. *J. Geophys. Res.* **81**, 6351-6356.

Lange, R.A. (1994) The effect of H_2O, CO_2 and F on the density and viscosity of silicate melts. *Rev. Mineral.* **30**, 331-365.

Lees, J. and Williamson, B.H.J. (1965) Combined very high pressure/high temperature calibration of the tetrahedral anvil apparatus, fusion curves of zinc, aluminium, germanium and silicon to 60 kilobars. *Nature* **208**, 278-279.

Liebske, C., Behrens, H., Holtz, F., and Lange, R.A. (2003) The influence of pressure and composition on the viscosity of andesitic melts. *Geochim. Cosmochim. Acta* **67**, 473-485.

Liebske, C., Schmickler, B., Terasaki, H., Poe, B.T., Suzuki, A., Funakoshi, K.-i., Ando, R., and Rubie, D.C. (2005) Viscosity of peridotite liquid up to 13 GPa: Implications for magma ocean viscosities. *Earth Planet. Sci. Lett.* **240**, 589-604.

Lillie, H.R. (1931) Viscosity of glass between the strain point and melting temperature. *J. Am. Ceram. Soc.* **14**, 502-512.

Liu, Y. and Zhang, Y. (2000) Bubble growth in rhyolitic melt. *Earth Planet. Sci. Lett.* **181**, 251-264.

Liu, Y., Behrens, H., and Zhang, Y. (2004a) The speciation of dissolved H_2O in dacitic melt. *Am. Mineral.* **89**, 277-284.

Liu, Y., Zhang, Y., and Behrens, H. (2004b) H_2O diffusion in dacitic melt. *Chem. Geol.* **209**, 327-340.

Liu, Y., Zhang, Y., and Behrens, H. (2005) Solubility of H_2O in rhyolitic melts at low pressures. *J. Volcanol. Geotherm. Res.* **143**, 219-235.

Martinez, L.-M. and Angell, C.A. (2001) A thermodynamic connection to the fragility of glass-forming liquids. *Nature* **410**, 663-667.

Moynihan, C.T., Easteal, A.J., Wilder, J., and Tucker, J. (1976) Dependence of the glass transition temperature on heating and cooling rate. *J. Phys. Chem.* **78**, 2673-2677.

Neuville, D.R. and Richet, P. (1991) Viscosity and mixing in molten (Ca, Mg) pyroxenes and garnets. *Geochim. Cosmochim. Acta* **55**, 1011-1019.

Neuville, D.R., Courtial, P., Dingwell, D.B., and Richet, P. (1993) Thermodynamic and rheological properties of rhyolite and andesite melts. *Contrib. Mineral. Petrol.* **113**, 572-581.

Newman, S., Stolper, E.M., and Epstein, S. (1986) Measurement of water in rhyolitic glasses: calibration of an infrared spectroscopic technique. *Am. Mineral.* **71**, 1527-1541.

Ni, H. and Zhang, Y. (2008) H_2O diffusion models in rhyolitic melt with new high pressure data. *Chem. Geol.* Revised.

Rapp, R.P. and Watson, E.B. (1995) Dehydration melting of metabasalt at 8-32 kbar: Implications for continental growth and crust-mantle recycling. *J. Petrol.* **36**, 891-931.

Reid, J. E., Suzuki, A., Funakoshi, K., Terasaki, H., Poe, B.T., Rubie, D.C., and Ohtani, E. (2003) The viscosity of $CaMgSi_2O_6$ liquid at pressures up to 13 GPa. *Phys. Earth Planet. Inter.* **139**, 45-54.

Richet, P., Lejeune, A.-M., Holtz, F., and Roux, J. (1996) Water and the viscosity of andesite melts. *Chem. Geol.* **128**, 185-197.

Rosenhauer, M., Scarfe, C.M., and Virgo, D. (1979) Pressure dependence of the glass transition temperature in glasses of diopside, albite, and sodium trisilicate composition. *Carnegie Inst. Washington Year Book* **78**, 556-559.

Rust, A.C. and Cashman, K.V. (2007) Multiple origins of obsidian pyroclasts and implications for changes in the dynamics of the 1300 B.P. eruption of Newberry Volcano, USA. *Bull. Volcanol.* **69**, 825-845.

Scarfe, C.M., Mysen, B.O., and Virgo, D. (1979) Changes in viscosity and density of melts of sodium disilicate, sodium metasilicate, and diopside composition with pressure. *Carnegie Inst. Washington Year Book* **78**, 547-551.

Scarfe,C.M., Mysen, B.O., and Virgo, D. (1987) Pressure dependence of the viscosity of silicate melts. In: Mysen, B.O. (ed) Magmatic Processes: Physicochemical Principles. *Geochem. Soc. Spec. Pub.* **1**, 59-67.

Scherer, G.W. (1984) Use of the Adam-Gibbs equation in the analysis of structural relaxation. *J. Am. Ceram. Soc.* **67**, 504-511.

Schulze, F., Behrens, H., and Hurkuck, W. (1999) Determination of the influence of pressure and dissolved water on the viscosity of highly viscous melts: Application of a new parallel-plate viscometer. *Am. Mineral.* **84**, 1512-1520.

Schulze, F., Behrens, H., Holtz, F., Roux, J., and Johannes, W. (1996) The influence of H_2O on the viscosity of a haplogranitic melt. *Am. Mineral.* **81**, 1155-1165.

Senkov, O.N. (2007) Correlation between fragility and glass-forming ability of metallic alloys. *Phys. Rev. B* **76**, 104202, DOI: 10.1103/PhysRevB.76.104202.

Shaw, H.R. (1963) Obsidian-H_2O viscosities at 1000 and 2000 bars in the temperature range 700° to 900°C. *J. Geophys. Res.* **68**, 6337-6343.

Shaw, H.R. (1972) Viscosities of magmatic silicate liquids: An empirical method of prediction. *Am. J. Sci.* **272**, 870-893.

Silver, L.A., Ihinger, P.D., and Stolper, E. (1990) The influence of bulk composition on the speciation of water in silicate glasses. *Contrib. Mineral. Petrol.* **104**, 142-162.

Stevenson, R.J., Dingwell, D.B., Webb, S.L., and Bagdassarov, N.S. (1995) The equivalence of enthalpy and shear stress relaxation in rhyolitic obsidians and quantification of the liquid-glass transition in volcanic processes. *J. Volcanol. Geotherm. Res.* **68**, 297-306.

Stolper, E.M. (1982a) The speciation of water in silicate melts. *Geochim. Cosmochim. Acta* **46**, 2609-2620.

Stolper, E.M. (1982b) Water in silicate glasses: an infrared spectroscopic study. *Contrib. Mineral. Petrol.* **81**, 1-17.

Sylvester, P.J. (1998) Post-collisional strongly peraluminous granites. *Lithos* **45**, 29-44.

Tinker, D., Lesher, C.E., Baxter, G.M., Uchida, T., and Wang, Y. (2004) High-pressure viscometry of polymerized silicate melts and limitations of the Eyring equation. *Am. Mineral.* **89**, 1701-1708.

Withers, A.C. and Behrens, H. (1999) Temperature-induced changes in the NIR spectra of hydrous albitic and rhyolitic glasses between 300 and 100 K. *Phys. Chem. Minerals* **27**, 119-132.

Xu, Z. and Zhang, Y. (2002) Quench rates in air, water, and liquid nitrogen, and inference of temperature in volcanic eruption columns. *Earth Planet. Sci. Lett.* **200**, 315-330.

Zhang, Y. (1994) Reaction kinetics, geospeedometry, and relaxation theory. *Earth Planet. Sci. Lett.* **122**, 373-391.

Zhang, Y. (1999) H_2O in rhyolitic glasses and melts: Measurement, speciation, solubility, and diffusion. *Rev. Geophys.* **37**, 493-516.

Zhang, Y. and Behrens, H. (2000) H_2O diffusion in rhyolitic melts and glasses. *Chem. Geol.* **169**, 243-262.

Zhang, Y., Belcher, R., Ihinger P.D., Wang, L., Xu, Z., and Newman, S. (1997a) New calibration of infrared measurement of dissolved water in rhyolitic glasses. *Geochim. Cosmochim. Acta* **61**, 3089-3100.

Zhang, Y., Jenkins, J., and Xu, Z. (1997b) Kinetics of the reaction H2O + O ⇔ 2OH in rhyolitic glasses upon cooling: Geospeedometry and comparison with glass transition. *Geochim. Cosmochim. Acta* **61**, 2167-2173.

Zhang, Y., Xu, Z., and Behrens, H. (2000) Hydrous species geospeedometer in rhyolite: Improved calibration and application. *Geochim. Cosmochim. Acta* **64**, 3347-3355.

Zhang, Y., Xu., Z., and Liu, Y. (2003) Viscosity of hydrous rhyolitic melts inferred from kinetic experiments, and a new viscosity model. *Am. Mineral.* **88**, 1741-1752.

Zhang,Y., and Xu, Z. (2007) A long-duration experiment on hydrous species geospeedometer and hydrous melt viscosity. *Geochim. Cosmochim. Acta* **71**, 5226-5232.

CHAPTER V

CONCLUSIONS

The goal of this dissertation is to understand viscosity of natural silicate melts. A two-pronged approach is used. One is to construct a general viscosity model using available viscosity data (mostly at pressures below 0.5 GPa) to predict viscosity of all natural silicate melts in all experimental temperature range at low pressures. The second is to experimentally investigate viscosity at high pressures and in the low temperature range (high viscosity range) because such data are lacking. Concerted effort on viscosity measurements at high pressures will allow an even more general viscosity model accounting for the effect of composition, temperature, and pressure.

A new empirical viscosity equation for all natural and nearly natural silicate melts at all experimentally covered temperature conditions is presented in Chapter II using the following formulation:

$$\log \eta = A + \frac{B}{T} + \exp\left(C + \frac{D}{T}\right),$$

where η is viscosity in Pa·s, T is temperature in K, and A, B, C, and D are linear functions of mole fractions of oxide components except for H_2O. The formulation is first applied successfully to fit the temperature and compositional dependence of viscosity for four binary systems. Then, a simpler version of the model with eight parameters is found to fit

the compositional and temperature dependence of the viscosity data of anhydrous natural silicate melts better than the best model in literature. A general viscosity equation with 37 parameters using this empirical formulation can fit the entire high- and low-temperature viscosity database (1451 data points) of all "natural" anhydrous and hydrous silicate melts:

$$\begin{aligned}\log\eta = &\left[-6.83X_{SiO_2} - 170.79X_{TiO_2} - 14.71X_{Al_2O_{3ex}} - 18.01X_{MgO} - 19.76X_{CaO}\right.\\ &\left.+34.31X_{(Na,\,K)_2O_{ex}} - 140.38Z + 159.26X_{H_2O} - 8.43X_{(Na,\,K)AlO_2}\right]\\ &+\left[18.14X_{SiO_2} + 248.93X_{TiO_2} + 32.61X_{Al_2O_{3ex}} + 25.96X_{MgO} + 22.64X_{CaO}\right.\\ &\left.-68.29X_{(Na,\,K)_2O_{ex}} + 38.84Z - 48.55X_{H_2O} + 16.12X_{(Na,\,K)AlO_2}\right]1000/T +\\ &\exp\left\{\left[21.73X_{Al_2O_{3ex}} - 61.98X_{(Fe,\,Mn)O} - 105.53X_{MgO} - 69.92X_{CaO}\right.\right.\\ &\left.-85.67X_{(Na,\,K)_2O_{ex}} + 332.01Z - 432.22X_{H_2O} - 3.16X_{(Na,\,K)AlO_2}\right]\\ &+\left[2.16X_{SiO_2} - 143.05X_{TiO_2} - 22.10X_{Al_2O_{3ex}} + 38.56X_{(Fe,\,Mn)O} + 110.83X_{MgO} + 67.12X_{CaO}\right.\\ &\left.\left.+58.01X_{(Na,\,K)_2O_{ex}} + 384.77X_{P_2O_5} - 404.97Z + 513.75X_{H_2O}\right]1000/T\right\}\end{aligned},$$

where η is viscosity in Pa·s, T is temperature in K, X_i means mole fraction of oxide component i, and $Z=(X_{H2O})^{1/[1+(185.797/T)]}$. Al_2O_{3ex} or $(Na, K)_2O_{ex}$ mean excess oxide after forming $(Na, K)AlO_2$. The 2σ deviation of the fit is 0.61 logη units. This general model can be used to calculate viscosity for modeling magma chamber processes and volcanic eruptions. It also can be used to calculate glass transition temperature for different silicate melts.

Temperature and melt composition affect melt viscosity, but pressure can also affect the viscosity of silicate melt. The pressure dependence of hydrous melt viscosity in the high viscosity range is not known. Hence the pressure dependence of rhyolitic melts in the high viscosity range has been investigated in this dissertation (Chapters III and IV). Hydrous species reaction viscometer in piston cylinder and parallel-plate creep viscometer in internally heated pressure vessel were used to investigate viscosity under

high pressure. In order to use hydrous species reaction viscometer under high pressure, it is necessary to study the speciation of dissolved water in rhyolitic melt under high pressure first.

The equilibrium of reaction between two dissolved water species (H_2O_m and OH) as a function of pressure (0.0001, 0.94, 1.89 and 2.83 GPa), temperature (624-1027 K), and H_2O concentrations (0.8% to 4.2 wt%) was investigated in this study. The speciation data with total H_2O content ≤ 2.2% can be described by an ideal mixing model, consistent with previous results. With inclusion of speciation data at higher water contents, one way to describe the speciation data is a regular solution model. A speciation model was constructed to accommodate the dependence of H_2O speciation in the rhyolitic melts on *T-P-X*:

$$\ln K = (1.8120 - 0.3832P) + \frac{1000}{T}\left((-3.0830 + 0.2999P + 0.0507P^{\frac{3}{2}}) + \right.$$
$$\left. (-7.4203 + 5.0262P - 3.1271P^{\frac{3}{2}})X_{H_2O_m} + (3.0437 - 5.4527P + 3.0464P^{\frac{3}{2}})X_{OH} \right),$$

where *P* is pressure in GPa, *T* is temperature in K and *X* is mole fraction of species H_2O_m or OH. This formulation can be used to predict species concentrations at P ≤ 2.83 GPa, total H_2O content ≤ 4.2 wt%, and temperature of 624-1027 K. Furthermore, it can be used to calculate apparent equilibrium temperature, which can then be used to infer viscosity of hydrous rhyolitic melts under high pressure. The results of Chapter III provide basis for the study of Chapter IV.

With the study of the speciation of dissolved water in rhyolitic melt under high pressure, viscosity of hydrous rhyolitic melts containing 0.8 to 4 wt% water was inferred using the hydrous species reaction viscometer at pressures up to 2.83 GPa. Viscosity of

rhyolitic melts with 0.13 wt% and 0.8 wt% water was also measured using the parallel plate creep viscometer at pressures up to 0.4 GPa, but no experiment method is available to determine viscosity of "dry" melt at pressures > 0.5 GPa. Combining the data of this study with previous data, an Arrhenian viscosity model in high viscosity range is constructed:

$$\begin{aligned}\log\eta = &\left(-7.8470+1.1472P^{\frac{1}{2}}\right)+\\ &\left(-12.4257+0.8080P^{\frac{1}{2}}\right)\left(1-\exp\left(-3.6440-10.1893P^{\frac{1}{2}}\right)x\right)+\\ &\left(\left(21.3531-2.1722P^{\frac{1}{2}}\right)+\right.\\ &\left.\left(-5.8335+4.0480P^{\frac{1}{2}}\right)\left(1-\exp\left(-89.3887-30.5499P^{\frac{1}{2}}\right)x\right)\right)1000/T\end{aligned},$$

where P is pressure in GPa, and X is mole fraction of total water content in the melt. This model can be utilized for interpolation, but is not recommended for extrapolation beyond the range of available data (Figure 4.6 in Chapter IV).

APPENDICES

APPENDIX A

VISCOSITY DATA OF NATURAL SILICATE MELTS

The viscosity data on the following pages are used to fit Eqn. 11 in Chapter II. The reference numbers of all the viscosity data points is the same as the ones in Table 2.3.

Table A.1 Viscosity database used to fit Eqn. 11.

#	Comp.	SiO_2 wt%	TiO_2 wt%	Al_2O_3 wt%	FeO_t wt%	MnO wt%	MgO wt%	CaO wt%	Na_2O wt%	K_2O wt%	P_2O_5 wt%	H_2O wt%	T K	measured logη Pa·s	calculated logη Pa·s	Δ	ref
1	Bn3	43.57	2.97	10.18	0	0	9.17	26.07	7.59	0.96	0	0.02	1573	0.41	0.02	-0.39	1
2	Bn3	43.57	2.97	10.18	0	0	9.17	26.07	7.59	0.96	0	0.02	977.4	9.16	9.17	0.01	1
3	Bn3	43.57	2.97	10.18	0	0	9.17	26.07	7.59	0.96	0	0.02	982.9	8.94	9.03	0.09	1
4	Bn3	43.57	2.97	10.18	0	0	9.17	26.07	7.59	0.96	0	0.02	992.7	8.66	8.77	0.11	1
5	Bn3	43.57	2.97	10.18	0	0	9.17	26.07	7.59	0.96	0	0.02	886.5	13.7	13.68	-0.02	1
6	Bn3	43.57	2.97	10.18	0	0	9.17	26.07	7.59	0.96	0	0.02	892.3	13.4	13.07	-0.33	1
7	Bn3	43.57	2.97	10.18	0	0	9.17	26.07	7.59	0.96	0	0.02	899.2	12.99	12.47	-0.52	1
8	Bn3	43.57	2.97	10.18	0	0	9.17	26.07	7.59	0.96	0	0.02	912.1	12.22	11.6	-0.62	1
9	Bn3	43.57	2.97	10.18	0	0	9.17	26.07	7.59	0.96	0	0.02	913.6	12.16	11.51	-0.65	1
10	Bn3	43.57	2.97	10.18	0	0	9.17	26.07	7.59	0.96	0	0.02	918.7	11.83	11.24	-0.59	1
11	Bn3	43.57	2.97	10.18	0	0	9.17	26.07	7.59	0.96	0	0.02	924.2	11.56	10.97	-0.59	1

12	Bn3	43.57	2.97	10.18	0	0	9.17	26.07	7.59	0.96	0	0.02	929.2	11.26	10.75	-0.51	1
13	Bn3	43.57	2.97	10.18	0	0	9.17	26.07	7.59	0.96	0	0.02	934.1	11.04	10.55	-0.49	1
14	Bn3	43.57	2.97	10.18	0	0	9.17	26.07	7.59	0.96	0	0.02	940.9	10.75	10.3	-0.45	1
15	Bn3	43.57	2.97	10.18	0	0	9.17	26.07	7.59	0.96	0	0.02	944.7	10.51	10.16	-0.35	1
16	Bn3	43.57	2.97	10.18	0	0	9.17	26.07	7.59	0.96	0	0.02	952.8	10.17	9.89	-0.28	1
17	Bn3	43.57	2.97	10.18	0	0	9.17	26.07	7.59	0.96	0	0.02	958.2	9.93	9.72	-0.21	1
18	Bn3	43.57	2.97	10.18	0	0	9.17	26.07	7.59	0.96	0	0.02	959.5	9.88	9.68	-0.2	1
19	Bn3	43.57	2.97	10.18	0	0	9.17	26.07	7.59	0.96	0	0.02	966.4	9.57	9.48	-0.09	1
20	Bn3	43.57	2.97	10.18	0	0	9.17	26.07	7.59	0.96	0	0.02	972	9.35	9.32	-0.03	1
21	Bn3	43.57	2.97	10.18	0	0	9.17	26.07	7.59	0.96	0	0.68	845.8	12.2	11.9	-0.3	1
22	Bn3	43.57	2.97	10.18	0	0	9.17	26.07	7.59	0.96	0	0.68	851.1	11.95	11.58	-0.37	1
23	Bn3	43.57	2.97	10.18	0	0	9.17	26.07	7.59	0.96	0	0.68	856	11.64	11.31	-0.33	1
24	Bn3	43.57	2.97	10.18	0	0	9.17	26.07	7.59	0.96	0	0.68	867.1	11.13	10.76	-0.37	1
25	Bn3	43.57	2.97	10.18	0	0	9.17	26.07	7.59	0.96	0	0.68	872.1	10.91	10.53	-0.38	1
26	Bn3	43.57	2.97	10.18	0	0	9.17	26.07	7.59	0.96	0	0.68	877.3	10.66	10.32	-0.34	1
27	Bn3	43.57	2.97	10.18	0	0	9.17	26.07	7.59	0.96	0	0.68	887.8	10.25	9.91	-0.34	1
28	Bn3	43.57	2.97	10.18	0	0	9.17	26.07	7.59	0.96	0	1	819.3	12.15	12.3	0.15	1
29	Bn3	43.57	2.97	10.18	0	0	9.17	26.07	7.59	0.96	0	1	826.9	11.76	11.82	0.06	1
30	Bn3	43.57	2.97	10.18	0	0	9.17	26.07	7.59	0.96	0	1	834.2	11.35	11.41	0.06	1
31	Bn3	43.57	2.97	10.18	0	0	9.17	26.07	7.59	0.96	0	1	840.9	11.08	11.06	-0.02	1
32	Bn3	43.57	2.97	10.18	0	0	9.17	26.07	7.59	0.96	0	1	845.6	10.84	10.84	0	1
33	Bn3	43.57	2.97	10.18	0	0	9.17	26.07	7.59	0.96	0	1	851.6	10.55	10.57	0.02	1
34	Bn3	43.57	2.97	10.18	0	0	9.17	26.07	7.59	0.96	0	1	856.3	10.35	10.37	0.02	1
35	Bn3	43.57	2.97	10.18	0	0	9.17	26.07	7.59	0.96	0	1	861.5	10.13	10.16	0.03	1
36	Bn3	43.57	2.97	10.18	0	0	9.17	26.07	7.59	0.96	0	1.26	800	12.38	12.59	0.21	1
37	Bn3	43.57	2.97	10.18	0	0	9.17	26.07	7.59	0.96	0	1.26	803.2	12.07	12.37	0.3	1
38	Bn3	43.57	2.97	10.18	0	0	9.17	26.07	7.59	0.96	0	1.26	809.5	11.88	11.98	0.1	1
39	Bn3	43.57	2.97	10.18	0	0	9.17	26.07	7.59	0.96	0	1.26	814.1	11.59	11.71	0.12	1
40	Bn3	43.57	2.97	10.18	0	0	9.17	26.07	7.59	0.96	0	1.26	820.6	11.36	11.36	0	1
41	Bn3	43.57	2.97	10.18	0	0	9.17	26.07	7.59	0.96	0	1.26	825.3	11.11	11.12	0.01	1
42	Bn3	43.57	2.97	10.18	0	0	9.17	26.07	7.59	0.96	0	1.26	830.5	10.86	10.88	0.02	1
43	Bn3	43.57	2.97	10.18	0	0	9.17	26.07	7.59	0.96	0	1.26	835.9	10.6	10.63	0.03	1

44	Bn3	43.57	2.97	10.18	0	0	9.17	26.07	7.59	0.96	0	1.26	841	10.39	10.42	0.03	1
45	Bn3	43.57	2.97	10.18	0	0	9.17	26.07	7.59	0.96	0	1.26	845.7	10.18	10.23	0.05	1
46	Bn3	43.57	2.97	10.18	0	0	9.17	26.07	7.59	0.96	0	1.35	794.5	12.33	12.62	0.29	1
47	Bn3	43.57	2.97	10.18	0	0	9.17	26.07	7.59	0.96	0	1.35	805.1	11.92	11.95	0.03	1
48	Bn3	43.57	2.97	10.18	0	0	9.17	26.07	7.59	0.96	0	1.35	820.4	11.02	11.14	0.12	1
49	Bn3	43.57	2.97	10.18	0	0	9.17	26.07	7.59	0.96	0	1.35	828.4	10.76	10.76	0	1
50	Bn3	43.57	2.97	10.18	0	0	9.17	26.07	7.59	0.96	0	1.35	836.2	10.34	10.43	0.09	1
51	Bn3	43.57	2.97	10.18	0	0	9.17	26.07	7.59	0.96	0	1.88	761.7	12.3	12.97	0.67	1
52	Bn3	43.57	2.97	10.18	0	0	9.17	26.07	7.59	0.96	0	1.88	802.3	10.72	10.83	0.11	1
53	Bn3	43.57	2.97	10.18	0	0	9.17	26.07	7.59	0.96	0	1.96	779.4	11.57	11.75	0.18	1
54	Te2	50.56	2.35	14.03	0	0	8.79	15	7.04	3.01	0	0.02	1413.9	1.96	2.94	0.98	1
55	Te2	50.56	2.35	14.03	0	0	8.79	15	7.04	3.01	0	0.02	1463.5	1.65	2.39	0.74	1
56	Te2	50.56	2.35	14.03	0	0	8.79	15	7.04	3.01	0	0.02	1497.5	1.45	2.03	0.58	1
57	Te2	50.56	2.35	14.03	0	0	8.79	15	7.04	3.01	0	0.02	1513.2	1.38	1.87	0.49	1
58	Te2	50.56	2.35	14.03	0	0	8.79	15	7.04	3.01	0	0.02	1565	1.13	1.36	0.23	1
59	Te2	50.56	2.35	14.03	0	0	8.79	15	7.04	3.01	0	0.02	1614.4	0.91	0.91	0	1
60	Te2	50.56	2.35	14.03	0	0	8.79	15	7.04	3.01	0	0.02	1666.2	0.7	0.47	-0.23	1
61	Te2	50.56	2.35	14.03	0	0	8.79	15	7.04	3.01	0	0.02	1718.6	0.5	0.04	-0.46	1
62	Te2	50.56	2.35	14.03	0	0	8.79	15	7.04	3.01	0	0.02	976.3	9.93	10.52	0.59	1
63	Te2	50.56	2.35	14.03	0	0	8.79	15	7.04	3.01	0	0.02	983.1	9.71	10.32	0.61	1
64	Te2	50.56	2.35	14.03	0	0	8.79	15	7.04	3.01	0	0.02	986.7	9.57	10.21	0.64	1
65	Te2	50.56	2.35	14.03	0	0	8.79	15	7.04	3.01	0	0.02	992.1	9.3	10.06	0.76	1
66	Te2	50.56	2.35	14.03	0	0	8.79	15	7.04	3.01	0	0.02	997.2	9.18	9.93	0.75	1
67	Te2	50.56	2.35	14.03	0	0	8.79	15	7.04	3.01	0	0.02	1008.1	8.73	9.64	0.91	1
68	Te2	50.56	2.35	14.03	0	0	8.79	15	7.04	3.01	0	0.02	918	12.85	12.94	0.09	1
69	Te2	50.56	2.35	14.03	0	0	8.79	15	7.04	3.01	0	0.02	930.7	12.05	12.25	0.2	1
70	Te2	50.56	2.35	14.03	0	0	8.79	15	7.04	3.01	0	0.02	934.1	11.86	12.09	0.23	1
71	Te2	50.56	2.35	14.03	0	0	8.79	15	7.04	3.01	0	0.02	946.4	11.32	11.56	0.24	1
72	Te2	50.56	2.35	14.03	0	0	8.79	15	7.04	3.01	0	0.02	956.7	10.75	11.17	0.42	1
73	Te2	50.56	2.35	14.03	0	0	8.79	15	7.04	3.01	0	0.02	960.6	10.61	11.03	0.42	1
74	Te2	50.56	2.35	14.03	0	0	8.79	15	7.04	3.01	0	0.02	967.3	10.38	10.8	0.42	1
75	Te2	50.56	2.35	14.03	0	0	8.79	15	7.04	3.01	0	0.02	971.2	10.21	10.68	0.47	1

76	Te2	50.56	2.35	14.03	0	0	8.79	15	7.04	3.01	0	0.12	905	12.7	12.72	0.02	1
77	Te2	50.56	2.35	14.03	0	0	8.79	15	7.04	3.01	0	0.12	915.6	12.01	12.18	0.17	1
78	Te2	50.56	2.35	14.03	0	0	8.79	15	7.04	3.01	0	0.12	926.5	11.77	11.69	-0.08	1
79	Te2	50.56	2.35	14.03	0	0	8.79	15	7.04	3.01	0	0.12	937.4	11.2	11.26	0.06	1
80	Te2	50.56	2.35	14.03	0	0	8.79	15	7.04	3.01	0	0.12	947.8	10.67	10.9	0.23	1
81	Te2	50.56	2.35	14.03	0	0	8.79	15	7.04	3.01	0	0.12	958.9	10.23	10.54	0.31	1
82	Te2	50.56	2.35	14.03	0	0	8.79	15	7.04	3.01	0	0.12	968.4	9.87	10.25	0.38	1
83	Te2	50.56	2.35	14.03	0	0	8.79	15	7.04	3.01	0	0.52	868.4	12.49	12.38	-0.11	1
84	Te2	50.56	2.35	14.03	0	0	8.79	15	7.04	3.01	0	0.52	878.5	11.97	11.93	-0.04	1
85	Te2	50.56	2.35	14.03	0	0	8.79	15	7.04	3.01	0	0.52	889.8	11.57	11.48	-0.09	1
86	Te2	50.56	2.35	14.03	0	0	8.79	15	7.04	3.01	0	0.52	899	10.99	11.14	0.15	1
87	Te2	50.56	2.35	14.03	0	0	8.79	15	7.04	3.01	0	0.88	834.2	12.38	12.58	0.2	1
88	Te2	50.56	2.35	14.03	0	0	8.79	15	7.04	3.01	0	0.88	844	11.78	12.16	0.38	1
89	Te2	50.56	2.35	14.03	0	0	8.79	15	7.04	3.01	0	0.88	855.5	11.58	11.71	0.13	1
90	Te2	50.56	2.35	14.03	0	0	8.79	15	7.04	3.01	0	0.88	866.5	11.21	11.3	0.09	1
91	Te2	50.56	2.35	14.03	0	0	8.79	15	7.04	3.01	0	0.88	876.1	10.77	10.97	0.2	1
92	Te2	50.56	2.35	14.03	0	0	8.79	15	7.04	3.01	0	0.92	830.4	12.39	12.62	0.23	1
93	Te2	50.56	2.35	14.03	0	0	8.79	15	7.04	3.01	0	0.92	841.6	12.15	12.14	-0.01	1
94	Te2	50.56	2.35	14.03	0	0	8.79	15	7.04	3.01	0	0.92	851.8	11.63	11.74	0.11	1
95	Te2	50.56	2.35	14.03	0	0	8.79	15	7.04	3.01	0	0.92	862.1	11.43	11.36	-0.07	1
96	Te2	50.56	2.35	14.03	0	0	8.79	15	7.04	3.01	0	0.92	869.5	10.49	11.1	0.61	1
97	Te2	50.56	2.35	14.03	0	0	8.79	15	7.04	3.01	0	0.92	882.8	10.41	10.65	0.24	1
98	Te2	50.56	2.35	14.03	0	0	8.79	15	7.04	3.01	0	0.92	893.5	9.95	10.32	0.37	1
99	Te2	50.56	2.35	14.03	0	0	8.79	15	7.04	3.01	0	0.92	918	8.92	9.61	0.69	1
100	Te2	50.56	2.35	14.03	0	0	8.79	15	7.04	3.01	0	1.36	822	12.51	11.79	-0.72	1
101	Te2	50.56	2.35	14.03	0	0	8.79	15	7.04	3.01	0	1.36	832	11.89	11.44	-0.45	1
102	Te2	50.56	2.35	14.03	0	0	8.79	15	7.04	3.01	0	1.36	836.6	11.41	11.28	-0.13	1
103	Te2	50.56	2.35	14.03	0	0	8.79	15	7.04	3.01	0	1.36	847.5	11.12	10.91	-0.21	1
104	Te2	50.56	2.35	14.03	0	0	8.79	15	7.04	3.01	0	1.6	825.5	11.31	11.21	-0.1	1
105	Te2	50.56	2.35	14.03	0	0	8.79	15	7.04	3.01	0	1.6	816	12.13	11.53	-0.6	1
106	Te2	50.56	2.35	14.03	0	0	8.79	15	7.04	3.01	0	1.6	847	10.91	10.52	-0.39	1
107	Te2	50.56	2.35	14.03	0	0	8.79	15	7.04	3.01	0	2.27	818	10.79	10.46	-0.33	1

108	Te2	50.56	2.35	14.03	0	0	8.79	15	7.04	3.01	0	2.27	782.7	12.6	11.58	-1.02	1
109	Ph4	58.82	0.79	19.42	0	0	1.87	2.35	9.31	7.44	0	0.02	1815.5	1.92	1.5	-0.42	2
110	Ph4	58.82	0.79	19.42	0	0	1.87	2.35	9.31	7.44	0	0.02	1766	2.12	1.76	-0.36	2
111	Ph4	58.82	0.79	19.42	0	0	1.87	2.35	9.31	7.44	0	0.02	1721.9	2.33	2.01	-0.32	2
112	Ph4	58.82	0.79	19.42	0	0	1.87	2.35	9.31	7.44	0	0.02	1669.4	2.57	2.33	-0.24	2
113	Ph4	58.82	0.79	19.42	0	0	1.87	2.35	9.31	7.44	0	0.02	1617.4	2.86	2.66	-0.2	2
114	Ph4	58.82	0.79	19.42	0	0	1.87	2.35	9.31	7.44	0	0.02	973.3	10.39	10.04	-0.35	2
115	Ph4	58.82	0.79	19.42	0	0	1.87	2.35	9.31	7.44	0	0.02	990	9.97	9.7	-0.27	2
116	Ph4	58.82	0.79	19.42	0	0	1.87	2.35	9.31	7.44	0	0.02	1005.1	9.62	9.4	-0.22	2
117	Ph4	58.82	0.79	19.42	0	0	1.87	2.35	9.31	7.44	0	0.02	1015.2	9.38	9.21	-0.17	2
118	Ph4	58.82	0.79	19.42	0	0	1.87	2.35	9.31	7.44	0	0.02	1026.8	9.15	9	-0.15	2
119	Ph4	58.82	0.79	19.42	0	0	1.87	2.35	9.31	7.44	0	0.02	1034.8	8.97	8.86	-0.11	2
120	Ph4	58.82	0.79	19.42	0	0	1.87	2.35	9.31	7.44	0	0.02	1046.4	8.66	8.66	0	2
121	Ph4	58.82	0.79	19.42	0	0	1.87	2.35	9.31	7.44	0	0.02	889.2	13.12	12.06	-1.06	2
122	Ph4	58.82	0.79	19.42	0	0	1.87	2.35	9.31	7.44	0	0.02	898.2	12.71	11.81	-0.9	2
123	Ph4	58.82	0.79	19.42	0	0	1.87	2.35	9.31	7.44	0	0.02	911	12.25	11.48	-0.77	2
124	Ph4	58.82	0.79	19.42	0	0	1.87	2.35	9.31	7.44	0	0.02	920	11.96	11.25	-0.71	2
125	Ph4	58.82	0.79	19.42	0	0	1.87	2.35	9.31	7.44	0	0.02	932.2	11.55	10.95	-0.6	2
126	Ph4	58.82	0.79	19.42	0	0	1.87	2.35	9.31	7.44	0	0.02	941.5	11.29	10.74	-0.55	2
127	Ph4	58.82	0.79	19.42	0	0	1.87	2.35	9.31	7.44	0	0.02	952.3	10.94	10.49	-0.45	2
128	Ph4	58.82	0.79	19.42	0	0	1.87	2.35	9.31	7.44	0	0.02	962.5	10.67	10.27	-0.4	2
129	Ph4	58.82	0.79	19.42	0	0	1.87	2.35	9.31	7.44	0	1.46	730.8	12.02	11.47	-0.55	2
130	Ph4	58.82	0.79	19.42	0	0	1.87	2.35	9.31	7.44	0	1.46	740.6	11.54	11.21	-0.33	2
131	Ph4	58.82	0.79	19.42	0	0	1.87	2.35	9.31	7.44	0	1.46	750.1	11.21	10.96	-0.25	2
132	Ph4	58.82	0.79	19.42	0	0	1.87	2.35	9.31	7.44	0	1.46	761.7	10.91	10.67	-0.24	2
133	Ph4	58.82	0.79	19.42	0	0	1.87	2.35	9.31	7.44	0	1.46	782.3	10.31	10.17	-0.14	2
134	Ph4	58.82	0.79	19.42	0	0	1.87	2.35	9.31	7.44	0	1.52	730.3	12.03	11.39	-0.64	2
135	Ph4	58.82	0.79	19.42	0	0	1.87	2.35	9.31	7.44	0	1.52	741	11.79	11.1	-0.69	2
136	Ph4	58.82	0.79	19.42	0	0	1.87	2.35	9.31	7.44	0	1.52	761.7	10.92	10.57	-0.35	2
137	Ph4	58.82	0.79	19.42	0	0	1.87	2.35	9.31	7.44	0	1.52	780.9	10.4	10.11	-0.29	2
138	Ph4	58.82	0.79	19.42	0	0	1.87	2.35	9.31	7.44	0	2.15	676.4	12.34	12.01	-0.33	2
139	Ph4	58.82	0.79	19.42	0	0	1.87	2.35	9.31	7.44	0	2.15	683.5	11.97	11.79	-0.18	2

140	Ph4	58.82	0.79	19.42	0	0	1.87	2.35	9.31	7.44	0	2.15	691.4	11.67	11.55	-0.12	2
141	Ph4	58.82	0.79	19.42	0	0	1.87	2.35	9.31	7.44	0	2.15	702.6	11.39	11.23	-0.16	2
142	Ph4	58.82	0.79	19.42	0	0	1.87	2.35	9.31	7.44	0	2.15	717.6	10.89	10.81	-0.08	2
143	Ph4	58.82	0.79	19.42	0	0	1.87	2.35	9.31	7.44	0	2.15	727.9	10.53	10.53	0	2
144	Ph4	58.82	0.79	19.42	0	0	1.87	2.35	9.31	7.44	0	2.15	738.1	10.22	10.27	0.05	2
145	Ph4	58.82	0.79	19.42	0	0	1.87	2.35	9.31	7.44	0	2.15	747.9	10.05	10.03	-0.02	2
146	Ph4	58.82	0.79	19.42	0	0	1.87	2.35	9.31	7.44	0	2.83	654.1	12.14	11.83	-0.31	2
147	Ph4	58.82	0.79	19.42	0	0	1.87	2.35	9.31	7.44	0	2.83	664	11.76	11.52	-0.24	2
148	Ph4	58.82	0.79	19.42	0	0	1.87	2.35	9.31	7.44	0	2.83	675.1	11.37	11.18	-0.19	2
149	Ph4	58.82	0.79	19.42	0	0	1.87	2.35	9.31	7.44	0	2.83	685.9	10.9	10.86	-0.04	2
150	Ph4	58.82	0.79	19.42	0	0	1.87	2.35	9.31	7.44	0	2.83	704.3	10.35	10.35	0	2
151	Ph4	58.82	0.79	19.42	0	0	1.87	2.35	9.31	7.44	0	2.83	716.4	9.96	10.03	0.07	2
152	Ph4	58.82	0.79	19.42	0	0	1.87	2.35	9.31	7.44	0	4.72	587	12.37	12.21	-0.16	2
153	Ph4	58.82	0.79	19.42	0	0	1.87	2.35	9.31	7.44	0	4.72	601.3	11.77	11.68	-0.09	2
154	Tr6	64.45	0.5	16.71	0	0	2.92	5.36	6.7	3.37	0	0.02	1827.7	1.86	1.42	-0.44	2
155	Tr6	64.45	0.5	16.71	0	0	2.92	5.36	6.7	3.37	0	0.02	1776.5	2.09	1.73	-0.36	2
156	Tr6	64.45	0.5	16.71	0	0	2.92	5.36	6.7	3.37	0	0.02	1725.8	2.32	2.05	-0.27	2
157	Tr6	64.45	0.5	16.71	0	0	2.92	5.36	6.7	3.37	0	0.02	1677.8	2.56	2.38	-0.18	2
158	Tr6	64.45	0.5	16.71	0	0	2.92	5.36	6.7	3.37	0	0.02	1628.5	2.83	2.73	-0.1	2
159	Tr6	64.45	0.5	16.71	0	0	2.92	5.36	6.7	3.37	0	0.02	1578	3.12	3.12	0	2
160	Tr6	64.45	0.5	16.71	0	0	2.92	5.36	6.7	3.37	0	0.02	1531.7	3.41	3.5	0.09	2
161	Tr6	64.45	0.5	16.71	0	0	2.92	5.36	6.7	3.37	0	0.02	973.3	11.96	12.43	0.47	2
162	Tr6	64.45	0.5	16.71	0	0	2.92	5.36	6.7	3.37	0	0.02	981.8	11.67	12.12	0.45	2
163	Tr6	64.45	0.5	16.71	0	0	2.92	5.36	6.7	3.37	0	0.02	994.2	11.23	11.7	0.47	2
164	Tr6	64.45	0.5	16.71	0	0	2.92	5.36	6.7	3.37	0	0.02	998.4	11.14	11.56	0.42	2
165	Tr6	64.45	0.5	16.71	0	0	2.92	5.36	6.7	3.37	0	0.02	999.2	11.09	11.53	0.44	2
166	Tr6	64.45	0.5	16.71	0	0	2.92	5.36	6.7	3.37	0	0.02	1014.6	10.59	11.06	0.47	2
167	Tr6	64.45	0.5	16.71	0	0	2.92	5.36	6.7	3.37	0	0.02	1036.1	10.04	10.46	0.42	2
168	Tr6	64.45	0.5	16.71	0	0	2.92	5.36	6.7	3.37	0	0.02	1045	9.82	10.23	0.41	2
169	Tr6	64.45	0.5	16.71	0	0	2.92	5.36	6.7	3.37	0	0.02	1057.2	9.53	9.93	0.4	2
170	Tr6	64.45	0.5	16.71	0	0	2.92	5.36	6.7	3.37	0	0.02	1065.8	9.34	9.73	0.39	2
171	Tr6	64.45	0.5	16.71	0	0	2.92	5.36	6.7	3.37	0	0.02	1082.6	8.99	9.35	0.36	2

172	Tr6	64.45	0.5	16.71	0	0	2.92	5.36	6.7	3.37	0	0.02	1092	8.81	9.15	0.34	2
173	Tr6	64.45	0.5	16.71	0	0	2.92	5.36	6.7	3.37	0	0.02	1103.1	8.58	8.92	0.34	2
174	Tr6	64.45	0.5	16.71	0	0	2.92	5.36	6.7	3.37	0	0.02	1113.7	8.37	8.71	0.34	2
175	Tr6	64.45	0.5	16.71	0	0	2.92	5.36	6.7	3.37	0	0.02	1928.7	1.46	0.86	-0.6	2
176	Tr6	64.45	0.5	16.71	0	0	2.92	5.36	6.7	3.37	0	0.02	1879.6	1.64	1.13	-0.51	2
177	Tr6	64.45	0.5	16.71	0	0	2.92	5.36	6.7	3.37	0	0.02	951.1	12.77	13.31	0.54	2
178	Tr6	64.45	0.5	16.71	0	0	2.92	5.36	6.7	3.37	0	0.57	879.2	12.16	11.75	-0.41	2
179	Tr6	64.45	0.5	16.71	0	0	2.92	5.36	6.7	3.37	0	0.57	889.5	11.78	11.5	-0.28	2
180	Tr6	64.45	0.5	16.71	0	0	2.92	5.36	6.7	3.37	0	0.57	909.9	11.14	11.02	-0.12	2
181	Tr6	64.45	0.5	16.71	0	0	2.92	5.36	6.7	3.37	0	0.57	930.9	10.5	10.54	0.04	2
182	Tr6	64.45	0.5	16.71	0	0	2.92	5.36	6.7	3.37	0	0.57	942.2	10.24	10.29	0.05	2
183	Tr6	64.45	0.5	16.71	0	0	2.92	5.36	6.7	3.37	0	0.57	957.9	9.85	9.95	0.1	2
184	Tr6	64.45	0.5	16.71	0	0	2.92	5.36	6.7	3.37	0	0.57	965.9	9.6	9.78	0.18	2
185	Tr6	64.45	0.5	16.71	0	0	2.92	5.36	6.7	3.37	0	0.57	979.3	9.31	9.51	0.2	2
186	Tr6	64.45	0.5	16.71	0	0	2.92	5.36	6.7	3.37	0	0.57	989.3	9.08	9.3	0.22	2
187	Tr6	64.45	0.5	16.71	0	0	2.92	5.36	6.7	3.37	0	0.83	832.4	12.2	12.02	-0.18	2
188	Tr6	64.45	0.5	16.71	0	0	2.92	5.36	6.7	3.37	0	0.83	836.2	12.08	11.93	-0.15	2
189	Tr6	64.45	0.5	16.71	0	0	2.92	5.36	6.7	3.37	0	0.83	837.1	11.99	11.91	-0.08	2
190	Tr6	64.45	0.5	16.71	0	0	2.92	5.36	6.7	3.37	0	0.83	842.6	11.83	11.78	-0.05	2
191	Tr6	64.45	0.5	16.71	0	0	2.92	5.36	6.7	3.37	0	0.83	847.2	11.73	11.67	-0.06	2
192	Tr6	64.45	0.5	16.71	0	0	2.92	5.36	6.7	3.37	0	0.83	858.2	11.42	11.41	-0.01	2
193	Tr6	64.45	0.5	16.71	0	0	2.92	5.36	6.7	3.37	0	0.83	869.8	11.04	11.15	0.11	2
194	Tr6	64.45	0.5	16.71	0	0	2.92	5.36	6.7	3.37	0	0.83	879.3	10.8	10.93	0.13	2
195	Tr6	64.45	0.5	16.71	0	0	2.92	5.36	6.7	3.37	0	0.83	889.9	10.49	10.7	0.21	2
196	Tr6	64.45	0.5	16.71	0	0	2.92	5.36	6.7	3.37	0	1.19	794.4	12.21	12.09	-0.12	2
197	Tr6	64.45	0.5	16.71	0	0	2.92	5.36	6.7	3.37	0	1.19	799.8	12.01	11.95	-0.06	2
198	Tr6	64.45	0.5	16.71	0	0	2.92	5.36	6.7	3.37	0	1.19	804.8	11.86	11.83	-0.03	2
199	Tr6	64.45	0.5	16.71	0	0	2.92	5.36	6.7	3.37	0	1.19	812.1	11.66	11.65	-0.01	2
200	Tr6	64.45	0.5	16.71	0	0	2.92	5.36	6.7	3.37	0	1.19	820.7	11.37	11.44	0.07	2
201	Tr6	64.45	0.5	16.71	0	0	2.92	5.36	6.7	3.37	0	1.19	828.6	11.15	11.26	0.11	2
202	Tr6	64.45	0.5	16.71	0	0	2.92	5.36	6.7	3.37	0	1.19	839.3	10.9	11.01	0.11	2
203	Tr6	64.45	0.5	16.71	0	0	2.92	5.36	6.7	3.37	0	1.19	846.6	10.66	10.84	0.18	2

204	Tr6	64.45	0.5	16.71	0	0	2.92	5.36	6.7	3.37	0	1.19	854.8	10.42	10.66	0.24	2
205	Tr6	64.45	0.5	16.71	0	0	2.92	5.36	6.7	3.37	0	2.19	725.4	12.31	12.38	0.07	2
206	Tr6	64.45	0.5	16.71	0	0	2.92	5.36	6.7	3.37	0	2.19	736	11.93	12.07	0.14	2
207	Tr6	64.45	0.5	16.71	0	0	2.92	5.36	6.7	3.37	0	2.19	743.6	11.57	11.85	0.28	2
208	Tr6	64.45	0.5	16.71	0	0	2.92	5.36	6.7	3.37	0	2.19	749.1	11.45	11.7	0.25	2
209	Tr6	64.45	0.5	16.71	0	0	2.92	5.36	6.7	3.37	0	2.19	757.8	11.19	11.46	0.27	2
210	Tr6	64.45	0.5	16.71	0	0	2.92	5.36	6.7	3.37	0	2.19	769	10.86	11.16	0.3	2
211	Tr6	64.45	0.5	16.71	0	0	2.92	5.36	6.7	3.37	0	2.19	780.6	10.57	10.86	0.29	2
212	Tr6	64.45	0.5	16.71	0	0	2.92	5.36	6.7	3.37	0	2.19	791.2	10.25	10.6	0.35	2
213	Tr6	64.45	0.5	16.71	0	0	2.92	5.36	6.7	3.37	0	2.19	802.2	10.01	10.33	0.32	2
214	Tr6	64.45	0.5	16.71	0	0	2.92	5.36	6.7	3.37	0	2.9	692.2	12.23	12.54	0.31	2
215	Tr6	64.45	0.5	16.71	0	0	2.92	5.36	6.7	3.37	0	2.9	703.3	11.89	12.18	0.29	2
216	Tr6	64.45	0.5	16.71	0	0	2.92	5.36	6.7	3.37	0	2.9	713	11.48	11.89	0.41	2
217	Tr6	64.45	0.5	16.71	0	0	2.92	5.36	6.7	3.37	0	2.9	722.9	11.21	11.59	0.38	2
218	Tr6	64.45	0.5	16.71	0	0	2.92	5.36	6.7	3.37	0	4.92	621.1	12.3	13	0.7	2
219	Tr6	64.45	0.5	16.71	0	0	2.92	5.36	6.7	3.37	0	4.92	630.8	11.89	12.64	0.75	2
220	H3	78.6	0	12.5	0	0	0	0	4.6	4.2	0	0.02	1453.2	6.79	7.36	0.57	3
221	H3	78.6	0	12.5	0	0	0	0	4.6	4.2	0	0.02	1154.9	11.02	11.17	0.15	4
222	H3	78.6	0	12.5	0	0	0	0	4.6	4.2	0	0.02	1178.2	10.63	10.8	0.17	4
223	H3	78.6	0	12.5	0	0	0	0	4.6	4.2	0	0.02	1198.9	10.28	10.48	0.2	4
224	H3	78.6	0	12.5	0	0	0	0	4.6	4.2	0	0.02	1212	10.16	10.29	0.13	4
225	H3	78.6	0	12.5	0	0	0	0	4.6	4.2	0	0.02	1670.2	4.9	5.48	0.58	4
226	H3	78.6	0	12.5	0	0	0	0	4.6	4.2	0	0.02	1719.2	4.53	5.12	0.59	4
227	H3	78.6	0	12.5	0	0	0	0	4.6	4.2	0	0.02	1768.2	4.15	4.78	0.63	4
228	H3	78.6	0	12.5	0	0	0	0	4.6	4.2	0	0.02	1817.2	3.81	4.46	0.65	4
229	H3	78.6	0	12.5	0	0	0	0	4.6	4.2	0	0.02	1867.2	3.58	4.16	0.58	4
230	H3	78.6	0	12.5	0	0	0	0	4.6	4.2	0	0.02	1916.2	3.24	3.87	0.63	4
231	H5	74.1	0	11.7	0	0	0	0	9	4.4	0	0.02	947.65	9.74	10.07	0.33	4
232	H5	74.1	0	11.7	0	0	0	0	9	4.4	0	0.02	919.65	10.45	10.63	0.18	4
233	H5	74.1	0	11.7	0	0	0	0	9	4.4	0	0.02	903.65	10.7	10.97	0.27	4
234	H5	74.1	0	11.7	0	0	0	0	9	4.4	0	0.02	883.45	11.35	11.42	0.07	4
235	H5	74.1	0	11.7	0	0	0	0	9	4.4	0	0.02	1213.2	6.01	6.39	0.38	4

236	H5	74.1	0	11.7	0	0	0	0	9	4.4	0	0.02	1143.2	6.84	7.16	0.32	4
237	H5	74.1	0	11.7	0	0	0	0	9	4.4	0	0.02	1073.2	7.84	8.04	0.2	4
238	H5	74.1	0	11.7	0	0	0	0	9	4.4	0	0.02	1293.2	5.33	5.64	0.31	4
239	H5	74.1	0	11.7	0	0	0	0	9	4.4	0	0.02	1768.2	2.53	2.68	0.15	4
240	H5	74.1	0	11.7	0	0	0	0	9	4.4	0	0.02	1719.2	2.72	2.9	0.18	4
241	H5	74.1	0	11.7	0	0	0	0	9	4.4	0	0.02	1670.2	2.91	3.14	0.23	4
242	H5	74.1	0	11.7	0	0	0	0	9	4.4	0	0.02	1621.2	3.14	3.4	0.26	4
243	H5	74.1	0	11.7	0	0	0	0	9	4.4	0	0.02	1571.2	3.38	3.67	0.29	4
244	H5	74.1	0	11.7	0	0	0	0	9	4.4	0	0.02	1522.2	3.61	3.96	0.35	4
245	H5	74.1	0	11.7	0	0	0	0	9	4.4	0	0.02	1473.2	3.87	4.27	0.4	4
246	H7	74.6	0	11.8	0	0	0	0	4.4	9.2	0	0.02	969.35	10.16	10.86	0.7	4
247	H7	74.6	0	11.8	0	0	0	0	4.4	9.2	0	0.02	945.75	10.65	11.35	0.7	4
248	H7	74.6	0	11.8	0	0	0	0	4.4	9.2	0	0.02	927.25	11.15	11.75	0.6	4
249	H7	74.6	0	11.8	0	0	0	0	4.4	9.2	0	0.02	1867.2	2.54	2.48	-0.06	4
250	H7	74.6	0	11.8	0	0	0	0	4.4	9.2	0	0.02	1817.2	2.72	2.71	-0.01	4
251	H7	74.6	0	11.8	0	0	0	0	4.4	9.2	0	0.02	1768.2	2.92	2.95	0.03	4
252	H7	74.6	0	11.8	0	0	0	0	4.4	9.2	0	0.02	1719.2	3.14	3.2	0.06	4
253	H7	74.6	0	11.8	0	0	0	0	4.4	9.2	0	0.02	1670.2	3.36	3.47	0.11	4
254	H7	74.6	0	11.8	0	0	0	0	4.4	9.2	0	0.02	1621.2	3.57	3.76	0.19	4
255	H7	74.6	0	11.8	0	0	0	0	4.4	9.2	0	0.02	1571.2	3.82	4.07	0.25	4
256	H2	77.9	0	11.89	0	0	0	0	4.53	4.17	0	0.02	1242.4	9.77	9.78	0.01	5
257	H2	77.9	0	11.89	0	0	0	0	4.53	4.17	0	0.02	1176.5	10.9	10.76	-0.14	5
258	H2	77.9	0	11.89	0	0	0	0	4.53	4.17	0	0.02	1117.4	11.5	11.73	0.23	5
259	H2	77.9	0	11.89	0	0	0	0	4.53	4.17	0	0.02	1965.2	2.98	3.53	0.55	5
260	H1	76.12	0	13.53	0	0	0	0	4.65	5.68	0	0.03	1673.2	4.91	5.02	0.11	6
261	H1	76.12	0	13.53	0	0	0	0	4.65	5.68	0	0.03	1673.2	4.92	5.02	0.1	6
262	H1	76.12	0	13.53	0	0	0	0	4.65	5.68	0	1.05	1473.2	4.21	5.05	0.84	6
263	H1	76.12	0	13.53	0	0	0	0	4.65	5.68	0	1.05	1573.2	3.77	4.35	0.58	6
264	H1	76.12	0	13.53	0	0	0	0	4.65	5.68	0	1.55	1473.2	3.85	4.37	0.52	6
265	H1	76.12	0	13.53	0	0	0	0	4.65	5.68	0	1.55	1573.2	3.45	3.71	0.26	6
266	H1	76.12	0	13.53	0	0	0	0	4.65	5.68	0	1.55	1673.2	2.98	3.08	0.1	6
267	H1	76.12	0	13.53	0	0	0	0	4.65	5.68	0	2.09	1473.2	3.61	3.77	0.16	6

268	H1	76.12	0	13.53	0	0	0	0	4.65	5.68	0	2.09	1573.2	3.2	3.13	-0.07	6
269	H1	76.12	0	13.53	0	0	0	0	4.65	5.68	0	2.58	1573.2	3.07	2.72	-0.35	6
270	H1	76.12	0	13.53	0	0	0	0	4.65	5.68	0	3.22	1473.2	3.27	2.88	-0.39	6
271	H1	76.12	0	13.53	0	0	0	0	4.65	5.68	0	3.22	1573.2	2.88	2.32	-0.56	6
272	H1	76.12	0	13.53	0	0	0	0	4.65	5.68	0	3.75	1573.2	2.54	2.08	-0.46	6
273	H1	76.12	0	13.53	0	0	0	0	4.65	5.68	0	5	1273.2	3.37	3.32	-0.05	6
274	H1	76.12	0	13.53	0	0	0	0	4.65	5.68	0	5	1423.2	2.75	2.46	-0.29	6
275	H1	76.12	0	13.53	0	0	0	0	4.65	5.68	0	5	1173.2	3.95	3.98	0.03	6
276	H1	76.12	0	13.53	0	0	0	0	4.65	5.68	0	5.9	1273.2	3.18	3.07	-0.11	6
277	H1	76.12	0	13.53	0	0	0	0	4.65	5.68	0	5.9	1173.2	3.71	3.7	-0.01	6
278	H1	76.12	0	13.53	0	0	0	0	4.65	5.68	0	5.9	1173.2	3.63	3.7	0.07	6
279	H1	76.12	0	13.53	0	0	0	0	4.65	5.68	0	5.9	1073.2	4.25	4.41	0.16	6
280	H1	76.12	0	13.53	0	0	0	0	4.65	5.68	0	7.03	1073.2	4.03	4.14	0.11	6
281	H1	76.12	0	13.53	0	0	0	0	4.65	5.68	0	7.03	1173.2	3.46	3.46	0	6
282	H1	76.12	0	13.53	0	0	0	0	4.65	5.68	0	8.21	1073.2	3.68	3.94	0.26	6
283	H1	76.12	0	13.53	0	0	0	0	4.65	5.68	0	8.21	1073.2	3.67	3.94	0.27	6
284	H1	76.12	0	13.53	0	0	0	0	4.65	5.68	0	8.21	1073.2	3.72	3.94	0.22	6
285	H1	76.12	0	13.53	0	0	0	0	4.65	5.68	0	8.21	1173.2	3.13	3.3	0.17	6
286	H1	76.12	0	13.53	0	0	0	0	4.65	5.68	0	8.21	1173.2	3.12	3.3	0.18	6
287	H3	78.6	0	12.5	0	0	0	0	4.6	4.2	0	0.41	976.75	10.76	11.2	0.44	7
288	H3	78.6	0	12.5	0	0	0	0	4.6	4.2	0	0.42	921.85	11.8	11.84	0.04	7
289	H3	78.6	0	12.5	0	0	0	0	4.6	4.2	0	0.42	960.45	11.4	11.34	-0.06	7
290	H3	78.6	0	12.5	0	0	0	0	4.6	4.2	0	0.95	939.75	9.42	9.92	0.5	7
291	H3	78.6	0	12.5	0	0	0	0	4.6	4.2	0	0.96	866.85	10.98	10.98	0	7
292	H3	78.6	0	12.5	0	0	0	0	4.6	4.2	0	0.96	884.55	10.45	10.68	0.23	7
293	H3	78.6	0	12.5	0	0	0	0	4.6	4.2	0	0.99	884.25	10.48	10.62	0.14	7
294	H3	78.6	0	12.5	0	0	0	0	4.6	4.2	0	0.99	922.75	9.68	10.05	0.37	7
295	H3	78.6	0	12.5	0	0	0	0	4.6	4.2	0	1.28	885.65	9.83	10.04	0.21	7
296	H3	78.6	0	12.5	0	0	0	0	4.6	4.2	0	1.3	894.55	9.6	9.86	0.26	7
297	H3	78.6	0	12.5	0	0	0	0	4.6	4.2	0	1.31	875.95	9.88	10.15	0.27	7
298	H3	78.6	0	12.5	0	0	0	0	4.6	4.2	0	1.32	856.05	10.38	10.48	0.1	7
299	H3	78.6	0	12.5	0	0	0	0	4.6	4.2	0	1.33	822.55	10.96	11.12	0.16	7

300	H3	78.6	0	12.5	0	0	0	0	4.6	4.2	0	1.35	801.55	11.39	11.54	0.15	7
301	H3	78.6	0	12.5	0	0	0	0	4.6	4.2	0	1.37	840.55	10.58	10.69	0.11	7
302	H3	78.6	0	12.5	0	0	0	0	4.6	4.2	0	1.8	849.75	9.69	9.87	0.18	7
303	H3	78.6	0	12.5	0	0	0	0	4.6	4.2	0	1.85	780.15	11.3	11.27	-0.03	7
304	H3	78.6	0	12.5	0	0	0	0	4.6	4.2	0	1.88	819.75	10.09	10.35	0.26	7
305	H3	78.6	0	12.5	0	0	0	0	4.6	4.2	0	2.25	818.45	9.62	9.92	0.3	7
306	H3	78.6	0	12.5	0	0	0	0	4.6	4.2	0	2.29	775.05	10.49	10.82	0.33	7
307	H3	78.6	0	12.5	0	0	0	0	4.6	4.2	0	2.61	821.85	9.12	9.46	0.34	7
308	H3	78.6	0	12.5	0	0	0	0	4.6	4.2	0	3.35	788.25	9.93	9.43	-0.5	7
309	A4	62.4	0.55	20.01	0.03	0.02	3.22	9.08	3.52	0.93	0.12	0	996.2	12.76	12.95	0.19	8
310	A4	62.4	0.55	20.01	0.03	0.02	3.22	9.08	3.52	0.93	0.12	0	1007.9	12.32	12.43	0.11	8
311	A4	62.4	0.55	20.01	0.03	0.02	3.22	9.08	3.52	0.93	0.12	0	1011.4	12.18	12.29	0.11	8
312	A4	62.4	0.55	20.01	0.03	0.02	3.22	9.08	3.52	0.93	0.12	0	1018.5	11.95	12	0.05	8
313	A4	62.4	0.55	20.01	0.03	0.02	3.22	9.08	3.52	0.93	0.12	0	1024.9	11.74	11.76	0.02	8
314	A4	62.4	0.55	20.01	0.03	0.02	3.22	9.08	3.52	0.93	0.12	0	1033.5	11.41	11.45	0.04	8
315	A4	62.4	0.55	20.01	0.03	0.02	3.22	9.08	3.52	0.93	0.12	0	1043.7	11.09	11.11	0.02	8
316	A4	62.4	0.55	20.01	0.03	0.02	3.22	9.08	3.52	0.93	0.12	0	1053.8	10.76	10.79	0.03	8
317	A4	62.4	0.55	20.01	0.03	0.02	3.22	9.08	3.52	0.93	0.12	0	1058.9	10.57	10.64	0.07	8
318	A4	62.4	0.55	20.01	0.03	0.02	3.22	9.08	3.52	0.93	0.12	0	1068.9	10.33	10.35	0.02	8
319	A4	62.4	0.55	20.01	0.03	0.02	3.22	9.08	3.52	0.93	0.12	0	1073	10.19	10.24	0.05	8
320	A4	62.4	0.55	20.01	0.03	0.02	3.22	9.08	3.52	0.93	0.12	0	1084.6	9.87	9.93	0.06	8
321	A4	62.4	0.55	20.01	0.03	0.02	3.22	9.08	3.52	0.93	0.12	0	1094.1	9.6	9.69	0.09	8
322	A4	62.4	0.55	20.01	0.03	0.02	3.22	9.08	3.52	0.93	0.12	0	1107.7	9.3	9.36	0.06	8
323	A4	62.4	0.55	20.01	0.03	0.02	3.22	9.08	3.52	0.93	0.12	0	1113.8	9.12	9.22	0.1	8
324	A4	62.4	0.55	20.01	0.03	0.02	3.22	9.08	3.52	0.93	0.12	0	1123.8	8.92	9	0.08	8
325	A4	62.4	0.55	20.01	0.03	0.02	3.22	9.08	3.52	0.93	0.12	0	1513.7	3.35	3.67	0.32	8
326	A4	62.4	0.55	20.01	0.03	0.02	3.22	9.08	3.52	0.93	0.12	0	1536.6	3.17	3.46	0.29	8
327	A4	62.4	0.55	20.01	0.03	0.02	3.22	9.08	3.52	0.93	0.12	0	1575.5	2.9	3.12	0.22	8
328	A4	62.4	0.55	20.01	0.03	0.02	3.22	9.08	3.52	0.93	0.12	0	1601.1	2.73	2.9	0.17	8
329	A4	62.4	0.55	20.01	0.03	0.02	3.22	9.08	3.52	0.93	0.12	0	1622.4	2.59	2.73	0.14	8
330	A4	62.4	0.55	20.01	0.03	0.02	3.22	9.08	3.52	0.93	0.12	0	1650.4	2.42	2.5	0.08	8
331	A4	62.4	0.55	20.01	0.03	0.02	3.22	9.08	3.52	0.93	0.12	0	1673.1	2.28	2.33	0.05	8

332 A4	62.4	0.55	20.01	0.03	0.02	3.22	9.08	3.52	0.93	0.12	0	1698.6	2.15	2.14	-0.01	8
333 A4	62.4	0.55	20.01	0.03	0.02	3.22	9.08	3.52	0.93	0.12	0	1728.6	1.97	1.92	-0.05	8
334 A4	62.4	0.55	20.01	0.03	0.02	3.22	9.08	3.52	0.93	0.12	0	1753.1	1.85	1.75	-0.1	8
335 A4	62.4	0.55	20.01	0.03	0.02	3.22	9.08	3.52	0.93	0.12	0	1776.2	1.74	1.59	-0.15	8
336 A4	62.4	0.55	20.01	0.03	0.02	3.22	9.08	3.52	0.93	0.12	0	1801.7	1.62	1.42	-0.2	8
337 A4	62.4	0.55	20.01	0.03	0.02	3.22	9.08	3.52	0.93	0.12	0	1803.9	1.6	1.41	-0.19	8
338 A4	62.4	0.55	20.01	0.03	0.02	3.22	9.08	3.52	0.93	0.12	0	1829.5	1.48	1.25	-0.23	8
339 A4	62.4	0.55	20.01	0.03	0.02	3.22	9.08	3.52	0.93	0.12	0	1852.2	1.39	1.1	-0.29	8
340 A4	62.4	0.55	20.01	0.03	0.02	3.22	9.08	3.52	0.93	0.12	0	1874.6	1.28	0.97	-0.31	8
341 A4	62.4	0.55	20.01	0.03	0.02	3.22	9.08	3.52	0.93	0.12	0	1904.1	1.16	0.79	-0.37	8
342 A4	62.4	0.55	20.01	0.03	0.02	3.22	9.08	3.52	0.93	0.12	0	1929.4	1.05	0.65	-0.4	8
343 A4	62.4	0.55	20.01	0.03	0.02	3.22	9.08	3.52	0.93	0.12	0	1952	0.96	0.52	-0.44	8
344 A4	62.4	0.55	20.01	0.03	0.02	3.22	9.08	3.52	0.93	0.12	0	1977.9	0.86	0.38	-0.48	8
345 A4	62.4	0.55	20.01	0.03	0.02	3.22	9.08	3.52	0.93	0.12	0.27	935.7	12.7	12.79	0.09	8
346 A4	62.4	0.55	20.01	0.03	0.02	3.22	9.08	3.52	0.93	0.12	0.27	946.1	12.32	12.42	0.1	8
347 A4	62.4	0.55	20.01	0.03	0.02	3.22	9.08	3.52	0.93	0.12	0.27	965.4	11.64	11.78	0.14	8
348 A4	62.4	0.55	20.01	0.03	0.02	3.22	9.08	3.52	0.93	0.12	0.27	982.4	11.09	11.25	0.16	8
349 A4	62.4	0.55	20.01	0.03	0.02	3.22	9.08	3.52	0.93	0.12	0.27	998.9	10.54	10.77	0.23	8
350 A4	62.4	0.55	20.01	0.03	0.02	3.22	9.08	3.52	0.93	0.12	0.27	1010.8	10.23	10.45	0.22	8
351 A4	62.4	0.55	20.01	0.03	0.02	3.22	9.08	3.52	0.93	0.12	0.27	1021.8	9.93	10.16	0.23	8
352 A4	62.4	0.55	20.01	0.03	0.02	3.22	9.08	3.52	0.93	0.12	0.27	1041.6	9.46	9.67	0.21	8
353 A4	62.4	0.55	20.01	0.03	0.02	3.22	9.08	3.52	0.93	0.12	0.27	1061.4	9.03	9.21	0.18	8
354 A4	62.4	0.55	20.01	0.03	0.02	3.22	9.08	3.52	0.93	0.12	0.27	1081.3	8.56	8.78	0.22	8
355 A4	62.4	0.55	20.01	0.03	0.02	3.22	9.08	3.52	0.93	0.12	1	864.5	12.19	11.8	-0.39	8
356 A4	62.4	0.55	20.01	0.03	0.02	3.22	9.08	3.52	0.93	0.12	1	877.6	11.73	11.47	-0.26	8
357 A4	62.4	0.55	20.01	0.03	0.02	3.22	9.08	3.52	0.93	0.12	1	898.4	11.03	10.97	-0.06	8
358 A4	62.4	0.55	20.01	0.03	0.02	3.22	9.08	3.52	0.93	0.12	1	911.4	10.62	10.66	0.04	8
359 A4	62.4	0.55	20.01	0.03	0.02	3.22	9.08	3.52	0.93	0.12	1	922.3	10.33	10.41	0.08	8
360 A4	62.4	0.55	20.01	0.03	0.02	3.22	9.08	3.52	0.93	0.12	1	942.3	9.78	9.96	0.18	8
361 A4	62.4	0.55	20.01	0.03	0.02	3.22	9.08	3.52	0.93	0.12	1	963.2	9.28	9.51	0.23	8
362 A4	62.4	0.55	20.01	0.03	0.02	3.22	9.08	3.52	0.93	0.12	1	986.1	8.74	9.03	0.29	8
363 A4	62.4	0.55	20.01	0.03	0.02	3.22	9.08	3.52	0.93	0.12	2	793.7	11.87	11.66	-0.21	8

364	A4	62.4	0.55	20.01	0.03	0.02	3.22	9.08	3.52	0.93	0.12	2	804	11.48	11.39	-0.09	8
365	A4	62.4	0.55	20.01	0.03	0.02	3.22	9.08	3.52	0.93	0.12	2	824.5	10.72	10.88	0.16	8
366	A4	62.4	0.55	20.01	0.03	0.02	3.22	9.08	3.52	0.93	0.12	2	825.1	10.75	10.87	0.12	8
367	A4	62.4	0.55	20.01	0.03	0.02	3.22	9.08	3.52	0.93	0.12	2	825.2	10.73	10.87	0.14	8
368	A4	62.4	0.55	20.01	0.03	0.02	3.22	9.08	3.52	0.93	0.12	2	825.5	10.74	10.86	0.12	8
369	A4	62.4	0.55	20.01	0.03	0.02	3.22	9.08	3.52	0.93	0.12	2	825.7	10.7	10.85	0.15	8
370	A4	62.4	0.55	20.01	0.03	0.02	3.22	9.08	3.52	0.93	0.12	2	846.1	10.08	10.38	0.3	8
371	A4	62.4	0.55	20.01	0.03	0.02	3.22	9.08	3.52	0.93	0.12	2	866.4	9.49	9.92	0.43	8
372	A4	62.4	0.55	20.01	0.03	0.02	3.22	9.08	3.52	0.93	0.12	2.66	721.5	13.42	12.88	-0.54	8
373	A4	62.4	0.55	20.01	0.03	0.02	3.22	9.08	3.52	0.93	0.12	2.66	742.6	12.66	12.23	-0.43	8
374	A4	62.4	0.55	20.01	0.03	0.02	3.22	9.08	3.52	0.93	0.12	2.66	753.7	12.2	11.9	-0.3	8
375	A4	62.4	0.55	20.01	0.03	0.02	3.22	9.08	3.52	0.93	0.12	2.66	765.1	11.7	11.58	-0.12	8
376	A4	62.4	0.55	20.01	0.03	0.02	3.22	9.08	3.52	0.93	0.12	2.66	786.7	10.9	11	0.1	8
377	A4	62.4	0.55	20.01	0.03	0.02	3.22	9.08	3.52	0.93	0.12	2.66	799.2	10.49	10.68	0.19	8
378	A4	62.4	0.55	20.01	0.03	0.02	3.22	9.08	3.52	0.93	0.12	2.66	823	9.75	10.11	0.36	8
379	A4	62.4	0.55	20.01	0.03	0.02	3.22	9.08	3.52	0.93	0.12	2.66	843.8	9.23	9.64	0.41	8
380	A4	62.4	0.55	20.01	0.03	0.02	3.22	9.08	3.52	0.93	0.12	2.66	864	8.75	9.21	0.46	8
381	A4	62.4	0.55	20.01	0.03	0.02	3.22	9.08	3.52	0.93	0.12	3.46	723	12.49	11.95	-0.54	8
382	A4	62.4	0.55	20.01	0.03	0.02	3.22	9.08	3.52	0.93	0.12	3.46	733.1	12.1	11.65	-0.45	8
383	A4	62.4	0.55	20.01	0.03	0.02	3.22	9.08	3.52	0.93	0.12	3.46	744.5	11.6	11.32	-0.28	8
384	A4	62.4	0.55	20.01	0.03	0.02	3.22	9.08	3.52	0.93	0.12	3.46	755.2	11.21	11.02	-0.19	8
385	A4	62.4	0.55	20.01	0.03	0.02	3.22	9.08	3.52	0.93	0.12	3.46	764.4	10.78	10.77	-0.01	8
386	A4	62.4	0.55	20.01	0.03	0.02	3.22	9.08	3.52	0.93	0.12	3.46	791.1	9.95	10.09	0.14	8
387	A4	62.4	0.55	20.01	0.03	0.02	3.22	9.08	3.52	0.93	0.12	3.46	797.8	9.76	9.93	0.17	8
388	A4	62.4	0.55	20.01	0.03	0.02	3.22	9.08	3.52	0.93	0.12	3.46	812.3	9.42	9.59	0.17	8
389	A4	62.4	0.55	20.01	0.03	0.02	3.22	9.08	3.52	0.93	0.12	3.46	834.8	8.75	9.09	0.34	8
390	R6	73.79	0.05	15.11	0.42	0.05	0.07	0.97	4.71	4.02	0.01	8.8	973.15	5.11	4.69	-0.42	9
391	R6	73.79	0.05	15.11	0.42	0.05	0.07	0.97	4.71	4.02	0.01	8.8	1073.2	4.14	3.92	-0.22	9
392	R6	73.79	0.05	15.11	0.42	0.05	0.07	0.97	4.71	4.02	0.01	8.8	1173.2	3.45	3.27	-0.18	9
393	R14	76.92	0.1	12.92	0.89	0.05	0.11	0.86	3.89	4.25	0.03	0.08	1221.2	8.64	8.85	0.21	10
394	R14	76.92	0.1	12.92	0.89	0.05	0.11	0.86	3.89	4.25	0.03	0.08	1206.2	8.81	9.06	0.25	10
395	R14	76.92	0.1	12.92	0.89	0.05	0.11	0.86	3.89	4.25	0.03	0.08	1179.2	9.2	9.45	0.25	10

396	R14	76.92	0.1	12.92	0.89	0.05	0.11	0.86	3.89	4.25	0.03	0.08	1151.2	9.65	9.87	0.22	10
397	R14	76.92	0.1	12.92	0.89	0.05	0.11	0.86	3.89	4.25	0.03	0.08	1138.2	9.82	10.07	0.25	10
398	R15	76.99	0.03	13.02	0.71	0.1	0.04	0.48	4.31	4.31	0	1.49	723.15	13.18	13.26	0.08	10
399	R15	76.99	0.03	13.02	0.71	0.1	0.04	0.48	4.31	4.31	0	1.49	737.15	12.85	12.86	0.01	10
400	R15	76.99	0.03	13.02	0.71	0.1	0.04	0.48	4.31	4.31	0	1.49	748.15	12.45	12.56	0.11	10
401	R15	76.99	0.03	13.02	0.71	0.1	0.04	0.48	4.31	4.31	0	1.49	758.15	12.14	12.3	0.16	10
402	R15	76.99	0.03	13.02	0.71	0.1	0.04	0.48	4.31	4.31	0	1.49	774.15	11.91	11.89	-0.02	10
403	R15	76.99	0.03	13.02	0.71	0.1	0.04	0.48	4.31	4.31	0	1.49	784.15	11.45	11.65	0.2	10
404	R15	76.99	0.03	13.02	0.71	0.1	0.04	0.48	4.31	4.31	0	1.49	794.15	11.55	11.41	-0.14	10
405	R15	76.99	0.03	13.02	0.71	0.1	0.04	0.48	4.31	4.31	0	1.49	804.15	10.92	11.19	0.27	10
406	R15	76.99	0.03	13.02	0.71	0.1	0.04	0.48	4.31	4.31	0	1.49	814.15	11.05	10.97	-0.08	10
407	R15	76.99	0.03	13.02	0.71	0.1	0.04	0.48	4.31	4.31	0	1.49	822.15	10.6	10.8	0.2	10
408	R15	76.99	0.03	13.02	0.71	0.1	0.04	0.48	4.31	4.31	0	1.49	832.15	10.58	10.59	0.01	10
409	R15	76.99	0.03	13.02	0.71	0.1	0.04	0.48	4.31	4.31	0	1.49	842.15	10.39	10.39	0	10
410	R15	76.99	0.03	13.02	0.71	0.1	0.04	0.48	4.31	4.31	0	1.49	851.15	10.26	10.22	-0.04	10
411	R15	76.99	0.03	13.02	0.71	0.1	0.04	0.48	4.31	4.31	0	1.49	862.15	10.1	10.01	-0.09	10
412	R17	77.01	0.03	13.14	0.71	0.1	0.04	0.51	4.28	4.18	0	0.01	1233.2	9.64	9.22	-0.42	10
413	R17	77.01	0.03	13.14	0.71	0.1	0.04	0.51	4.28	4.18	0	0.01	1205.2	9.93	9.63	-0.3	10
414	R17	77.01	0.03	13.14	0.71	0.1	0.04	0.51	4.28	4.18	0	0.01	1158.2	10.69	10.38	-0.31	10
415	R17	77.01	0.03	13.14	0.71	0.1	0.04	0.51	4.28	4.18	0	0.01	1135.2	11.2	10.77	-0.43	10
416	R17	77.01	0.03	13.14	0.71	0.1	0.04	0.51	4.28	4.18	0	0.01	1111.2	11.27	11.19	-0.08	10
417	R17	77.01	0.03	13.14	0.71	0.1	0.04	0.51	4.28	4.18	0	0.01	1088.2	11.95	11.62	-0.33	10
418	R17	77.01	0.03	13.14	0.71	0.1	0.04	0.51	4.28	4.18	0	0.01	1064.2	12.38	12.09	-0.29	10
419	R19	77.08	0.09	12.44	1.3	0.02	0.02	0.36	4.49	4.2	0	0.04	1231.2	8.84	8.69	-0.15	10
420	R19	77.08	0.09	12.44	1.3	0.02	0.02	0.36	4.49	4.2	0	0.04	1206.7	9.16	9.02	-0.14	10
421	R19	77.08	0.09	12.44	1.3	0.02	0.02	0.36	4.49	4.2	0	0.04	1179.2	9.51	9.42	-0.09	10
422	R19	77.08	0.09	12.44	1.3	0.02	0.02	0.36	4.49	4.2	0	0.04	1161.2	9.71	9.68	-0.03	10
423	R19	77.08	0.09	12.44	1.3	0.02	0.02	0.36	4.49	4.2	0	0.04	1142.2	9.98	9.97	-0.01	10
424	R21	77.17	0.08	12.4	1.3	0.02	0.01	0.35	4.5	4.2	0	0.12	1070.2	10.16	10.64	0.48	10
425	R21	77.17	0.08	12.4	1.3	0.02	0.01	0.35	4.5	4.2	0	0.12	1092.2	10.08	10.3	0.22	10
426	R21	77.17	0.08	12.4	1.3	0.02	0.01	0.35	4.5	4.2	0	0.12	1100.2	9.93	10.18	0.25	10
427	R21	77.17	0.08	12.4	1.3	0.02	0.01	0.35	4.5	4.2	0	0.12	1129.2	9.53	9.76	0.23	10

428	R21	77.17	0.08	12.4	1.3	0.02	0.01	0.35	4.5	4.2	0	0.12	1158.2	8.96	9.35	0.39	10
429	R21	77.17	0.08	12.4	1.3	0.02	0.01	0.35	4.5	4.2	0	0.12	1187.2	8.57	8.96	0.39	10
430	R26	77.48	0.17	12.2	1.3	0.05	0.17	1.14	3.9	3.6	0	0.13	1188.2	8.5	8.72	0.22	10
431	R26	77.48	0.17	12.2	1.3	0.05	0.17	1.14	3.9	3.6	0	0.13	1152.2	9.1	9.23	0.13	10
432	R26	77.48	0.17	12.2	1.3	0.05	0.17	1.14	3.9	3.6	0	0.13	1127.2	9.51	9.6	0.09	10
433	R26	77.48	0.17	12.2	1.3	0.05	0.17	1.14	3.9	3.6	0	0.13	1093.2	10.05	10.13	0.08	10
434	R26	77.48	0.17	12.2	1.3	0.05	0.17	1.14	3.9	3.6	0	0.13	1093.2	10.25	10.13	-0.12	10
435	R26	77.48	0.17	12.2	1.3	0.05	0.17	1.14	3.9	3.6	0	0.13	1061.2	10.62	10.65	0.03	10
436	R27	77.53	0.17	12.17	1.3	0.05	0.17	1.13	3.89	3.6	0	0.04	1134.2	10.07	9.96	-0.11	10
437	R27	77.53	0.17	12.17	1.3	0.05	0.17	1.13	3.89	3.6	0	0.04	1152.2	9.81	9.67	-0.14	10
438	R27	77.53	0.17	12.17	1.3	0.05	0.17	1.13	3.89	3.6	0	0.04	1159.2	9.62	9.56	-0.06	10
439	R27	77.53	0.17	12.17	1.3	0.05	0.17	1.13	3.89	3.6	0	0.04	1178.2	9.34	9.26	-0.08	10
440	R27	77.53	0.17	12.17	1.3	0.05	0.17	1.13	3.89	3.6	0	0.04	1187.2	9.09	9.12	0.03	10
441	R27	77.53	0.17	12.17	1.3	0.05	0.17	1.13	3.89	3.6	0	0.04	1196.2	9.04	8.99	-0.05	10
442	R27	77.53	0.17	12.17	1.3	0.05	0.17	1.13	3.89	3.6	0	0.04	1224.7	8.62	8.58	-0.04	10
443	R28	77.88	0.07	12.73	0.76	0.04	0.06	0.5	3.93	4.03	0.01	0.02	1185.2	10.12	9.98	-0.14	10
444	R28	77.88	0.07	12.73	0.76	0.04	0.06	0.5	3.93	4.03	0.01	0.02	1208.2	9.79	9.63	-0.16	10
445	R31	78	0.09	12.15	0.54	0.07	0.06	0.5	4.08	4.48	0.02	0.06	1238.2	8.66	8.95	0.29	10
446	R31	78	0.09	12.15	0.54	0.07	0.06	0.5	4.08	4.48	0.02	0.06	1223.2	8.89	9.15	0.26	10
447	R31	78	0.09	12.15	0.54	0.07	0.06	0.5	4.08	4.48	0.02	0.06	1204.2	9.06	9.42	0.36	10
448	R31	78	0.09	12.15	0.54	0.07	0.06	0.5	4.08	4.48	0.02	0.06	1185.2	9.48	9.69	0.21	10
449	R31	78	0.09	12.15	0.54	0.07	0.06	0.5	4.08	4.48	0.02	0.06	1171.2	9.51	9.9	0.39	10
450	R31	78	0.09	12.15	0.54	0.07	0.06	0.5	4.08	4.48	0.02	0.06	1165.7	9.69	9.98	0.29	10
451	R31	78	0.09	12.15	0.54	0.07	0.06	0.5	4.08	4.48	0.02	0.06	1136.9	10.04	10.42	0.38	10
452	R31	78	0.09	12.15	0.54	0.07	0.06	0.5	4.08	4.48	0.02	0.06	1119.9	10.29	10.69	0.4	10
453	R31	78	0.09	12.15	0.54	0.07	0.06	0.5	4.08	4.48	0.02	0.06	1077.8	10.89	11.4	0.51	10
454	R31	78	0.09	12.15	0.54	0.07	0.06	0.5	4.08	4.48	0.02	0.06	1040.3	11.65	12.07	0.42	10
455	R32	78	0.09	12.15	0.54	0.07	0.07	0.5	4.08	4.48	0	0.13	1171.2	9.2	9.5	0.3	10
456	R32	78	0.09	12.15	0.54	0.07	0.07	0.5	4.08	4.48	0	0.13	1120.2	9.99	10.22	0.23	10
457	R32	78	0.09	12.15	0.54	0.07	0.07	0.5	4.08	4.48	0	0.13	1078.2	10.49	10.84	0.35	10
458	R32	78	0.09	12.15	0.54	0.07	0.07	0.5	4.08	4.48	0	0.13	1024.2	11.54	11.7	0.16	10
459	R32	78	0.09	12.15	0.54	0.07	0.07	0.5	4.08	4.48	0	0.13	992.15	12	12.24	0.24	10

460	A3	61.17	0.84	17.29	5.39	0	3.35	5.83	3.85	1.39	0	0.02	981.1	11.33	11.17	-0.16	11
461	A3	61.17	0.84	17.29	5.39	0	3.35	5.83	3.85	1.39	0	0.02	992.2	10.83	10.89	0.06	11
462	A3	61.17	0.84	17.29	5.39	0	3.35	5.83	3.85	1.39	0	0.02	1011.8	10.25	10.42	0.17	11
463	A3	61.17	0.84	17.29	5.39	0	3.35	5.83	3.85	1.39	0	0.02	1025.5	9.9	10.12	0.22	11
464	A3	61.17	0.84	17.29	5.39	0	3.35	5.83	3.85	1.39	0	0.02	1036.8	9.67	9.87	0.2	11
465	A3	61.17	0.84	17.29	5.39	0	3.35	5.83	3.85	1.39	0	0.02	1670	2.19	2.3	0.11	11
466	A3	61.17	0.84	17.29	5.39	0	3.35	5.83	3.85	1.39	0	0.02	1719	1.97	1.96	-0.01	11
467	A3	61.17	0.84	17.29	5.39	0	3.35	5.83	3.85	1.39	0	0.02	1768	1.74	1.64	-0.1	11
468	A3	61.17	0.84	17.29	5.39	0	3.35	5.83	3.85	1.39	0	0.02	1818	1.52	1.33	-0.19	11
469	A3	61.17	0.84	17.29	5.39	0	3.35	5.83	3.85	1.39	0	0.02	1867	1.33	1.04	-0.29	11
470	A3	61.17	0.84	17.29	5.39	0	3.35	5.83	3.85	1.39	0	0.02	939.3	12.66	12.35	-0.31	11
471	A3	61.17	0.84	17.29	5.39	0	3.35	5.83	3.85	1.39	0	0.02	950.6	12.3	12.01	-0.29	11
472	A3	61.17	0.84	17.29	5.39	0	3.35	5.83	3.85	1.39	0	0.02	961.7	11.85	11.69	-0.16	11
473	A3	61.17	0.84	17.29	5.39	0	3.35	5.83	3.85	1.39	0	0.02	971.8	11.64	11.41	-0.23	11
474	R30	77.9	0.07	12.05	0.76	0	0.05	0.52	4.01	4.06	0	0	1670	4.79	4.73	-0.06	11
475	R30	77.9	0.07	12.05	0.76	0	0.05	0.52	4.01	4.06	0	0	1719	4.41	4.38	-0.03	11
476	R30	77.9	0.07	12.05	0.76	0	0.05	0.52	4.01	4.06	0	0	1768	4.09	4.04	-0.05	11
477	R30	77.9	0.07	12.05	0.76	0	0.05	0.52	4.01	4.06	0	0	1817	3.81	3.73	-0.08	11
478	R30	77.9	0.07	12.05	0.76	0	0.05	0.52	4.01	4.06	0	0	1867	3.5	3.43	-0.07	11
479	R30	77.9	0.07	12.05	0.76	0	0.05	0.52	4.01	4.06	0	0	1051	12.1	12.59	0.49	11
480	R30	77.9	0.07	12.05	0.76	0	0.05	0.52	4.01	4.06	0	0	1070.6	11.92	12.17	0.25	11
481	R30	77.9	0.07	12.05	0.76	0	0.05	0.52	4.01	4.06	0	0	1081.3	11.81	11.94	0.13	11
482	R30	77.9	0.07	12.05	0.76	0	0.05	0.52	4.01	4.06	0	0	1100.6	11.34	11.56	0.22	11
483	R30	77.9	0.07	12.05	0.76	0	0.05	0.52	4.01	4.06	0	0	1098.4	11.27	11.6	0.33	11
484	R30	77.9	0.07	12.05	0.76	0	0.05	0.52	4.01	4.06	0	0	1111.1	11.05	11.36	0.31	11
485	R30	77.9	0.07	12.05	0.76	0	0.05	0.52	4.01	4.06	0	0	1126.9	10.89	11.06	0.17	11
486	R30	77.9	0.07	12.05	0.76	0	0.05	0.52	4.01	4.06	0	0	1127.2	10.73	11.06	0.33	11
487	R30	77.9	0.07	12.05	0.76	0	0.05	0.52	4.01	4.06	0	0	1167.4	10.19	10.35	0.16	11
488	R30	77.9	0.07	12.05	0.76	0	0.05	0.52	4.01	4.06	0	0	1193.5	9.78	9.92	0.14	11
489	R30	77.9	0.07	12.05	0.76	0	0.05	0.52	4.01	4.06	0	0	1096.9	11.37	11.63	0.26	11
490	R30	77.9	0.07	12.05	0.76	0	0.05	0.52	4.01	4.06	0	0	1097.6	11.34	11.62	0.28	11
491	R30	77.9	0.07	12.05	0.76	0	0.05	0.52	4.01	4.06	0	0	1106.8	11.18	11.44	0.26	11

492	R30	77.9	0.07	12.05	0.76	0	0.05	0.52	4.01	4.06	0	0	1120.3	10.92	11.18	0.26	11
493	R30	77.9	0.07	12.05	0.76	0	0.05	0.52	4.01	4.06	0	0	1126.1	10.81	11.08	0.27	11
494	R30	77.9	0.07	12.05	0.76	0	0.05	0.52	4.01	4.06	0	0	1130.5	10.77	10.99	0.22	11
495	R30	77.9	0.07	12.05	0.76	0	0.05	0.52	4.01	4.06	0	0	1134.5	10.66	10.92	0.26	11
496	R30	77.9	0.07	12.05	0.76	0	0.05	0.52	4.01	4.06	0	0	1134.7	10.63	10.92	0.29	11
497	R30	77.9	0.07	12.05	0.76	0	0.05	0.52	4.01	4.06	0	0	1146.9	10.42	10.7	0.28	11
498	R30	77.9	0.07	12.05	0.76	0	0.05	0.52	4.01	4.06	0	0	1155.1	10.31	10.56	0.25	11
499	R30	77.9	0.07	12.05	0.76	0	0.05	0.52	4.01	4.06	0	0	1156.3	10.3	10.54	0.24	11
500	R30	77.9	0.07	12.05	0.76	0	0.05	0.52	4.01	4.06	0	0	1167.1	10.15	10.35	0.2	11
501	R30	77.9	0.07	12.05	0.76	0	0.05	0.52	4.01	4.06	0	0	1177.1	9.99	10.18	0.19	11
502	R30	77.9	0.07	12.05	0.76	0	0.05	0.52	4.01	4.06	0	0	1194.1	9.73	9.91	0.18	11
503	R30	77.9	0.07	12.05	0.76	0	0.05	0.52	4.01	4.06	0	0	1213.3	9.36	9.61	0.25	11
504	R30	77.9	0.07	12.05	0.76	0	0.05	0.52	4.01	4.06	0	0	1098.3	11.56	11.6	0.04	11
505	R30	77.9	0.07	12.05	0.76	0	0.05	0.52	4.01	4.06	0	0	1110.6	11.37	11.37	0	11
506	R30	77.9	0.07	12.05	0.76	0	0.05	0.52	4.01	4.06	0	0	1120.3	11.21	11.18	-0.03	11
507	R30	77.9	0.07	12.05	0.76	0	0.05	0.52	4.01	4.06	0	0	1134.4	10.93	10.92	-0.01	11
508	R30	77.9	0.07	12.05	0.76	0	0.05	0.52	4.01	4.06	0	0	1151.3	10.65	10.62	-0.03	11
509	R30	77.9	0.07	12.05	0.76	0	0.05	0.52	4.01	4.06	0	0	1166.1	10.36	10.37	0.01	11
510	R30	77.9	0.07	12.05	0.76	0	0.05	0.52	4.01	4.06	0	0	1175.7	10.18	10.21	0.03	11
511	R30	77.9	0.07	12.05	0.76	0	0.05	0.52	4.01	4.06	0	0	1190.2	9.95	9.97	0.02	11
512	R30	77.9	0.07	12.05	0.76	0	0.05	0.52	4.01	4.06	0	0	1204.5	9.74	9.74	0	11
513	R30	77.9	0.07	12.05	0.76	0	0.05	0.52	4.01	4.06	0	0	1219.1	9.54	9.52	-0.02	11
514	R30	77.9	0.07	12.05	0.76	0	0.05	0.52	4.01	4.06	0	0	1230.8	9.36	9.34	-0.02	11
515	R30	77.9	0.07	12.05	0.76	0	0.05	0.52	4.01	4.06	0	0	988	13.77	14.08	0.31	11
516	R30	77.9	0.07	12.05	0.76	0	0.05	0.52	4.01	4.06	0	0	1063	12.49	12.33	-0.16	11
517	R30	77.9	0.07	12.05	0.76	0	0.05	0.52	4.01	4.06	0	0	1068	12.26	12.22	-0.04	11
518	R30	77.9	0.07	12.05	0.76	0	0.05	0.52	4.01	4.06	0	0	1091	11.87	11.75	-0.12	11
519	R30	77.9	0.07	12.05	0.76	0	0.05	0.52	4.01	4.06	0	0	1094	11.51	11.69	0.18	11
520	R30	77.9	0.07	12.05	0.76	0	0.05	0.52	4.01	4.06	0	0	1128	11.02	11.04	0.02	11
521	R30	77.9	0.07	12.05	0.76	0	0.05	0.52	4.01	4.06	0	0	1129	11.02	11.02	0	11
522	R30	77.9	0.07	12.05	0.76	0	0.05	0.52	4.01	4.06	0	0	1131	10.92	10.99	0.07	11
523	R30	77.9	0.07	12.05	0.76	0	0.05	0.52	4.01	4.06	0	0	1135	10.87	10.91	0.04	11

524	R30	77.9	0.07	12.05	0.76	0	0.05	0.52	4.01	4.06	0	0	1136	10.9	10.89	-0.01	11
525	R30	77.9	0.07	12.05	0.76	0	0.05	0.52	4.01	4.06	0	0	1138	10.84	10.86	0.02	11
526	R30	77.9	0.07	12.05	0.76	0	0.05	0.52	4.01	4.06	0	0	1157	10.62	10.52	-0.1	11
527	R30	77.9	0.07	12.05	0.76	0	0.05	0.52	4.01	4.06	0	0	1186	10.07	10.04	-0.03	11
528	R30	77.9	0.07	12.05	0.76	0	0.05	0.52	4.01	4.06	0	0	1219	9.55	9.52	-0.03	11
529	R30	77.9	0.07	12.05	0.76	0	0.05	0.52	4.01	4.06	0	0	1221	9.57	9.49	-0.08	11
530	R30	77.9	0.07	12.05	0.76	0	0.05	0.52	4.01	4.06	0	0	1253	9.19	9.02	-0.17	11
531	R30	77.9	0.07	12.05	0.76	0	0.05	0.52	4.01	4.06	0	0	920	15.08	16.01	0.93	11
532	R30	77.9	0.07	12.05	0.76	0	0.05	0.52	4.01	4.06	0	0	1916	3.22	3.15	-0.07	11
533	R20	77.15	0.09	12.82	0.56	0.07	0.07	0.52	4.11	4.61	0.01	0.12	1231.3	8.68	8.74	0.06	12
534	R20	77.15	0.09	12.82	0.56	0.07	0.07	0.52	4.11	4.61	0.01	0.12	1219	8.89	8.9	0.01	12
535	R20	77.15	0.09	12.82	0.56	0.07	0.07	0.52	4.11	4.61	0.01	0.12	1201	9.12	9.13	0.01	12
536	R20	77.15	0.09	12.82	0.56	0.07	0.07	0.52	4.11	4.61	0.01	0.12	1176.5	9.47	9.46	-0.01	12
537	R20	77.15	0.09	12.82	0.56	0.07	0.07	0.52	4.11	4.61	0.01	0.12	1149.3	9.91	9.83	-0.08	12
538	R22	77.18	0.09	12.91	0.61	0.07	0.07	0.51	4.05	4.52	0.01	0.1	1238.2	8.66	8.74	0.08	12
539	R22	77.18	0.09	12.91	0.61	0.07	0.07	0.51	4.05	4.52	0.01	0.1	1223.2	8.89	8.93	0.04	12
540	R22	77.18	0.09	12.91	0.61	0.07	0.07	0.51	4.05	4.52	0.01	0.1	1204.2	9.06	9.19	0.13	12
541	R22	77.18	0.09	12.91	0.61	0.07	0.07	0.51	4.05	4.52	0.01	0.1	1185.2	9.48	9.44	-0.04	12
542	R22	77.18	0.09	12.91	0.61	0.07	0.07	0.51	4.05	4.52	0.01	0.1	1166.2	9.69	9.71	0.02	12
543	R22	77.18	0.09	12.91	0.61	0.07	0.07	0.51	4.05	4.52	0.01	0.1	1137.2	10.04	10.12	0.08	12
544	R29	77.88	0.16	12.03	1.19	0.05	0.05	1.06	3.64	3.88	0.01	0.11	1188.2	8.88	8.97	0.09	12
545	R29	77.88	0.16	12.03	1.19	0.05	0.05	1.06	3.64	3.88	0.01	0.11	1178.2	9.13	9.11	-0.02	12
546	R29	77.88	0.16	12.03	1.19	0.05	0.05	1.06	3.64	3.88	0.01	0.11	1164.2	9.31	9.31	0	12
547	R29	77.88	0.16	12.03	1.19	0.05	0.05	1.06	3.64	3.88	0.01	0.11	1153.2	9.54	9.47	-0.07	12
548	R29	77.88	0.16	12.03	1.19	0.05	0.05	1.06	3.64	3.88	0.01	0.11	1148.8	9.48	9.53	0.05	12
549	R29	77.88	0.16	12.03	1.19	0.05	0.05	1.06	3.64	3.88	0.01	0.11	1141.2	9.75	9.65	-0.1	12
550	R29	77.88	0.16	12.03	1.19	0.05	0.05	1.06	3.64	3.88	0.01	0.11	1121.2	10.03	9.95	-0.08	12
551	R29	77.88	0.16	12.03	1.19	0.05	0.05	1.06	3.64	3.88	0.01	0.11	1116.2	10.21	10.03	-0.18	12
552	R29	77.88	0.16	12.03	1.19	0.05	0.05	1.06	3.64	3.88	0.01	0.11	1092.2	10.5	10.4	-0.1	12
553	R29	77.88	0.16	12.03	1.19	0.05	0.05	1.06	3.64	3.88	0.01	0.11	1074.2	10.73	10.7	-0.03	12
554	R10	76.38	0.06	11.59	1.03	0.05	0.36	3.25	2.44	4.66	0	0.02	1048.2	11.61	11.68	0.07	13
555	R10	76.38	0.06	11.59	1.03	0.05	0.36	3.25	2.44	4.66	0	0.02	1073.2	11.01	11.09	0.08	13

556	R10	76.38	0.06	11.59	1.03	0.05	0.36	3.25	2.44	4.66	0	0.02	1098.2	10.48	10.54	0.06	13
557	R10	76.38	0.06	11.59	1.03	0.05	0.36	3.25	2.44	4.66	0	0.02	1123.2	10.02	10.03	0.01	13
558	R10	76.38	0.06	11.59	1.03	0.05	0.36	3.25	2.44	4.66	0	0.02	1148.2	9.57	9.55	-0.02	13
559	R10	76.38	0.06	11.59	1.03	0.05	0.36	3.25	2.44	4.66	0	0.02	1073.2	11	11.09	0.09	13
560	R10	76.38	0.06	11.59	1.03	0.05	0.36	3.25	2.44	4.66	0	0.02	1123.2	9.97	10.03	0.06	13
561	R10	76.38	0.06	11.59	1.03	0.05	0.36	3.25	2.44	4.66	0	0.02	1173.2	9.12	9.1	-0.02	13
562	R10	76.38	0.06	11.59	1.03	0.05	0.36	3.25	2.44	4.66	0	0.02	1198.2	8.75	8.68	-0.07	13
563	R11	76.57	0.06	11.65	1.04	0.07	0.36	3.23	2.46	4.62	0	0.17	998.15	11.65	11.58	-0.07	13
564	R11	76.57	0.06	11.65	1.04	0.07	0.36	3.23	2.46	4.62	0	0.17	1023.2	10.91	11.07	0.16	13
565	R11	76.57	0.06	11.65	1.04	0.07	0.36	3.23	2.46	4.62	0	0.17	1023.2	10.94	11.07	0.13	13
566	R11	76.57	0.06	11.65	1.04	0.07	0.36	3.23	2.46	4.62	0	0.17	1048.2	10.36	10.59	0.23	13
567	R11	76.57	0.06	11.65	1.04	0.07	0.36	3.23	2.46	4.62	0	0.17	1073.2	9.87	10.12	0.25	13
568	R11	76.57	0.06	11.65	1.04	0.07	0.36	3.23	2.46	4.62	0	0.17	1098.2	9.42	9.68	0.26	13
569	R11	76.57	0.06	11.65	1.04	0.07	0.36	3.23	2.46	4.62	0	0.17	1123.2	9.06	9.26	0.2	13
570	R16	77	0.06	11.77	1	0.06	0.36	3.29	2.48	4.68	0	0.55	948.15	11.46	10.69	-0.77	13
571	R16	77	0.06	11.77	1	0.06	0.36	3.29	2.48	4.68	0	0.55	973.15	10.85	10.29	-0.56	13
572	R16	77	0.06	11.77	1	0.06	0.36	3.29	2.48	4.68	0	0.55	973.15	10.88	10.29	-0.59	13
573	R16	77	0.06	11.77	1	0.06	0.36	3.29	2.48	4.68	0	0.55	998.15	10.5	9.9	-0.6	13
574	R16	77	0.06	11.77	1	0.06	0.36	3.29	2.48	4.68	0	0.55	1023.2	9.96	9.52	-0.44	13
575	R16	77	0.06	11.77	1	0.06	0.36	3.29	2.48	4.68	0	0.55	1023.2	9.94	9.52	-0.42	13
576	R16	77	0.06	11.77	1	0.06	0.36	3.29	2.48	4.68	0	0.55	1073.2	9.05	8.8	-0.25	13
577	R18	77.07	0.06	11.67	0.99	0.07	0.35	3.28	2.42	4.62	0	0.27	973.15	11.54	11.5	-0.04	13
578	R18	77.07	0.06	11.67	0.99	0.07	0.35	3.28	2.42	4.62	0	0.27	998.15	11.28	11.03	-0.25	13
579	R18	77.07	0.06	11.67	0.99	0.07	0.35	3.28	2.42	4.62	0	0.27	998.15	11.23	11.03	-0.2	13
580	R18	77.07	0.06	11.67	0.99	0.07	0.35	3.28	2.42	4.62	0	0.27	1023.2	10.57	10.58	0.01	13
581	R18	77.07	0.06	11.67	0.99	0.07	0.35	3.28	2.42	4.62	0	0.27	1023.2	10.83	10.58	-0.25	13
582	R18	77.07	0.06	11.67	0.99	0.07	0.35	3.28	2.42	4.62	0	0.27	1048.2	10.02	10.14	0.12	13
583	R18	77.07	0.06	11.67	0.99	0.07	0.35	3.28	2.42	4.62	0	0.27	1073.2	9.57	9.72	0.15	13
584	R18	77.07	0.06	11.67	0.99	0.07	0.35	3.28	2.42	4.62	0	0.27	1073.2	9.81	9.72	-0.09	13
585	R18	77.07	0.06	11.67	0.99	0.07	0.35	3.28	2.42	4.62	0	0.27	1098.2	9.37	9.31	-0.06	13
586	R18	77.07	0.06	11.67	0.99	0.07	0.35	3.28	2.42	4.62	0	0.27	998.15	11.51	11.03	-0.48	13
587	R18	77.07	0.06	11.67	0.99	0.07	0.35	3.28	2.42	4.62	0	0.27	1023.2	10.83	10.58	-0.25	13

588	R18	77.07	0.06	11.67	0.99	0.07	0.35	3.28	2.42	4.62	0	0.27	1023.2	10.89	10.58	-0.31	13
589	R18	77.07	0.06	11.67	0.99	0.07	0.35	3.28	2.42	4.62	0	0.27	1073.2	9.84	9.72	-0.12	13
590	R23	77.27	0.03	11.75	1.05	0.05	0.36	3.31	2.43	4.73	0	0.58	973.15	10.71	10.2	-0.51	13
591	R23	77.27	0.03	11.75	1.05	0.05	0.36	3.31	2.43	4.73	0	0.58	998.15	10.29	9.82	-0.47	13
592	R23	77.27	0.03	11.75	1.05	0.05	0.36	3.31	2.43	4.73	0	0.58	1023.2	9.86	9.44	-0.42	13
593	R23	77.27	0.03	11.75	1.05	0.05	0.36	3.31	2.43	4.73	0	0.58	1048.2	9.43	9.08	-0.35	13
594	R23	77.27	0.03	11.75	1.05	0.05	0.36	3.31	2.43	4.73	0	0.58	1073.2	9.02	8.73	-0.29	13
595	R23	77.27	0.03	11.75	1.05	0.05	0.36	3.31	2.43	4.73	0	0.58	1098.2	8.66	8.38	-0.28	13
596	R24	77.38	0.05	11.7	1.03	0.05	0.36	3.24	2.44	4.8	0	0.37	1023.2	10.16	10.14	-0.02	13
597	R24	77.38	0.05	11.7	1.03	0.05	0.36	3.24	2.44	4.8	0	0.37	1023.2	10.42	10.14	-0.28	13
598	R24	77.38	0.05	11.7	1.03	0.05	0.36	3.24	2.44	4.8	0	0.37	1048.2	9.69	9.74	0.05	13
599	R24	77.38	0.05	11.7	1.03	0.05	0.36	3.24	2.44	4.8	0	0.37	1073.2	9.32	9.34	0.02	13
600	R24	77.38	0.05	11.7	1.03	0.05	0.36	3.24	2.44	4.8	0	0.37	1073.2	9.47	9.34	-0.13	13
601	R24	77.38	0.05	11.7	1.03	0.05	0.36	3.24	2.44	4.8	0	0.37	1098.2	8.96	8.96	0	13
602	R24	77.38	0.05	11.7	1.03	0.05	0.36	3.24	2.44	4.8	0	0.37	1123.2	8.75	8.59	-0.16	13
603	R24	77.38	0.05	11.7	1.03	0.05	0.36	3.24	2.44	4.8	0	0.37	1023.2	10.14	10.14	0	13
604	R24	77.38	0.05	11.7	1.03	0.05	0.36	3.24	2.44	4.8	0	0.37	1023.2	10.34	10.14	-0.2	13
605	R24	77.38	0.05	11.7	1.03	0.05	0.36	3.24	2.44	4.8	0	0.37	1048.2	9.74	9.74	0	13
606	R24	77.38	0.05	11.7	1.03	0.05	0.36	3.24	2.44	4.8	0	0.37	1073.2	9.35	9.34	-0.01	13
607	R24	77.38	0.05	11.7	1.03	0.05	0.36	3.24	2.44	4.8	0	0.37	1073.2	9.51	9.34	-0.17	13
608	R24	77.38	0.05	11.7	1.03	0.05	0.36	3.24	2.44	4.8	0	0.37	1098.2	9.03	8.96	-0.07	13
609	R24	77.38	0.05	11.7	1.03	0.05	0.36	3.24	2.44	4.8	0	0.37	1123.2	8.79	8.59	-0.2	13
610	R25	77.46	0.05	11.64	1.04	0.07	0.35	3.23	2.45	4.7	0	0.31	998.15	10.95	10.82	-0.13	13
611	R25	77.46	0.05	11.64	1.04	0.07	0.35	3.23	2.45	4.7	0	0.31	1023.2	10.44	10.39	-0.05	13
612	R25	77.46	0.05	11.64	1.04	0.07	0.35	3.23	2.45	4.7	0	0.31	1048.2	9.97	9.97	0	13
613	R25	77.46	0.05	11.64	1.04	0.07	0.35	3.23	2.45	4.7	0	0.31	1073.2	9.53	9.56	0.03	13
614	R25	77.46	0.05	11.64	1.04	0.07	0.35	3.23	2.45	4.7	0	0.31	1098.2	9.12	9.16	0.04	13
615	R25	77.46	0.05	11.64	1.04	0.07	0.35	3.23	2.45	4.7	0	0.31	1123.2	8.82	8.78	-0.04	13
616	R25	77.46	0.05	11.64	1.04	0.07	0.35	3.23	2.45	4.7	0	0.31	948.15	12.44	11.73	-0.71	13
617	R25	77.46	0.05	11.64	1.04	0.07	0.35	3.23	2.45	4.7	0	0.31	973.15	11.7	11.27	-0.43	13
618	R25	77.46	0.05	11.64	1.04	0.07	0.35	3.23	2.45	4.7	0	0.31	998.15	11.31	10.82	-0.49	13
619	R9	76.03	0.06	11.48	1.05	0.06	0.36	3.21	2.42	4.6	0	0	1073.2	11.48	11.35	-0.13	13

620	R9	76.03	0.06	11.48	1.05	0.06	0.36	3.21	2.42	4.6	0	0	1098.2	10.86	10.76	-0.1	13
621	R9	76.03	0.06	11.48	1.05	0.06	0.36	3.21	2.42	4.6	0	0	1123.2	10.4	10.22	-0.18	13
622	R9	76.03	0.06	11.48	1.05	0.06	0.36	3.21	2.42	4.6	0	0	1148.2	9.91	9.72	-0.19	13
623	R9	76.03	0.06	11.48	1.05	0.06	0.36	3.21	2.42	4.6	0	0	1173.2	9.46	9.26	-0.2	13
624	R9	76.03	0.06	11.48	1.05	0.06	0.36	3.21	2.42	4.6	0	0	1198.2	9.13	8.82	-0.31	13
625	R12	76.59	0.08	12.67	1	0	0.03	0.52	3.98	4.88	0	1.68	738	12.35	12.52	0.17	14
626	R12	76.59	0.08	12.67	1	0	0.03	0.52	3.98	4.88	0	1.73	710	13.22	13.24	0.02	14
627	R12	76.59	0.08	12.67	1	0	0.03	0.52	3.98	4.88	0	1.57	671	15.2	14.76	-0.44	14
628	R12	76.59	0.08	12.67	1	0	0.03	0.52	3.98	4.88	0	1.82	709	13.23	13.13	-0.1	14
629	R12	76.59	0.08	12.67	1	0	0.03	0.52	3.98	4.88	0	1.86	731	12.34	12.44	0.1	14
630	R12	76.59	0.08	12.67	1	0	0.03	0.52	3.98	4.88	0	1.88	755	11.53	11.77	0.24	14
631	R12	76.59	0.08	12.67	1	0	0.03	0.52	3.98	4.88	0	2.37	729	11.62	11.8	0.18	14
632	R12	76.59	0.08	12.67	1	0	0.03	0.52	3.98	4.88	0	2.55	804	9.68	9.8	0.12	14
633	R12	76.59	0.08	12.67	1	0	0.03	0.52	3.98	4.88	0	1.84	845	9.63	9.82	0.19	14
634	R12	76.59	0.08	12.67	1	0	0.03	0.52	3.98	4.88	0	2.63	678	13.22	12.96	-0.26	14
635	R12	76.59	0.08	12.67	1	0	0.03	0.52	3.98	4.88	0	3.06	682	12.42	12.33	-0.09	14
636	R12	76.59	0.08	12.67	1	0	0.03	0.52	3.98	4.88	0	3	710	11.71	11.58	-0.13	14
637	R12	76.59	0.08	12.67	1	0	0.03	0.52	3.98	4.88	0	1.42	730	13.22	13.17	-0.05	14
638	R12	76.59	0.08	12.67	1	0	0.03	0.52	3.98	4.88	0	1.43	757	12.3	12.41	0.11	14
639	R12	76.59	0.08	12.67	1	0	0.03	0.52	3.98	4.88	0	1.42	787	11.57	11.68	0.11	14
640	R12	76.59	0.08	12.67	1	0	0.03	0.52	3.98	4.88	0	0.93	769	13.23	13.05	-0.18	14
641	R12	76.59	0.08	12.67	1	0	0.03	0.52	3.98	4.88	0	1.12	780	12.27	12.38	0.11	14
642	R12	76.59	0.08	12.67	1	0	0.03	0.52	3.98	4.88	0	1.16	810	11.49	11.6	0.11	14
643	R12	76.59	0.08	12.67	1	0	0.03	0.52	3.98	4.88	0	2.39	643	15.2	14.46	-0.74	14
644	R12	76.59	0.08	12.67	1	0	0.03	0.52	3.98	4.88	0	0.51	841	13.23	12.53	-0.7	14
645	R12	76.59	0.08	12.67	1	0	0.03	0.52	3.98	4.88	0	2.03	873	8.72	9.07	0.35	14
646	R12	76.59	0.08	12.67	1	0	0.03	0.52	3.98	4.88	0	1.97	798	10.3	10.62	0.32	14
647	R12	76.59	0.08	12.67	1	0	0.03	0.52	3.98	4.88	0	1.97	773	10.82	11.2	0.38	14
648	R12	76.59	0.08	12.67	1	0	0.03	0.52	3.98	4.88	0	2.04	848	9.26	9.51	0.25	14
649	R12	76.59	0.08	12.67	1	0	0.03	0.52	3.98	4.88	0	2.03	824	9.68	9.99	0.31	14
650	R12	76.59	0.08	12.67	1	0	0.03	0.52	3.98	4.88	0	1.36	873	9.7	9.99	0.29	14
651	R12	76.59	0.08	12.67	1	0	0.03	0.52	3.98	4.88	0	1.41	848	10.3	10.38	0.08	14

652	R12	76.59	0.08	12.67	1	0	0.03	0.52	3.98	4.88	0	1.46	873	9.62	9.84	0.22	14
653	R12	76.59	0.08	12.67	1	0	0.03	0.52	3.98	4.88	0	3.8	750	9.62	9.81	0.19	14
654	R12	76.59	0.08	12.67	1	0	0.03	0.52	3.98	4.88	0	3.8	642	13	12.81	-0.19	14
655	R12	76.59	0.08	12.67	1	0	0.03	0.52	3.98	4.88	0	3.8	625	14.23	13.39	-0.84	14
656	R12	76.59	0.08	12.67	1	0	0.03	0.52	3.98	4.88	0	5.6	707	9.6	9.5	-0.1	14
657	R12	76.59	0.08	12.67	1	0	0.03	0.52	3.98	4.88	0	5.6	604	13.24	12.49	-0.75	14
658	R12	76.59	0.08	12.67	1	0	0.03	0.52	3.98	4.88	0	5.6	648	11.44	11.07	-0.37	14
659	R12	76.59	0.08	12.67	1	0	0.03	0.52	3.98	4.88	0	7.7	670	9.6	9.21	-0.39	14
660	R12	76.59	0.08	12.67	1	0	0.03	0.52	3.98	4.88	0	7.7	573	13.24	12.11	-1.13	14
661	R12	76.59	0.08	12.67	1	0	0.03	0.52	3.98	4.88	0	7.7	603	11.45	11.08	-0.37	14
662	R12	76.59	0.08	12.67	1	0	0.03	0.52	3.98	4.88	0	0.78	825	12.24	12.07	-0.17	14
663	R12	76.59	0.08	12.67	1	0	0.03	0.52	3.98	4.88	0	0.8	823	12.24	12.07	-0.17	14
664	R12	76.59	0.08	12.67	1	0	0.03	0.52	3.98	4.88	0	0.82	820	12.24	12.09	-0.15	14
665	R12	76.59	0.08	12.67	1	0	0.03	0.52	3.98	4.88	0	0.79	971	9.61	9.62	0.01	14
666	R12	76.59	0.08	12.67	1	0	0.03	0.52	3.98	4.88	0	0.84	846	11.53	11.5	-0.03	14
667	R12	76.59	0.08	12.67	1	0	0.03	0.52	3.98	4.88	0	0.83	892	10.64	10.69	0.05	14
668	R12	76.59	0.08	12.67	1	0	0.03	0.52	3.98	4.88	0	0.89	772	13.23	13.05	-0.18	14
669	R12	76.59	0.08	12.67	1	0	0.03	0.52	3.98	4.88	0	0.81	804	12.76	12.46	-0.3	14
670	R12	76.59	0.08	12.67	1	0	0.03	0.52	3.98	4.88	0	0.84	765	13.71	13.35	-0.36	14
671	R12	76.59	0.08	12.67	1	0	0.03	0.52	3.98	4.88	0	0.84	752	14.2	13.7	-0.5	14
672	R12	76.59	0.08	12.67	1	0	0.03	0.52	3.98	4.88	0	0.83	784	13.2	12.89	-0.31	14
673	R12	76.59	0.08	12.67	1	0	0.03	0.52	3.98	4.88	0	0.84	779	13.2	12.99	-0.21	14
674	R12	76.59	0.08	12.67	1	0	0.03	0.52	3.98	4.88	0	0.81	728	15.2	14.46	-0.74	14
675	R12	76.59	0.08	12.67	1	0	0.03	0.52	3.98	4.88	0	1.14	748	13.22	13.18	-0.04	14
676	R12	76.59	0.08	12.67	1	0	0.03	0.52	3.98	4.88	0	1.17	897	9.48	9.91	0.43	14
677	R13	76.6	0.1	12.7	1.17	0	0.02	0.31	4.1	4.6	0	4.3	1073	5.51	5	-0.51	15
678	R13	76.6	0.1	12.7	1.17	0	0.02	0.31	4.1	4.6	0	4.3	1073	5.45	5	-0.45	15
679	R13	76.6	0.1	12.7	1.17	0	0.02	0.31	4.1	4.6	0	4.3	1123	5.26	4.6	-0.66	15
680	R13	76.6	0.1	12.7	1.17	0	0.02	0.31	4.1	4.6	0	4.3	1123	5.17	4.6	-0.57	15
681	R13	76.6	0.1	12.7	1.17	0	0.02	0.31	4.1	4.6	0	4.3	1173	4.88	4.22	-0.66	15
682	R13	76.6	0.1	12.7	1.17	0	0.02	0.31	4.1	4.6	0	6.2	973	5.52	5.2	-0.32	15
683	R13	76.6	0.1	12.7	1.17	0	0.02	0.31	4.1	4.6	0	6.2	1023	5.05	4.75	-0.3	15

684	R13	76.6	0.1	12.7	1.17	0	0.02	0.31	4.1	4.6	0	6.2	1073	4.57	4.35	-0.22	15
685	R13	76.6	0.1	12.7	1.17	0	0.02	0.31	4.1	4.6	0	6.2	1073	4.63	4.35	-0.28	15
686	R13	76.6	0.1	12.7	1.17	0	0.02	0.31	4.1	4.6	0	6.2	1123	4.25	3.98	-0.27	15
687	R1	66.77	0.39	20.15	4.31	0.01	0.72	3.64	1.37	2.17	0	0.02	1573.2	3.77	3.99	0.22	16
688	R1	66.77	0.39	20.15	4.31	0.01	0.72	3.64	1.37	2.17	0	0.02	1623.2	3.29	3.59	0.3	16
689	R1	66.77	0.39	20.15	4.31	0.01	0.72	3.64	1.37	2.17	0	0.02	1673.2	2.9	3.22	0.32	16
690	R1	66.77	0.39	20.15	4.31	0.01	0.72	3.64	1.37	2.17	0	0.02	1723.2	2.67	2.87	0.2	16
691	R1	66.77	0.39	20.15	4.31	0.01	0.72	3.64	1.37	2.17	0	0.02	1723.2	2.64	2.87	0.23	16
692	R1	66.77	0.39	20.15	4.31	0.01	0.72	3.64	1.37	2.17	0	0.02	1773.2	2.35	2.54	0.19	16
693	R1	66.77	0.39	20.15	4.31	0.01	0.72	3.64	1.37	2.17	0	0.02	1823.2	2.09	2.23	0.14	16
694	R1	66.77	0.39	20.15	4.31	0.01	0.72	3.64	1.37	2.17	0	0.02	1873.2	1.86	1.93	0.07	16
695	R2	67.16	0.01	21.65	2.81	0.01	0.73	2.65	2.85	1.82	0	0.02	1723.2	2.88	3.31	0.43	16
696	R2	67.16	0.01	21.65	2.81	0.01	0.73	2.65	2.85	1.82	0	0.02	1773.2	2.6	2.98	0.38	16
697	R2	67.16	0.01	21.65	2.81	0.01	0.73	2.65	2.85	1.82	0	0.02	1823.2	2.33	2.66	0.33	16
698	R2	67.16	0.01	21.65	2.81	0.01	0.73	2.65	2.85	1.82	0	0.02	1873.2	2.09	2.37	0.28	16
699	R3	71.22	0.24	16.8	2.91	0.06	0.8	2.62	3.09	1.94	0	0.02	1623.2	3.92	3.79	-0.13	16
700	R3	71.22	0.24	16.8	2.91	0.06	0.8	2.62	3.09	1.94	0	0.02	1673.2	3.61	3.42	-0.19	16
701	R3	71.22	0.24	16.8	2.91	0.06	0.8	2.62	3.09	1.94	0	0.02	1723.2	3.28	3.07	-0.21	16
702	R3	71.22	0.24	16.8	2.91	0.06	0.8	2.62	3.09	1.94	0	0.02	1773.2	3	2.75	-0.25	16
703	R3	71.22	0.24	16.8	2.91	0.06	0.8	2.62	3.09	1.94	0	0.02	1823.2	2.73	2.44	-0.29	16
704	R3	71.22	0.24	16.8	2.91	0.06	0.8	2.62	3.09	1.94	0	0.02	1873.2	2.48	2.15	-0.33	16
705	R4	71.42	0.01	16.1	4.58	0.01	1.57	0.94	1.94	2.92	0	0.02	1573.2	4.19	4.23	0.04	16
706	R4	71.42	0.01	16.1	4.58	0.01	1.57	0.94	1.94	2.92	0	0.02	1623.2	3.87	3.85	-0.02	16
707	R4	71.42	0.01	16.1	4.58	0.01	1.57	0.94	1.94	2.92	0	0.02	1673.2	3.52	3.49	-0.03	16
708	R4	71.42	0.01	16.1	4.58	0.01	1.57	0.94	1.94	2.92	0	0.02	1723.2	3.22	3.16	-0.06	16
709	R4	71.42	0.01	16.1	4.58	0.01	1.57	0.94	1.94	2.92	0	0.02	1773.2	2.92	2.85	-0.07	16
710	R4	71.42	0.01	16.1	4.58	0.01	1.57	0.94	1.94	2.92	0	0.02	1823.2	2.65	2.55	-0.1	16
711	R4	71.42	0.01	16.1	4.58	0.01	1.57	0.94	1.94	2.92	0	0.02	1873.2	2.4	2.28	-0.12	16
712	Tr10	73.35	0.9	14.83	2.38	0.07	0	1.64	1.87	4.7	0	0.02	1673.2	3.85	3.57	-0.28	16
713	Tr10	73.35	0.9	14.83	2.38	0.07	0	1.64	1.87	4.7	0	0.02	1713.2	3.59	3.28	-0.31	16
714	Tr10	73.35	0.9	14.83	2.38	0.07	0	1.64	1.87	4.7	0	0.02	1753.2	3.37	3.01	-0.36	16
715	Tr10	73.35	0.9	14.83	2.38	0.07	0	1.64	1.87	4.7	0	0.02	1793.2	3.1	2.75	-0.35	16

716	Tr10	73.35	0.9	14.83	2.38	0.07	0	1.64	1.87	4.7	0	0.02	1833.2	2.92	2.5	-0.42	16
717	Tr10	73.35	0.9	14.83	2.38	0.07	0	1.64	1.87	4.7	0	0.02	1873.2	2.76	2.26	-0.5	16
718	Tr7	66.95	0.87	21.24	2.57	0.06	0.01	1.63	1.83	4.55	0	0.02	1753.2	3.19	3.11	-0.08	16
719	Tr7	66.95	0.87	21.24	2.57	0.06	0.01	1.63	1.83	4.55	0	0.02	1793.2	3	2.85	-0.15	16
720	Tr7	66.95	0.87	21.24	2.57	0.06	0.01	1.63	1.83	4.55	0	0.02	1813.2	2.57	2.72	0.15	16
721	Tr7	66.95	0.87	21.24	2.57	0.06	0.01	1.63	1.83	4.55	0	0.02	1833.2	2.42	2.59	0.17	16
722	Tr7	66.95	0.87	21.24	2.57	0.06	0.01	1.63	1.83	4.55	0	0.02	1853.2	2.31	2.47	0.16	16
723	Tr7	66.95	0.87	21.24	2.57	0.06	0.01	1.63	1.83	4.55	0	0.02	1873.2	2.22	2.35	0.13	16
724	Tr8	68.71	0.9	19.28	2.59	0.06	0	1.65	1.87	4.66	0	0.02	1653.2	3.68	3.75	0.07	16
725	Tr8	68.71	0.9	19.28	2.59	0.06	0	1.65	1.87	4.66	0	0.02	1673.2	3.55	3.6	0.05	16
726	Tr8	68.71	0.9	19.28	2.59	0.06	0	1.65	1.87	4.66	0	0.02	1693.2	3.42	3.46	0.04	16
727	Tr8	68.71	0.9	19.28	2.59	0.06	0	1.65	1.87	4.66	0	0.02	1713.2	3.26	3.31	0.05	16
728	Tr8	68.71	0.9	19.28	2.59	0.06	0	1.65	1.87	4.66	0	0.02	1733.2	3.11	3.17	0.06	16
729	Tr8	68.71	0.9	19.28	2.59	0.06	0	1.65	1.87	4.66	0	0.02	1753.2	3	3.04	0.04	16
730	Tr8	68.71	0.9	19.28	2.59	0.06	0	1.65	1.87	4.66	0	0.02	1773.2	2.85	2.91	0.06	16
731	Tr8	68.71	0.9	19.28	2.59	0.06	0	1.65	1.87	4.66	0	0.02	1793.2	2.75	2.78	0.03	16
732	Tr8	68.71	0.9	19.28	2.59	0.06	0	1.65	1.87	4.66	0	0.02	1813.2	2.64	2.65	0.01	16
733	Tr8	68.71	0.9	19.28	2.59	0.06	0	1.65	1.87	4.66	0	0.02	1833.2	2.55	2.52	-0.03	16
734	Tr8	68.71	0.9	19.28	2.59	0.06	0	1.65	1.87	4.66	0	0.02	1853.2	2.42	2.4	-0.02	16
735	Tr8	68.71	0.9	19.28	2.59	0.06	0	1.65	1.87	4.66	0	0.02	1873.2	2.34	2.28	-0.06	16
736	Tr9	70.16	0.92	17.18	2.74	0.06	0	1.7	2.07	4.88	0	0.02	1633.2	4.1	3.77	-0.33	16
737	Tr9	70.16	0.92	17.18	2.74	0.06	0	1.7	2.07	4.88	0	0.02	1673.2	3.71	3.47	-0.24	16
738	Tr9	70.16	0.92	17.18	2.74	0.06	0	1.7	2.07	4.88	0	0.02	1713.2	3.44	3.19	-0.25	16
739	Tr9	70.16	0.92	17.18	2.74	0.06	0	1.7	2.07	4.88	0	0.02	1753.2	3.18	2.92	-0.26	16
740	Tr9	70.16	0.92	17.18	2.74	0.06	0	1.7	2.07	4.88	0	0.02	1793.2	2.95	2.66	-0.29	16
741	Tr9	70.16	0.92	17.18	2.74	0.06	0	1.7	2.07	4.88	0	0.02	1833.2	2.73	2.41	-0.32	16
742	Tr9	70.16	0.92	17.18	2.74	0.06	0	1.7	2.07	4.88	0	0.02	1873.2	2.59	2.17	-0.42	16
743	Bl2	47.81	1.94	17.91	10.9	0.19	4.75	9.96	3.94	2.11	0.48	0	1020.2	9.94	9.56	-0.38	17
744	Bl2	47.81	1.94	17.91	10.9	0.19	4.75	9.96	3.94	2.11	0.48	0	946.15	11.65	11.34	-0.31	17
745	Bn2	41.22	2.74	12.12	10.03	0	11.26	15.69	2.76	3.05	1.02	0	983.15	9.94	10.08	0.14	17
746	Bn2	41.22	2.74	12.12	10.03	0	11.26	15.69	2.76	3.05	1.02	0	1013.2	8.69	9.25	0.56	17
747	Bn2	41.22	2.74	12.12	10.03	0	11.26	15.69	2.76	3.05	1.02	0	953.15	11.41	11.17	-0.24	17

748	R8	75.37	0.07	12.84	1.57	0.07	0.04	0.72	4.19	5.13	0	0.14	993.15	11.1	11.46	0.36	17
749	R8	75.37	0.07	12.84	1.57	0.07	0.04	0.72	4.19	5.13	0	0.14	1011.2	10.78	11.15	0.37	17
750	R8	75.37	0.07	12.84	1.57	0.07	0.04	0.72	4.19	5.13	0	0.14	1043.2	10.18	10.62	0.44	17
751	R8	75.37	0.07	12.84	1.57	0.07	0.04	0.72	4.19	5.13	0	0.14	1084.2	9.56	9.97	0.41	17
752	R8	75.37	0.07	12.84	1.57	0.07	0.04	0.72	4.19	5.13	0	0.14	1114.2	9.15	9.52	0.37	17
753	R7	74.7	0.08	13.28	1.65	0	0	0.77	4.3	5.22	0	0	1273.2	7.85	7.92	0.07	18
754	R7	74.7	0.08	13.28	1.65	0	0	0.77	4.3	5.22	0	0	1273.2	7.82	7.92	0.1	18
755	R7	74.7	0.08	13.28	1.65	0	0	0.77	4.3	5.22	0	0	1273.2	7.87	7.92	0.05	18
756	R7	74.7	0.08	13.28	1.65	0	0	0.77	4.3	5.22	0	0	1323.2	7.26	7.3	0.04	18
757	R7	74.7	0.08	13.28	1.65	0	0	0.77	4.3	5.22	0	0	1373.2	6.79	6.73	-0.06	18
758	R7	74.7	0.08	13.28	1.65	0	0	0.77	4.3	5.22	0	0	1373.2	6.77	6.73	-0.04	18
759	R7	74.7	0.08	13.28	1.65	0	0	0.77	4.3	5.22	0	0	1423.2	6.25	6.2	-0.05	18
760	Bn1	41.15	2.74	12.1	10.11	0	11.24	15.66	2.76	3.04	1.02	0.02	1744	-0.22	-0.68	-0.46	19
761	Bn1	41.15	2.74	12.1	10.11	0	11.24	15.66	2.76	3.04	1.02	0.02	1719.4	-0.16	-0.49	-0.33	19
762	Bn1	41.15	2.74	12.1	10.11	0	11.24	15.66	2.76	3.04	1.02	0.02	1694.8	-0.09	-0.29	-0.2	19
763	Bn1	41.15	2.74	12.1	10.11	0	11.24	15.66	2.76	3.04	1.02	0.02	1670.2	-0.02	-0.09	-0.07	19
764	Bn1	41.15	2.74	12.1	10.11	0	11.24	15.66	2.76	3.04	1.02	0.02	1645.6	0.07	0.12	0.05	19
765	Bn1	41.15	2.74	12.1	10.11	0	11.24	15.66	2.76	3.04	1.02	0.02	1621	0.16	0.34	0.18	19
766	Bn1	41.15	2.74	12.1	10.11	0	11.24	15.66	2.76	3.04	1.02	0.02	975.15	10.26	10.14	-0.12	19
767	Bn1	41.15	2.74	12.1	10.11	0	11.24	15.66	2.76	3.04	1.02	0.02	982.75	9.81	9.91	0.1	19
768	Bn1	41.15	2.74	12.1	10.11	0	11.24	15.66	2.76	3.04	1.02	0.02	983.15	10.05	9.9	-0.15	19
769	Bn1	41.15	2.74	12.1	10.11	0	11.24	15.66	2.76	3.04	1.02	0.02	965	10.77	10.48	-0.29	19
770	Ph1	51.2	0.67	18.6	6.1	0.13	2.5	7.3	3.75	7.9	0.4	0.02	1817.9	0.97	0.92	-0.05	19
771	Ph1	51.2	0.67	18.6	6.1	0.13	2.5	7.3	3.75	7.9	0.4	0.02	1793.3	1.07	1.07	0	19
772	Ph1	51.2	0.67	18.6	6.1	0.13	2.5	7.3	3.75	7.9	0.4	0.02	1768.7	1.17	1.21	0.04	19
773	Ph1	51.2	0.67	18.6	6.1	0.13	2.5	7.3	3.75	7.9	0.4	0.02	1744	1.28	1.36	0.08	19
774	Ph1	51.2	0.67	18.6	6.1	0.13	2.5	7.3	3.75	7.9	0.4	0.02	1719.4	1.38	1.52	0.14	19
775	Ph1	51.2	0.67	18.6	6.1	0.13	2.5	7.3	3.75	7.9	0.4	0.02	1694.8	1.5	1.68	0.18	19
776	Ph1	51.2	0.67	18.6	6.1	0.13	2.5	7.3	3.75	7.9	0.4	0.02	1670.2	1.63	1.84	0.21	19
777	Ph1	51.2	0.67	18.6	6.1	0.13	2.5	7.3	3.75	7.9	0.4	0.02	1645.6	1.75	2.01	0.26	19
778	Ph1	51.2	0.67	18.6	6.1	0.13	2.5	7.3	3.75	7.9	0.4	0.02	1621	1.88	2.19	0.31	19
779	Ph1	51.2	0.67	18.6	6.1	0.13	2.5	7.3	3.75	7.9	0.4	0.02	978.15	10.66	10.34	-0.32	19

780	Ph1	51.2	0.67	18.6	6.1	0.13	2.5	7.3	3.75	7.9	0.4	0.02	997.5	10.15	9.85	-0.3	19
781	Ph1	51.2	0.67	18.6	6.1	0.13	2.5	7.3	3.75	7.9	0.4	0.02	1016.4	9.75	9.42	-0.33	19
782	Ph5	59.7	0.46	18.52	3.6	0.17	0.65	2.8	3.89	8.45	0.15	0.02	1744	2.45	2.3	-0.15	19
783	Ph5	59.7	0.46	18.52	3.6	0.17	0.65	2.8	3.89	8.45	0.15	0.02	1719.4	2.58	2.45	-0.13	19
784	Ph5	59.7	0.46	18.52	3.6	0.17	0.65	2.8	3.89	8.45	0.15	0.02	1694.8	2.72	2.61	-0.11	19
785	Ph5	59.7	0.46	18.52	3.6	0.17	0.65	2.8	3.89	8.45	0.15	0.02	1621	3.16	3.11	-0.05	19
786	Ph5	59.7	0.46	18.52	3.6	0.17	0.65	2.8	3.89	8.45	0.15	0.02	1596.4	3.32	3.29	-0.03	19
787	Ph5	59.7	0.46	18.52	3.6	0.17	0.65	2.8	3.89	8.45	0.15	0.02	1571.8	3.48	3.48	0	19
788	Ph5	59.7	0.46	18.52	3.6	0.17	0.65	2.8	3.89	8.45	0.15	0.02	1547.2	3.66	3.67	0.01	19
789	Ph5	59.7	0.46	18.52	3.6	0.17	0.65	2.8	3.89	8.45	0.15	0.02	1522.6	3.83	3.86	0.03	19
790	Ph5	59.7	0.46	18.52	3.6	0.17	0.65	2.8	3.89	8.45	0.15	0.02	1497.9	4.02	4.07	0.05	19
791	Ph5	59.7	0.46	18.52	3.6	0.17	0.65	2.8	3.89	8.45	0.15	0.02	1473.3	4.2	4.28	0.08	19
792	Ph5	59.7	0.46	18.52	3.6	0.17	0.65	2.8	3.89	8.45	0.15	0.02	1448.7	4.4	4.5	0.1	19
793	Ph5	59.7	0.46	18.52	3.6	0.17	0.65	2.8	3.89	8.45	0.15	0.02	1424.1	4.6	4.72	0.12	19
794	Ph5	59.7	0.46	18.52	3.6	0.17	0.65	2.8	3.89	8.45	0.15	0.02	1034.6	10.3	9.96	-0.34	19
795	Ph5	59.7	0.46	18.52	3.6	0.17	0.65	2.8	3.89	8.45	0.15	0.02	1047.7	10.11	9.71	-0.4	19
796	Ph5	59.7	0.46	18.52	3.6	0.17	0.65	2.8	3.89	8.45	0.15	0.02	1067.5	9.73	9.34	-0.39	19
797	Ph5	59.7	0.46	18.52	3.6	0.17	0.65	2.8	3.89	8.45	0.15	0.02	1083.8	9.55	9.05	-0.5	19
798	Ph5	59.7	0.46	18.52	3.6	0.17	0.65	2.8	3.89	8.45	0.15	0.02	1104.1	9.11	8.71	-0.4	19
799	Te1	49.2	0.83	16.4	7.2	0.13	5.1	10.2	2.7	6.5	0.72	0.02	1817.9	0.53	0.38	-0.15	19
800	Te1	49.2	0.83	16.4	7.2	0.13	5.1	10.2	2.7	6.5	0.72	0.02	1793.3	0.62	0.52	-0.1	19
801	Te1	49.2	0.83	16.4	7.2	0.13	5.1	10.2	2.7	6.5	0.72	0.02	1768.7	0.71	0.68	-0.03	19
802	Te1	49.2	0.83	16.4	7.2	0.13	5.1	10.2	2.7	6.5	0.72	0.02	1744	0.81	0.83	0.02	19
803	Te1	49.2	0.83	16.4	7.2	0.13	5.1	10.2	2.7	6.5	0.72	0.02	1719.4	0.9	0.99	0.09	19
804	Te1	49.2	0.83	16.4	7.2	0.13	5.1	10.2	2.7	6.5	0.72	0.02	1694.8	1.01	1.16	0.15	19
805	Te1	49.2	0.83	16.4	7.2	0.13	5.1	10.2	2.7	6.5	0.72	0.02	1670.2	1.12	1.33	0.21	19
806	Te1	49.2	0.83	16.4	7.2	0.13	5.1	10.2	2.7	6.5	0.72	0.02	1645.6	1.24	1.5	0.26	19
807	Te1	49.2	0.83	16.4	7.2	0.13	5.1	10.2	2.7	6.5	0.72	0.02	1621	1.36	1.69	0.33	19
808	Te1	49.2	0.83	16.4	7.2	0.13	5.1	10.2	2.7	6.5	0.72	0.02	980.6	10.55	10.41	-0.14	19
809	Te1	49.2	0.83	16.4	7.2	0.13	5.1	10.2	2.7	6.5	0.72	0.02	993.35	10.17	9.97	-0.2	19
810	Te1	49.2	0.83	16.4	7.2	0.13	5.1	10.2	2.7	6.5	0.72	0.02	1002.3	9.78	9.69	-0.09	19
811	Te1	49.2	0.83	16.4	7.2	0.13	5.1	10.2	2.7	6.5	0.72	0.02	1017.9	9.51	9.25	-0.26	19

812	Te1	49.2	0.83	16.4	7.2	0.13	5.1	10.2	2.7	6.5	0.72	0.02	1029.4	9.13	8.95	-0.18	19
813	Te1	49.2	0.83	16.4	7.2	0.13	5.1	10.2	2.7	6.5	0.72	0.02	1040.1	8.79	8.7	-0.09	19
814	Te1	49.2	0.83	16.4	7.2	0.13	5.1	10.2	2.7	6.5	0.72	0.02	969.95	10.98	10.84	-0.14	19
815	Tr5	63.99	0.45	16.96	2.55	0.14	0.32	0.83	6.33	6.37	0.09	0.02	1867.1	2.14	1.98	-0.16	19
816	Tr5	63.99	0.45	16.96	2.55	0.14	0.32	0.83	6.33	6.37	0.09	0.02	1842.5	2.25	2.11	-0.14	19
817	Tr5	63.99	0.45	16.96	2.55	0.14	0.32	0.83	6.33	6.37	0.09	0.02	1817.9	2.37	2.25	-0.12	19
818	Tr5	63.99	0.45	16.96	2.55	0.14	0.32	0.83	6.33	6.37	0.09	0.02	1793.3	2.5	2.39	-0.11	19
819	Tr5	63.99	0.45	16.96	2.55	0.14	0.32	0.83	6.33	6.37	0.09	0.02	1768.7	2.63	2.53	-0.1	19
820	Tr5	63.99	0.45	16.96	2.55	0.14	0.32	0.83	6.33	6.37	0.09	0.02	1744	2.76	2.68	-0.08	19
821	Tr5	63.99	0.45	16.96	2.55	0.14	0.32	0.83	6.33	6.37	0.09	0.02	1719.4	2.91	2.83	-0.08	19
822	Tr5	63.99	0.45	16.96	2.55	0.14	0.32	0.83	6.33	6.37	0.09	0.02	1694.8	3.05	2.99	-0.06	19
823	Tr5	63.99	0.45	16.96	2.55	0.14	0.32	0.83	6.33	6.37	0.09	0.02	1670.2	3.2	3.15	-0.05	19
824	Tr5	63.99	0.45	16.96	2.55	0.14	0.32	0.83	6.33	6.37	0.09	0.02	1645.6	3.36	3.31	-0.05	19
825	Tr5	63.99	0.45	16.96	2.55	0.14	0.32	0.83	6.33	6.37	0.09	0.02	1621	3.52	3.48	-0.04	19
826	Tr5	63.99	0.45	16.96	2.55	0.14	0.32	0.83	6.33	6.37	0.09	0.02	1596.4	3.68	3.66	-0.02	19
827	Tr5	63.99	0.45	16.96	2.55	0.14	0.32	0.83	6.33	6.37	0.09	0.02	1571.8	3.85	3.84	-0.01	19
828	Tr5	63.99	0.45	16.96	2.55	0.14	0.32	0.83	6.33	6.37	0.09	0.02	1547.2	4	4.03	0.03	19
829	Tr5	63.99	0.45	16.96	2.55	0.14	0.32	0.83	6.33	6.37	0.09	0.02	1522.6	4.21	4.23	0.02	19
830	Tr5	63.99	0.45	16.96	2.55	0.14	0.32	0.83	6.33	6.37	0.09	0.02	1497.9	4.4	4.43	0.03	19
831	Tr5	63.99	0.45	16.96	2.55	0.14	0.32	0.83	6.33	6.37	0.09	0.02	1473.3	4.59	4.64	0.05	19
832	Tr5	63.99	0.45	16.96	2.55	0.14	0.32	0.83	6.33	6.37	0.09	0.02	996.03	10.77	10.91	0.14	19
833	Tr5	63.99	0.45	16.96	2.55	0.14	0.32	0.83	6.33	6.37	0.09	0.02	1010.3	10.53	10.62	0.09	19
834	Tr5	63.99	0.45	16.96	2.55	0.14	0.32	0.83	6.33	6.37	0.09	0.02	1011.7	10.41	10.6	0.19	19
835	Tr5	63.99	0.45	16.96	2.55	0.14	0.32	0.83	6.33	6.37	0.09	0.02	1016.3	10.49	10.51	0.02	19
836	Tr5	63.99	0.45	16.96	2.55	0.14	0.32	0.83	6.33	6.37	0.09	0.02	1022.9	10.19	10.38	0.19	19
837	Tr5	63.99	0.45	16.96	2.55	0.14	0.32	0.83	6.33	6.37	0.09	0.02	1033.8	9.95	10.18	0.23	19
838	Tr5	63.99	0.45	16.96	2.55	0.14	0.32	0.83	6.33	6.37	0.09	0.02	1055	9.63	9.79	0.16	19
839	Tr5	63.99	0.45	16.96	2.55	0.14	0.32	0.83	6.33	6.37	0.09	0.02	1079.7	9.11	9.37	0.26	19
840	Tr1	60.74	0.27	19.22	3.37	0.18	0.28	2.11	5.28	6.32	0.06	0	1769.2	2.37	2.48	0.11	20
841	Tr1	60.74	0.27	19.22	3.37	0.18	0.28	2.11	5.28	6.32	0.06	0	1744.2	2.49	2.63	0.14	20
842	Tr1	60.74	0.27	19.22	3.37	0.18	0.28	2.11	5.28	6.32	0.06	0	1719.2	2.63	2.79	0.16	20
843	Tr1	60.74	0.27	19.22	3.37	0.18	0.28	2.11	5.28	6.32	0.06	0	1695.2	2.77	2.94	0.17	20

844	Tr1	60.74	0.27	19.22	3.37	0.18	0.28	2.11	5.28	6.32	0.06	0	1670.2	2.92	3.1	0.18	20
845	Tr1	60.74	0.27	19.22	3.37	0.18	0.28	2.11	5.28	6.32	0.06	0	1646.2	3.08	3.27	0.19	20
846	Tr1	60.74	0.27	19.22	3.37	0.18	0.28	2.11	5.28	6.32	0.06	0	1621.2	3.24	3.44	0.2	20
847	Tr1	60.74	0.27	19.22	3.37	0.18	0.28	2.11	5.28	6.32	0.06	0	1596.2	3.4	3.63	0.23	20
848	Tr1	60.74	0.27	19.22	3.37	0.18	0.28	2.11	5.28	6.32	0.06	0	1572.2	3.58	3.81	0.23	20
849	Tr1	60.74	0.27	19.22	3.37	0.18	0.28	2.11	5.28	6.32	0.06	0	1547.2	3.76	4	0.24	20
850	Tr1	60.74	0.27	19.22	3.37	0.18	0.28	2.11	5.28	6.32	0.06	0	1522.2	3.94	4.2	0.26	20
851	Tr1	60.74	0.27	19.22	3.37	0.18	0.28	2.11	5.28	6.32	0.06	0	1498.2	4.14	4.4	0.26	20
852	Tr1	60.74	0.27	19.22	3.37	0.18	0.28	2.11	5.28	6.32	0.06	0	1473.2	4.34	4.62	0.28	20
853	Tr1	60.74	0.27	19.22	3.37	0.18	0.28	2.11	5.28	6.32	0.06	0	1449.2	4.54	4.83	0.29	20
854	Tr1	60.74	0.27	19.22	3.37	0.18	0.28	2.11	5.28	6.32	0.06	0	1134.2	9.32	8.57	-0.75	20
855	Tr1	60.74	0.27	19.22	3.37	0.18	0.28	2.11	5.28	6.32	0.06	0	1109.2	9.84	8.98	-0.86	20
856	Tr1	60.74	0.27	19.22	3.37	0.18	0.28	2.11	5.28	6.32	0.06	0	1076.2	10.44	9.54	-0.9	20
857	Tr1	60.74	0.27	19.22	3.37	0.18	0.28	2.11	5.28	6.32	0.06	0	1056.2	10.83	9.91	-0.92	20
858	Tr1	60.74	0.27	19.22	3.37	0.18	0.28	2.11	5.28	6.32	0.06	0.81	835.15	11.12	11.22	0.1	20
859	Tr1	60.74	0.27	19.22	3.37	0.18	0.28	2.11	5.28	6.32	0.06	0.81	842.15	10.94	11.07	0.13	20
860	Tr1	60.74	0.27	19.22	3.37	0.18	0.28	2.11	5.28	6.32	0.06	0.81	852.15	10.75	10.86	0.11	20
861	Tr1	60.74	0.27	19.22	3.37	0.18	0.28	2.11	5.28	6.32	0.06	0.81	868.15	10.44	10.52	0.08	20
862	Tr1	60.74	0.27	19.22	3.37	0.18	0.28	2.11	5.28	6.32	0.06	0.81	869.15	10.3	10.5	0.2	20
863	Tr1	60.74	0.27	19.22	3.37	0.18	0.28	2.11	5.28	6.32	0.06	0.81	877.15	10.09	10.34	0.25	20
864	Tr1	60.74	0.27	19.22	3.37	0.18	0.28	2.11	5.28	6.32	0.06	1.54	802.15	10.86	10.65	-0.21	20
865	Tr1	60.74	0.27	19.22	3.37	0.18	0.28	2.11	5.28	6.32	0.06	1.54	819.15	10.36	10.27	-0.09	20
866	Tr1	60.74	0.27	19.22	3.37	0.18	0.28	2.11	5.28	6.32	0.06	1.54	826.15	10.14	10.11	-0.03	20
867	Tr1	60.74	0.27	19.22	3.37	0.18	0.28	2.11	5.28	6.32	0.06	2.01	781.15	10.52	10.48	-0.04	20
868	Tr1	60.74	0.27	19.22	3.37	0.18	0.28	2.11	5.28	6.32	0.06	2.01	779.15	10.44	10.53	0.09	20
869	Tr1	60.74	0.27	19.22	3.37	0.18	0.28	2.11	5.28	6.32	0.06	2.01	811.15	9.94	9.8	-0.14	20
870	Tr1	60.74	0.27	19.22	3.37	0.18	0.28	2.11	5.28	6.32	0.06	2.96	732.15	10.76	10.58	-0.18	20
871	Tr1	60.74	0.27	19.22	3.37	0.18	0.28	2.11	5.28	6.32	0.06	2.96	740.15	10.27	10.38	0.11	20
872	Tr1	60.74	0.27	19.22	3.37	0.18	0.28	2.11	5.28	6.32	0.06	3.41	691.15	11.28	11.23	-0.05	20
873	Tr1	60.74	0.27	19.22	3.37	0.18	0.28	2.11	5.28	6.32	0.06	3.41	715.15	10.45	10.57	0.12	20
874	Tr1	60.74	0.27	19.22	3.37	0.18	0.28	2.11	5.28	6.32	0.06	3.41	730.15	9.88	10.18	0.3	20
875	Tr4	63.88	0.31	17.1	2.9	0.13	0.24	1.82	5.67	6.82	0.05	0.02	1768.7	2.5	2.45	-0.05	20

876 Tr4	63.88	0.31	17.1	2.9	0.13	0.24	1.82	5.67	6.82	0.05	0.02	1744	2.62	2.59	-0.03	20
877 Tr4	63.88	0.31	17.1	2.9	0.13	0.24	1.82	5.67	6.82	0.05	0.02	1719.4	2.75	2.74	-0.01	20
878 Tr4	63.88	0.31	17.1	2.9	0.13	0.24	1.82	5.67	6.82	0.05	0.02	1694.8	2.89	2.9	0.01	20
879 Tr4	63.88	0.31	17.1	2.9	0.13	0.24	1.82	5.67	6.82	0.05	0.02	1670.2	3.03	3.06	0.03	20
880 Tr4	63.88	0.31	17.1	2.9	0.13	0.24	1.82	5.67	6.82	0.05	0.02	1645.6	3.18	3.22	0.04	20
881 Tr4	63.88	0.31	17.1	2.9	0.13	0.24	1.82	5.67	6.82	0.05	0.02	1621	3.33	3.39	0.06	20
882 Tr4	63.88	0.31	17.1	2.9	0.13	0.24	1.82	5.67	6.82	0.05	0.02	1596.4	3.49	3.57	0.08	20
883 Tr4	63.88	0.31	17.1	2.9	0.13	0.24	1.82	5.67	6.82	0.05	0.02	1571.8	3.65	3.75	0.1	20
884 Tr4	63.88	0.31	17.1	2.9	0.13	0.24	1.82	5.67	6.82	0.05	0.02	1547.2	3.82	3.94	0.12	20
885 Tr4	63.88	0.31	17.1	2.9	0.13	0.24	1.82	5.67	6.82	0.05	0.02	1522.6	3.97	4.13	0.16	20
886 Tr4	63.88	0.31	17.1	2.9	0.13	0.24	1.82	5.67	6.82	0.05	0.02	1497.9	4.17	4.34	0.17	20
887 Tr4	63.88	0.31	17.1	2.9	0.13	0.24	1.82	5.67	6.82	0.05	0.02	1473.3	4.36	4.54	0.18	20
888 Tr4	63.88	0.31	17.1	2.9	0.13	0.24	1.82	5.67	6.82	0.05	0.02	1448.7	4.55	4.76	0.21	20
889 Tr4	63.88	0.31	17.1	2.9	0.13	0.24	1.82	5.67	6.82	0.05	0.02	1017	10.03	10.46	0.43	20
890 Tr4	63.88	0.31	17.1	2.9	0.13	0.24	1.82	5.67	6.82	0.05	0.02	979.25	10.71	11.24	0.53	20
891 Tr4	63.88	0.31	17.1	2.9	0.13	0.24	1.82	5.67	6.82	0.05	0.02	1090	8.76	9.13	0.37	20
892 Tr4	63.88	0.31	17.1	2.9	0.13	0.24	1.82	5.67	6.82	0.05	0.02	1042.5	9.56	9.97	0.41	20
893 Tr4	63.88	0.31	17.1	2.9	0.13	0.24	1.82	5.67	6.82	0.05	0.02	958.6	11.08	11.69	0.61	20
894 Tr4	63.88	0.31	17.1	2.9	0.13	0.24	1.82	5.67	6.82	0.05	1	839.15	10.64	10.66	0.02	20
895 Tr4	63.88	0.31	17.1	2.9	0.13	0.24	1.82	5.67	6.82	0.05	1	848.15	10.47	10.47	0	20
896 Tr4	63.88	0.31	17.1	2.9	0.13	0.24	1.82	5.67	6.82	0.05	1	862.15	10.22	10.19	-0.03	20
897 Tr4	63.88	0.31	17.1	2.9	0.13	0.24	1.82	5.67	6.82	0.05	1	870.15	10.08	10.03	-0.05	20
898 Tr4	63.88	0.31	17.1	2.9	0.13	0.24	1.82	5.67	6.82	0.05	1.39	788.15	10.97	11.13	0.16	20
899 Tr4	63.88	0.31	17.1	2.9	0.13	0.24	1.82	5.67	6.82	0.05	1.39	818.15	10.31	10.44	0.13	20
900 Tr4	63.88	0.31	17.1	2.9	0.13	0.24	1.82	5.67	6.82	0.05	1.39	843.15	9.9	9.9	0	20
901 Tr4	63.88	0.31	17.1	2.9	0.13	0.24	1.82	5.67	6.82	0.05	2.41	745.15	10.59	10.77	0.18	20
902 Tr4	63.88	0.31	17.1	2.9	0.13	0.24	1.82	5.67	6.82	0.05	2.41	788.15	9.67	9.74	0.07	20
903 Tr4	63.88	0.31	17.1	2.9	0.13	0.24	1.82	5.67	6.82	0.05	3.86	674.15	10.85	11.18	0.33	20
904 Tr4	63.88	0.31	17.1	2.9	0.13	0.24	1.82	5.67	6.82	0.05	3.86	673.15	10.8	11.2	0.4	20
905 Tr4	63.88	0.31	17.1	2.9	0.13	0.24	1.82	5.67	6.82	0.05	3.86	671.15	10.79	11.26	0.47	20
906 Tr4	63.88	0.31	17.1	2.9	0.13	0.24	1.82	5.67	6.82	0.05	3.86	658.15	11.6	11.66	0.06	20
907 A1	58.56	0.64	18.98	7.45	0	3.48	6.17	3.24	0.92	0	0.83	1473.2	2.75	2.59	-0.16	21

908	A1	58.56	0.64	18.98	7.45	0	3.48	6.17	3.24	0.92	0	0.83	1573.2	2.22	1.85	-0.37	21
909	A1	58.56	0.64	18.98	7.45	0	3.48	6.17	3.24	0.92	0	0.83	1573.2	2.15	1.85	-0.3	21
910	A1	58.56	0.64	18.98	7.45	0	3.48	6.17	3.24	0.92	0	0.83	1623.2	1.76	1.52	-0.24	21
911	A1	58.56	0.64	18.98	7.45	0	3.48	6.17	3.24	0.92	0	0.72	1473.2	2.37	2.7	0.33	21
912	A1	58.56	0.64	18.98	7.45	0	3.48	6.17	3.24	0.92	0	1	1423.2	2.5	2.83	0.33	21
913	A1	58.56	0.64	18.98	7.45	0	3.48	6.17	3.24	0.92	0	1	1473.2	2.25	2.44	0.19	21
914	A1	58.56	0.64	18.98	7.45	0	3.48	6.17	3.24	0.92	0	1	1373.2	3.64	3.26	-0.38	21
915	A1	58.56	0.64	18.98	7.45	0	3.48	6.17	3.24	0.92	0	1	1473.2	2.01	2.44	0.43	21
916	A1	58.56	0.64	18.98	7.45	0	3.48	6.17	3.24	0.92	0	4.6	1373.2	1.8	1.74	-0.06	21
917	A1	58.56	0.64	18.98	7.45	0	3.48	6.17	3.24	0.92	0	4.6	1473.2	1.45	1.18	-0.27	21
918	Bl3	48.21	1.25	15.5	10.64	0	9.08	11.92	2.4	0.08	0.14	0.22	1373.2	2.86	3.19	0.33	21
919	Bl3	48.21	1.25	15.5	10.64	0	9.08	11.92	2.4	0.08	0.14	0.22	1523.2	2.3	1.74	-0.56	21
920	Bl4	53.54	1.05	17.29	7.82	0	5.46	8.32	3.59	1.64	0.2	2.5	1373.2	1.74	1.83	0.09	21
921	Bl4	53.54	1.05	17.29	7.82	0	5.46	8.32	3.59	1.64	0.2	2.5	1573.2	0.91	0.48	-0.43	21
922	Bl4	53.54	1.05	17.29	7.82	0	5.46	8.32	3.59	1.64	0.2	2.5	1373.2	1.42	1.83	0.41	21
923	Bl4	53.54	1.05	17.29	7.82	0	5.46	8.32	3.59	1.64	0.2	2.5	1573.2	0.8	0.48	-0.32	21
924	Bl4	53.54	1.05	17.29	7.82	0	5.46	8.32	3.59	1.64	0.2	6.36	1273.2	1.3	1.77	0.47	21
925	Bl4	53.54	1.05	17.29	7.82	0	5.46	8.32	3.59	1.64	0.2	6.36	1573.2	0.27	0.21	-0.06	21
926	Bl4	53.54	1.05	17.29	7.82	0	5.46	8.32	3.59	1.64	0.2	0	1473.2	3.6	3.39	-0.21	21
927	Bl4	53.54	1.05	17.29	7.82	0	5.46	8.32	3.59	1.64	0.2	0	1573.2	2.16	2.5	0.34	21
928	Bl4	53.54	1.05	17.29	7.82	0	5.46	8.32	3.59	1.64	0.2	0	1473.2	3.4	3.39	-0.01	21
929	Bl4	53.54	1.05	17.29	7.82	0	5.46	8.32	3.59	1.64	0.2	0	1573.2	2.94	2.5	-0.44	21
930	R5	73.23	0.19	13.6	2.78	0	0.17	1.69	3.78	4.11	0.13	2.1	1073.2	6.1	6.19	0.09	21
931	R5	73.23	0.19	13.6	2.78	0	0.17	1.69	3.78	4.11	0.13	2.1	1373.2	3.25	3.56	0.31	21
932	R5	73.23	0.19	13.6	2.78	0	0.17	1.69	3.78	4.11	0.13	3	1073.2	4.8	5.48	0.68	21
933	R5	73.23	0.19	13.6	2.78	0	0.17	1.69	3.78	4.11	0.13	3.3	1473.2	2.25	2.29	0.04	21
934	R5	73.23	0.19	13.6	2.78	0	0.17	1.69	3.78	4.11	0.13	5.2	1073.2	3.97	4.44	0.47	21
935	R5	73.23	0.19	13.6	2.78	0	0.17	1.69	3.78	4.11	0.13	5.2	1473.2	1.67	1.88	0.21	21
936	R5	73.23	0.19	13.6	2.78	0	0.17	1.69	3.78	4.11	0.13	12.3	1123.2	3.2	3.25	0.05	21
937	R5	73.23	0.19	13.6	2.78	0	0.17	1.69	3.78	4.11	0.13	12.3	1223.2	2.4	2.81	0.41	21
938	Ph6	60.46	0.56	18.81	3.31	0.2	0.36	0.67	9.76	5.45	0.06	0.02	1773.2	2.2	2.13	-0.07	22
939	Ph6	60.46	0.56	18.81	3.31	0.2	0.36	0.67	9.76	5.45	0.06	0.02	1748.2	2.32	2.26	-0.06	22

940	Ph6	60.46	0.56	18.81	3.31	0.2	0.36	0.67	9.76	5.45	0.06	0.02	1723.2	2.44	2.4	-0.04	22
941	Ph6	60.46	0.56	18.81	3.31	0.2	0.36	0.67	9.76	5.45	0.06	0.02	1698.2	2.57	2.54	-0.03	22
942	Ph6	60.46	0.56	18.81	3.31	0.2	0.36	0.67	9.76	5.45	0.06	0.02	1673.2	2.7	2.68	-0.02	22
943	Ph6	60.46	0.56	18.81	3.31	0.2	0.36	0.67	9.76	5.45	0.06	0.02	1648.2	2.83	2.83	0	22
944	Ph6	60.46	0.56	18.81	3.31	0.2	0.36	0.67	9.76	5.45	0.06	0.02	1623.2	2.97	2.98	0.01	22
945	Ph6	60.46	0.56	18.81	3.31	0.2	0.36	0.67	9.76	5.45	0.06	0.02	1598.2	3.11	3.14	0.03	22
946	Ph6	60.46	0.56	18.81	3.31	0.2	0.36	0.67	9.76	5.45	0.06	0.02	1573.2	3.26	3.31	0.05	22
947	Ph6	60.46	0.56	18.81	3.31	0.2	0.36	0.67	9.76	5.45	0.06	0.02	1548.2	3.42	3.48	0.06	22
948	Ph6	60.46	0.56	18.81	3.31	0.2	0.36	0.67	9.76	5.45	0.06	0.02	1523.2	3.57	3.65	0.08	22
949	Ph6	60.46	0.56	18.81	3.31	0.2	0.36	0.67	9.76	5.45	0.06	0.02	1498.2	3.74	3.83	0.09	22
950	Ph6	60.46	0.56	18.81	3.31	0.2	0.36	0.67	9.76	5.45	0.06	0.02	1473.2	3.91	4.02	0.11	22
951	Ph6	60.46	0.56	18.81	3.31	0.2	0.36	0.67	9.76	5.45	0.06	0.02	1448.2	4.07	4.21	0.14	22
952	Ph6	60.46	0.56	18.81	3.31	0.2	0.36	0.67	9.76	5.45	0.06	0.02	1423.2	4.27	4.41	0.14	22
953	Ph6	60.46	0.56	18.81	3.31	0.2	0.36	0.67	9.76	5.45	0.06	0.02	1398.2	4.46	4.62	0.16	22
954	Ph6	60.46	0.56	18.81	3.31	0.2	0.36	0.67	9.76	5.45	0.06	0.02	1373.2	4.65	4.84	0.19	22
955	Ph6	60.46	0.56	18.81	3.31	0.2	0.36	0.67	9.76	5.45	0.06	0.02	1010.4	8.99	9.25	0.26	22
956	Ph6	60.46	0.56	18.81	3.31	0.2	0.36	0.67	9.76	5.45	0.06	0.02	887.85	11.63	11.64	0.01	22
957	Ph6	60.46	0.56	18.81	3.31	0.2	0.36	0.67	9.76	5.45	0.06	0.02	923.95	10.85	10.86	0.01	22
958	Ph6	60.46	0.56	18.81	3.31	0.2	0.36	0.67	9.76	5.45	0.06	0.02	945.85	10.31	10.42	0.11	22
959	Ph6	60.46	0.56	18.81	3.31	0.2	0.36	0.67	9.76	5.45	0.06	0.02	964.75	10	10.06	0.06	22
960	Ph6	60.46	0.56	18.81	3.31	0.2	0.36	0.67	9.76	5.45	0.06	0.85	867.05	8.79	9.25	0.46	22
961	Ph6	60.46	0.56	18.81	3.31	0.2	0.36	0.67	9.76	5.45	0.06	0.85	804.55	10.33	10.52	0.19	22
962	Ph6	60.46	0.56	18.81	3.31	0.2	0.36	0.67	9.76	5.45	0.06	0.85	793.95	10.59	10.75	0.16	22
963	Ph6	60.46	0.56	18.81	3.31	0.2	0.36	0.67	9.76	5.45	0.06	0.85	780.45	11.05	11.07	0.02	22
964	Ph6	60.46	0.56	18.81	3.31	0.2	0.36	0.67	9.76	5.45	0.06	0.85	821.75	9.9	10.15	0.25	22
965	Ph6	60.46	0.56	18.81	3.31	0.2	0.36	0.67	9.76	5.45	0.06	0.95	763.75	10.84	11.26	0.42	22
966	Ph6	60.46	0.56	18.81	3.31	0.2	0.36	0.67	9.76	5.45	0.06	0.95	774.95	10.82	10.99	0.17	22
967	Ph6	60.46	0.56	18.81	3.31	0.2	0.36	0.67	9.76	5.45	0.06	0.95	778.45	10.45	10.91	0.46	22
968	Ph6	60.46	0.56	18.81	3.31	0.2	0.36	0.67	9.76	5.45	0.06	0.95	785.65	10.25	10.74	0.49	22
969	Ph6	60.46	0.56	18.81	3.31	0.2	0.36	0.67	9.76	5.45	0.06	2.1	742.15	10.16	9.94	-0.22	22
970	Ph6	60.46	0.56	18.81	3.31	0.2	0.36	0.67	9.76	5.45	0.06	2.1	728.35	10.55	10.27	-0.28	22
971	Ph6	60.46	0.56	18.81	3.31	0.2	0.36	0.67	9.76	5.45	0.06	2.1	759.05	9.59	9.55	-0.04	22

972	Ph6	60.46	0.56	18.81	3.31	0.2	0.36	0.67	9.76	5.45	0.06	3.75	703.35	9.57	9.12	-0.45	22
973	Ph6	60.46	0.56	18.81	3.31	0.2	0.36	0.67	9.76	5.45	0.06	3.75	662.85	11	10.17	-0.83	22
974	Ph6	60.46	0.56	18.81	3.31	0.2	0.36	0.67	9.76	5.45	0.06	3.75	675.35	10.5	9.83	-0.67	22
975	Ph2	53.14	0.59	19.84	4.72	0.13	1.77	6.75	4.77	8.28	0	0.02	1670.2	2.28	2.01	-0.27	23
976	Ph2	53.14	0.59	19.84	4.72	0.13	1.77	6.75	4.77	8.28	0	0.02	1621	2.54	2.35	-0.19	23
977	Ph2	53.14	0.59	19.84	4.72	0.13	1.77	6.75	4.77	8.28	0	0.02	1571.8	2.83	2.71	-0.12	23
978	Ph2	53.14	0.59	19.84	4.72	0.13	1.77	6.75	4.77	8.28	0	0.02	1522.6	3.15	3.1	-0.05	23
979	Ph2	53.14	0.59	19.84	4.72	0.13	1.77	6.75	4.77	8.28	0	0.02	1473.3	3.48	3.51	0.03	23
980	Ph2	53.14	0.59	19.84	4.72	0.13	1.77	6.75	4.77	8.28	0	0.02	1424.1	3.87	3.95	0.08	23
981	Ph2	53.14	0.59	19.84	4.72	0.13	1.77	6.75	4.77	8.28	0	0.02	1374.9	4.29	4.43	0.14	23
982	Ph2	53.14	0.59	19.84	4.72	0.13	1.77	6.75	4.77	8.28	0	0.02	1325.7	4.75	4.94	0.19	23
983	Ph2	53.14	0.59	19.84	4.72	0.13	1.77	6.75	4.77	8.28	0	0.02	980.4	10.66	10.19	-0.47	23
984	Ph2	53.14	0.59	19.84	4.72	0.13	1.77	6.75	4.77	8.28	0	0.02	999.85	10.2	9.77	-0.43	23
985	Ph2	53.14	0.59	19.84	4.72	0.13	1.77	6.75	4.77	8.28	0	0.02	1029.5	9.78	9.17	-0.61	23
986	Ph2	53.14	0.59	19.84	4.72	0.13	1.77	6.75	4.77	8.28	0	0.02	1044.3	9.58	8.88	-0.7	23
987	Ph2	53.14	0.59	19.84	4.72	0.13	1.77	6.75	4.77	8.28	0	0.02	1078.3	8.81	8.28	-0.53	23
988	Ph2	53.14	0.59	19.84	4.72	0.13	1.77	6.75	4.77	8.28	0	0.02	962.1	11.05	10.62	-0.43	23
989	Ph2	53.14	0.59	19.84	4.72	0.13	1.77	6.75	4.77	8.28	0	1.26	848.25	9.4	9.67	0.27	23
990	Ph2	53.14	0.59	19.84	4.72	0.13	1.77	6.75	4.77	8.28	0	1.26	836.75	9.71	9.93	0.22	23
991	Ph2	53.14	0.59	19.84	4.72	0.13	1.77	6.75	4.77	8.28	0	1.26	815.35	10.35	10.43	0.08	23
992	Ph2	53.14	0.59	19.84	4.72	0.13	1.77	6.75	4.77	8.28	0	1.26	783.15	11.29	11.24	-0.05	23
993	Ph2	53.14	0.59	19.84	4.72	0.13	1.77	6.75	4.77	8.28	0	2.04	795.15	9.16	9.77	0.61	23
994	Ph2	53.14	0.59	19.84	4.72	0.13	1.77	6.75	4.77	8.28	0	2.04	779.05	9.62	10.17	0.55	23
995	Ph2	53.14	0.59	19.84	4.72	0.13	1.77	6.75	4.77	8.28	0	2.04	759.45	10.16	10.67	0.51	23
996	Ph2	53.14	0.59	19.84	4.72	0.13	1.77	6.75	4.77	8.28	0	2.04	734.45	11	11.36	0.36	23
997	Ph2	53.14	0.59	19.84	4.72	0.13	1.77	6.75	4.77	8.28	0	3.07	736.05	9.84	10.1	0.26	23
998	Ph2	53.14	0.59	19.84	4.72	0.13	1.77	6.75	4.77	8.28	0	3.07	717.65	10.33	10.6	0.27	23
999	Ph2	53.14	0.59	19.84	4.72	0.13	1.77	6.75	4.77	8.28	0	3.07	708.85	10.61	10.85	0.24	23
1000	Ph3	53.52	0.6	19.84	4.8	0.14	1.76	6.76	4.66	7.91	0	0.02	1670.2	1.96	2.03	0.07	23
1001	Ph3	53.52	0.6	19.84	4.8	0.14	1.76	6.76	4.66	7.91	0	0.02	1621	2.25	2.37	0.12	23
1002	Ph3	53.52	0.6	19.84	4.8	0.14	1.76	6.76	4.66	7.91	0	0.02	1571.8	2.56	2.74	0.18	23
1003	Ph3	53.52	0.6	19.84	4.8	0.14	1.76	6.76	4.66	7.91	0	0.02	1522.6	2.91	3.12	0.21	23

1004	Ph3	53.52	0.6	19.84	4.8	0.14	1.76	6.76	4.66	7.91	0	0.02	1473.3	3.29	3.54	0.25	23
1005	Ph3	53.52	0.6	19.84	4.8	0.14	1.76	6.76	4.66	7.91	0	0.02	1424.1	3.72	3.98	0.26	23
1006	Ph3	53.52	0.6	19.84	4.8	0.14	1.76	6.76	4.66	7.91	0	0.02	1374.9	4.22	4.46	0.24	23
1007	Ph3	53.52	0.6	19.84	4.8	0.14	1.76	6.76	4.66	7.91	0	0.02	1325.7	4.77	4.97	0.2	23
1008	Ph3	53.52	0.6	19.84	4.8	0.14	1.76	6.76	4.66	7.91	0	0.02	981.65	10.26	10.22	-0.04	23
1009	Ph3	53.52	0.6	19.84	4.8	0.14	1.76	6.76	4.66	7.91	0	0.02	996.1	9.97	9.9	-0.07	23
1010	Ph3	53.52	0.6	19.84	4.8	0.14	1.76	6.76	4.66	7.91	0	0.02	1025.4	9.44	9.3	-0.14	23
1011	Ph3	53.52	0.6	19.84	4.8	0.14	1.76	6.76	4.66	7.91	0	0.02	1028.3	9.01	9.24	0.23	23
1012	Ph3	53.52	0.6	19.84	4.8	0.14	1.76	6.76	4.66	7.91	0	0.02	1043.2	8.98	8.95	-0.03	23
1013	Ph3	53.52	0.6	19.84	4.8	0.14	1.76	6.76	4.66	7.91	0	0.02	962.35	10.68	10.67	-0.01	23
1014	Ph3	53.52	0.6	19.84	4.8	0.14	1.76	6.76	4.66	7.91	0	1.17	867.35	9.17	9.47	0.3	23
1015	Ph3	53.52	0.6	19.84	4.8	0.14	1.76	6.76	4.66	7.91	0	1.17	860.05	9.2	9.63	0.43	23
1016	Ph3	53.52	0.6	19.84	4.8	0.14	1.76	6.76	4.66	7.91	0	1.17	840.65	9.84	10.06	0.22	23
1017	Ph3	53.52	0.6	19.84	4.8	0.14	1.76	6.76	4.66	7.91	0	1.17	818.85	10.32	10.57	0.25	23
1018	Ph3	53.52	0.6	19.84	4.8	0.14	1.76	6.76	4.66	7.91	0	1.17	805.55	10.64	10.9	0.26	23
1019	Ph3	53.52	0.6	19.84	4.8	0.14	1.76	6.76	4.66	7.91	0	1.17	789.55	11.05	11.3	0.25	23
1020	Ph3	53.52	0.6	19.84	4.8	0.14	1.76	6.76	4.66	7.91	0	3.32	753.75	9.32	9.47	0.15	23
1021	Ph3	53.52	0.6	19.84	4.8	0.14	1.76	6.76	4.66	7.91	0	3.32	748.75	9.46	9.6	0.14	23
1022	Ph3	53.52	0.6	19.84	4.8	0.14	1.76	6.76	4.66	7.91	0	3.32	727.75	9.82	10.15	0.33	23
1023	Ph3	53.52	0.6	19.84	4.8	0.14	1.76	6.76	4.66	7.91	0	3.32	717.65	10.25	10.42	0.17	23
1024	Ph3	53.52	0.6	19.84	4.8	0.14	1.76	6.76	4.66	7.91	0	3.32	704.35	10.82	10.8	-0.02	23
1025	Ph3	53.52	0.6	19.84	4.8	0.14	1.76	6.76	4.66	7.91	0	2.21	799.95	8.9	9.52	0.62	23
1026	Ph3	53.52	0.6	19.84	4.8	0.14	1.76	6.76	4.66	7.91	0	2.21	778.55	9.4	10.03	0.63	23
1027	Ph3	53.52	0.6	19.84	4.8	0.14	1.76	6.76	4.66	7.91	0	2.21	746.75	10.29	10.86	0.57	23
1028	Tr2	60.86	0.39	18.27	3.88	0.12	0.9	2.96	4.12	8.5	0	0.02	1769.2	2.49	2.1	-0.39	23
1029	Tr2	60.86	0.39	18.27	3.88	0.12	0.9	2.96	4.12	8.5	0	0.02	1719.2	2.74	2.4	-0.34	23
1030	Tr2	60.86	0.39	18.27	3.88	0.12	0.9	2.96	4.12	8.5	0	0.02	1670.2	3.01	2.72	-0.29	23
1031	Tr2	60.86	0.39	18.27	3.88	0.12	0.9	2.96	4.12	8.5	0	0.02	1621.2	3.3	3.05	-0.25	23
1032	Tr2	60.86	0.39	18.27	3.88	0.12	0.9	2.96	4.12	8.5	0	0.02	1572.2	3.62	3.41	-0.21	23
1033	Tr2	60.86	0.39	18.27	3.88	0.12	0.9	2.96	4.12	8.5	0	0.02	1522.2	3.96	3.79	-0.17	23
1034	Tr2	60.86	0.39	18.27	3.88	0.12	0.9	2.96	4.12	8.5	0	0.02	1473.2	4.33	4.2	-0.13	23
1035	Tr2	60.86	0.39	18.27	3.88	0.12	0.9	2.96	4.12	8.5	0	0.02	1424.2	4.73	4.63	-0.1	23

1036	Tr2	60.86	0.39	18.27	3.88	0.12	0.9	2.96	4.12	8.5	0	0.02	1087.3	8.45	8.81	0.36	23
1037	Tr2	60.86	0.39	18.27	3.88	0.12	0.9	2.96	4.12	8.5	0	0.02	1038.5	9.32	9.68	0.36	23
1038	Tr2	60.86	0.39	18.27	3.88	0.12	0.9	2.96	4.12	8.5	0	0.02	1009.7	9.77	10.24	0.47	23
1039	Tr2	60.86	0.39	18.27	3.88	0.12	0.9	2.96	4.12	8.5	0	0.02	985.15	10.56	10.76	0.2	23
1040	Tr2	60.86	0.39	18.27	3.88	0.12	0.9	2.96	4.12	8.5	0	0.02	973.35	10.75	11.02	0.27	23
1041	Tr2	60.86	0.39	18.27	3.88	0.12	0.9	2.96	4.12	8.5	0	0.02	956.95	11.29	11.4	0.11	23
1042	Tr2	60.86	0.39	18.27	3.88	0.12	0.9	2.96	4.12	8.5	0	3.75	723.65	9.9	9.95	0.05	23
1043	Tr2	60.86	0.39	18.27	3.88	0.12	0.9	2.96	4.12	8.5	0	3.75	709.35	10.31	10.32	0.01	23
1044	Tr2	60.86	0.39	18.27	3.88	0.12	0.9	2.96	4.12	8.5	0	3.75	688.85	11.05	10.89	-0.16	23
1045	Tr2	60.86	0.39	18.27	3.88	0.12	0.9	2.96	4.12	8.5	0	2.38	794.55	9.7	9.62	-0.08	23
1046	Tr2	60.86	0.39	18.27	3.88	0.12	0.9	2.96	4.12	8.5	0	2.38	776.65	10.05	10.03	-0.02	23
1047	Tr2	60.86	0.39	18.27	3.88	0.12	0.9	2.96	4.12	8.5	0	2.38	761.25	10.65	10.4	-0.25	23
1048	Tr2	60.86	0.39	18.27	3.88	0.12	0.9	2.96	4.12	8.5	0	2.38	743.85	10.97	10.85	-0.12	23
1049	Tr2	60.86	0.39	18.27	3.88	0.12	0.9	2.96	4.12	8.5	0	2.04	821.65	9.55	9.43	-0.12	23
1050	Tr2	60.86	0.39	18.27	3.88	0.12	0.9	2.96	4.12	8.5	0	2.04	795.45	10.2	10.01	-0.19	23
1051	Tr2	60.86	0.39	18.27	3.88	0.12	0.9	2.96	4.12	8.5	0	2.04	775.75	10.8	10.47	-0.33	23
1052	Tr2	60.86	0.39	18.27	3.88	0.12	0.9	2.96	4.12	8.5	0	2.04	763.85	11.04	10.77	-0.27	23
1053	Tr2	60.86	0.39	18.27	3.88	0.12	0.9	2.96	4.12	8.5	0	1.15	917.45	9.04	8.81	-0.23	23
1054	Tr2	60.86	0.39	18.27	3.88	0.12	0.9	2.96	4.12	8.5	0	1.15	885.45	9.72	9.4	-0.32	23
1055	Tr2	60.86	0.39	18.27	3.88	0.12	0.9	2.96	4.12	8.5	0	1.15	865.05	10.08	9.8	-0.28	23
1056	Tr2	60.86	0.39	18.27	3.88	0.12	0.9	2.96	4.12	8.5	0	1.15	849.85	10.42	10.12	-0.3	23
1057	Tr2	60.86	0.39	18.27	3.88	0.12	0.9	2.96	4.12	8.5	0	1.15	819.65	11.24	10.78	-0.46	23
1058	Tr3	61.26	0.38	18.38	3.5	0.14	0.74	2.97	4.58	8.04	0	0.02	1719.4	2.79	2.44	-0.35	23
1059	Tr3	61.26	0.38	18.38	3.5	0.14	0.74	2.97	4.58	8.04	0	0.02	1670.2	3.06	2.75	-0.31	23
1060	Tr3	61.26	0.38	18.38	3.5	0.14	0.74	2.97	4.58	8.04	0	0.02	1621	3.35	3.09	-0.26	23
1061	Tr3	61.26	0.38	18.38	3.5	0.14	0.74	2.97	4.58	8.04	0	0.02	1571.8	3.67	3.45	-0.22	23
1062	Tr3	61.26	0.38	18.38	3.5	0.14	0.74	2.97	4.58	8.04	0	0.02	1522.6	4.02	3.83	-0.19	23
1063	Tr3	61.26	0.38	18.38	3.5	0.14	0.74	2.97	4.58	8.04	0	0.02	1473.3	4.39	4.24	-0.15	23
1064	Tr3	61.26	0.38	18.38	3.5	0.14	0.74	2.97	4.58	8.04	0	0.02	1424.1	4.8	4.68	-0.12	23
1065	Tr3	61.26	0.38	18.38	3.5	0.14	0.74	2.97	4.58	8.04	0	0.02	1005.6	10.39	10.39	0	23
1066	Tr3	61.26	0.38	18.38	3.5	0.14	0.74	2.97	4.58	8.04	0	0.02	1041.4	9.41	9.68	0.27	23
1067	Tr3	61.26	0.38	18.38	3.5	0.14	0.74	2.97	4.58	8.04	0	0.02	1057.9	9.06	9.38	0.32	23

1068	Tr3	61.26	0.38	18.38	3.5	0.14	0.74	2.97	4.58	8.04	0	0.02	967.08	11.18	11.22	0.04	23
1069	Tr3	61.26	0.38	18.38	3.5	0.14	0.74	2.97	4.58	8.04	0	1.26	872.85	9.33	9.49	0.16	23
1070	Tr3	61.26	0.38	18.38	3.5	0.14	0.74	2.97	4.58	8.04	0	1.26	853.75	9.74	9.88	0.14	23
1071	Tr3	61.26	0.38	18.38	3.5	0.14	0.74	2.97	4.58	8.04	0	1.26	830.85	10.09	10.36	0.27	23
1072	Tr3	61.26	0.38	18.38	3.5	0.14	0.74	2.97	4.58	8.04	0	1.26	814.15	10.56	10.74	0.18	23
1073	Tr3	61.26	0.38	18.38	3.5	0.14	0.74	2.97	4.58	8.04	0	1.26	811.25	10.62	10.81	0.19	23
1074	Tr3	61.26	0.38	18.38	3.5	0.14	0.74	2.97	4.58	8.04	0	1.26	799.15	10.85	11.09	0.24	23
1075	Tr3	61.26	0.38	18.38	3.5	0.14	0.74	2.97	4.58	8.04	0	1.26	794.65	11.19	11.2	0.01	23
1076	Tr3	61.26	0.38	18.38	3.5	0.14	0.74	2.97	4.58	8.04	0	3.78	724.25	9.85	9.93	0.08	23
1077	Tr3	61.26	0.38	18.38	3.5	0.14	0.74	2.97	4.58	8.04	0	3.78	718.05	10.05	10.09	0.04	23
1078	Tr3	61.26	0.38	18.38	3.5	0.14	0.74	2.97	4.58	8.04	0	3.78	698.75	10.52	10.61	0.09	23
1079	Tr3	61.26	0.38	18.38	3.5	0.14	0.74	2.97	4.58	8.04	0	3.78	693.35	10.95	10.76	-0.19	23
1080	Tr3	61.26	0.38	18.38	3.5	0.14	0.74	2.97	4.58	8.04	0	3.78	679.45	11.33	11.16	-0.17	23
1081	Tr3	61.26	0.38	18.38	3.5	0.14	0.74	2.97	4.58	8.04	0	3.78	677.35	11.43	11.22	-0.21	23
1082	Tr3	61.26	0.38	18.38	3.5	0.14	0.74	2.97	4.58	8.04	0	1.19	862.75	9.54	9.81	0.27	23
1083	Tr3	61.26	0.38	18.38	3.5	0.14	0.74	2.97	4.58	8.04	0	1.19	845.05	10.01	10.18	0.17	23
1084	Tr3	61.26	0.38	18.38	3.5	0.14	0.74	2.97	4.58	8.04	0	1.19	827.55	10.24	10.56	0.32	23
1085	Tr3	61.26	0.38	18.38	3.5	0.14	0.74	2.97	4.58	8.04	0	1.19	802.85	10.74	11.13	0.39	23
1086	Tr3	61.26	0.38	18.38	3.5	0.14	0.74	2.97	4.58	8.04	0	1.19	798.25	11.02	11.24	0.22	23
1087	Tr3	61.26	0.38	18.38	3.5	0.14	0.74	2.97	4.58	8.04	0	1.19	786.45	11.56	11.53	-0.03	23
1088	Tr3	61.26	0.38	18.38	3.5	0.14	0.74	2.97	4.58	8.04	0	0.79	959.45	8.83	8.75	-0.08	23
1089	Tr3	61.26	0.38	18.38	3.5	0.14	0.74	2.97	4.58	8.04	0	0.79	901.55	9.88	9.79	-0.09	23
1090	Tr3	61.26	0.38	18.38	3.5	0.14	0.74	2.97	4.58	8.04	0	0.79	859.05	10.7	10.65	-0.05	23
1091	Tr3	61.26	0.38	18.38	3.5	0.14	0.74	2.97	4.58	8.04	0	0.79	840.75	11.35	11.05	-0.3	23
1092	D2	66	0.36	15.23	4.08	0.1	2.21	5.01	3.84	2.16	0.14	0.02	1744	2.09	2.16	0.07	24
1093	D2	66	0.36	15.23	4.08	0.1	2.21	5.01	3.84	2.16	0.14	0.02	1719.4	2.21	2.31	0.1	24
1094	D2	66	0.36	15.23	4.08	0.1	2.21	5.01	3.84	2.16	0.14	0.02	1694.8	2.34	2.48	0.14	24
1095	D2	66	0.36	15.23	4.08	0.1	2.21	5.01	3.84	2.16	0.14	0.02	1670.2	2.48	2.64	0.16	24
1096	D2	66	0.36	15.23	4.08	0.1	2.21	5.01	3.84	2.16	0.14	0.02	1645.6	2.62	2.81	0.19	24
1097	D2	66	0.36	15.23	4.08	0.1	2.21	5.01	3.84	2.16	0.14	0.02	1621	2.76	2.99	0.23	24
1098	D2	66	0.36	15.23	4.08	0.1	2.21	5.01	3.84	2.16	0.14	0.02	1596.4	2.92	3.17	0.25	24
1099	D2	66	0.36	15.23	4.08	0.1	2.21	5.01	3.84	2.16	0.14	0.02	1571.8	3.08	3.36	0.28	24

1100	D2	66	0.36	15.23	4.08	0.1	2.21	5.01	3.84	2.16	0.14	0.02	1547.2	3.25	3.55	0.3	24
1101	D2	66	0.36	15.23	4.08	0.1	2.21	5.01	3.84	2.16	0.14	0.02	1522.6	3.43	3.76	0.33	24
1102	D2	66	0.36	15.23	4.08	0.1	2.21	5.01	3.84	2.16	0.14	0.02	1497.9	3.61	3.96	0.35	24
1103	D2	66	0.36	15.23	4.08	0.1	2.21	5.01	3.84	2.16	0.14	0.02	1473.3	3.8	4.18	0.38	24
1104	D2	66	0.36	15.23	4.08	0.1	2.21	5.01	3.84	2.16	0.14	0.02	1448.7	4	4.4	0.4	24
1105	D2	66	0.36	15.23	4.08	0.1	2.21	5.01	3.84	2.16	0.14	0.02	1424.1	4.21	4.63	0.42	24
1106	D2	66	0.36	15.23	4.08	0.1	2.21	5.01	3.84	2.16	0.14	0.02	1399.5	4.44	4.88	0.44	24
1107	D2	66	0.36	15.23	4.08	0.1	2.21	5.01	3.84	2.16	0.14	0.02	1374.9	4.66	5.13	0.47	24
1108	D2	66	0.36	15.23	4.08	0.1	2.21	5.01	3.84	2.16	0.14	0.02	1034.2	10.5	10.34	-0.16	24
1109	D2	66	0.36	15.23	4.08	0.1	2.21	5.01	3.84	2.16	0.14	0.02	1057.8	9.85	9.79	-0.06	24
1110	D2	66	0.36	15.23	4.08	0.1	2.21	5.01	3.84	2.16	0.14	0.02	1074.2	9.28	9.44	0.16	24
1111	D2	66	0.36	15.23	4.08	0.1	2.21	5.01	3.84	2.16	0.14	0.02	1091.2	8.91	9.1	0.19	24
1112	D2	66	0.36	15.23	4.08	0.1	2.21	5.01	3.84	2.16	0.14	1.31	862.05	10.56	10.17	-0.39	24
1113	D2	66	0.36	15.23	4.08	0.1	2.21	5.01	3.84	2.16	0.14	1.31	835.05	11.18	10.76	-0.42	24
1114	D2	66	0.36	15.23	4.08	0.1	2.21	5.01	3.84	2.16	0.14	1.64	772.05	11.95	11.73	-0.22	24
1115	D2	66	0.36	15.23	4.08	0.1	2.21	5.01	3.84	2.16	0.14	1.64	807.95	11.12	10.84	-0.28	24
1116	D2	66	0.36	15.23	4.08	0.1	2.21	5.01	3.84	2.16	0.14	1.64	808.45	10.93	10.83	-0.1	24
1117	D2	66	0.36	15.23	4.08	0.1	2.21	5.01	3.84	2.16	0.14	1.64	838.55	9.86	10.15	0.29	24
1118	D2	66	0.36	15.23	4.08	0.1	2.21	5.01	3.84	2.16	0.14	1.98	803.95	10.48	10.45	-0.03	24
1119	D2	66	0.36	15.23	4.08	0.1	2.21	5.01	3.84	2.16	0.14	1.98	815.05	9.99	10.2	0.21	24
1120	D2	66	0.36	15.23	4.08	0.1	2.21	5.01	3.84	2.16	0.14	1.98	833.55	9.63	9.79	0.16	24
1121	Bl1	47.03	1.61	16.28	10.88	0.2	5.17	10.47	3.75	1.94	0.59	0.5	848.35	11.6	11.93	0.33	25
1122	Bl1	47.03	1.61	16.28	10.88	0.2	5.17	10.47	3.75	1.94	0.59	0.5	870.35	10.8	11.23	0.43	25
1123	Bl1	47.03	1.61	16.28	10.88	0.2	5.17	10.47	3.75	1.94	0.59	0.5	875.05	10.74	11.09	0.35	25
1124	Bl1	47.03	1.61	16.28	10.88	0.2	5.17	10.47	3.75	1.94	0.59	0.5	884.75	10.5	10.81	0.31	25
1125	Bl1	47.03	1.61	16.28	10.88	0.2	5.17	10.47	3.75	1.94	0.59	0.5	891.65	10.42	10.61	0.19	25
1126	Bl1	47.03	1.61	16.28	10.88	0.2	5.17	10.47	3.75	1.94	0.59	0.5	892.55	10.33	10.59	0.26	25
1127	Bl1	47.03	1.61	16.28	10.88	0.2	5.17	10.47	3.75	1.94	0.59	1.03	826.35	10.99	11.2	0.21	25
1128	Bl1	47.03	1.61	16.28	10.88	0.2	5.17	10.47	3.75	1.94	0.59	1.03	831.05	10.89	11.06	0.17	25
1129	Bl1	47.03	1.61	16.28	10.88	0.2	5.17	10.47	3.75	1.94	0.59	1.03	837.65	10.73	10.87	0.14	25
1130	Bl1	47.03	1.61	16.28	10.88	0.2	5.17	10.47	3.75	1.94	0.59	1.03	848.45	10.37	10.57	0.2	25
1131	Bl1	47.03	1.61	16.28	10.88	0.2	5.17	10.47	3.75	1.94	0.59	1.5	805.45	11.2	10.93	-0.27	25

1132	Bl1	47.03	1.61	16.28	10.88	0.2	5.17	10.47	3.75	1.94	0.59	1.5	817.75	10.88	10.59	-0.29	25
1133	Bl1	47.03	1.61	16.28	10.88	0.2	5.17	10.47	3.75	1.94	0.59	1.5	822.35	10.57	10.46	-0.11	25
1134	Bl1	47.03	1.61	16.28	10.88	0.2	5.17	10.47	3.75	1.94	0.59	1.5	824.85	10.54	10.39	-0.15	25
1135	Bl1	47.03	1.61	16.28	10.88	0.2	5.17	10.47	3.75	1.94	0.59	1.5	829.95	10.25	10.26	0.01	25
1136	Bl1	47.03	1.61	16.28	10.88	0.2	5.17	10.47	3.75	1.94	0.59	1.5	849.95	9.75	9.74	-0.01	25
1137	Bl1	47.03	1.61	16.28	10.88	0.2	5.17	10.47	3.75	1.94	0.59	2.29	797.75	10.16	10.05	-0.11	25
1138	Bl1	47.03	1.61	16.28	10.88	0.2	5.17	10.47	3.75	1.94	0.59	2.29	807.95	9.77	9.78	0.01	25
1139	Bl1	47.03	1.61	16.28	10.88	0.2	5.17	10.47	3.75	1.94	0.59	2.29	818.05	9.57	9.52	-0.05	25
1140	Bl1	47.03	1.61	16.28	10.88	0.2	5.17	10.47	3.75	1.94	0.59	0.02	1817.9	0.18	0.1	-0.08	25
1141	Bl1	47.03	1.61	16.28	10.88	0.2	5.17	10.47	3.75	1.94	0.59	0.02	1793.3	0.26	0.26	0	25
1142	Bl1	47.03	1.61	16.28	10.88	0.2	5.17	10.47	3.75	1.94	0.59	0.02	1768.7	0.34	0.42	0.08	25
1143	Bl1	47.03	1.61	16.28	10.88	0.2	5.17	10.47	3.75	1.94	0.59	0.02	1744.1	0.43	0.59	0.16	25
1144	Bl1	47.03	1.61	16.28	10.88	0.2	5.17	10.47	3.75	1.94	0.59	0.02	1739.5	0.52	0.62	0.1	25
1145	Bl1	47.03	1.61	16.28	10.88	0.2	5.17	10.47	3.75	1.94	0.59	0.02	1694.9	0.62	0.94	0.32	25
1146	Bl1	47.03	1.61	16.28	10.88	0.2	5.17	10.47	3.75	1.94	0.59	0.02	1670.3	0.72	1.12	0.4	25
1147	Bl1	47.03	1.61	16.28	10.88	0.2	5.17	10.47	3.75	1.94	0.59	0.02	985.05	10.82	9.93	-0.89	25
1148	Bl1	47.03	1.61	16.28	10.88	0.2	5.17	10.47	3.75	1.94	0.59	0.02	989.05	10.7	9.83	-0.87	25
1149	Bl1	47.03	1.61	16.28	10.88	0.2	5.17	10.47	3.75	1.94	0.59	0.02	1004.2	10.23	9.49	-0.74	25
1150	A2	58.69	0.01	21.57	0.02	0.02	5.38	9.49	3.3	1.57	0	0	1036	11.58	11.51	-0.07	26
1151	A2	58.69	0.01	21.57	0.02	0.02	5.38	9.49	3.3	1.57	0	0	1054	10.77	10.74	-0.03	26
1152	A2	58.69	0.01	21.57	0.02	0.02	5.38	9.49	3.3	1.57	0	0	1065	10.45	10.34	-0.11	26
1153	A2	58.69	0.01	21.57	0.02	0.02	5.38	9.49	3.3	1.57	0	0	1075	10.16	10	-0.16	26
1154	A2	58.69	0.01	21.57	0.02	0.02	5.38	9.49	3.3	1.57	0	0	1084	9.87	9.72	-0.15	26
1155	A2	58.69	0.01	21.57	0.02	0.02	5.38	9.49	3.3	1.57	0	0	1096	9.55	9.38	-0.17	26
1156	A2	58.69	0.01	21.57	0.02	0.02	5.38	9.49	3.3	1.57	0	0	1106	9.3	9.11	-0.19	26
1157	A2	58.69	0.01	21.57	0.02	0.02	5.38	9.49	3.3	1.57	0	0	1116	9.06	8.86	-0.2	26
1158	A2	58.69	0.01	21.57	0.02	0.02	5.38	9.49	3.3	1.57	0	0	1036	11.32	11.51	0.19	26
1159	A2	58.69	0.01	21.57	0.02	0.02	5.38	9.49	3.3	1.57	0	0	1054	10.83	10.74	-0.09	26
1160	A2	58.69	0.01	21.57	0.02	0.02	5.38	9.49	3.3	1.57	0	0	1062	10.3	10.44	0.14	26
1161	A2	58.69	0.01	21.57	0.02	0.02	5.38	9.49	3.3	1.57	0	0	1065	10.44	10.34	-0.1	26
1162	A2	58.69	0.01	21.57	0.02	0.02	5.38	9.49	3.3	1.57	0	0	1074	10.15	10.03	-0.12	26
1163	A2	58.69	0.01	21.57	0.02	0.02	5.38	9.49	3.3	1.57	0	0	1083	9.74	9.75	0.01	26

1164 A2	58.69	0.01	21.57	0.02	0.02	5.38	9.49	3.3	1.57	0	0	1088	9.63	9.6	-0.03	26
1165 A2	58.69	0.01	21.57	0.02	0.02	5.38	9.49	3.3	1.57	0	0	1094	9.48	9.43	-0.05	26
1166 A2	58.69	0.01	21.57	0.02	0.02	5.38	9.49	3.3	1.57	0	0	1103	9.25	9.19	-0.06	26
1167 A2	58.69	0.01	21.57	0.02	0.02	5.38	9.49	3.3	1.57	0	0	1113	8.99	8.93	-0.06	26
1168 A2	58.69	0.01	21.57	0.02	0.02	5.38	9.49	3.3	1.57	0	0	1123	8.75	8.7	-0.05	26
1169 A2	58.69	0.01	21.57	0.02	0.02	5.38	9.49	3.3	1.57	0	0	1081	10.02	9.81	-0.21	26
1170 A2	58.69	0.01	21.57	0.02	0.02	5.38	9.49	3.3	1.57	0	0	1091	9.72	9.52	-0.2	26
1171 A2	58.69	0.01	21.57	0.02	0.02	5.38	9.49	3.3	1.57	0	0	1100	9.44	9.27	-0.17	26
1172 A2	58.69	0.01	21.57	0.02	0.02	5.38	9.49	3.3	1.57	0	0	1110	9.17	9.01	-0.16	26
1173 A2	58.69	0.01	21.57	0.02	0.02	5.38	9.49	3.3	1.57	0	0	1120	8.91	8.77	-0.14	26
1174 A2	58.69	0.01	21.57	0.02	0.02	5.38	9.49	3.3	1.57	0	0	1130	8.67	8.54	-0.13	26
1175 A2	58.69	0.01	21.57	0.02	0.02	5.38	9.49	3.3	1.57	0	1.06	917	10.55	10.67	0.12	26
1176 A2	58.69	0.01	21.57	0.02	0.02	5.38	9.49	3.3	1.57	0	1.06	928	10.44	10.35	-0.09	26
1177 A2	58.69	0.01	21.57	0.02	0.02	5.38	9.49	3.3	1.57	0	1.06	937	10.07	10.1	0.03	26
1178 A2	58.69	0.01	21.57	0.02	0.02	5.38	9.49	3.3	1.57	0	1.06	935	9.97	10.16	0.19	26
1179 A2	58.69	0.01	21.57	0.02	0.02	5.38	9.49	3.3	1.57	0	1.06	954	9.54	9.64	0.1	26
1180 A2	58.69	0.01	21.57	0.02	0.02	5.38	9.49	3.3	1.57	0	1.06	976	9	9.08	0.08	26
1181 A2	58.69	0.01	21.57	0.02	0.02	5.38	9.49	3.3	1.57	0	1.06	985	8.74	8.87	0.13	26
1182 A2	58.69	0.01	21.57	0.02	0.02	5.38	9.49	3.3	1.57	0	1.06	996	8.54	8.61	0.07	26
1183 A2	58.69	0.01	21.57	0.02	0.02	5.38	9.49	3.3	1.57	0	1.06	1013	8.13	8.23	0.1	26
1184 A2	58.69	0.01	21.57	0.02	0.02	5.38	9.49	3.3	1.57	0	1.06	908	11.03	10.93	-0.1	26
1185 A2	58.69	0.01	21.57	0.02	0.02	5.38	9.49	3.3	1.57	0	1.06	918	10.65	10.64	-0.01	26
1186 A2	58.69	0.01	21.57	0.02	0.02	5.38	9.49	3.3	1.57	0	1.06	938	10.07	10.07	0	26
1187 A2	58.69	0.01	21.57	0.02	0.02	5.38	9.49	3.3	1.57	0	1.06	948	9.81	9.8	-0.01	26
1188 A2	58.69	0.01	21.57	0.02	0.02	5.38	9.49	3.3	1.57	0	1.06	948	9.78	9.8	0.02	26
1189 A2	58.69	0.01	21.57	0.02	0.02	5.38	9.49	3.3	1.57	0	1.06	957	9.57	9.56	-0.01	26
1190 A2	58.69	0.01	21.57	0.02	0.02	5.38	9.49	3.3	1.57	0	1.06	977	9.04	9.06	0.02	26
1191 A2	58.69	0.01	21.57	0.02	0.02	5.38	9.49	3.3	1.57	0	1.06	987	8.77	8.82	0.05	26
1192 A2	58.69	0.01	21.57	0.02	0.02	5.38	9.49	3.3	1.57	0	1.96	840	10.8	10.57	-0.23	26
1193 A2	58.69	0.01	21.57	0.02	0.02	5.38	9.49	3.3	1.57	0	1.96	849	10.52	10.36	-0.16	26
1194 A2	58.69	0.01	21.57	0.02	0.02	5.38	9.49	3.3	1.57	0	1.96	851	10.43	10.32	-0.11	26
1195 A2	58.69	0.01	21.57	0.02	0.02	5.38	9.49	3.3	1.57	0	1.96	859	10.2	10.13	-0.07	26

1196	A2	58.69	0.01	21.57	0.02	0.02	5.38	9.49	3.3	1.57	0	1.96	870	9.85	9.88	0.03	26
1197	A2	58.69	0.01	21.57	0.02	0.02	5.38	9.49	3.3	1.57	0	1.96	879	9.57	9.68	0.11	26
1198	A2	58.69	0.01	21.57	0.02	0.02	5.38	9.49	3.3	1.57	0	1.96	889	9.32	9.45	0.13	26
1199	A2	58.69	0.01	21.57	0.02	0.02	5.38	9.49	3.3	1.57	0	1.96	844	10.8	10.48	-0.32	26
1200	A2	58.69	0.01	21.57	0.02	0.02	5.38	9.49	3.3	1.57	0	1.96	853	10.51	10.27	-0.24	26
1201	A2	58.69	0.01	21.57	0.02	0.02	5.38	9.49	3.3	1.57	0	1.96	863	10.17	10.04	-0.13	26
1202	A2	58.69	0.01	21.57	0.02	0.02	5.38	9.49	3.3	1.57	0	1.96	864	10.15	10.02	-0.13	26
1203	A2	58.69	0.01	21.57	0.02	0.02	5.38	9.49	3.3	1.57	0	1.96	873	9.86	9.81	-0.05	26
1204	A2	58.69	0.01	21.57	0.02	0.02	5.38	9.49	3.3	1.57	0	1.96	883	9.56	9.59	0.03	26
1205	A2	58.69	0.01	21.57	0.02	0.02	5.38	9.49	3.3	1.57	0	1.96	893	9.27	9.36	0.09	26
1206	Pr	45.83	0.18	4.87	8.63	0	31.63	6.37	0.32	0	0	0	1006	10.73	11.24	0.51	27
1207	Pr	45.83	0.18	4.87	8.63	0	31.63	6.37	0.32	0	0	0	1013	10.52	10.3	-0.22	27
1208	Pr	45.83	0.18	4.87	8.63	0	31.63	6.37	0.32	0	0	0	1013	10.43	10.3	-0.13	27
1209	Pr	45.83	0.18	4.87	8.63	0	31.63	6.37	0.32	0	0	0	1017	10.25	9.89	-0.36	27
1210	Pr	45.83	0.18	4.87	8.63	0	31.63	6.37	0.32	0	0	0	1018	10.13	9.8	-0.33	27
1211	Pr	45.83	0.18	4.87	8.63	0	31.63	6.37	0.32	0	0	0	1866.9	-0.97	-1.01	-0.04	27
1212	Pr	45.83	0.18	4.87	8.63	0	31.63	6.37	0.32	0	0	0	1857.1	-0.94	-0.95	-0.01	27
1213	Pr	45.83	0.18	4.87	8.63	0	31.63	6.37	0.32	0	0	0	1847.3	-0.9	-0.89	0.01	27
1214	Bl5	49.61	4.27	11.01	14.73	0	4.46	10.04	2.81	0.47	2.51	0.02	1873.2	-0.06	-0.93	-0.86	28
1215	Bl5	49.61	4.27	11.01	14.73	0	4.46	10.04	2.81	0.47	2.51	0.02	1823.2	0.08	-0.56	-0.64	28
1216	Bl5	49.61	4.27	11.01	14.73	0	4.46	10.04	2.81	0.47	2.51	0.02	1773.2	0.23	-0.18	-0.4	28
1217	Bl5	49.61	4.27	11.01	14.73	0	4.46	10.04	2.81	0.47	2.51	0.02	1723.2	0.39	0.23	-0.16	28
1218	Bl5	49.61	4.27	11.01	14.73	0	4.46	10.04	2.81	0.47	2.51	0.02	1673.2	0.55	0.66	0.11	28
1219	Bl5	49.61	4.27	11.01	14.73	0	4.46	10.04	2.81	0.47	2.51	0.02	1623.2	0.73	1.11	0.38	28
1220	Bl5	49.61	4.27	11.01	14.73	0	4.46	10.04	2.81	0.47	2.51	0.02	1573.2	0.94	1.6	0.66	28
1221	Bl5	49.61	4.27	11.01	14.73	0	4.46	10.04	2.81	0.47	2.51	0.02	1523.2	1.17	2.12	0.94	28
1222	Bl6	50.66	3.95	11.35	13.9	0	3.94	9.6	2.98	0.51	2.4	0.02	1867.2	-0.05	-0.69	-0.63	28
1223	Bl6	50.66	3.95	11.35	13.9	0	3.94	9.6	2.98	0.51	2.4	0.02	1818.2	0.09	-0.33	-0.42	28
1224	Bl6	50.66	3.95	11.35	13.9	0	3.94	9.6	2.98	0.51	2.4	0.02	1769.2	0.24	0.04	-0.2	28
1225	Bl6	50.66	3.95	11.35	13.9	0	3.94	9.6	2.98	0.51	2.4	0.02	1719.2	0.4	0.44	0.04	28
1226	Bl6	50.66	3.95	11.35	13.9	0	3.94	9.6	2.98	0.51	2.4	0.02	1670.2	0.57	0.85	0.28	28
1227	Bl8	50.84	4.26	11.38	15.05	0	4.42	10.18	3.01	0.55	0.04	0.02	1873.2	-0.05	-0.89	-0.84	28

1228	Bl8	50.84	4.26	11.38	15.05	0	4.42	10.18	3.01	0.55	0.04	0.02	1823.2	0.08	-0.52	-0.6	28
1229	Bl8	50.84	4.26	11.38	15.05	0	4.42	10.18	3.01	0.55	0.04	0.02	1773.2	0.22	-0.14	-0.35	28
1230	Bl8	50.84	4.26	11.38	15.05	0	4.42	10.18	3.01	0.55	0.04	0.02	1723.2	0.37	0.27	-0.1	28
1231	Bl8	50.84	4.26	11.38	15.05	0	4.42	10.18	3.01	0.55	0.04	0.02	1673.2	0.53	0.7	0.17	28
1232	Bl8	50.84	4.26	11.38	15.05	0	4.42	10.18	3.01	0.55	0.04	0.02	1623.2	0.72	1.16	0.44	28
1233	Bl8	50.84	4.26	11.38	15.05	0	4.42	10.18	3.01	0.55	0.04	0.02	1573.2	0.92	1.64	0.73	28
1234	Bl8	50.84	4.26	11.38	15.05	0	4.42	10.18	3.01	0.55	0.04	0.02	1523.2	1.16	2.16	1.01	28
1235	Bl9	50.87	4.05	11.36	14.2	0	4.23	9.62	3.06	0.52	0.09	0.02	1867.2	-0.02	-0.73	-0.71	28
1236	Bl9	50.87	4.05	11.36	14.2	0	4.23	9.62	3.06	0.52	0.09	0.02	1818.2	0.11	-0.37	-0.49	28
1237	Bl9	50.87	4.05	11.36	14.2	0	4.23	9.62	3.06	0.52	0.09	0.02	1769.2	0.26	0	-0.26	28
1238	Bl9	50.87	4.05	11.36	14.2	0	4.23	9.62	3.06	0.52	0.09	0.02	1719.2	0.42	0.41	-0.02	28
1239	Bl9	50.87	4.05	11.36	14.2	0	4.23	9.62	3.06	0.52	0.09	0.02	1670.2	0.59	0.83	0.24	28
1240	Bl9	50.87	4.05	11.36	14.2	0	4.23	9.62	3.06	0.52	0.09	0.02	1621.2	0.77	1.27	0.51	28
1241	Bl9	50.87	4.05	11.36	14.2	0	4.23	9.62	3.06	0.52	0.09	0.02	1572.2	0.98	1.75	0.77	28
1242	Bl9	50.87	4.05	11.36	14.2	0	4.23	9.62	3.06	0.52	0.09	0.02	1522.2	1.22	2.26	1.05	28
1243	A5	59.46	0.73	17.9	5.18	0.13	3.71	6.45	4.23	1.47	0	0	1623.2	2.22	2.62	0.4	29
1244	A5	59.46	0.73	17.9	5.18	0.13	3.71	6.45	4.23	1.47	0	0	1523.2	2.74	3.44	0.7	29
1245	Bl7	50.01	2.6	12.56	10.79	0.33	9.39	10.88	2.33	0.48	0	0.02	1773.2	0.09	-0.04	-0.13	29
1246	Bl7	50.01	2.6	12.56	10.79	0.33	9.39	10.88	2.33	0.48	0	0.02	1673.2	0.35	0.74	0.39	29
1247	Bl7	50.01	2.6	12.56	10.79	0.33	9.39	10.88	2.33	0.48	0	0.02	1523.2	1.03	2.11	1.08	29
1248	D1	65.28	0.59	17.05	4.02	0.08	1.82	4.7	4.34	1.29	0.13	0.02	1571.2	3.22	3.43	0.21	30
1249	D1	65.28	0.59	17.05	4.02	0.08	1.82	4.7	4.34	1.29	0.13	0.02	1620.2	2.91	3.05	0.14	30
1250	D1	65.28	0.59	17.05	4.02	0.08	1.82	4.7	4.34	1.29	0.13	0.02	1670.2	2.61	2.69	0.08	30
1251	D1	65.28	0.59	17.05	4.02	0.08	1.82	4.7	4.34	1.29	0.13	0.02	1719.2	2.35	2.35	0	30
1252	D1	65.28	0.59	17.05	4.02	0.08	1.82	4.7	4.34	1.29	0.13	0.02	1768.2	2.11	2.04	-0.07	30
1253	D1	65.28	0.59	17.05	4.02	0.08	1.82	4.7	4.34	1.29	0.13	0.02	1817.2	1.87	1.74	-0.13	30
1254	D1	65.28	0.59	17.05	4.02	0.08	1.82	4.7	4.34	1.29	0.13	0.02	1867.2	1.66	1.45	-0.21	30
1255	D1	65.28	0.59	17.05	4.02	0.08	1.82	4.7	4.34	1.29	0.13	0.02	1009.1	10.6	10.99	0.39	30
1256	D1	65.28	0.59	17.05	4.02	0.08	1.82	4.7	4.34	1.29	0.13	0.02	1023.5	10.25	10.65	0.4	30
1257	D1	65.28	0.59	17.05	4.02	0.08	1.82	4.7	4.34	1.29	0.13	0.02	1037.7	10	10.33	0.33	30
1258	D1	65.28	0.59	17.05	4.02	0.08	1.82	4.7	4.34	1.29	0.13	0.02	1057.1	9.53	9.91	0.38	30
1259	D1	65.28	0.59	17.05	4.02	0.08	1.82	4.7	4.34	1.29	0.13	0.02	1075.9	9.25	9.53	0.28	30

1260	R33	73.12	0.19	13.56	3.19	0	0.18	1.68	3.86	4.2	0	2.1	1273.2	3.85	4.19	0.34	31
1261	R33	73.12	0.19	13.56	3.19	0	0.18	1.68	3.86	4.2	0	2.1	1373.2	3.32	3.43	0.11	31
1262	R33	73.12	0.19	13.56	3.19	0	0.18	1.68	3.86	4.2	0	2.1	1473.2	2.73	2.75	0.02	31
1263	R33	73.12	0.19	13.56	3.19	0	0.18	1.68	3.86	4.2	0	5.2	1173.2	3.69	3.57	-0.12	31
1264	R33	73.12	0.19	13.56	3.19	0	0.18	1.68	3.86	4.2	0	5.2	1273.2	3.05	2.89	-0.16	31
1265	R33	73.12	0.19	13.56	3.19	0	0.18	1.68	3.86	4.2	0	5.2	1373.2	2.51	2.32	-0.19	31
1266	R33	73.12	0.19	13.56	3.19	0	0.18	1.68	3.86	4.2	0	5.2	1473.2	2.03	1.84	-0.19	31
1267	R33	73.12	0.19	13.56	3.19	0	0.18	1.68	3.86	4.2	0	5.6	1173.2	3.6	3.47	-0.13	31
1268	R33	73.12	0.19	13.56	3.19	0	0.18	1.68	3.86	4.2	0	5.6	1273.2	2.97	2.81	-0.16	31
1269	R33	73.12	0.19	13.56	3.19	0	0.18	1.68	3.86	4.2	0	5.6	1373.2	2.42	2.27	-0.15	31
1270	R33	73.12	0.19	13.56	3.19	0	0.18	1.68	3.86	4.2	0	5.6	1473.2	1.85	1.81	-0.04	31
1271	R33	73.12	0.19	13.56	3.19	0	0.18	1.68	3.86	4.2	0	8.8	1173.2	3	3.04	0.04	31
1272	R33	73.12	0.19	13.56	3.19	0	0.18	1.68	3.86	4.2	0	8.8	1473.2	1.47	1.81	0.34	31
1273	A6	62.15	0.76	16.8	4.96	0.25	3.26	5.08	5.02	1.72	0	0	1623.2	2.6	2.77	0.17	32
1274	A6	62.15	0.76	16.8	4.96	0.25	3.26	5.08	5.02	1.72	0	0	1623.2	2.52	2.77	0.25	32
1275	H4	73.6	0	15.6	0	0	0	2.1	4.4	3.8	0	2.1	880.45	8.97	8.99	0.02	33
1276	H4	73.6	0	15.6	0	0	0	2.1	4.4	3.8	0	2.1	835.95	9.79	9.8	0.01	33
1277	H4	73.6	0	15.6	0	0	0	2.1	4.4	3.8	0	2.1	795.95	10.85	10.65	-0.2	33
1278	H4	73.6	0	15.6	0	0	0	2.1	4.4	3.8	0	2.1	794.95	10.99	10.67	-0.32	33
1279	H4	73.6	0	15.6	0	0	0	2.1	4.4	3.8	0	0.89	951.35	9.62	9.84	0.22	33
1280	H4	73.6	0	15.6	0	0	0	2.1	4.4	3.8	0	0.89	976.15	9.15	9.52	0.37	33
1281	H4	73.6	0	15.6	0	0	0	2.1	4.4	3.8	0	0.89	938.35	10.3	10.02	-0.28	33
1282	H4	73.6	0	15.6	0	0	0	2.1	4.4	3.8	0	0.89	916.75	10.81	10.34	-0.47	33
1283	R34	73.89	0.06	15.77	0.75	0	0.14	0.58	4.62	4.19	0	6.66	1228.2	3	3.21	0.22	34
1284	R34	73.89	0.06	15.77	0.75	0	0.14	0.58	4.62	4.19	0	6.66	1086.2	3.86	4.19	0.33	34
1285	R34	73.89	0.06	15.77	0.75	0	0.14	0.58	4.62	4.19	0	3.98	1373.2	3.1	3.02	-0.08	34
1286	R34	73.89	0.06	15.77	0.75	0	0.14	0.58	4.62	4.19	0	3.98	1274.2	3.78	3.67	-0.11	34
1287	R34	73.89	0.06	15.77	0.75	0	0.14	0.58	4.62	4.19	0	3.98	1180.2	4.45	4.35	-0.1	34
1288	R34	73.89	0.06	15.77	0.75	0	0.14	0.58	4.62	4.19	0	6.66	1133.2	3.58	3.84	0.27	34
1289	R34	73.89	0.06	15.77	0.75	0	0.14	0.58	4.62	4.19	0	6.66	1183.2	3.24	3.5	0.26	34
1290	R34	73.89	0.06	15.77	0.75	0	0.14	0.58	4.62	4.19	0	6.66	1128.2	3.54	3.88	0.34	34
1291	R34	73.89	0.06	15.77	0.75	0	0.14	0.58	4.62	4.19	0	6.66	1073.2	3.94	4.29	0.35	34

1292	R34	73.89	0.06	15.77	0.75	0	0.14	0.58	4.62	4.19	0	6.66	1138.2	3.54	3.81	0.27	34
1293	R34	73.89	0.06	15.77	0.75	0	0.14	0.58	4.62	4.19	0	6.66	1133.2	3.52	3.84	0.33	34
1294	H5	74.1	0	11.7	0	0	0	0	9	4.4	0	2.9	622.35	10.05	10.14	0.09	35
1295	H5	74.1	0	11.7	0	0	0	0	9	4.4	0	2.9	661.45	8.69	9.15	0.46	35
1296	H5	74.1	0	11.7	0	0	0	0	9	4.4	0	2.9	599.65	10.94	10.8	-0.14	35
1297	H5	74.1	0	11.7	0	0	0	0	9	4.4	0	2.9	643.75	9.08	9.58	0.5	35
1298	H5	74.1	0	11.7	0	0	0	0	9	4.4	0	1.81	653.65	10.82	10.73	-0.09	35
1299	H5	74.1	0	11.7	0	0	0	0	9	4.4	0	1.81	698.45	9.44	9.64	0.2	35
1300	H5	74.1	0	11.7	0	0	0	0	9	4.4	0	1.81	685.15	9.68	9.94	0.26	35
1301	H5	74.1	0	11.7	0	0	0	0	9	4.4	0	6.97	493.45	10.68	10.93	0.25	35
1302	H5	74.1	0	11.7	0	0	0	0	9	4.4	0	6.97	517.45	9.1	9.99	0.89	35
1303	H5	74.1	0	11.7	0	0	0	0	9	4.4	0	6.97	524.95	8.7	9.72	1.02	35
1304	H5	74.1	0	11.7	0	0	0	0	9	4.4	0	0.92	744.75	10.03	10.14	0.11	35
1305	H5	74.1	0	11.7	0	0	0	0	9	4.4	0	0.92	716.85	10.94	10.74	-0.2	35
1306	H5	74.1	0	11.7	0	0	0	0	9	4.4	0	1.29	745.35	9.28	9.44	0.16	35
1307	H5	74.1	0	11.7	0	0	0	0	9	4.4	0	1.29	707.25	10.38	10.26	-0.12	35
1308	H5	74.1	0	11.7	0	0	0	0	9	4.4	0	1.29	686.55	10.62	10.74	0.12	35
1309	H5	74.1	0	11.7	0	0	0	0	9	4.4	0	0.63	776.45	10.17	10.17	0	35
1310	H5	74.1	0	11.7	0	0	0	0	9	4.4	0	0.63	756.35	10.96	10.57	-0.39	35
1311	H5	74.1	0	11.7	0	0	0	0	9	4.4	0	0.63	804.45	9.31	9.66	0.35	35
1312	H5	74.1	0	11.7	0	0	0	0	9	4.4	0	0.77	774.05	9.48	9.88	0.4	35
1313	H5	74.1	0	11.7	0	0	0	0	9	4.4	0	0.77	744.15	10.8	10.48	-0.32	35
1314	H6	74.1	0	12.2	0	0	0	5.2	4.4	4	0	0.02	1032.3	10.91	11.87	0.96	36
1315	H6	74.1	0	12.2	0	0	0	5.2	4.4	4	0	0.02	1053.5	10.34	11.3	0.96	36
1316	H6	74.1	0	12.2	0	0	0	5.2	4.4	4	0	0.02	1076	9.64	10.75	1.11	36
1317	H6	74.1	0	12.2	0	0	0	5.2	4.4	4	0	0.02	1473.2	4.49	4.88	0.39	36
1318	H6	74.1	0	12.2	0	0	0	5.2	4.4	4	0	0.02	1522.2	4.15	4.43	0.28	36
1319	H6	74.1	0	12.2	0	0	0	5.2	4.4	4	0	0.02	1571.2	3.83	4.01	0.18	36
1320	H6	74.1	0	12.2	0	0	0	5.2	4.4	4	0	0.02	1621.2	3.52	3.62	0.1	36
1321	H6	74.1	0	12.2	0	0	0	5.2	4.4	4	0	0.02	1670.2	3.26	3.26	0	36
1322	H6	74.1	0	12.2	0	0	0	5.2	4.4	4	0	0.02	1719.2	3	2.92	-0.08	36
1323	H6	74.1	0	12.2	0	0	0	5.2	4.4	4	0	0.02	1768.2	2.77	2.61	-0.16	36

1324	H6	74.1	0	12.2	0	0	0	5.2	4.4	4	0	0.02	1817.2	2.55	2.31	-0.24	36
1325	H6	74.1	0	12.2	0	0	0	5.2	4.4	4	0	0.02	1867.2	2.33	2.03	-0.3	36
1326	H9	75.6	0	12	0	0	4.9	0	4.5	4	0	0.02	1078.8	11	11.45	0.45	36
1327	H9	75.6	0	12	0	0	4.9	0	4.5	4	0	0.02	1096.9	10.66	10.85	0.19	36
1328	H9	75.6	0	12	0	0	4.9	0	4.5	4	0	0.02	1113.6	10.14	10.35	0.21	36
1329	H9	75.6	0	12	0	0	4.9	0	4.5	4	0	0.02	1130.1	9.71	9.9	0.19	36
1330	H9	75.6	0	12	0	0	4.9	0	4.5	4	0	0.02	1522.4	4.41	4.31	-0.1	36
1331	H9	75.6	0	12	0	0	4.9	0	4.5	4	0	0.02	1571.6	4.06	3.91	-0.15	36
1332	H9	75.6	0	12	0	0	4.9	0	4.5	4	0	0.02	1620.8	3.72	3.53	-0.19	36
1333	H9	75.6	0	12	0	0	4.9	0	4.5	4	0	0.02	1670	3.4	3.18	-0.22	36
1334	H9	75.6	0	12	0	0	4.9	0	4.5	4	0	0.02	1719.2	3.12	2.85	-0.27	36
1335	H9	75.6	0	12	0	0	4.9	0	4.5	4	0	0.02	1768.4	2.86	2.54	-0.32	36
1336	H9	75.6	0	12	0	0	4.9	0	4.5	4	0	0.02	1817.6	2.61	2.25	-0.36	36
1337	H9	75.6	0	12	0	0	4.9	0	4.5	4	0	0.02	1866.8	2.35	1.97	-0.38	36
1338	H11	77.2	0	13.9	0	0	0	0	4.5	4.3	0	0	1176.1	11.3	11.09	-0.21	37
1339	H11	77.2	0	13.9	0	0	0	0	4.5	4.3	0	0	1198.1	11.08	10.74	-0.34	37
1340	H11	77.2	0	13.9	0	0	0	0	4.5	4.3	0	0	1217.2	10.48	10.44	-0.04	37
1341	H11	77.2	0	13.9	0	0	0	0	4.5	4.3	0	0	1234.4	10.14	10.19	0.05	37
1342	H11	77.2	0	13.9	0	0	0	0	4.5	4.3	0	0	1257.4	10.07	9.86	-0.21	37
1343	H11	77.2	0	13.9	0	0	0	0	4.5	4.3	0	1.07	869.35	11	10.75	-0.25	37
1344	H11	77.2	0	13.9	0	0	0	0	4.5	4.3	0	1.07	908.75	10.55	10.12	-0.43	37
1345	H11	77.2	0	13.9	0	0	0	0	4.5	4.3	0	2.18	815.05	10.64	10.14	-0.5	37
1346	H11	77.2	0	13.9	0	0	0	0	4.5	4.3	0	2.54	767.25	10.58	10.78	0.2	37
1347	H11	77.2	0	13.9	0	0	0	0	4.5	4.3	0	2.54	794.55	10.19	10.16	-0.03	37
1348	H11	77.2	0	13.9	0	0	0	0	4.5	4.3	0	2.54	747.05	11.2	11.27	0.07	37
1349	H8	75.4	0	16.1	0	0	0	0	4.7	4.3	0	0	1252.9	10.12	9.96	-0.16	37
1350	H8	75.4	0	16.1	0	0	0	0	4.7	4.3	0	0	1233.9	10.35	10.23	-0.12	37
1351	H8	75.4	0	16.1	0	0	0	0	4.7	4.3	0	0	1216.1	10.7	10.49	-0.21	37
1352	H8	75.4	0	16.1	0	0	0	0	4.7	4.3	0	0	1267.9	9.85	9.76	-0.09	37
1353	H8	75.4	0	16.1	0	0	0	0	4.7	4.3	0	0	1213	10.58	10.53	-0.05	37
1354	H8	75.4	0	16.1	0	0	0	0	4.7	4.3	0	1.17	891.55	10.52	10.22	-0.3	37
1355	H8	75.4	0	16.1	0	0	0	0	4.7	4.3	0	1.17	869.75	10.85	10.6	-0.25	37

1356	H8	75.4	0	16.1	0	0	0	0	4.7	4.3	0	1.17	856.55	11.12	10.84	-0.28	37
1357	H8	75.4	0	16.1	0	0	0	0	4.7	4.3	0	2.03	819.45	10.42	10.29	-0.13	37
1358	H8	75.4	0	16.1	0	0	0	0	4.7	4.3	0	2.03	832.85	9.84	10.02	0.18	37
1359	H8	75.4	0	16.1	0	0	0	0	4.7	4.3	0	2.03	801.35	10.7	10.68	-0.02	37
1360	H8	75.4	0	16.1	0	0	0	0	4.7	4.3	0	2.03	792.65	10.8	10.88	0.08	37
1361	H8	75.4	0	16.1	0	0	0	0	4.7	4.3	0	2.77	764.75	10.14	10.66	0.52	37
1362	H8	75.4	0	16.1	0	0	0	0	4.7	4.3	0	2.77	755.55	10.6	10.88	0.28	37
1363	H8	75.4	0	16.1	0	0	0	0	4.7	4.3	0	2.77	792.85	9.91	10.02	0.11	37
1364	H8	75.4	0	16.1	0	0	0	0	4.7	4.3	0	2.77	747.85	10.75	11.07	0.32	37
1365	H10	76.88	0	11.45	0	0	0	0	3.6	5.6	0	0.02	1277.2	9.15	8.98	-0.17	38
1366	H10	76.88	0	11.45	0	0	0	0	3.6	5.6	0	0.02	1243.5	9.57	9.43	-0.14	38
1367	H10	76.88	0	11.45	0	0	0	0	3.6	5.6	0	0.02	1210.7	9.99	9.89	-0.1	38
1368	H10	76.88	0	11.45	0	0	0	0	3.6	5.6	0	0.02	1155.9	10.85	10.73	-0.12	38
1369	H10	76.88	0	11.45	0	0	0	0	3.6	5.6	0	0.02	1123.2	11.35	11.27	-0.08	38
1370	H12	78.14	0	11.64	0	0	0	0	1.26	9.11	0	0.02	1261.2	9.6	9.41	-0.19	38
1371	H12	78.14	0	11.64	0	0	0	0	1.26	9.11	0	0.02	1244	9.86	9.65	-0.21	38
1372	H12	78.14	0	11.64	0	0	0	0	1.26	9.11	0	0.02	1216.1	10.31	10.05	-0.26	38
1373	H12	78.14	0	11.64	0	0	0	0	1.26	9.11	0	0.02	1195.3	10.75	10.36	-0.39	38
1374	H12	78.14	0	11.64	0	0	0	0	1.26	9.11	0	0.02	1123.2	12.12	11.53	-0.59	38
1375	H13	78.21	0	11.69	0	0	0	0	2.41	7.43	0	0.02	1263.5	9.72	9.34	-0.38	38
1376	H13	78.21	0	11.69	0	0	0	0	2.41	7.43	0	0.02	1245	9.92	9.59	-0.33	38
1377	H13	78.21	0	11.69	0	0	0	0	2.41	7.43	0	0.02	1199.4	10.52	10.25	-0.27	38
1378	H13	78.21	0	11.69	0	0	0	0	2.41	7.43	0	0.02	1196.5	10.72	10.3	-0.42	38
1379	H13	78.21	0	11.69	0	0	0	0	2.41	7.43	0	0.02	1123.2	11.8	11.48	-0.32	38
1380	H14	78.28	0	11.92	0	0	0	0	5.91	2.23	0	0.02	1247.8	9.02	9.6	0.58	38
1381	H14	78.28	0	11.92	0	0	0	0	5.91	2.23	0	0.02	1225.3	9.34	9.92	0.58	38
1382	H14	78.28	0	11.92	0	0	0	0	5.91	2.23	0	0.02	1204.8	9.6	10.21	0.61	38
1383	H14	78.28	0	11.92	0	0	0	0	5.91	2.23	0	0.02	1183.8	9.94	10.53	0.59	38
1384	H14	78.28	0	11.92	0	0	0	0	5.91	2.23	0	0.02	1173.2	10.13	10.7	0.57	38
1385	H14	78.28	0	11.92	0	0	0	0	5.91	2.23	0	0.02	1123.2	10.92	11.52	0.6	38
1386	H15	78.6	0	11.99	0	0	0	0	4.57	4.2	0	0.02	1154.9	11.02	11.12	0.1	38
1387	H15	78.6	0	11.99	0	0	0	0	4.57	4.2	0	0.02	1178.2	10.63	10.74	0.11	38

1388	H15	78.6	0	11.99	0	0	0	0	4.57	4.2	0	0.02	1198.9	10.28	10.43	0.15	38
1389	H15	78.6	0	11.99	0	0	0	0	4.57	4.2	0	0.02	1212	10.16	10.23	0.07	38
1390	H15	78.6	0	11.99	0	0	0	0	4.57	4.2	0	0.02	1123.2	11.53	11.65	0.12	38
1391	H16	81.03	0	9.91	0	0	0	0	1.24	7.39	0	0.02	1266.8	10.25	9.85	-0.4	38
1392	H16	81.03	0	9.91	0	0	0	0	1.24	7.39	0	0.02	1256.7	10.36	9.99	-0.37	38
1393	H16	81.03	0	9.91	0	0	0	0	1.24	7.39	0	0.02	1236	10.56	10.29	-0.27	38
1394	H16	81.03	0	9.91	0	0	0	0	1.24	7.39	0	0.02	1237.5	10.63	10.27	-0.36	38
1395	H16	81.03	0	9.91	0	0	0	0	1.24	7.39	0	0.02	1222.5	10.97	10.49	-0.48	38
1396	H16	81.03	0	9.91	0	0	0	0	1.24	7.39	0	0.02	1224.3	11	10.46	-0.54	38
1397	H16	81.03	0	9.91	0	0	0	0	1.24	7.39	0	0.02	1213.7	11.27	10.62	-0.65	38
1398	H16	81.03	0	9.91	0	0	0	0	1.24	7.39	0	0.02	1123.2	13.08	12.12	-0.96	38
1399	H17	81.74	0	10.03	0	0	0	0	2.47	5.66	0	0.02	1263.7	9.97	9.86	-0.11	38
1400	H17	81.74	0	10.03	0	0	0	0	2.47	5.66	0	0.02	1241.6	10.23	10.17	-0.06	38
1401	H17	81.74	0	10.03	0	0	0	0	2.47	5.66	0	0.02	1217.3	10.59	10.53	-0.06	38
1402	H17	81.74	0	10.03	0	0	0	0	2.47	5.66	0	0.02	1194.1	11	10.89	-0.11	38
1403	H17	81.74	0	10.03	0	0	0	0	2.47	5.66	0	0.02	1123.2	12.16	12.08	-0.08	38
1404	H18	82.22	0	10.17	0	0	0	0	3.66	3.89	0	0.02	1270.8	9.86	9.84	-0.02	38
1405	H18	82.22	0	10.17	0	0	0	0	3.66	3.89	0	0.02	1253.8	10.15	10.08	-0.07	38
1406	H18	82.22	0	10.17	0	0	0	0	3.66	3.89	0	0.02	1226.2	10.44	10.48	0.04	38
1407	H18	82.22	0	10.17	0	0	0	0	3.66	3.89	0	0.02	1197	10.95	10.93	-0.02	38
1408	H18	82.22	0	10.17	0	0	0	0	3.66	3.89	0	0.02	1123.2	12.12	12.17	0.05	38
1409	H19	82.31	0	10.16	0	0	0	0	5.89	0.7	0	0.02	1242.5	9.86	10.04	0.18	38
1410	H19	82.31	0	10.16	0	0	0	0	5.89	0.7	0	0.02	1226.8	10.18	10.27	0.09	38
1411	H19	82.31	0	10.16	0	0	0	0	5.89	0.7	0	0.02	1203.3	10.54	10.62	0.08	38
1412	H19	82.31	0	10.16	0	0	0	0	5.89	0.7	0	0.02	1176.8	10.91	11.04	0.13	38
1413	H19	82.31	0	10.16	0	0	0	0	5.89	0.7	0	0.02	1123.2	11.87	11.96	0.09	38
1414	H20	82.94	0	10.3	0	0	0	0	4.68	2.41	0	0.01	1260.5	9.73	10.05	0.32	38
1415	H20	82.94	0	10.3	0	0	0	0	4.68	2.41	0	0.01	1236.7	10.1	10.4	0.3	38
1416	H20	82.94	0	10.3	0	0	0	0	4.68	2.41	0	0.01	1215.5	10.59	10.72	0.13	38
1417	H20	82.94	0	10.3	0	0	0	0	4.68	2.41	0	0.01	1217.3	10.6	10.69	0.09	38
1418	H20	82.94	0	10.3	0	0	0	0	4.68	2.41	0	0.01	1191.5	11.14	11.1	-0.04	38
1419	H20	82.94	0	10.3	0	0	0	0	4.68	2.41	0	0.01	1123.2	12.72	12.27	-0.45	38

1420	H21	73.49	0	13.26	0	0	0	0	2.4	8.98	0	0.03	1246.3	9.86	9.08	-0.78	38
1421	H21	73.49	0	13.26	0	0	0	0	2.4	8.98	0	0.03	1221.3	10.22	9.41	-0.81	38
1422	H21	73.49	0	13.26	0	0	0	0	2.4	8.98	0	0.03	1202.5	10.49	9.67	-0.82	38
1423	H21	73.49	0	13.26	0	0	0	0	2.4	8.98	0	0.03	1177	10.89	10.04	-0.85	38
1424	H21	73.49	0	13.26	0	0	0	0	2.4	8.98	0	0.03	1123.2	11.77	10.88	-0.89	38
1425	H22	74.9	0	13.52	0	0	0	0	3.64	7.22	0	0.02	1267.9	9.46	8.91	-0.55	38
1426	H22	74.9	0	13.52	0	0	0	0	3.64	7.22	0	0.02	1240.3	9.9	9.27	-0.63	38
1427	H22	74.9	0	13.52	0	0	0	0	3.64	7.22	0	0.02	1226.6	10.1	9.46	-0.64	38
1428	H22	74.9	0	13.52	0	0	0	0	3.64	7.22	0	0.02	1191.4	10.6	9.96	-0.64	38
1429	H22	74.9	0	13.52	0	0	0	0	3.64	7.22	0	0.02	1123.2	11.76	11.01	-0.75	38
1430	H23	75.52	0	13.9	0	0	0	0	4.77	5.53	0	0.02	1265.2	9.36	9.15	-0.21	38
1431	H23	75.52	0	13.9	0	0	0	0	4.77	5.53	0	0.02	1236.4	9.96	9.54	-0.42	38
1432	H23	75.52	0	13.9	0	0	0	0	4.77	5.53	0	0.02	1223	10.12	9.72	-0.4	38
1433	H23	75.52	0	13.9	0	0	0	0	4.77	5.53	0	0.02	1188.4	10.66	10.22	-0.44	38
1434	H23	75.52	0	13.9	0	0	0	0	4.77	5.53	0	0.02	1123.2	11.92	11.25	-0.67	38
1435	H24	76.08	0	13.89	0	0	0	0	5.96	3.84	0	0.02	1217.4	9.54	9.76	0.22	38
1436	H24	76.08	0	13.89	0	0	0	0	5.96	3.84	0	0.02	1192.3	10.13	10.13	0	38
1437	H24	76.08	0	13.89	0	0	0	0	5.96	3.84	0	0.02	1176.9	10.5	10.36	-0.14	38
1438	H24	76.08	0	13.89	0	0	0	0	5.96	3.84	0	0.02	1151.3	10.9	10.75	-0.15	38
1439	H24	76.08	0	13.89	0	0	0	0	5.96	3.84	0	0.02	1123.2	11.59	11.21	-0.38	38
1440	H25	76.52	0	14.05	0	0	0	0	7.14	2.19	0	0.02	1218.8	9.64	9.72	0.08	38
1441	H25	76.52	0	14.05	0	0	0	0	7.14	2.19	0	0.02	1197.6	9.99	10.02	0.03	38
1442	H25	76.52	0	14.05	0	0	0	0	7.14	2.19	0	0.02	1175	10.34	10.36	0.02	38
1443	H25	76.52	0	14.05	0	0	0	0	7.14	2.19	0	0.02	1150	10.8	10.74	-0.06	38
1444	H25	76.52	0	14.05	0	0	0	0	7.14	2.19	0	0.02	1123.2	11.27	11.18	-0.09	38
1445	H26	78.98	0	12.11	0	0	0	0	7.04	0.62	0	0.01	1271.1	9.15	9.35	0.2	38
1446	H26	78.98	0	12.11	0	0	0	0	7.04	0.62	0	0.01	1258.6	9.45	9.52	0.07	38
1447	H26	78.98	0	12.11	0	0	0	0	7.04	0.62	0	0.01	1239.4	9.65	9.79	0.14	38
1448	H26	78.98	0	12.11	0	0	0	0	7.04	0.62	0	0.01	1209.9	10.35	10.22	-0.13	38
1449	H26	78.98	0	12.11	0	0	0	0	7.04	0.62	0	0.01	1189.3	10.74	10.53	-0.21	38
1450	H26	78.98	0	12.11	0	0	0	0	7.04	0.62	0	0.01	1168.6	11.24	10.86	-0.38	38
1451	H26	78.98	0	12.11	0	0	0	0	7.04	0.62	0	0.01	1123.2	12.24	11.62	-0.62	38

APPENDIX B

FTIR SPECTRA FOR EQUILIBRIUM SPECIATION EXPERIMENTS

The FTIR spectra on the following pages are for the measurements listed in Table 3.3 in Chapter III. All spectra were normalized to the sample thickness (mm).

Fig. B.1 FTIR spectra for equilibrium speciation experiments.

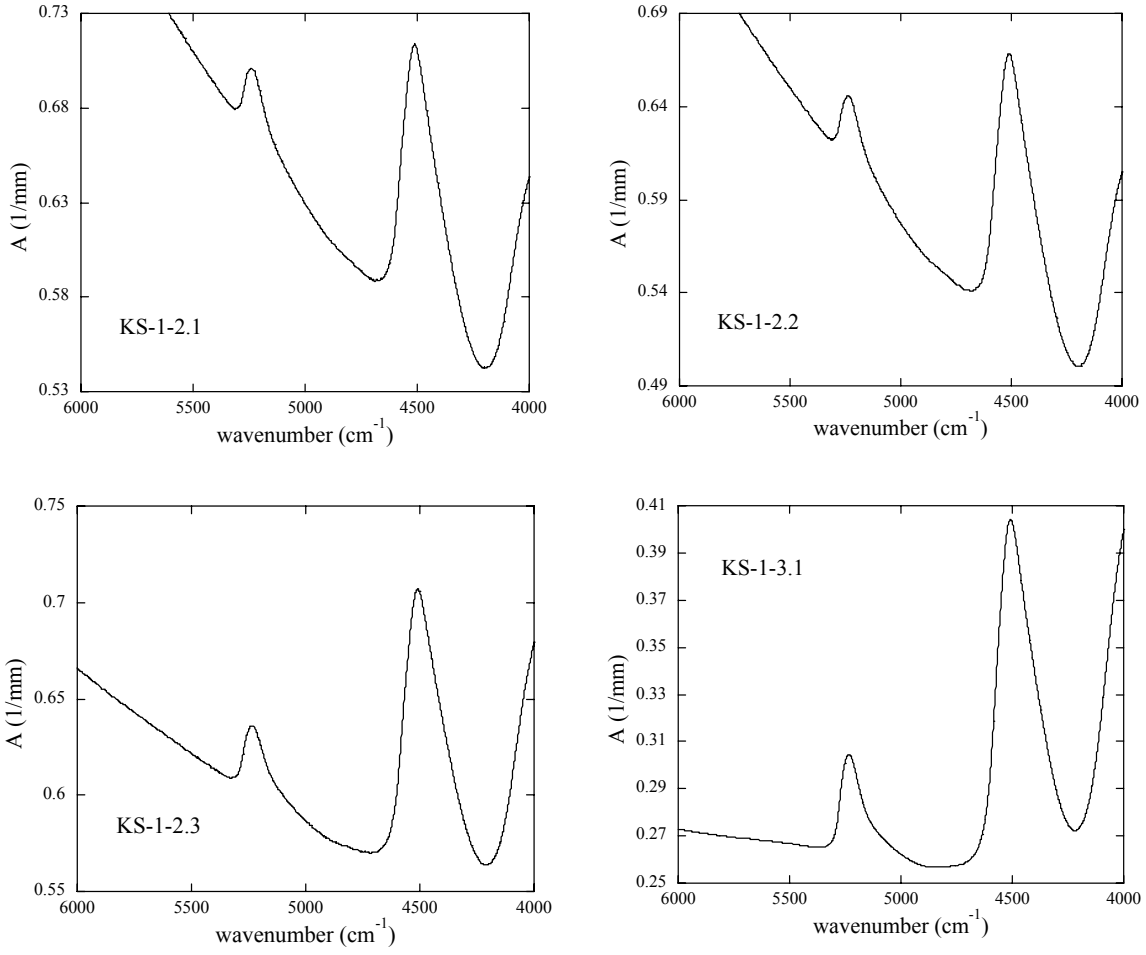

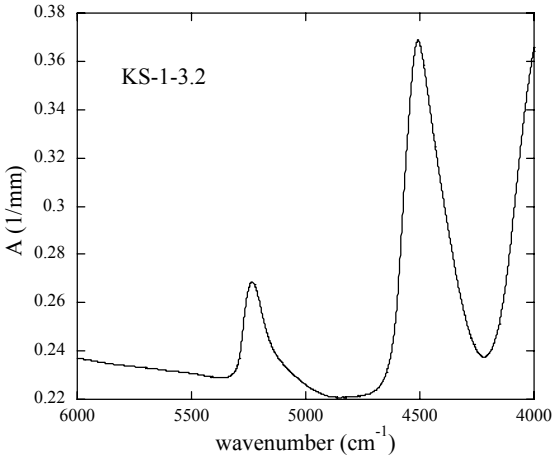
KS-1-3.2
A (1/mm)
wavenumber (cm-1)

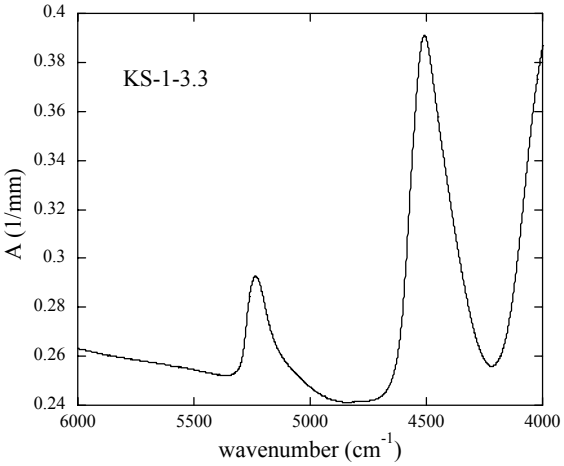
KS-1-3.3
A (1/mm)
wavenumber (cm-1)

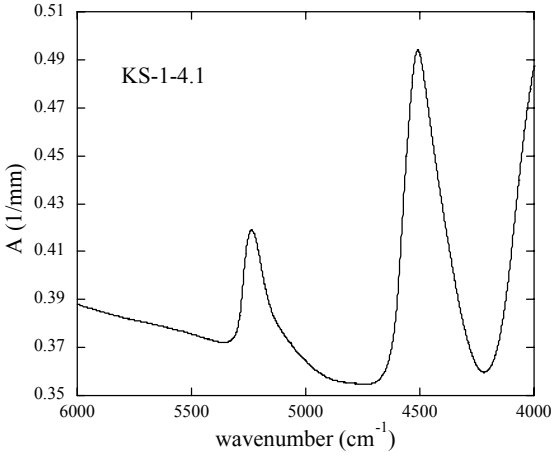
KS-1-4.1
A (1/mm)
wavenumber (cm-1)

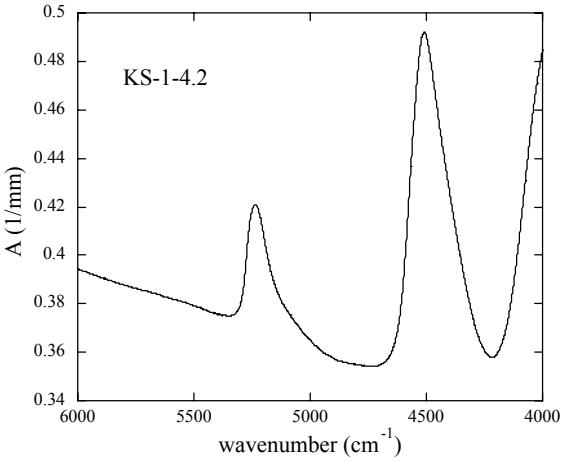
KS-1-4.2
A (1/mm)
wavenumber (cm-1)

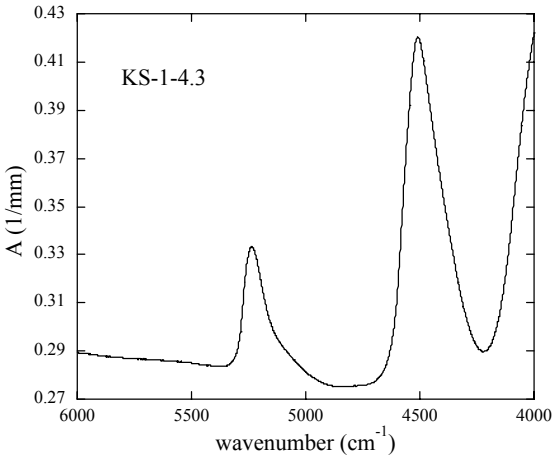
KS-1-4.3
A (1/mm)
wavenumber (cm-1)

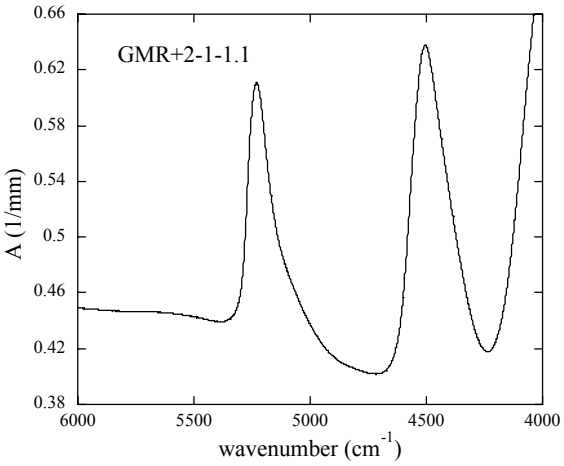
GMR+2-1-1.1
A (1/mm)
wavenumber (cm-1)

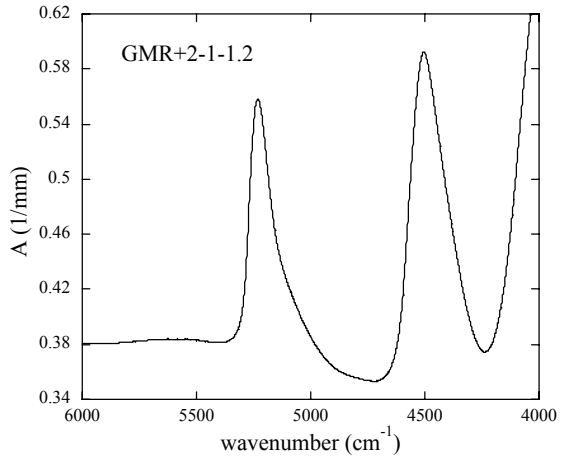
GMR+2-1-1.2
A (1/mm)
wavenumber (cm-1)

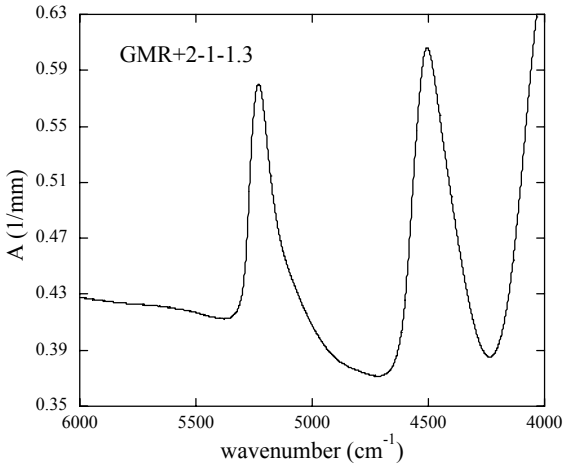
GMR+2-1-1.3
A (1/mm)
wavenumber (cm-1)

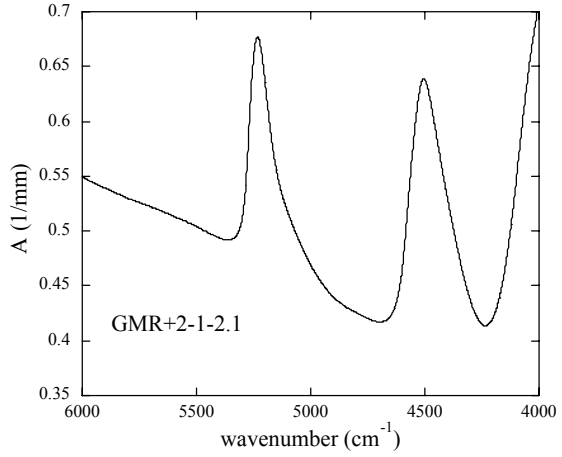
GMR+2-1-2.1
A (1/mm)
wavenumber (cm-1)

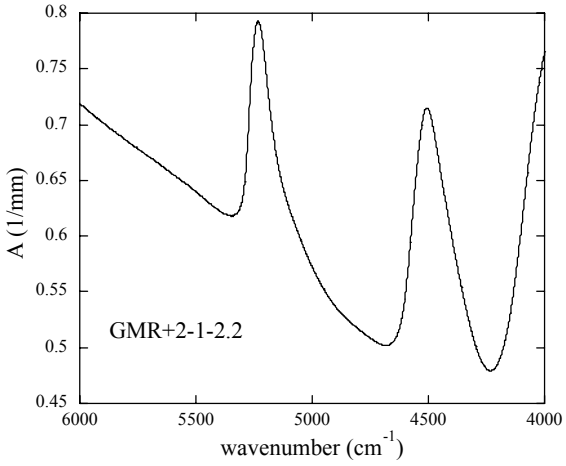
GMR+2-1-2.2
A (1/mm)
wavenumber (cm-1)

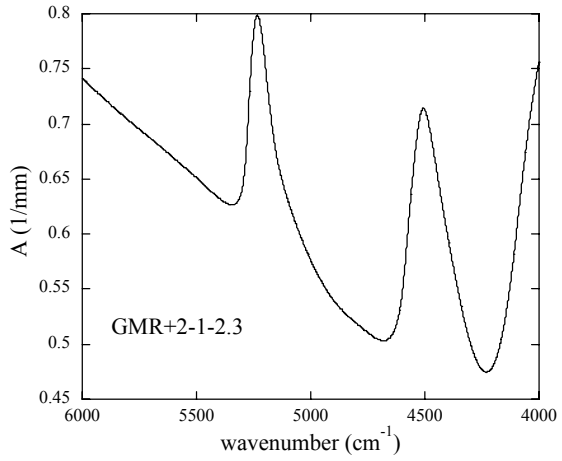
GMR+2-1-2.3
A (1/mm)
wavenumber (cm-1)

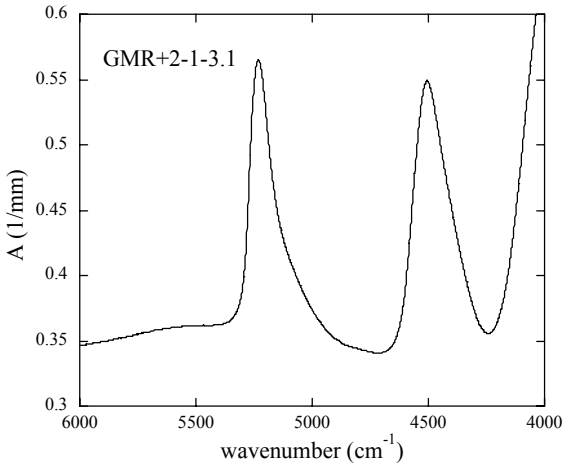
GMR+2-1-3.1
A (1/mm)
wavenumber (cm-1)

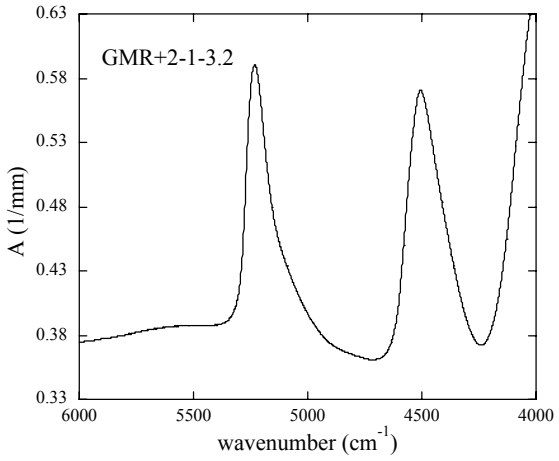
GMR+2-1-3.2
A (1/mm)
wavenumber (cm-1)

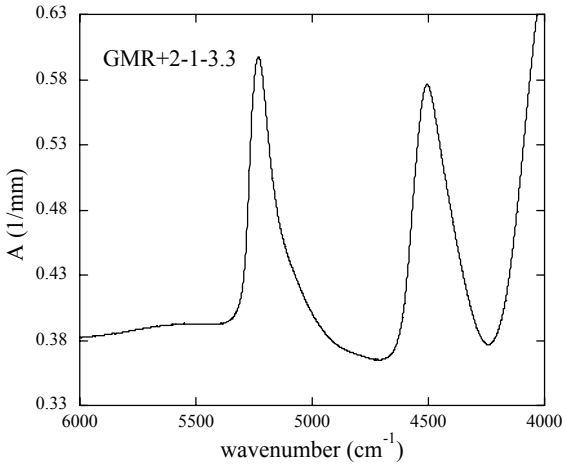
GMR+2-1-3.3
A (1/mm)
wavenumber (cm-1)

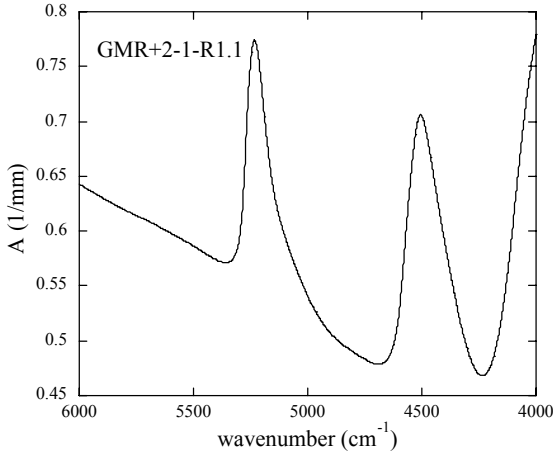
GMR+2-1-R1.1
A (1/mm)
wavenumber (cm-1)

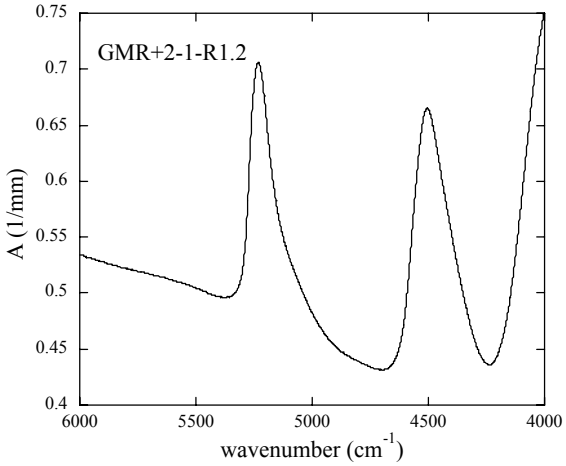
GMR+2-1-R1.2
A (1/mm)
wavenumber (cm-1)

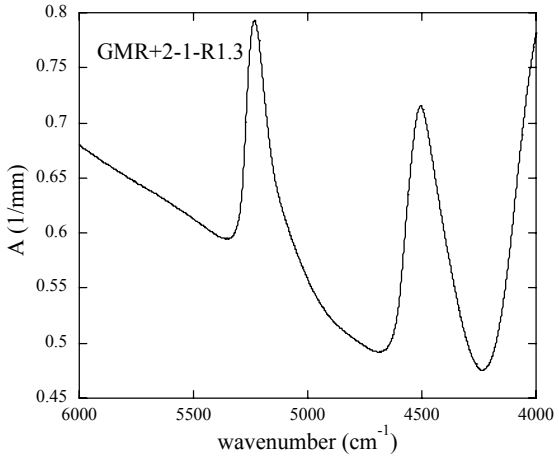
GMR+2-1-R1.3
A (1/mm)
wavenumber (cm-1)

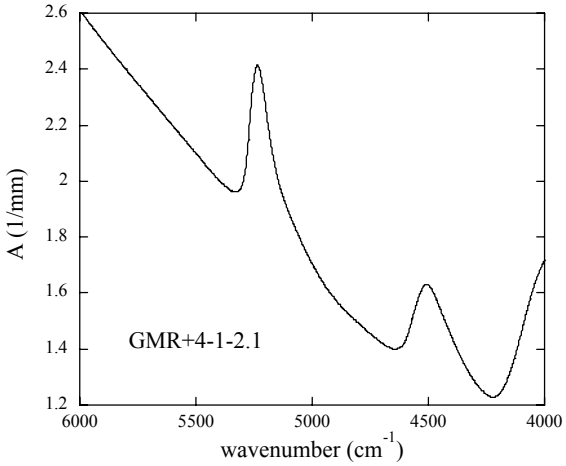
GMR+4-1-2.1
A (1/mm)
wavenumber (cm-1)

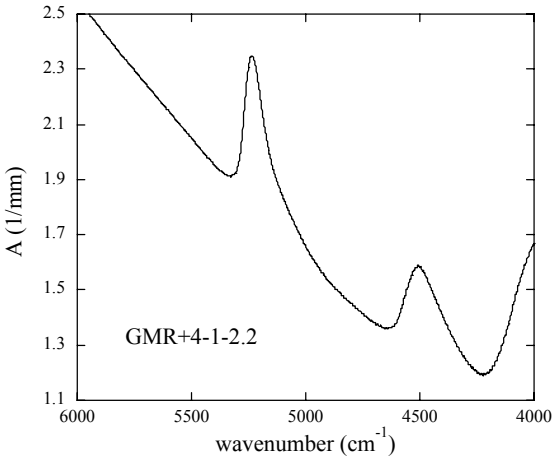
GMR+4-1-2.2
A (1/mm)
wavenumber (cm-1)

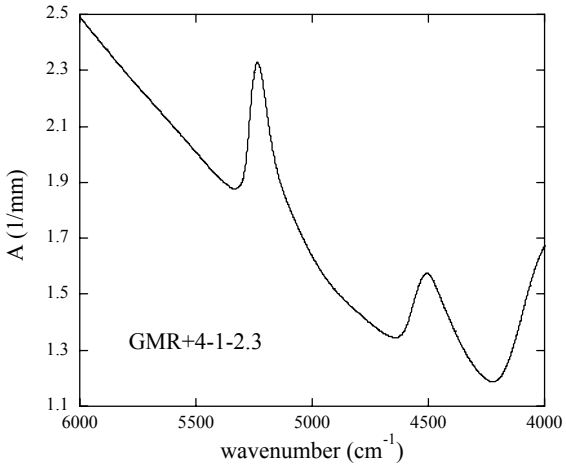
GMR+4-1-2.3
A (1/mm)
wavenumber (cm-1)

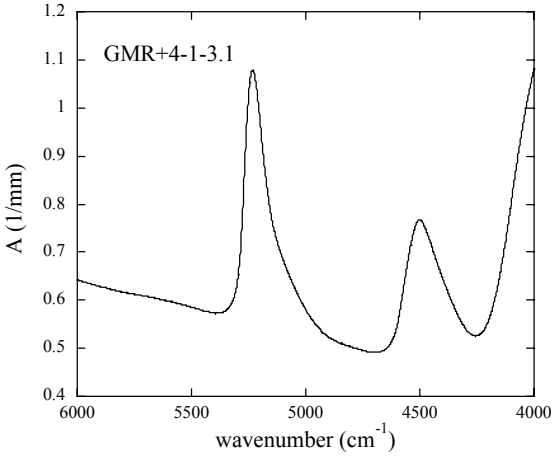
GMR+4-1-3.1
A (1/mm)
wavenumber (cm-1)

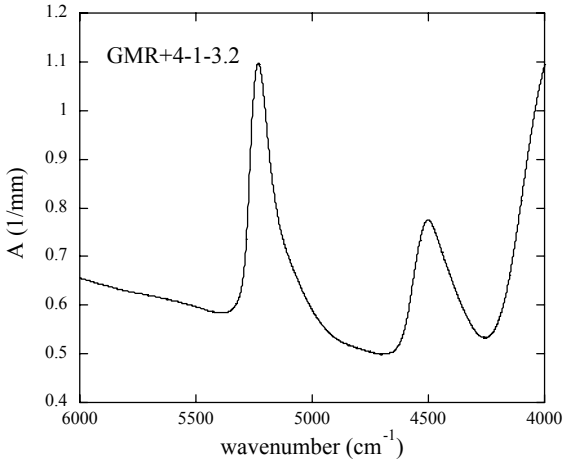
GMR+4-1-3.2
A (1/mm)
wavenumber (cm-1)

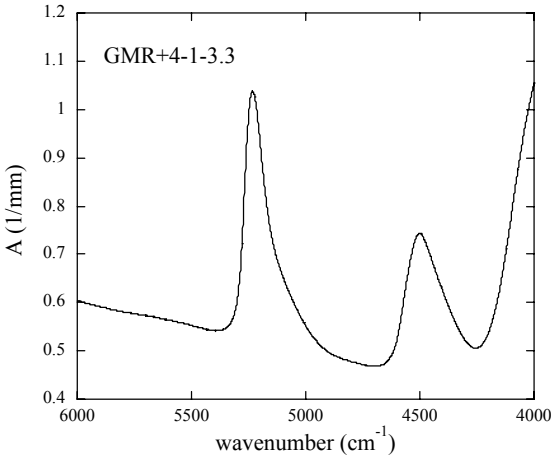
GMR+4-1-3.3
A (1/mm)
wavenumber (cm-1)

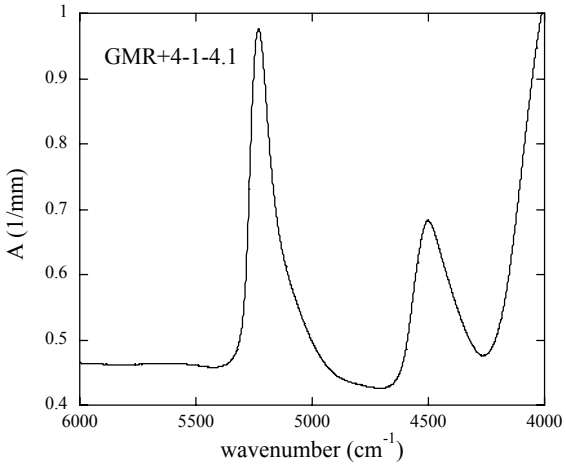
GMR+4-1-4.1
A (1/mm)
wavenumber (cm-1)

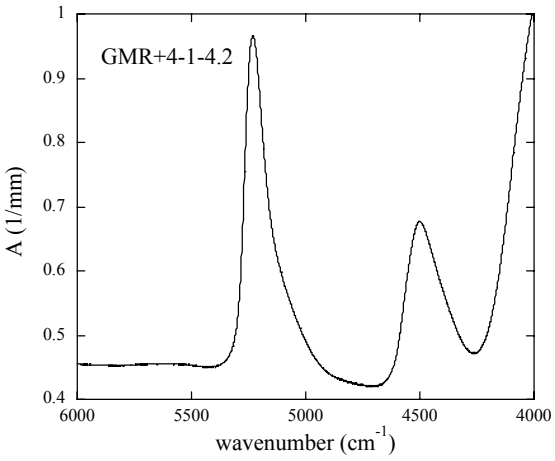
GMR+4-1-4.2
A (1/mm)
wavenumber (cm-1)

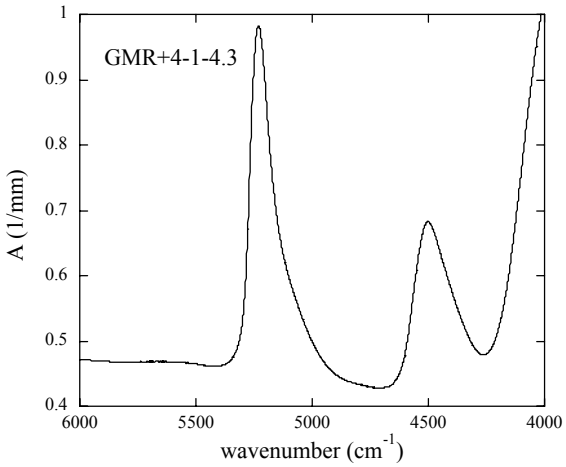
GMR+4-1-4.3
A (1/mm)
wavenumber (cm-1)

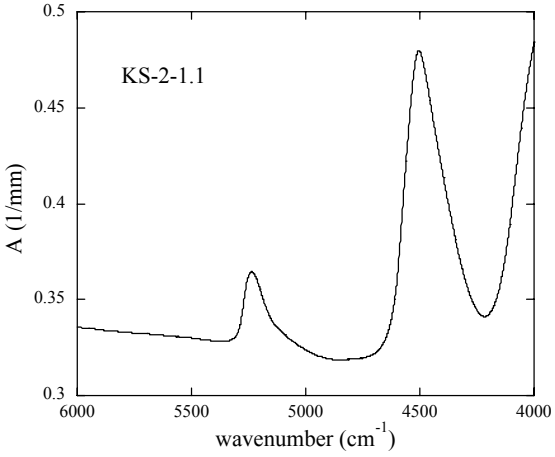
KS-2-1.1
A (1/mm)
wavenumber (cm-1)

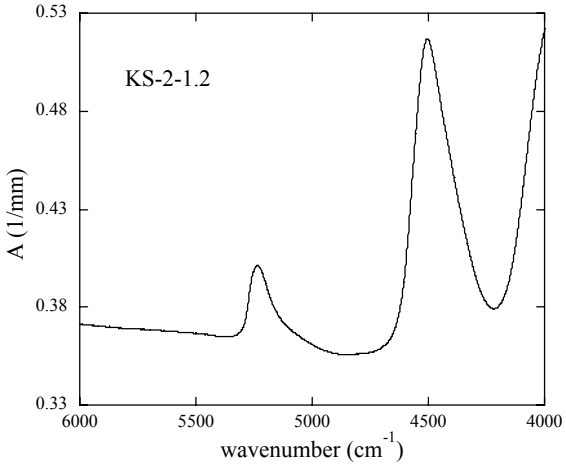
KS-2-1.2
A (1/mm)
wavenumber (cm-1)

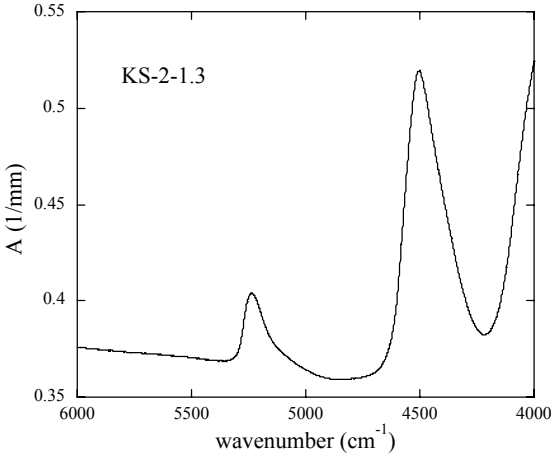
KS-2-1.3
A (1/mm)
wavenumber (cm-1)

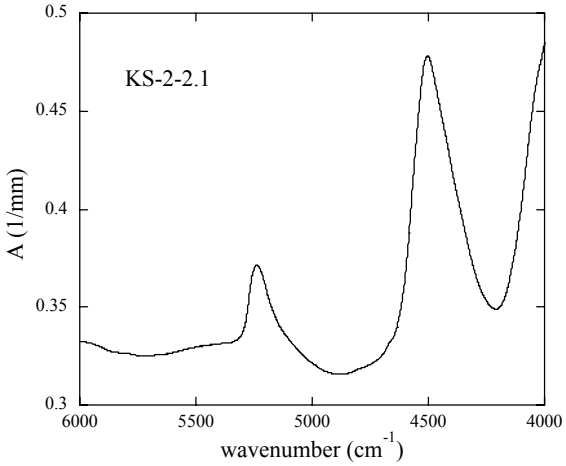
KS-2-2.1
A (1/mm)
wavenumber (cm-1)

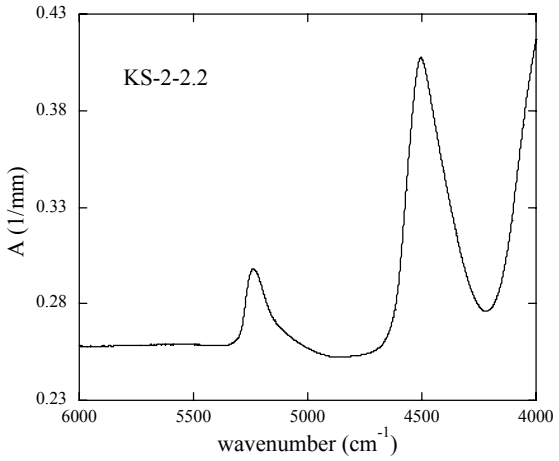
KS-2-2.2
A (1/mm)
wavenumber (cm-1)

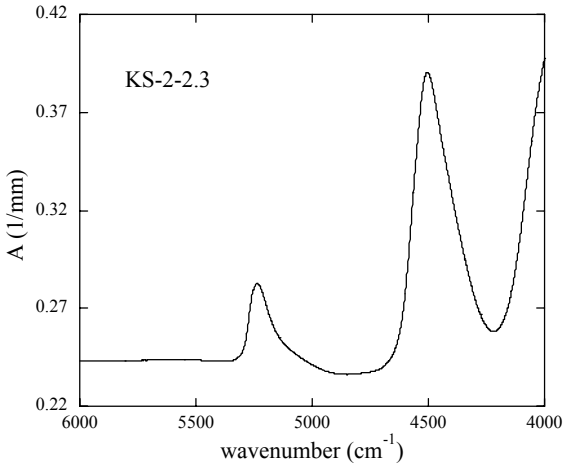
KS-2-2.3
A (1/mm)
wavenumber (cm-1)

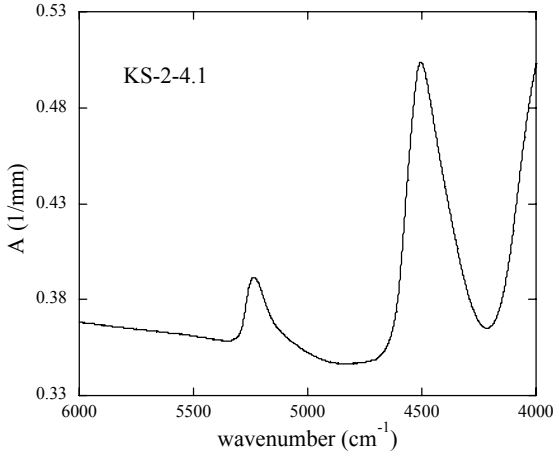
KS-2-4.1
A (1/mm)
wavenumber (cm-1)

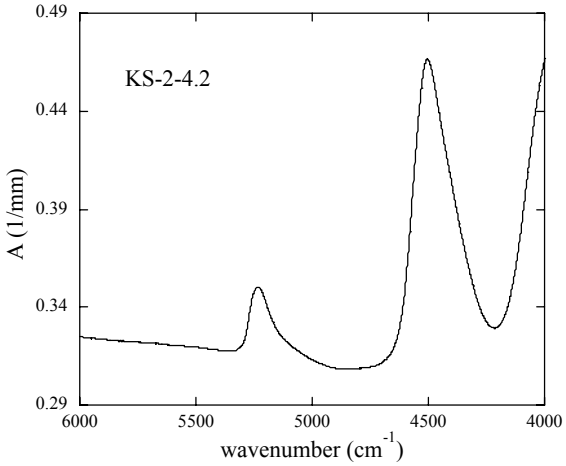
KS-2-4.2
A (1/mm)
wavenumber (cm-1)

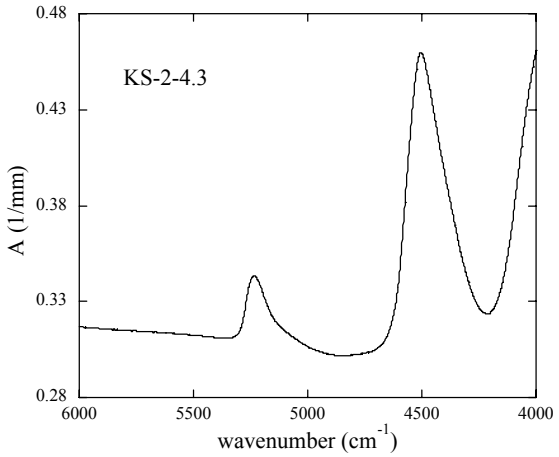
KS-2-4.3
A (1/mm)
wavenumber (cm-1)

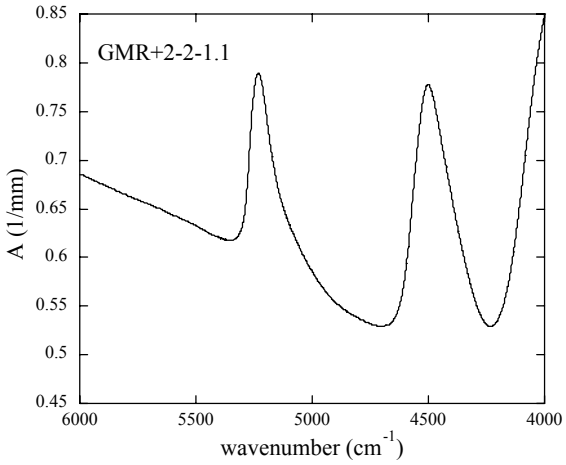
GMR+2-2-1.1
A (1/mm)
wavenumber (cm-1)

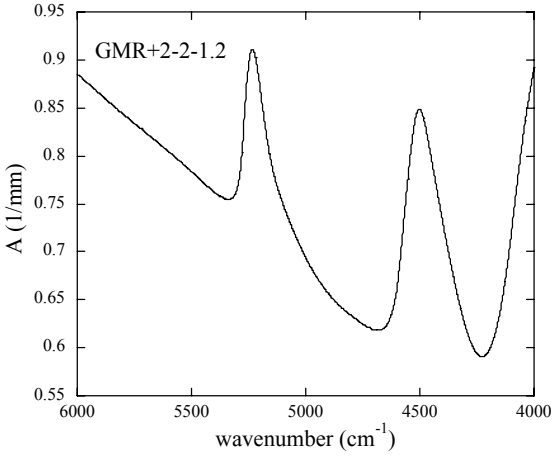
GMR+2-2-1.2
A (1/mm)
wavenumber (cm-1)

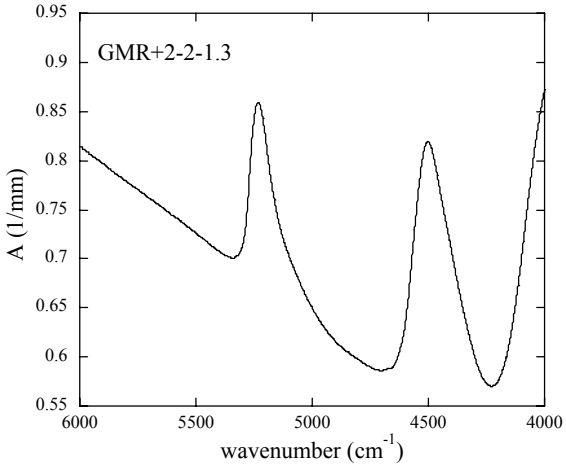
GMR+2-2-1.3
A (1/mm)
wavenumber (cm-1)

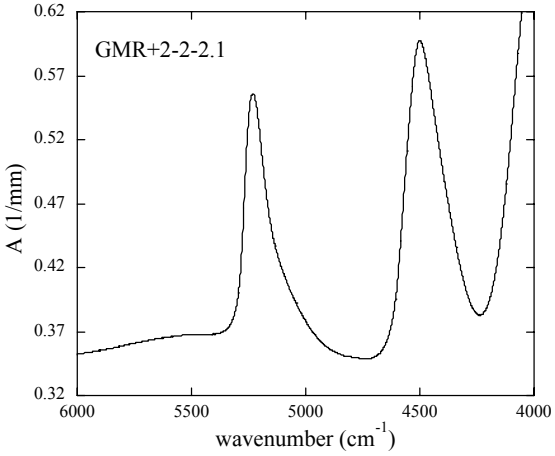
GMR+2-2-2.1
A (1/mm)
wavenumber (cm-1)

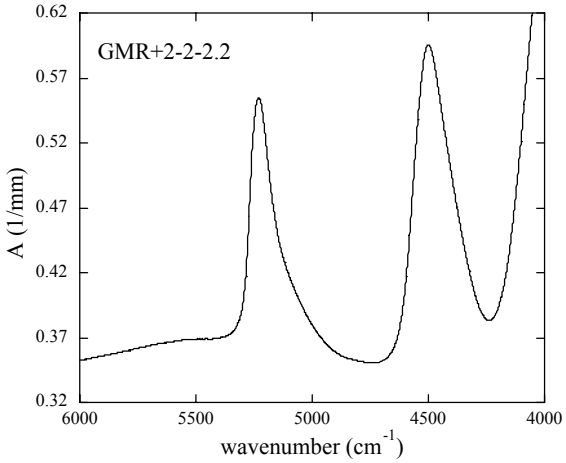
GMR+2-2-2.2
A (1/mm)
wavenumber (cm-1)

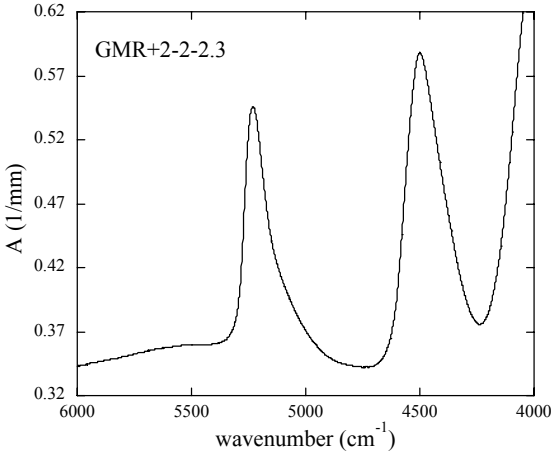
GMR+2-2-2.3
A (1/mm)
wavenumber (cm-1)

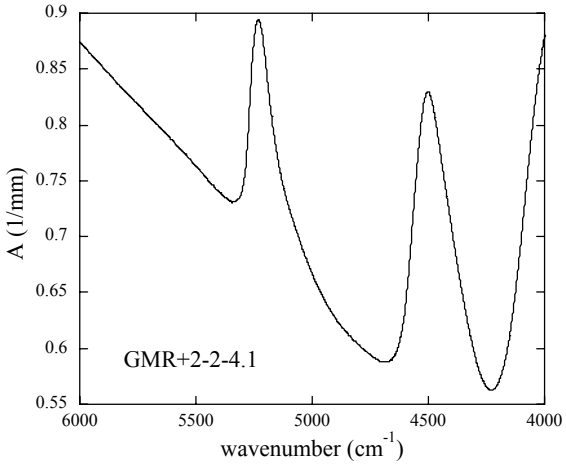
GMR+2-2-4.1
A (1/mm)
wavenumber (cm-1)

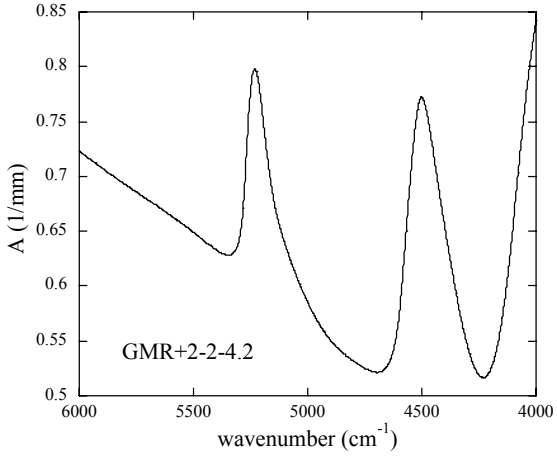
GMR+2-2-4.2
A (1/mm)
wavenumber (cm-1)

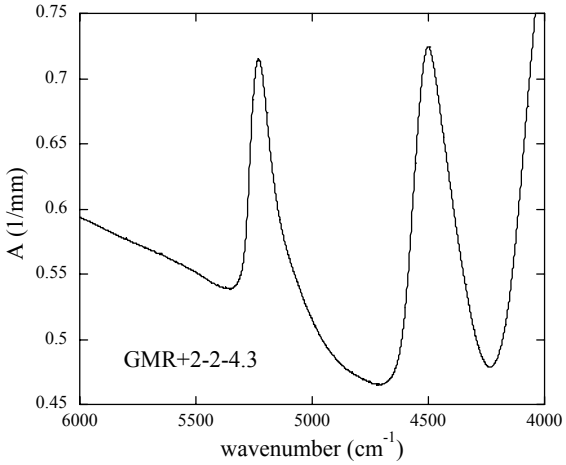
GMR+2-2-4.3
A (1/mm)
wavenumber (cm-1)

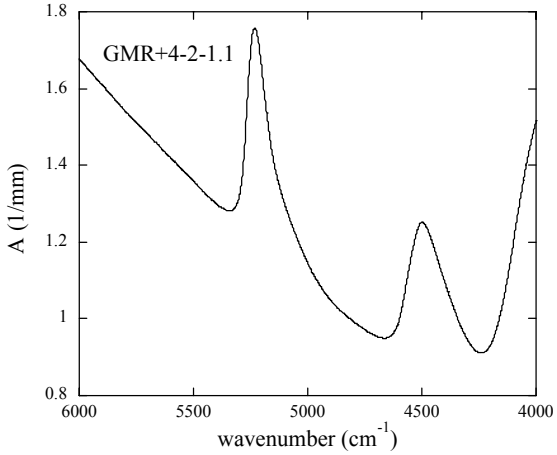
GMR+4-2-1.1
A (1/mm)
wavenumber (cm-1)

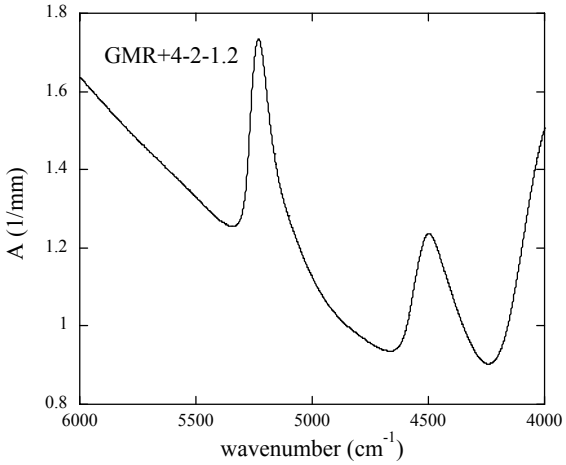
GMR+4-2-1.2
A (1/mm)
wavenumber (cm-1)

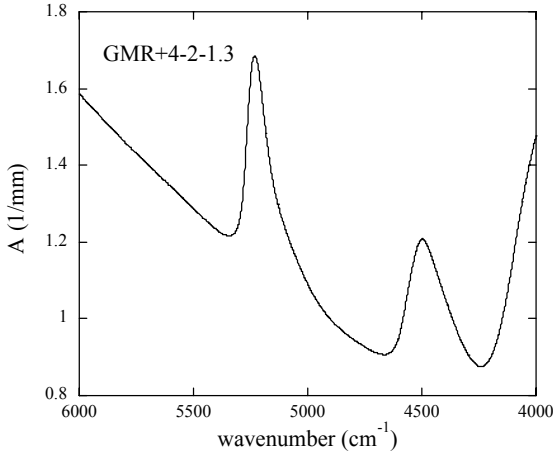
GMR+4-2-1.3
A (1/mm)
wavenumber (cm-1)

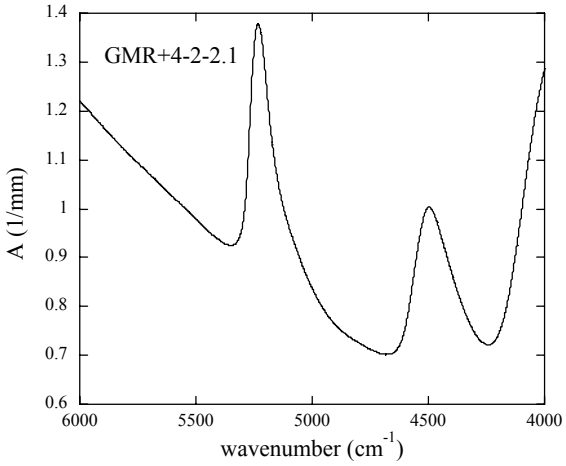
GMR+4-2-2.1
A (1/mm)
wavenumber (cm-1)

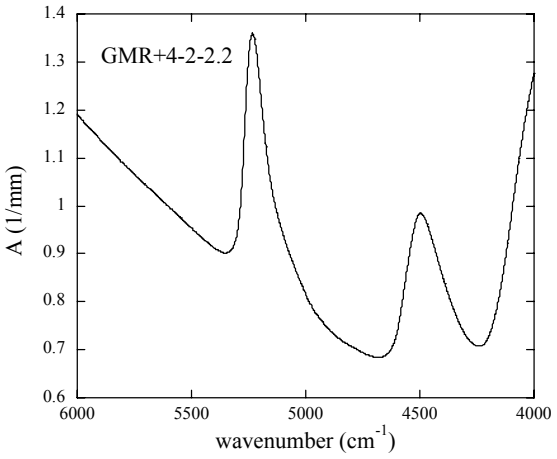
GMR+4-2-2.2
A (1/mm)
wavenumber (cm-1)

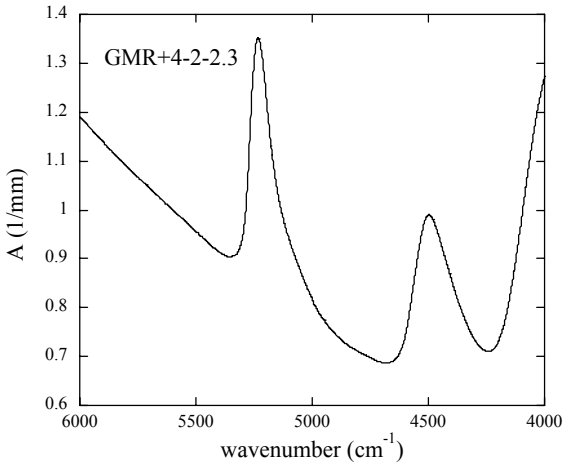
GMR+4-2-2.3
A (1/mm)
wavenumber (cm-1)

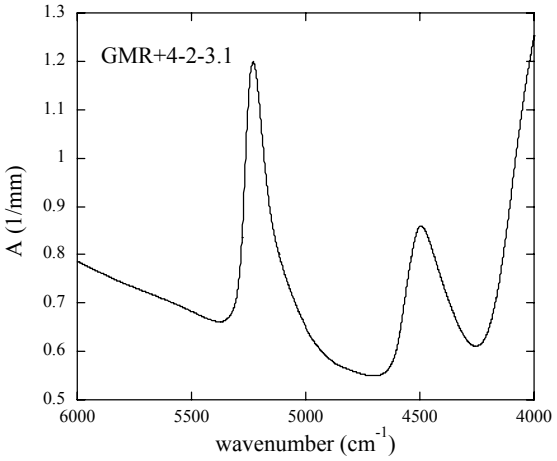
GMR+4-2-3.1
A (1/mm)
wavenumber (cm-1)

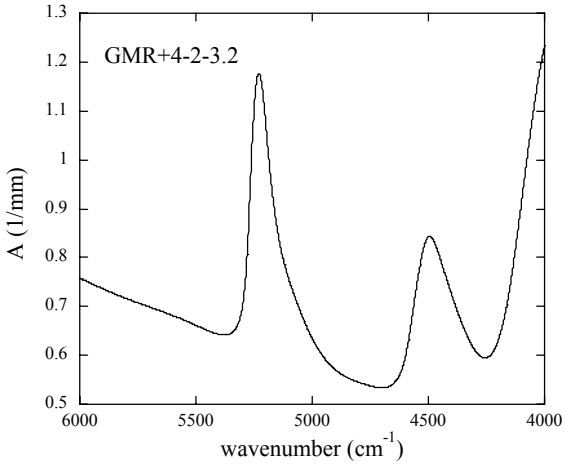
GMR+4-2-3.2
A (1/mm)
wavenumber (cm-1)

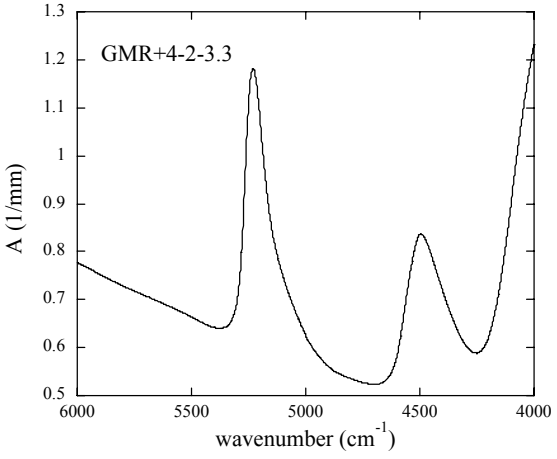
GMR+4-2-3.3
A (1/mm)
wavenumber (cm-1)

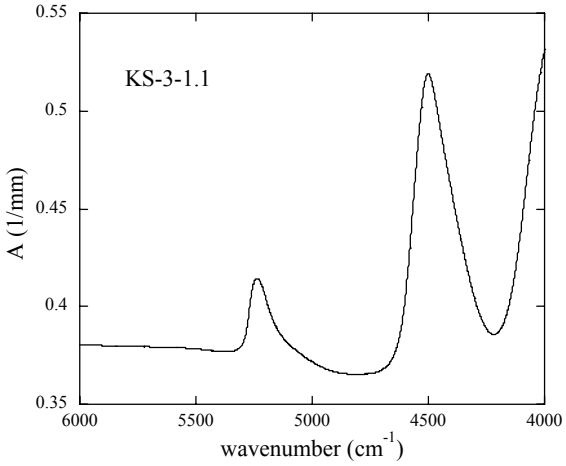
KS-3-1.1
A (1/mm)
wavenumber (cm-1)

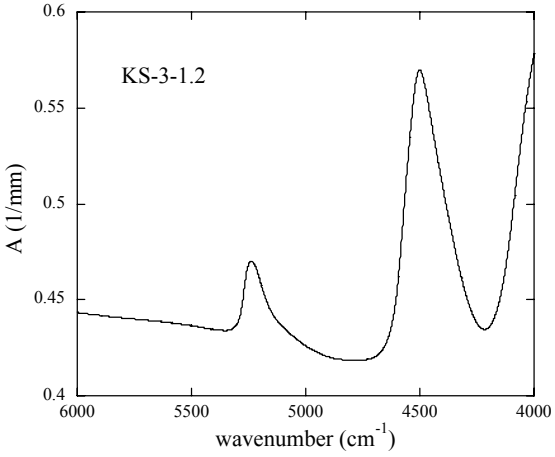
KS-3-1.2
A (1/mm)
wavenumber (cm-1)

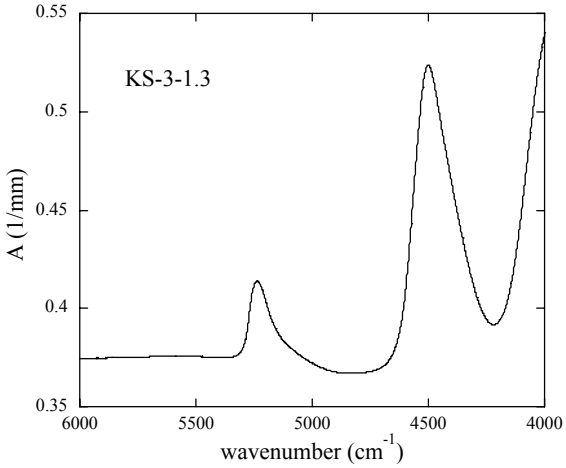
KS-3-1.3
A (1/mm)
wavenumber (cm-1)

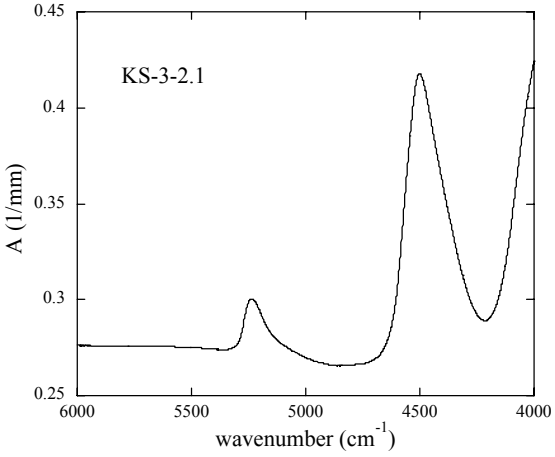
KS-3-2.1
A (1/mm)
wavenumber (cm-1)

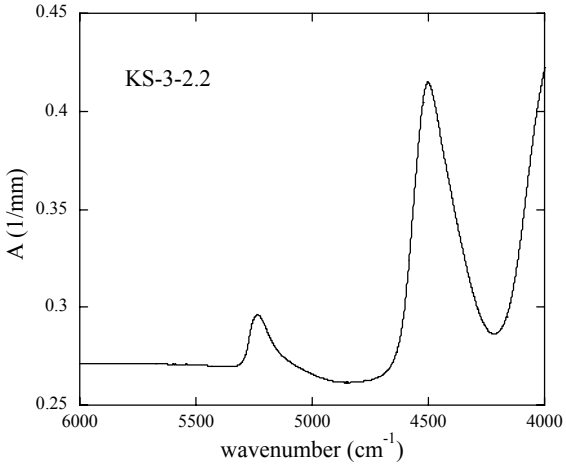
KS-3-2.2
A (1/mm)
wavenumber (cm-1)

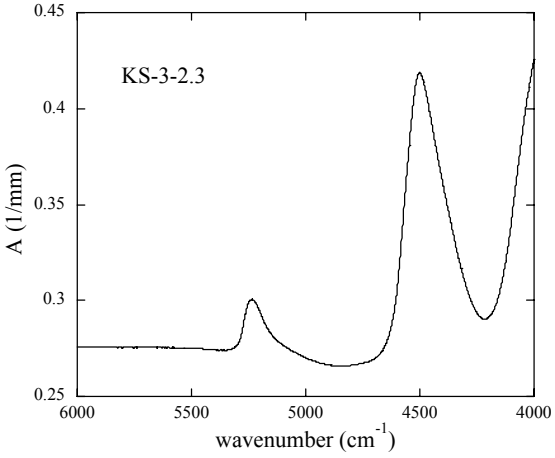
KS-3-2.3
A (1/mm)
wavenumber (cm-1)

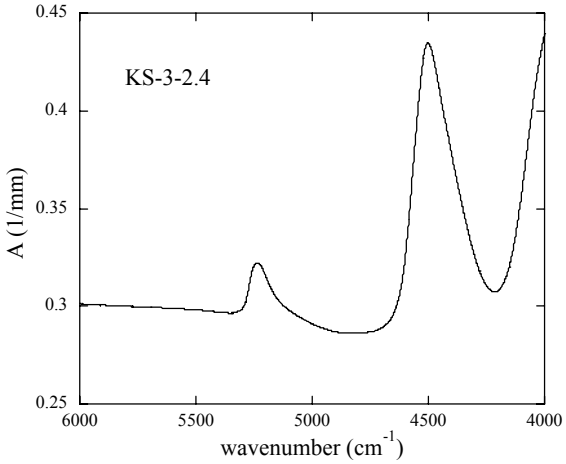
KS-3-2.4
A (1/mm)
wavenumber (cm-1)

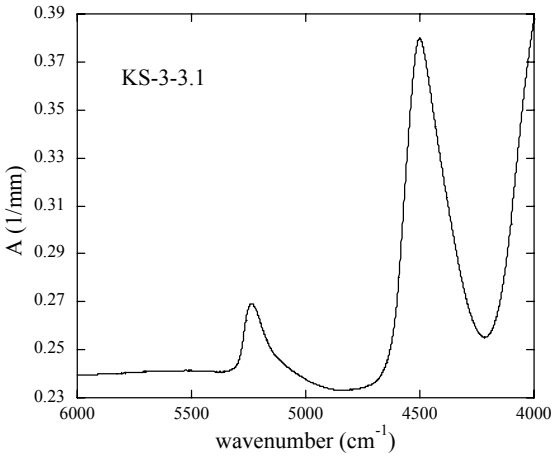
KS-3-3.1
A (1/mm)
wavenumber (cm-1)

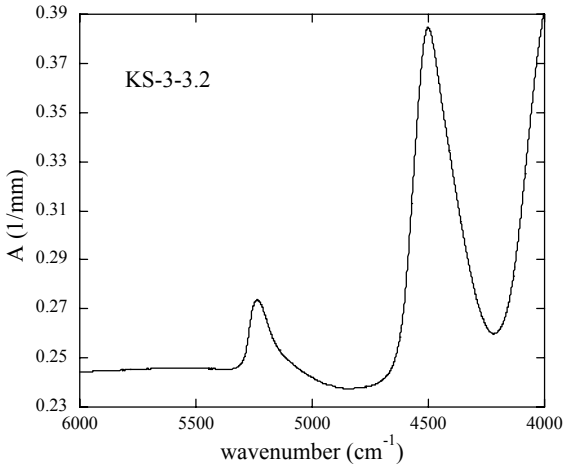
KS-3-3.2
A (1/mm)
wavenumber (cm-1)

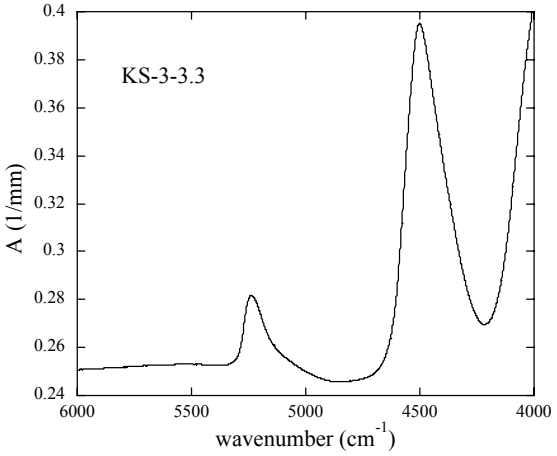
KS-3-3.3
A (1/mm)
wavenumber (cm-1)

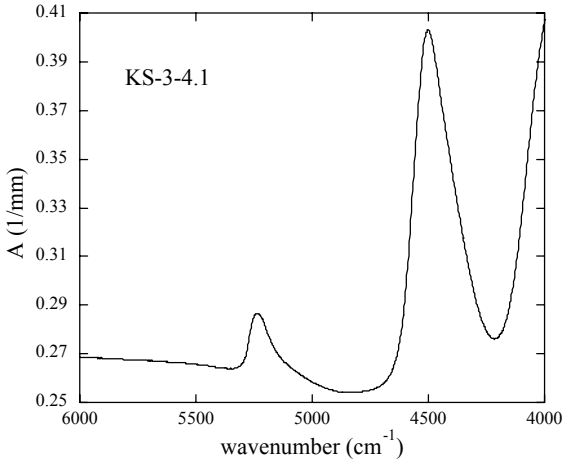
KS-3-4.1
A (1/mm)
wavenumber (cm-1)

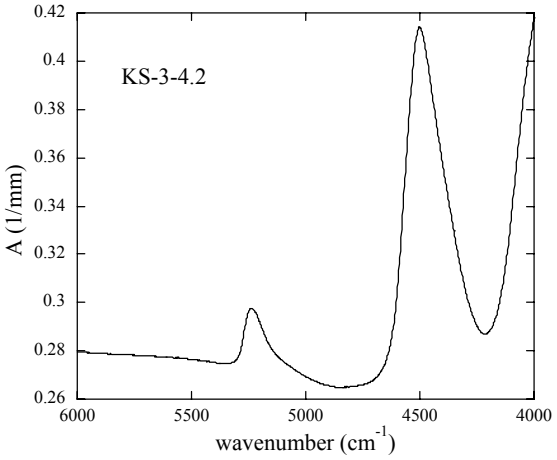
KS-3-4.2
A (1/mm)
wavenumber (cm-1)

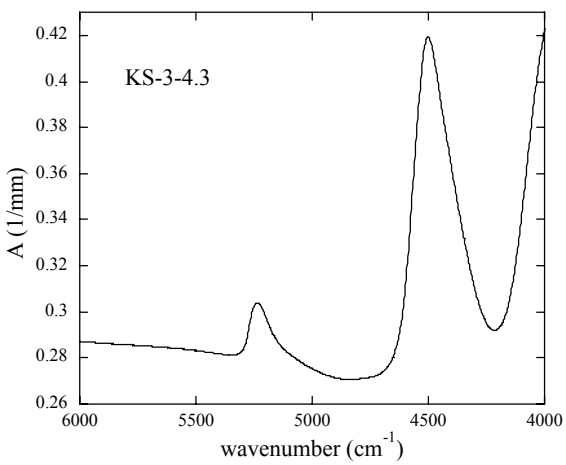
KS-3-4.3
A (1/mm)
wavenumber (cm-1)

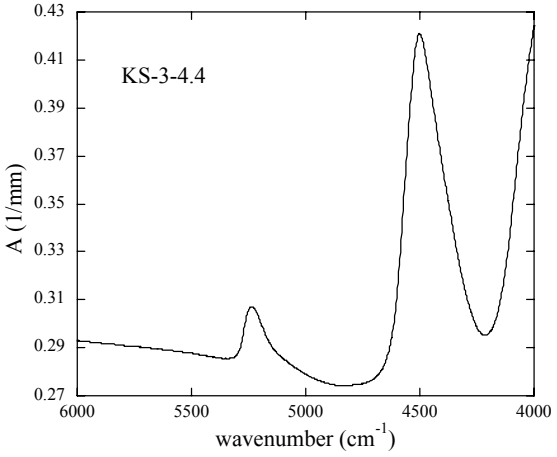
KS-3-4.4
A (1/mm)
wavenumber (cm-1)

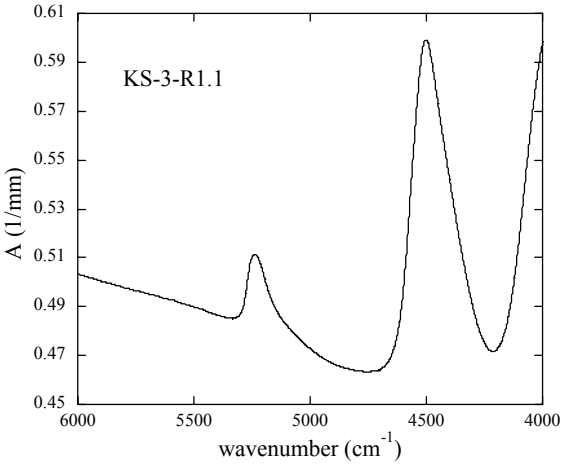
KS-3-R1.1
A (1/mm)
wavenumber (cm-1)

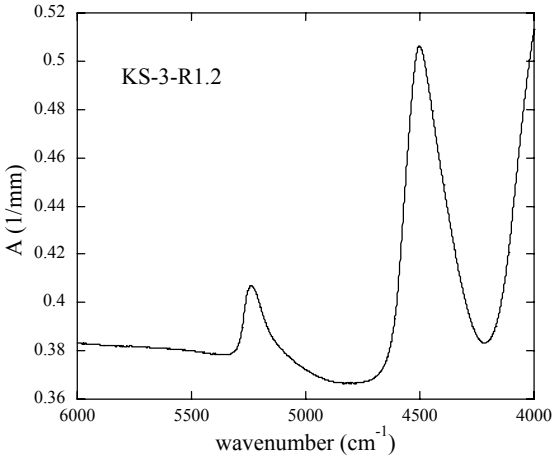
KS-3-R1.2
A (1/mm)
wavenumber (cm-1)

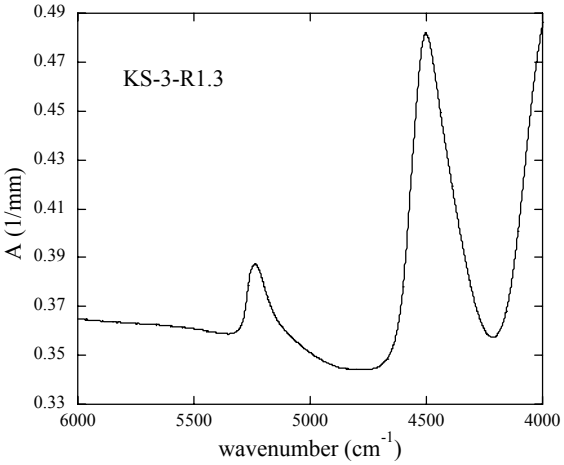
KS-3-R1.3
A (1/mm)
wavenumber (cm-1)

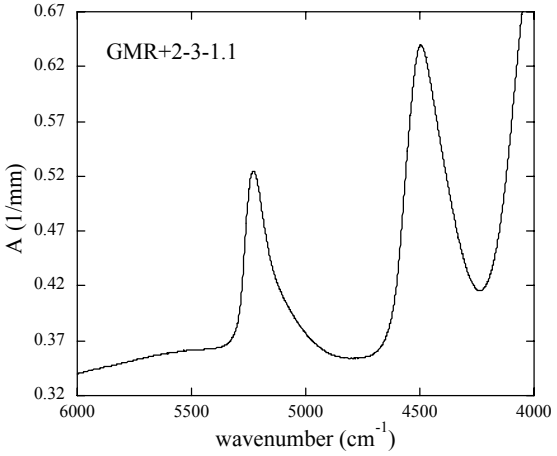
GMR+2-3-1.1
A (1/mm)
wavenumber (cm-1)

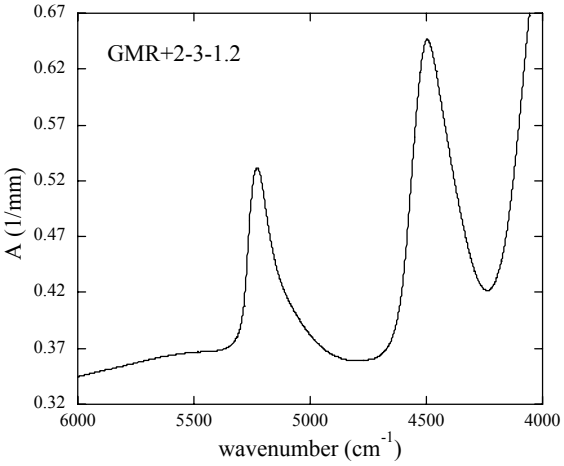
GMR+2-3-1.2
A (1/mm)
wavenumber (cm-1)

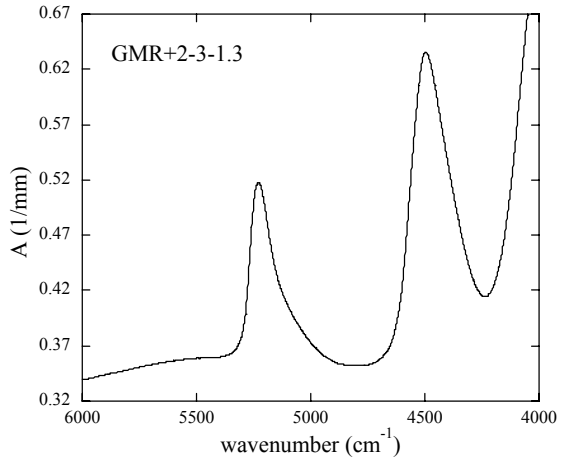
GMR+2-3-1.3
A (1/mm)
wavenumber (cm-1)

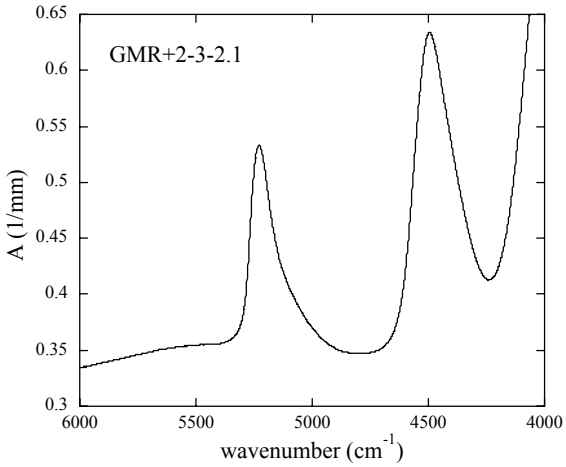
GMR+2-3-2.1
A (1/mm)
wavenumber (cm-1)

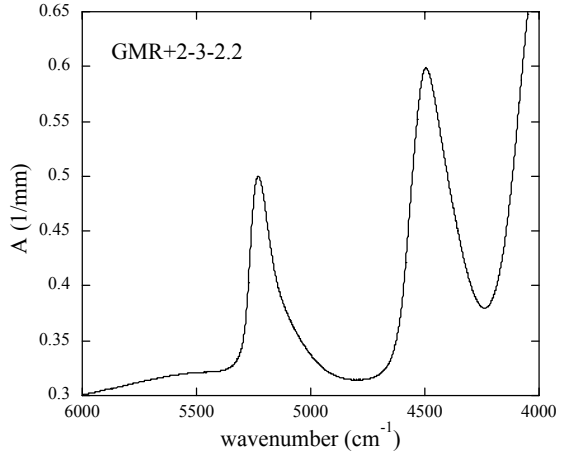
GMR+2-3-2.2
A (1/mm)
wavenumber (cm-1)

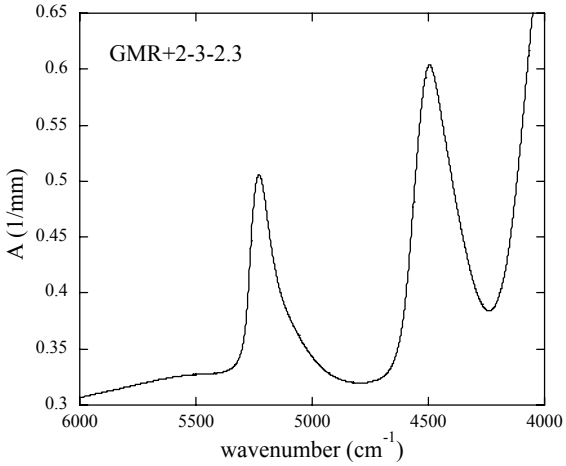
GMR+2-3-2.3
A (1/mm)
wavenumber (cm-1)

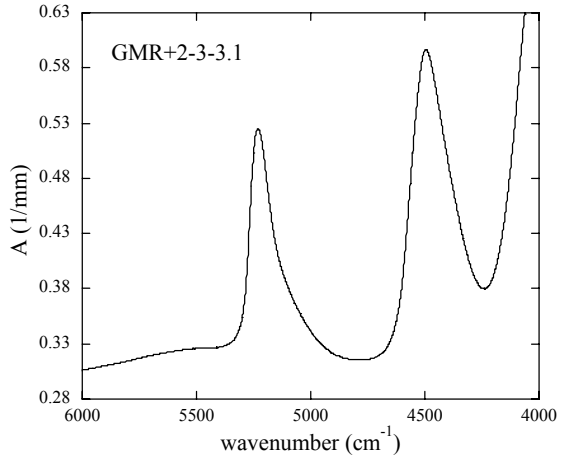
GMR+2-3-3.1
A (1/mm)
wavenumber (cm-1)

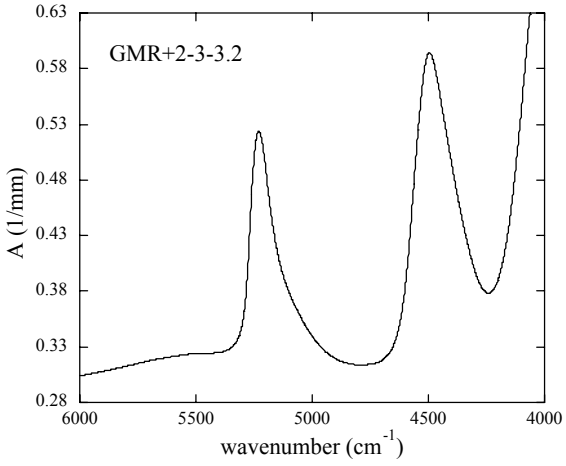
GMR+2-3-3.2
A (1/mm)
wavenumber (cm-1)

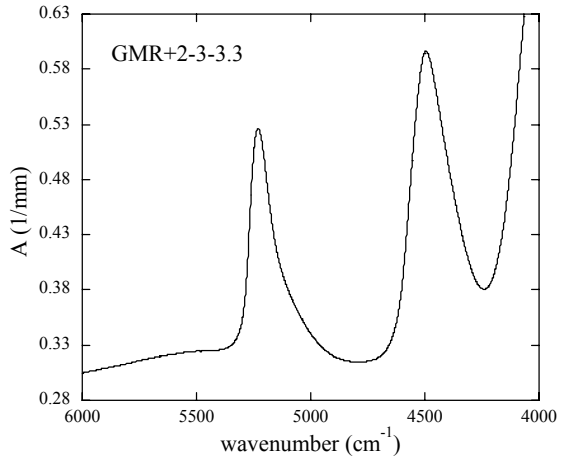
GMR+2-3-3.3
A (1/mm)
wavenumber (cm-1)

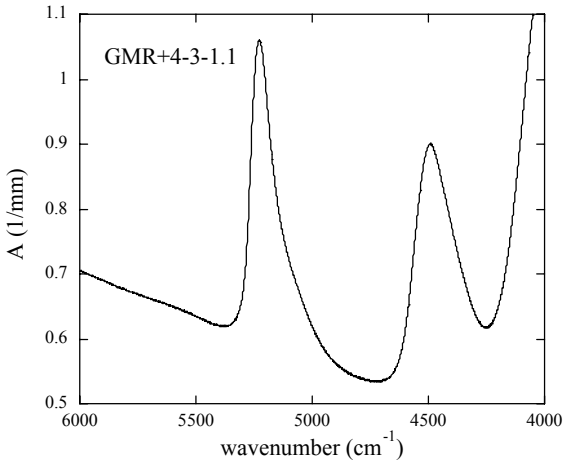
GMR+4-3-1.1
A (1/mm)
wavenumber (cm-1)

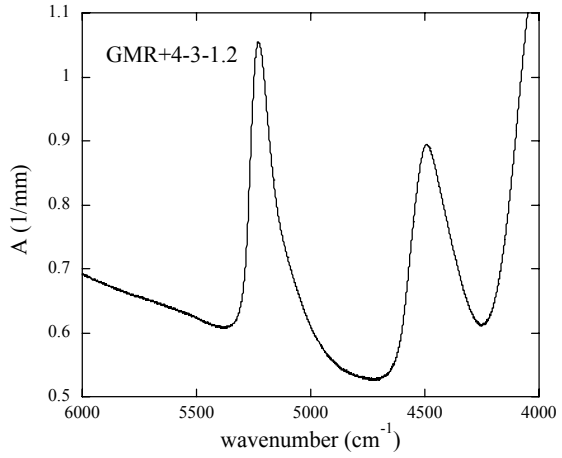
GMR+4-3-1.2
A (1/mm)
wavenumber (cm-1)

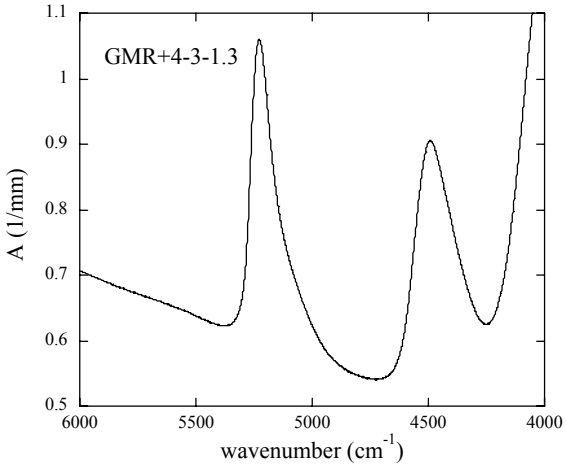
GMR+4-3-1.3
A (1/mm)
wavenumber (cm-1)

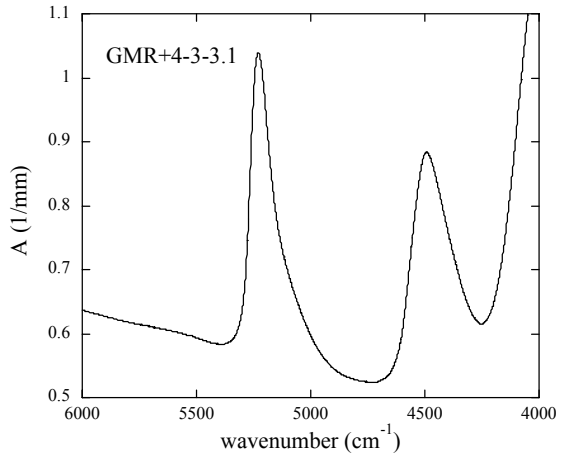
GMR+4-3-3.1
A (1/mm)
wavenumber (cm-1)

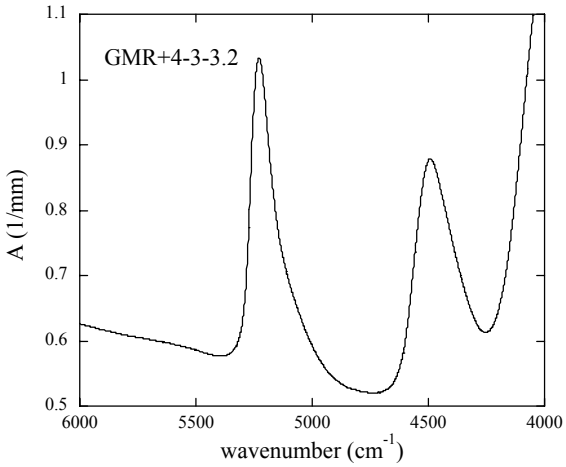
GMR+4-3-3.2
A (1/mm)
wavenumber (cm-1)

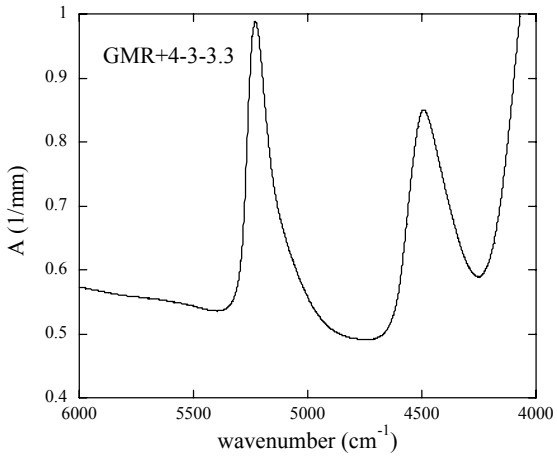
GMR+4-3-3.3
A (1/mm)
wavenumber (cm-1)

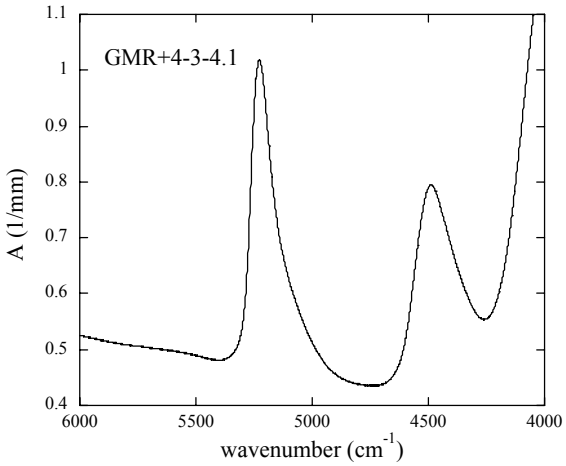
GMR+4-3-4.1
A (1/mm)
wavenumber (cm-1)

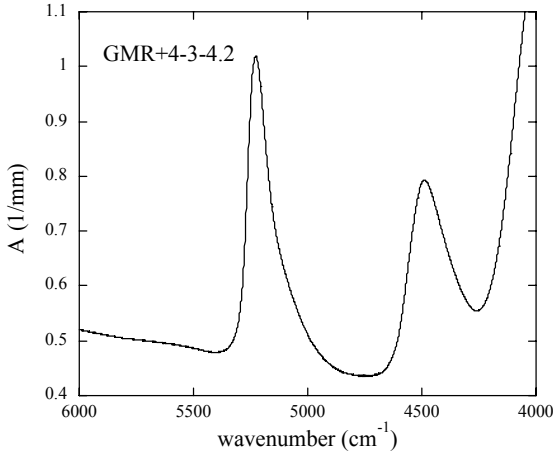
GMR+4-3-4.2
A (1/mm)
wavenumber (cm-1)

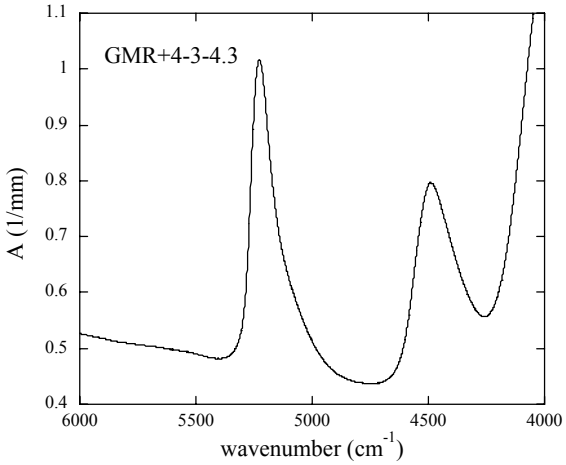
GMR+4-3-4.3
A (1/mm)
wavenumber (cm-1)

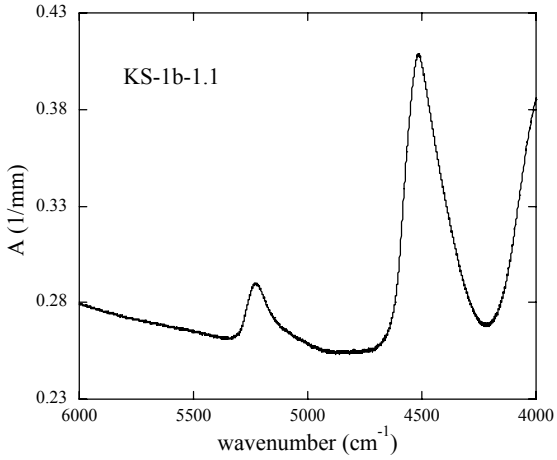
KS-1b-1.1
A (1/mm)
wavenumber (cm-1)

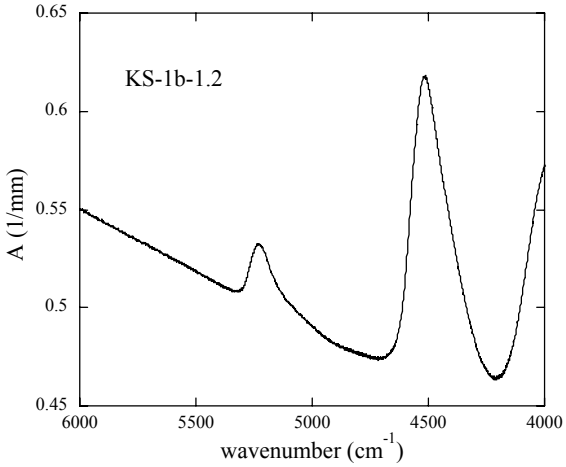
KS-1b-1.2
A (1/mm)
wavenumber (cm-1)

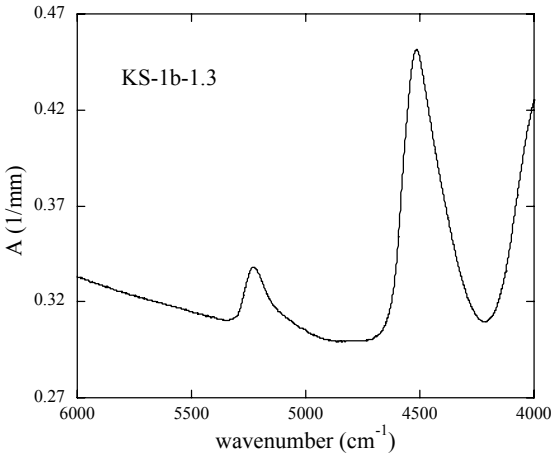
KS-1b-1.3
A (1/mm)
wavenumber (cm-1)

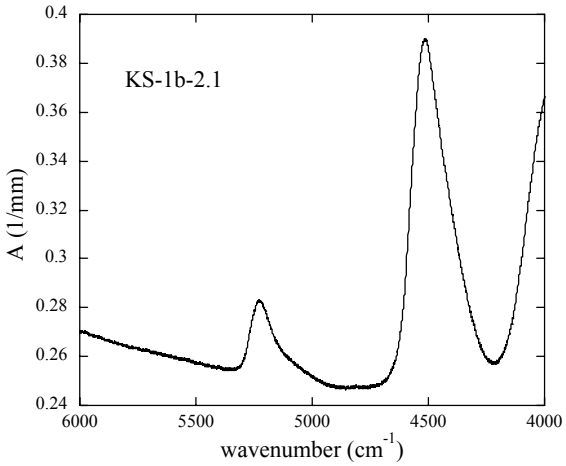
KS-1b-2.1
A (1/mm)
wavenumber (cm-1)

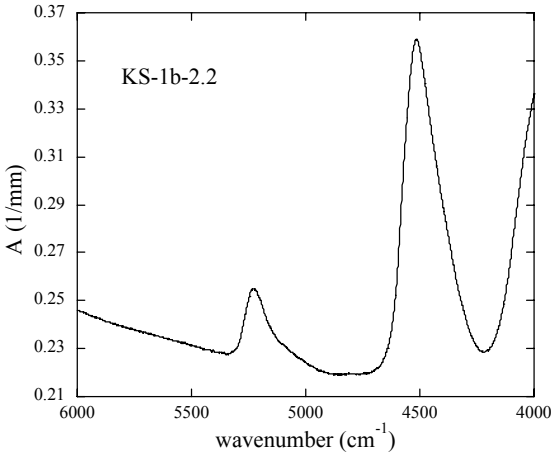
KS-1b-2.2
A (1/mm)
wavenumber (cm-1)

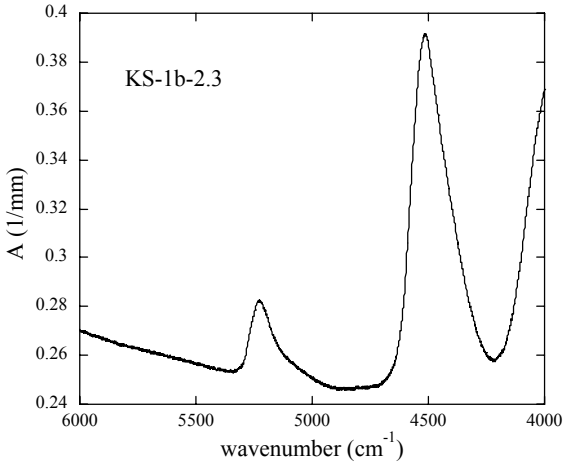
KS-1b-2.3
A (1/mm)
wavenumber (cm-1)

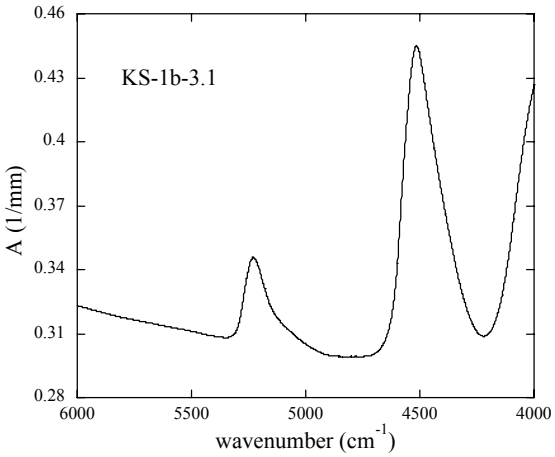
KS-1b-3.1
A (1/mm)
wavenumber (cm-1)

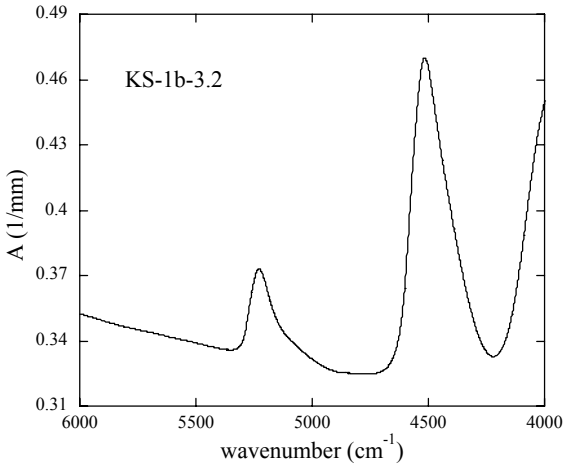
KS-1b-3.2
A (1/mm)
wavenumber (cm-1)

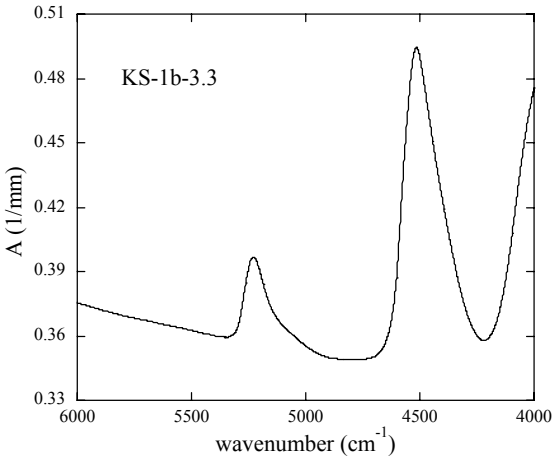
KS-1b-3.3
A (1/mm)
wavenumber (cm-1)

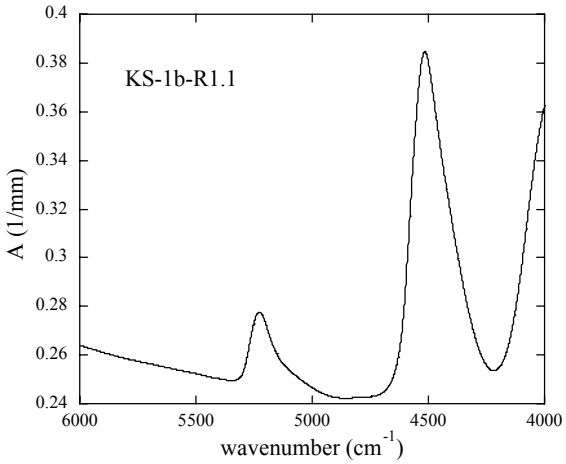
KS-1b-R1.1
A (1/mm)
wavenumber (cm-1)

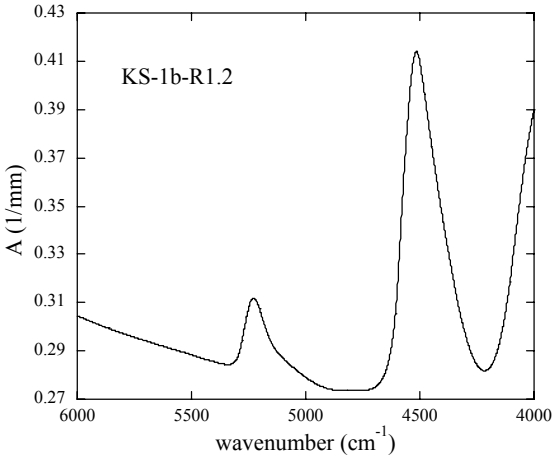
KS-1b-R1.2
A (1/mm)
wavenumber (cm-1)

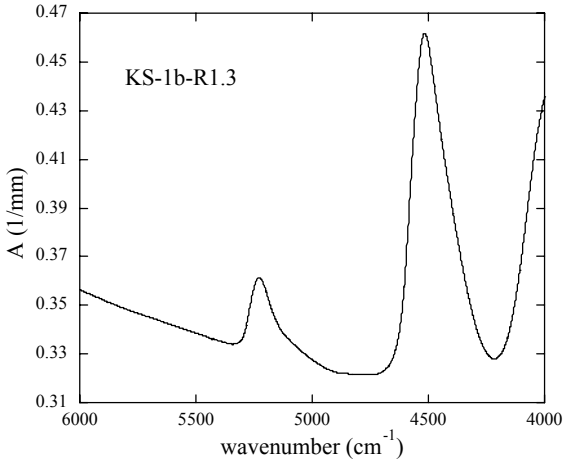
KS-1b-R1.3
A (1/mm)
wavenumber (cm-1)

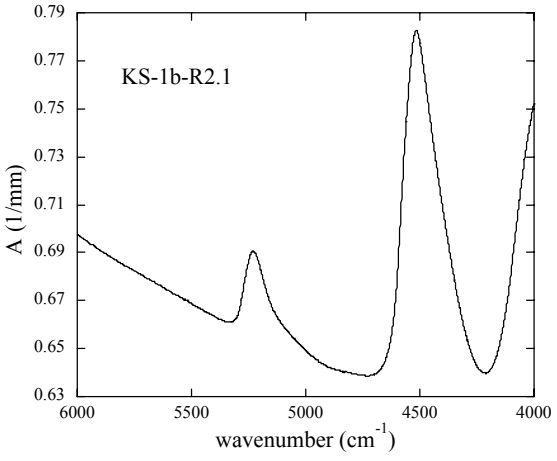
KS-1b-R2.1
A (1/mm)
wavenumber (cm-1)

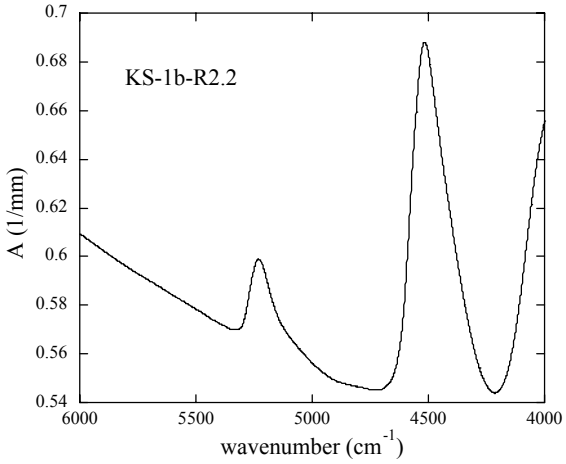
KS-1b-R2.2
A (1/mm)
wavenumber (cm-1)

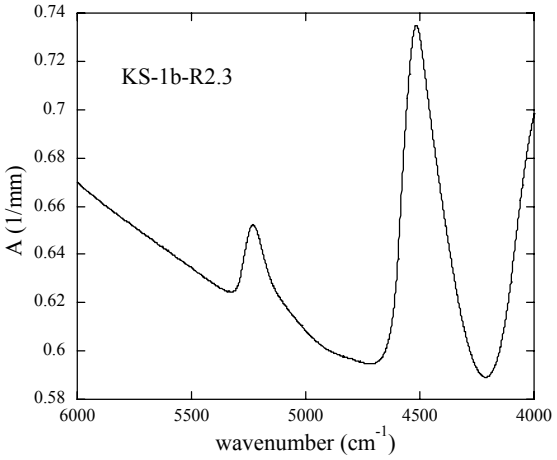
KS-1b-R2.3
A (1/mm)
wavenumber (cm-1)
0.74
0.72
0.7
0.68
0.66
0.64
0.62
0.6
0.58
6000
5500
5000
4500
4000

APPENDIX C

FTIR SPECTRA FOR COOLING EXPERIMENTS

The FTIR spectra on the following pages are for the measurements listed in Table 4.3 in Chapter IV. All spectra were normalized to the sample thickness (mm).

Fig. C.1 FTIR spectra for cooling experiments.

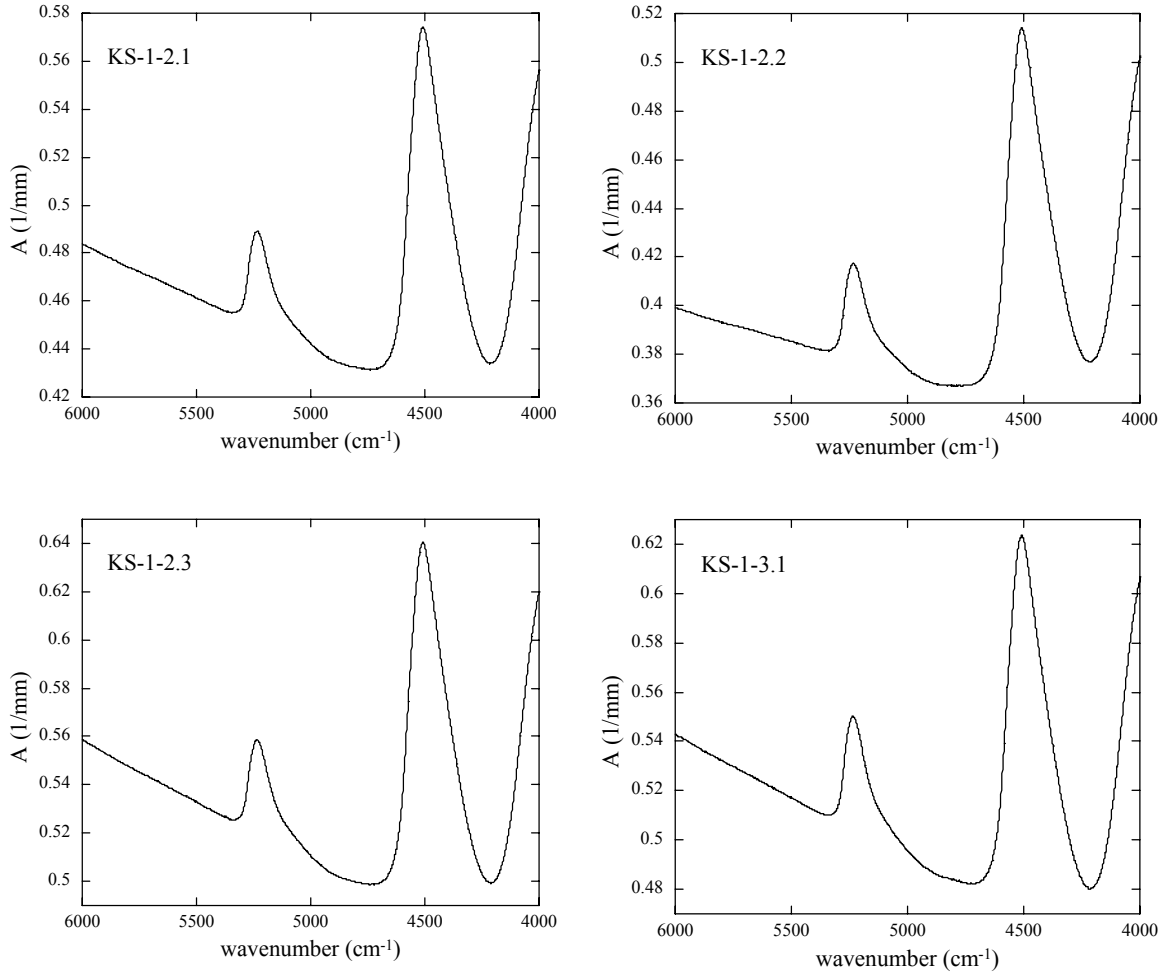

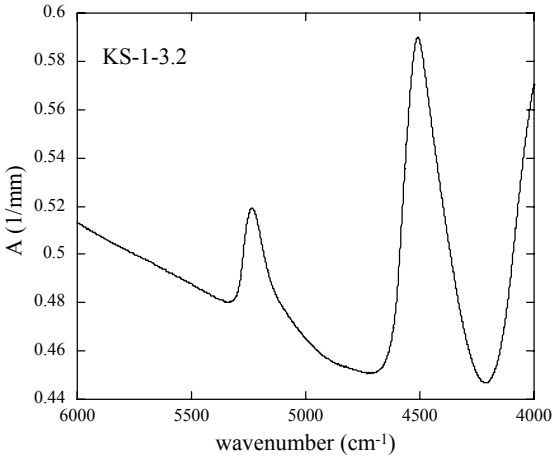
KS-1-3.2
A (1/mm)
wavenumber (cm-1)

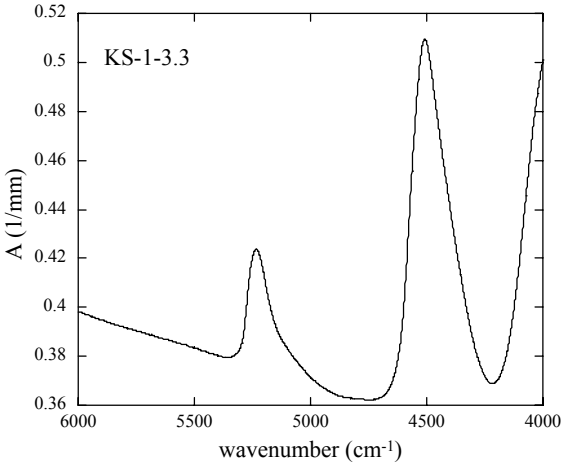
KS-1-3.3
A (1/mm)
wavenumber (cm-1)

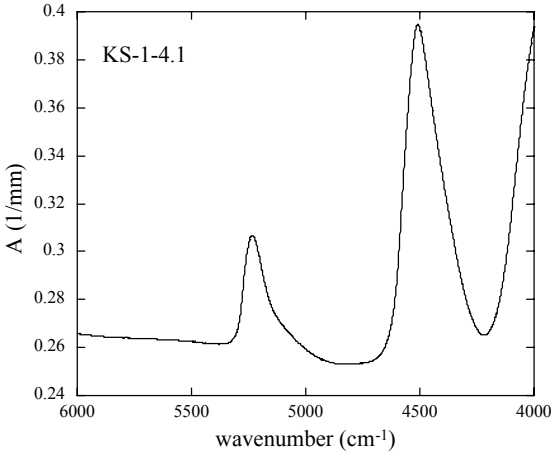
KS-1-4.1
A (1/mm)
wavenumber (cm-1)

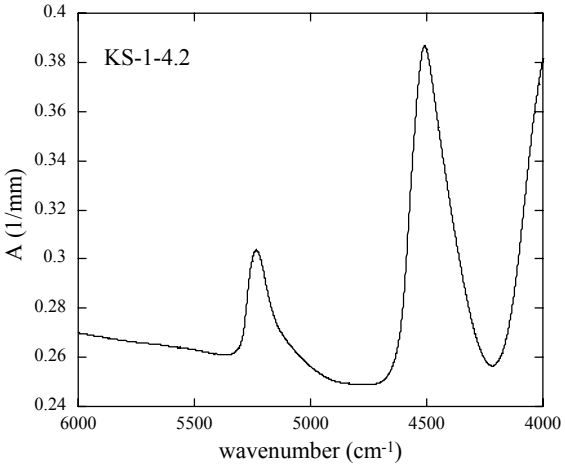
KS-1-4.2
A (1/mm)
wavenumber (cm-1)

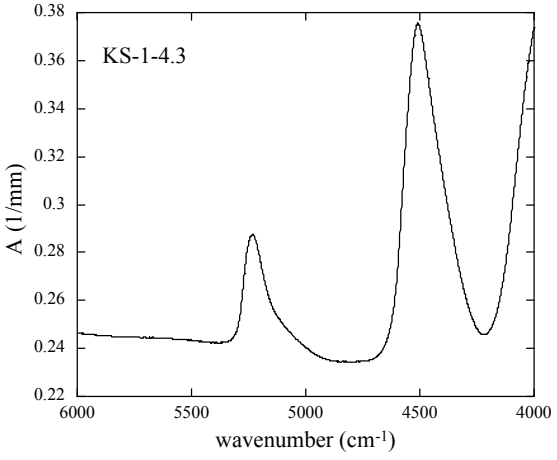
KS-1-4.3
A (1/mm)
wavenumber (cm-1)

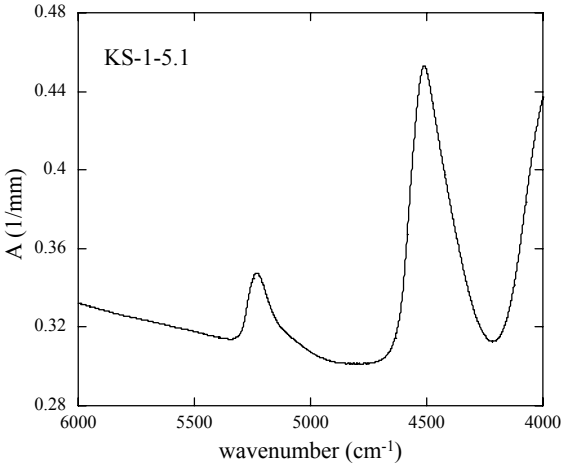
KS-1-5.1
A (1/mm)
wavenumber (cm-1)

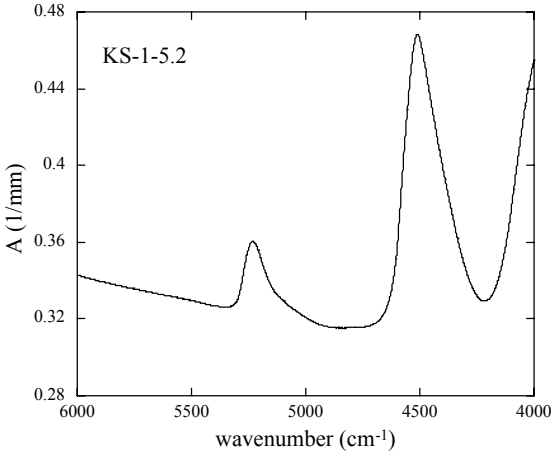
KS-1-5.2
A (1/mm)
wavenumber (cm-1)

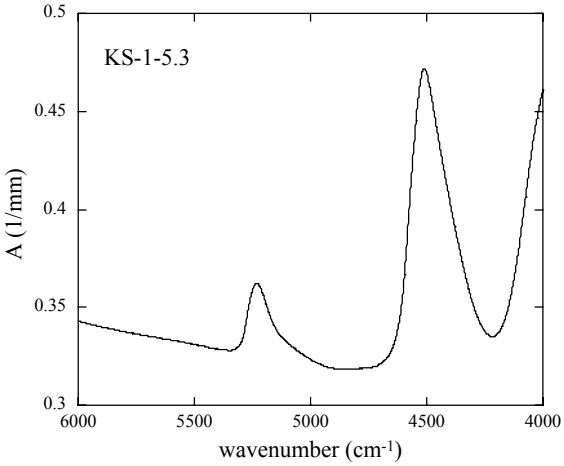
KS-1-5.3
A (1/mm)
wavenumber (cm-1)

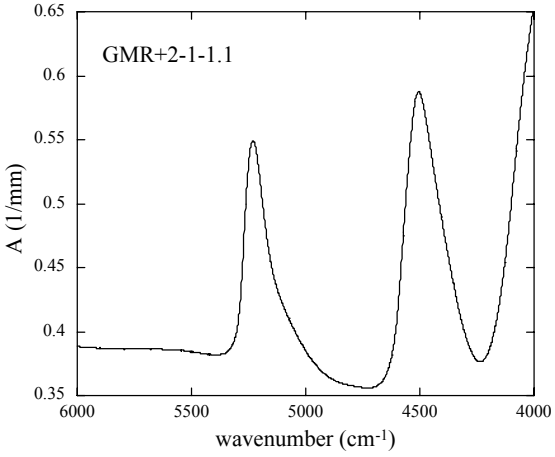
GMR+2-1-1.1
A (1/mm)
wavenumber (cm-1)

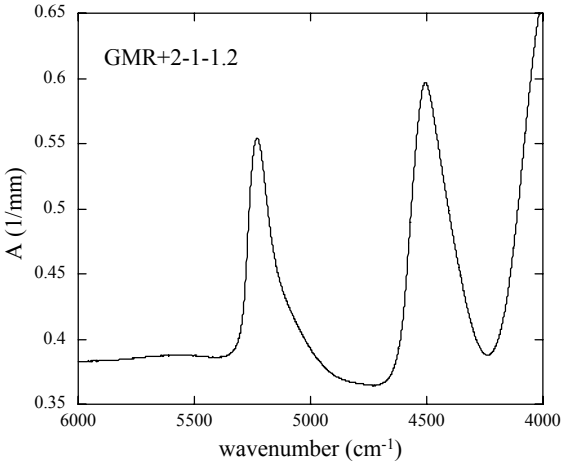
GMR+2-1-1.2
A (1/mm)
wavenumber (cm-1)

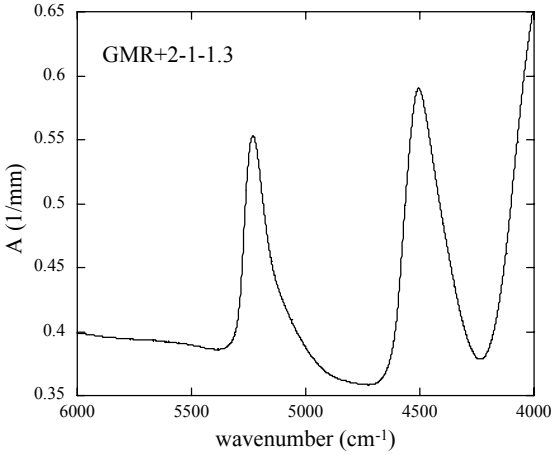
GMR+2-1-1.3
A (1/mm)
wavenumber (cm-1)

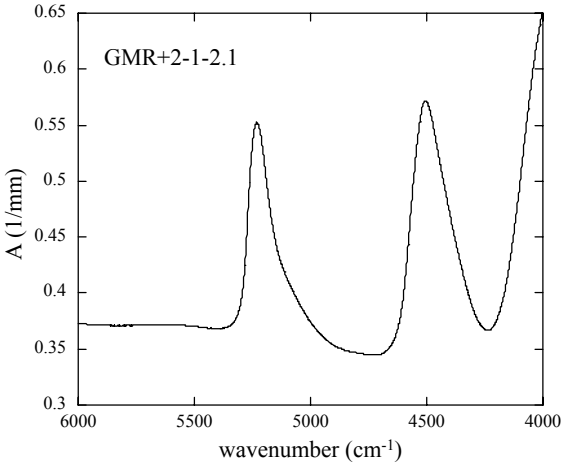
GMR+2-1-2.1
A (1/mm)
wavenumber (cm-1)

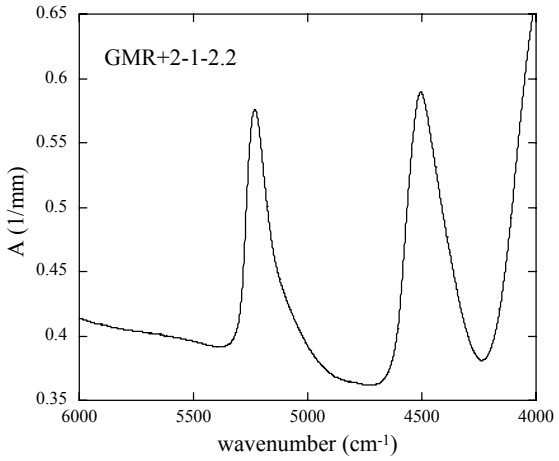
GMR+2-1-2.2
A (1/mm)
wavenumber (cm-1)

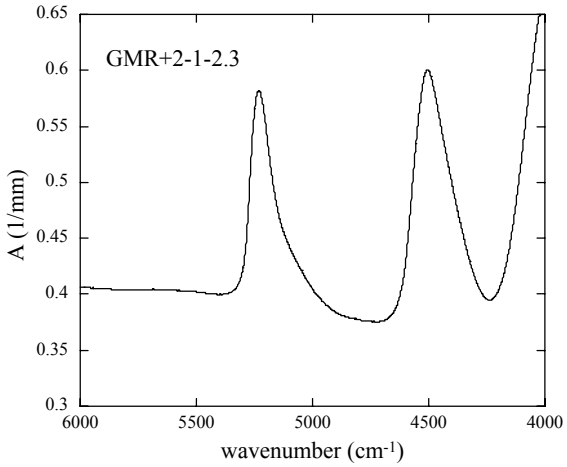
GMR+2-1-2.3
A (1/mm)
wavenumber (cm-1)

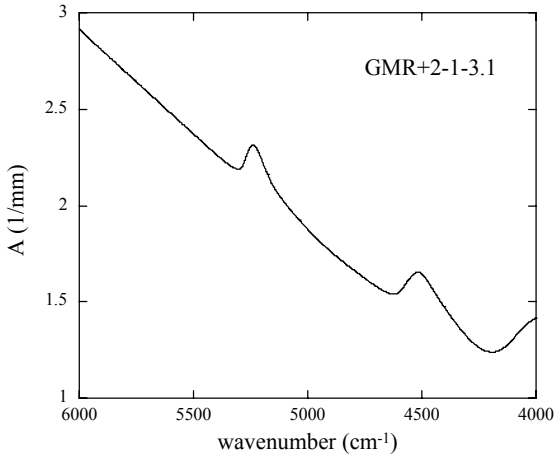
GMR+2-1-3.1
A (1/mm)
wavenumber (cm-1)

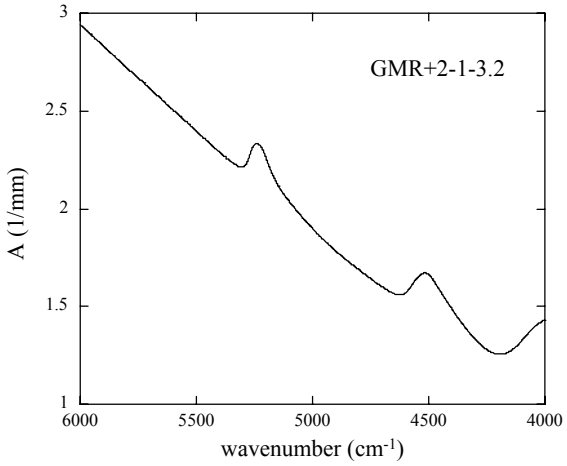
GMR+2-1-3.2
A (1/mm)
wavenumber (cm-1)

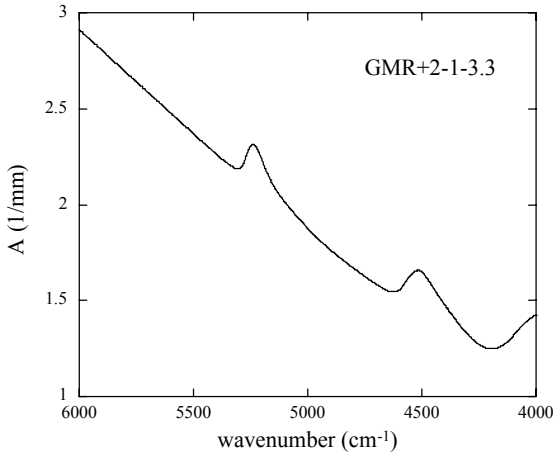
GMR+2-1-3.3
A (1/mm)
wavenumber (cm-1)

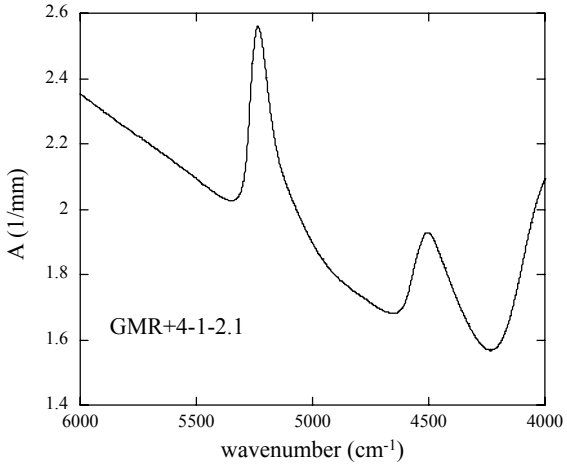
GMR+4-1-2.1
A (1/mm)
wavenumber (cm-1)

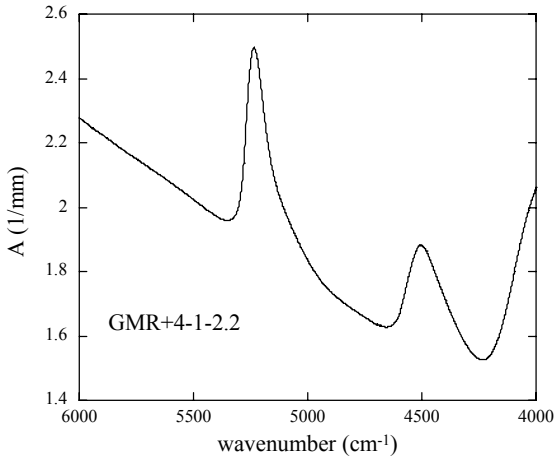
A (1/mm)
wavenumber (cm-1)
GMR+4-1-2.2

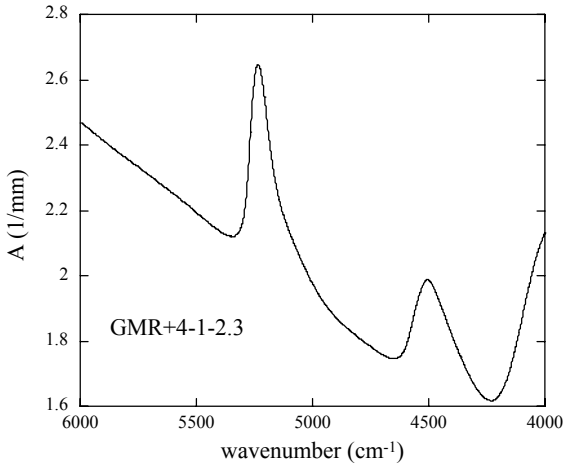
A (1/mm)
wavenumber (cm-1)
GMR+4-1-2.3

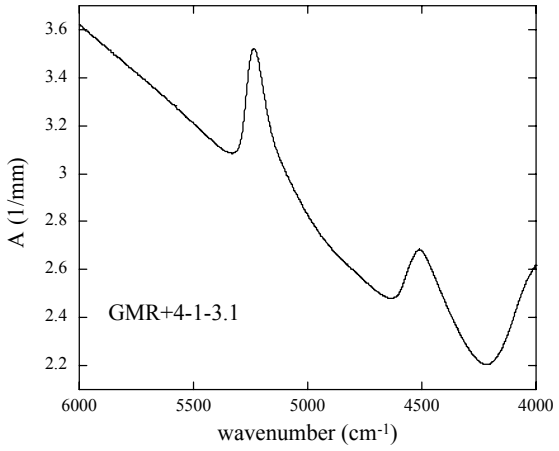
A (1/mm)
wavenumber (cm-1)
GMR+4-1-3.1

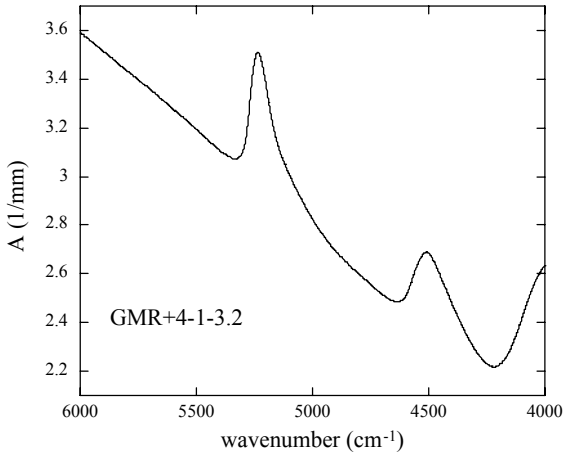
A (1/mm)
wavenumber (cm-1)
GMR+4-1-3.2

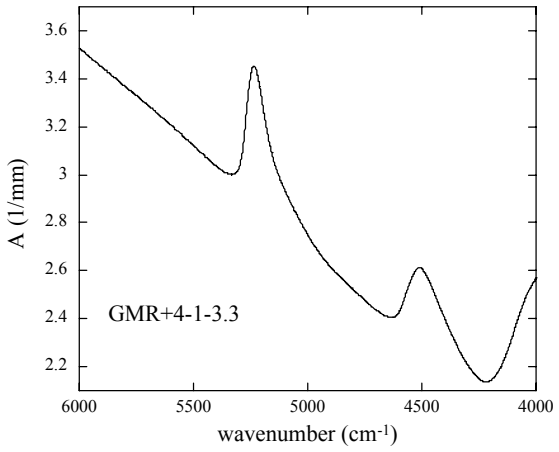
A (1/mm)
wavenumber (cm-1)
GMR+4-1-3.3

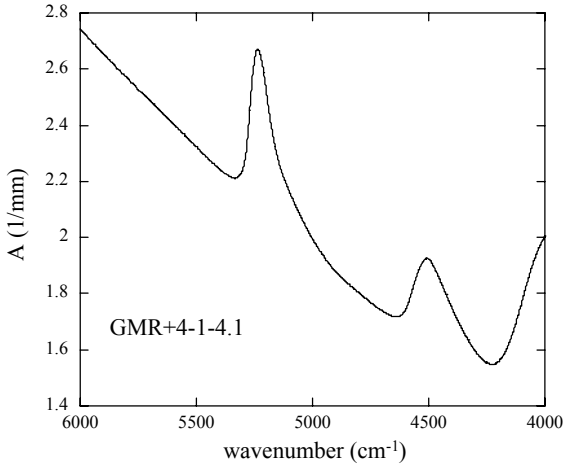
A (1/mm)
wavenumber (cm-1)
GMR+4-1-4.1

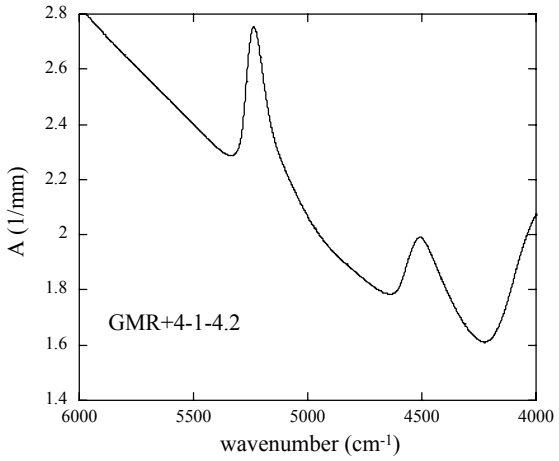
GMR+4-1-4.2
A (1/mm)
wavenumber (cm-1)

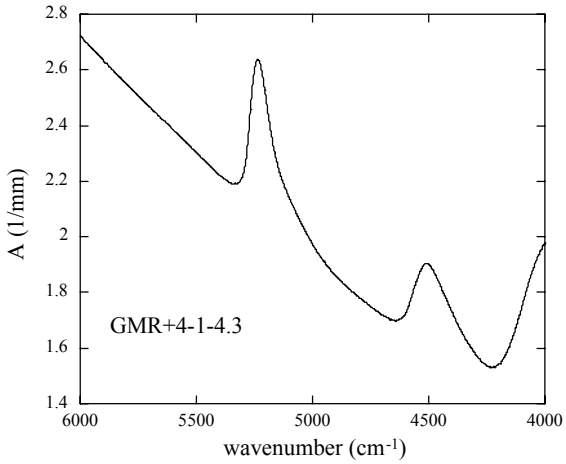
GMR+4-1-4.3
A (1/mm)
wavenumber (cm-1)

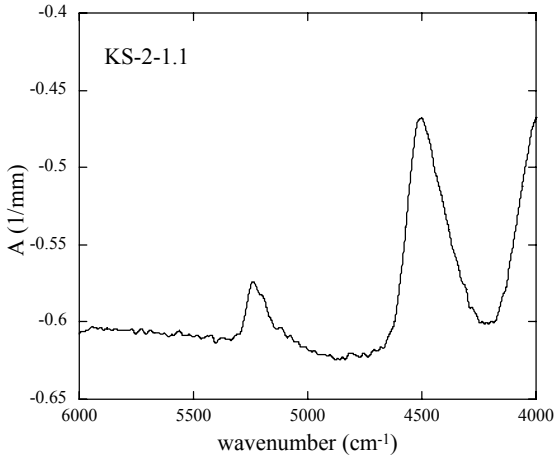
KS-2-1.1
A (1/mm)
wavenumber (cm-1)

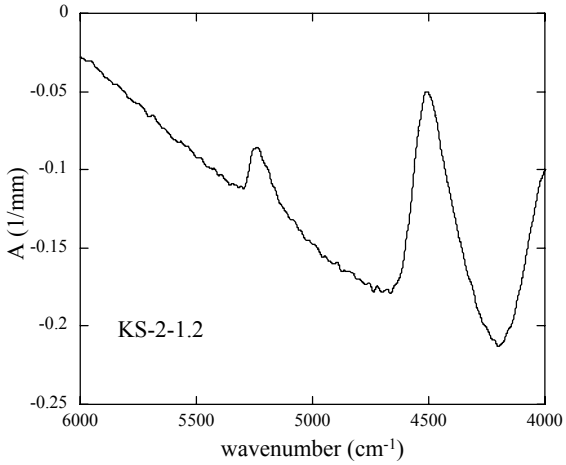
KS-2-1.2
A (1/mm)
wavenumber (cm-1)

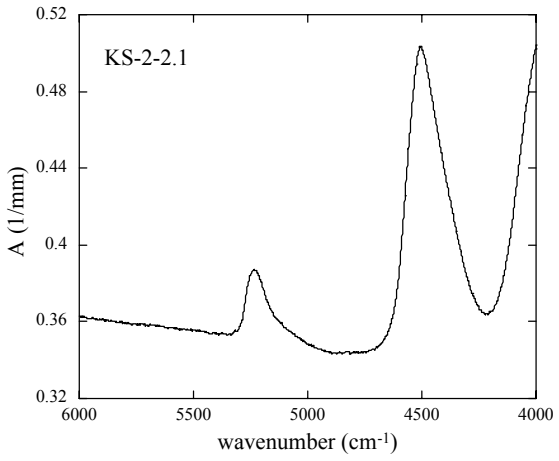
KS-2-2.1
A (1/mm)
wavenumber (cm-1)

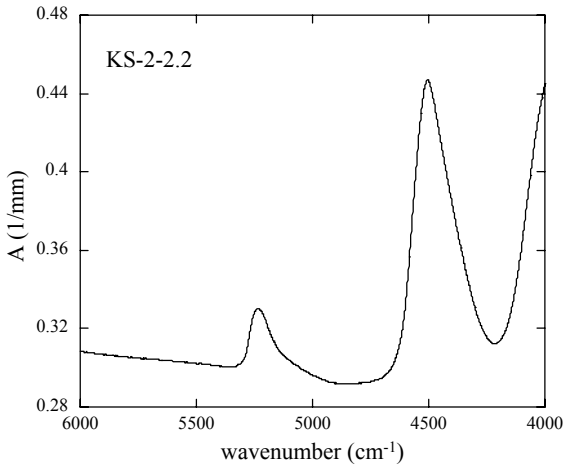
KS-2-2.2
A (1/mm)
wavenumber (cm-1)

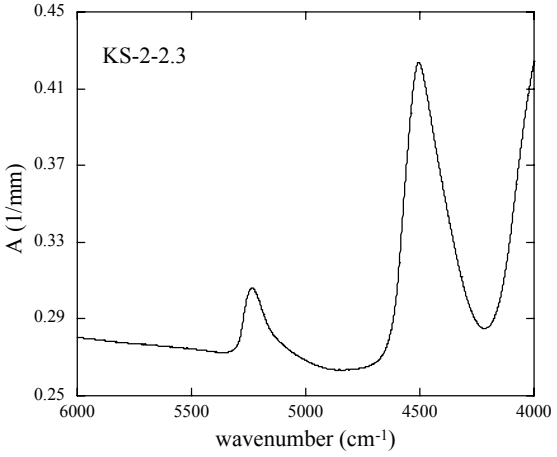
KS-2-2.3
A (1/mm)
0.45
0.41
0.37
0.33
0.29
0.25
6000
5500
5000
4500
4000
wavenumber (cm-1)

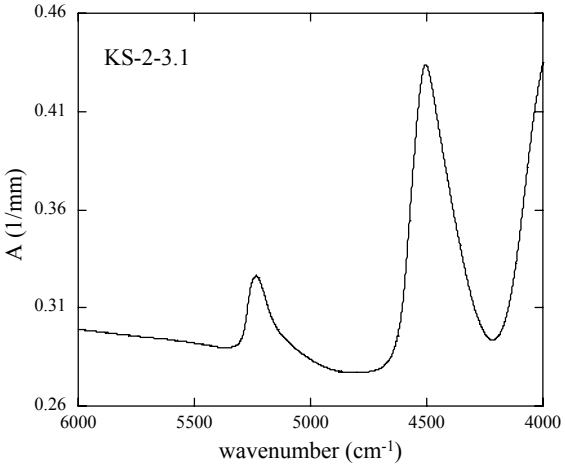
KS-2-3.1
A (1/mm)
0.46
0.41
0.36
0.31
0.26
6000
5500
5000
4500
4000
wavenumber (cm-1)

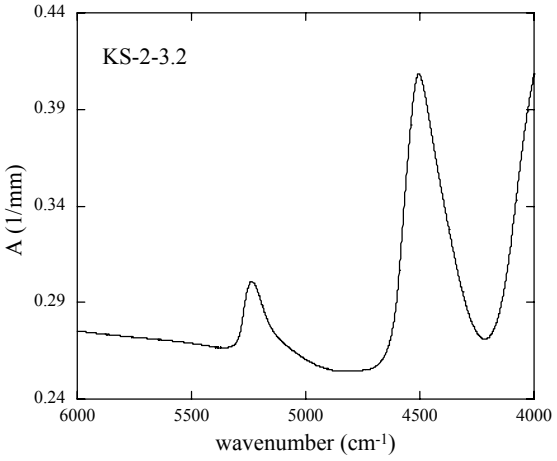
KS-2-3.2
A (1/mm)
0.44
0.39
0.34
0.29
0.24
6000
5500
5000
4500
4000
wavenumber (cm-1)

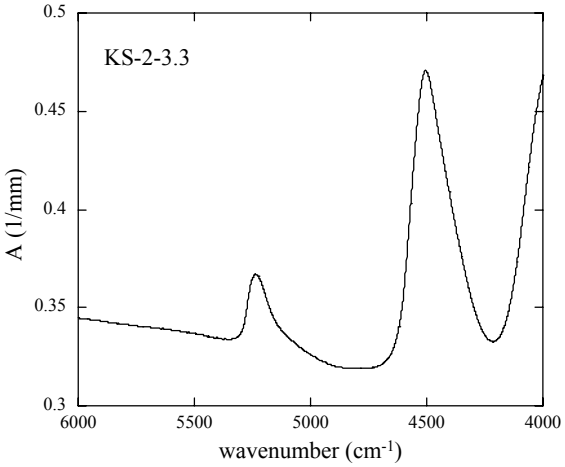
KS-2-3.3
A (1/mm)
0.5
0.45
0.4
0.35
0.3
6000
5500
5000
4500
4000
wavenumber (cm-1)

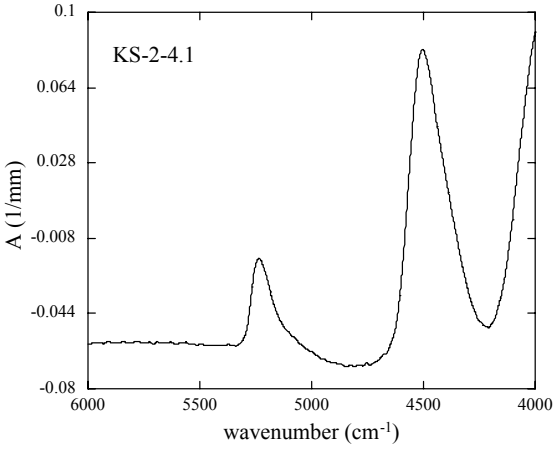
KS-2-4.1
A (1/mm)
0.1
0.064
0.028
-0.008
-0.044
-0.08
6000
5500
5000
4500
4000
wavenumber (cm-1)

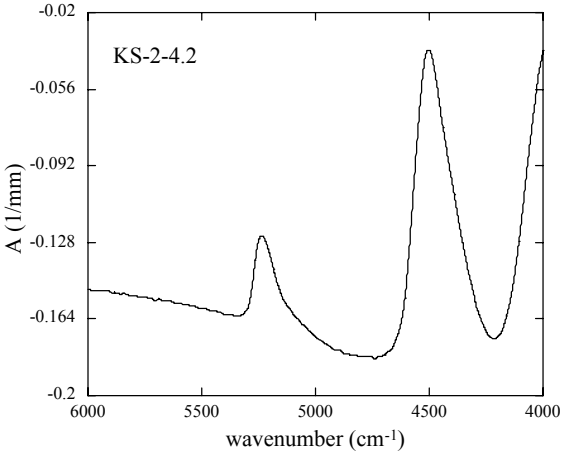
KS-2-4.2
A (1/mm)
-0.02
-0.056
-0.092
-0.128
-0.164
-0.2
6000
5500
5000
4500
4000
wavenumber (cm-1)

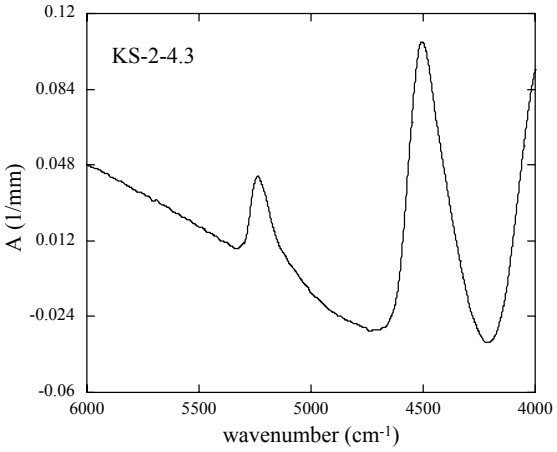
KS-2-4.3
A (1/mm)
wavenumber (cm-1)

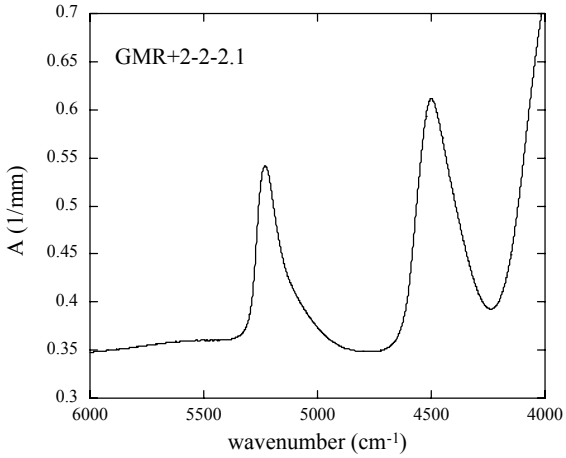
GMR+2-2-2.1
A (1/mm)
wavenumber (cm-1)

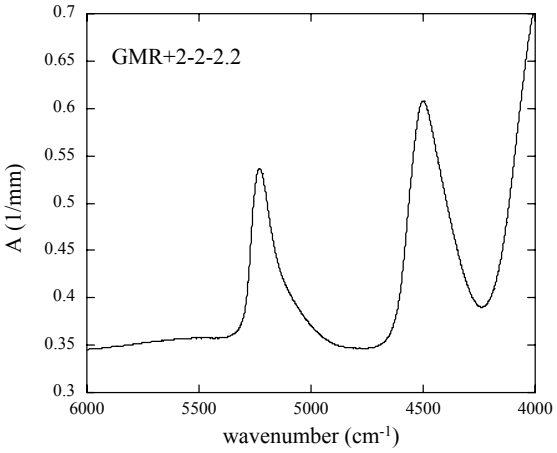
GMR+2-2-2.2
A (1/mm)
wavenumber (cm-1)

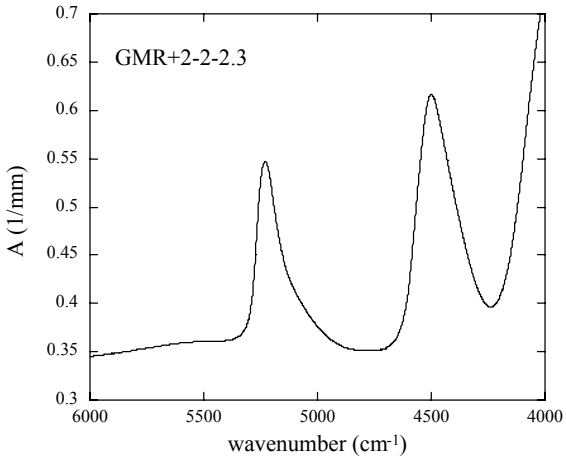
GMR+2-2-2.3
A (1/mm)
wavenumber (cm-1)

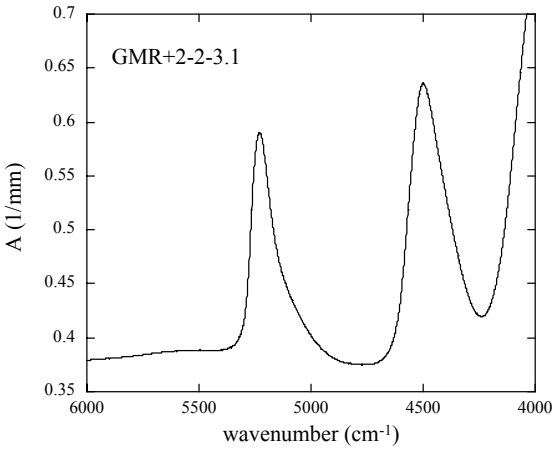
GMR+2-2-3.1
A (1/mm)
wavenumber (cm-1)

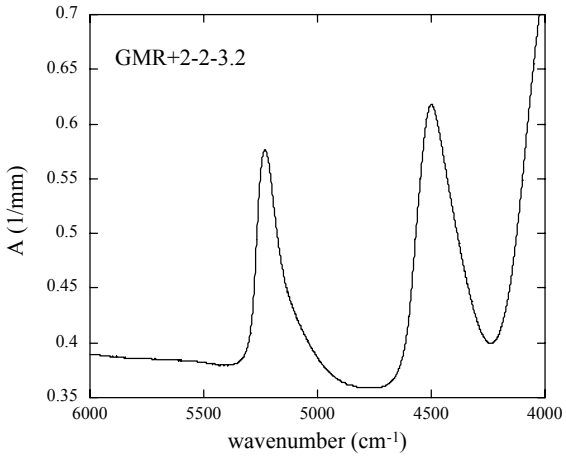
GMR+2-2-3.2
A (1/mm)
wavenumber (cm-1)

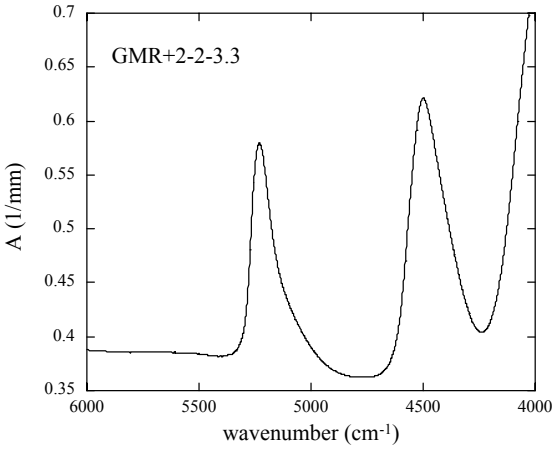
GMR+2-2-3.3
A (1/mm)
wavenumber (cm-1)

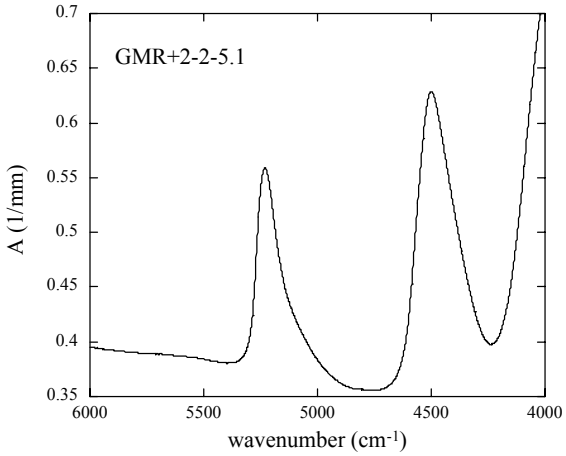
GMR+2-2-5.1
A (1/mm)
wavenumber (cm-1)

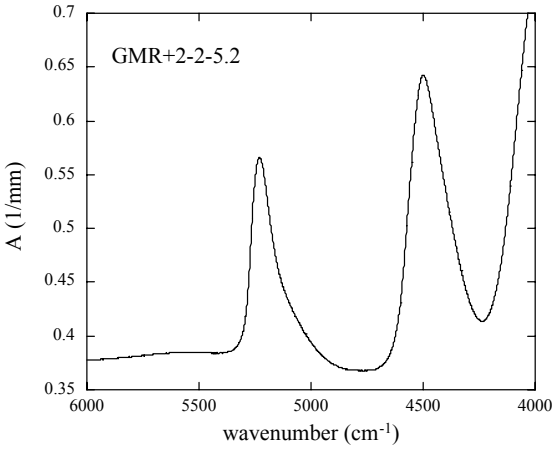
GMR+2-2-5.2
A (1/mm)
wavenumber (cm-1)

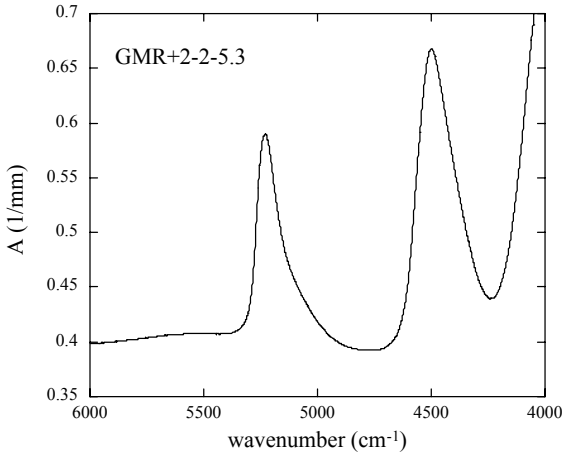
GMR+2-2-5.3
A (1/mm)
wavenumber (cm-1)

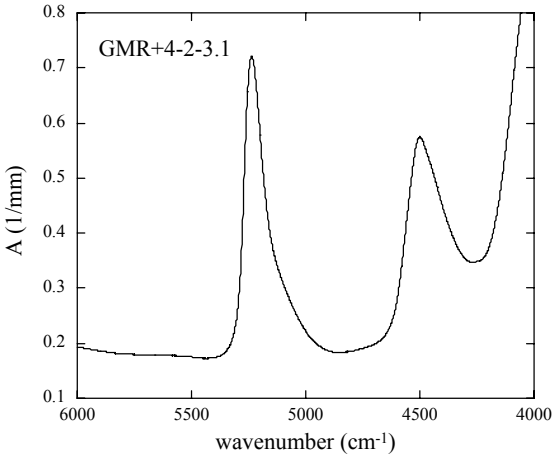
GMR+4-2-3.1
A (1/mm)
wavenumber (cm-1)

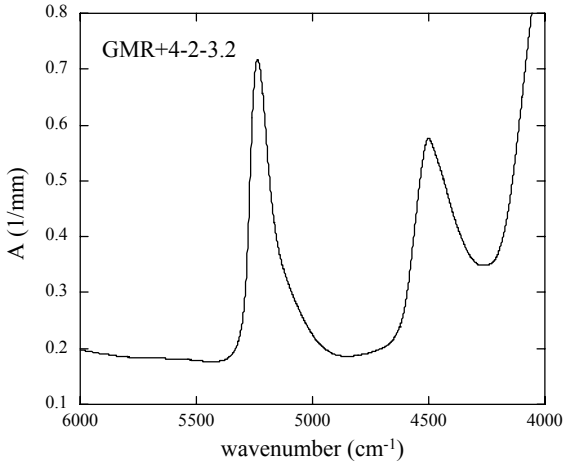
GMR+4-2-3.2
A (1/mm)
wavenumber (cm-1)

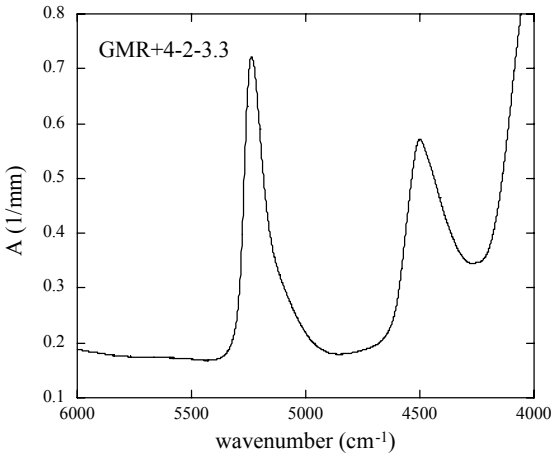
GMR+4-2-3.3
A (1/mm)
wavenumber (cm-1)

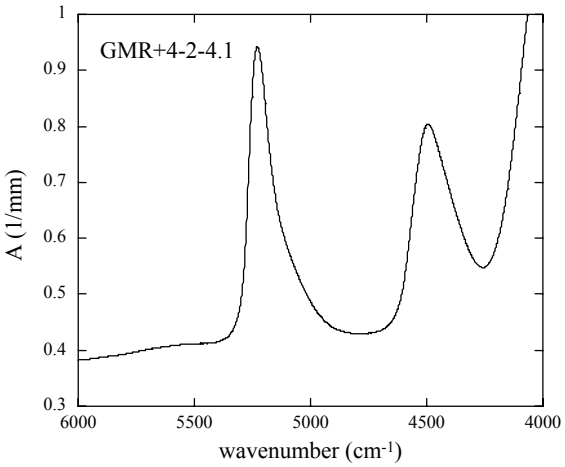
GMR+4-2-4.1
A (1/mm)
wavenumber (cm-1)

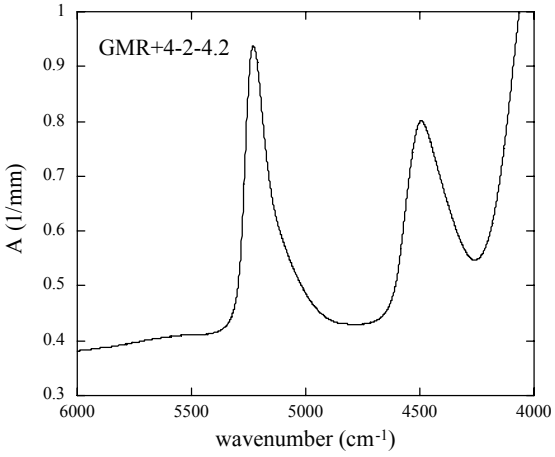
GMR+4-2-4.2
A (1/mm)
wavenumber (cm-1)

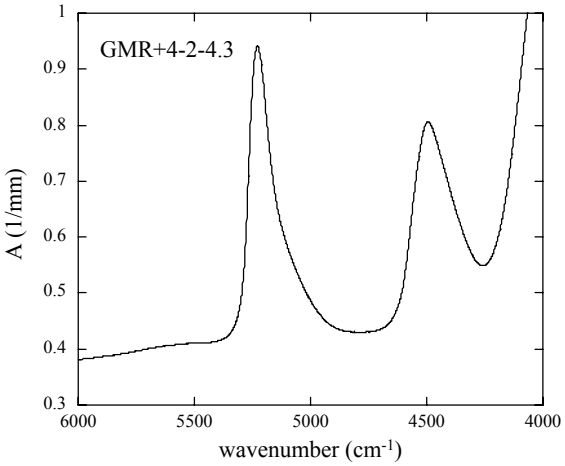
GMR+4-2-4.3
A (1/mm)
wavenumber (cm-1)

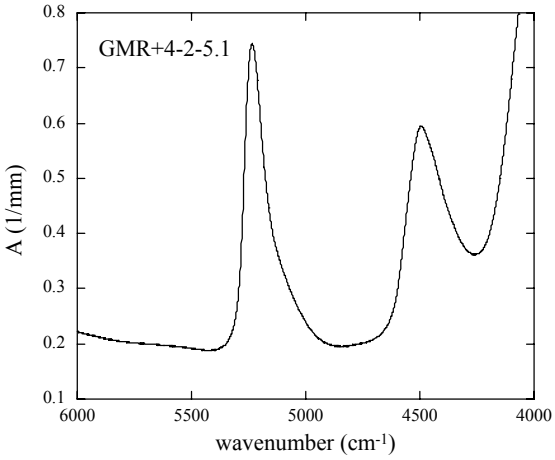
GMR+4-2-5.1
A (1/mm)
wavenumber (cm-1)

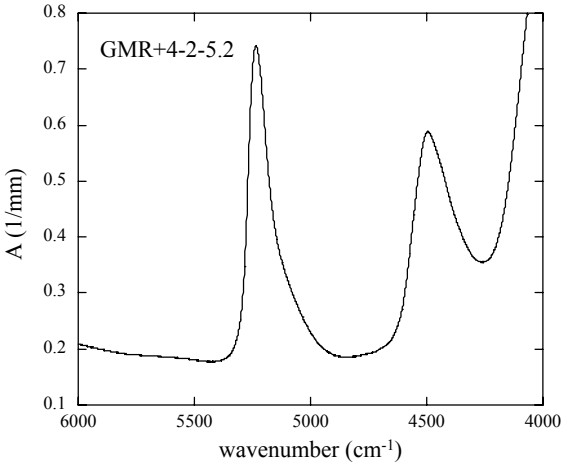
GMR+4-2-5.2
A (1/mm)
wavenumber (cm-1)

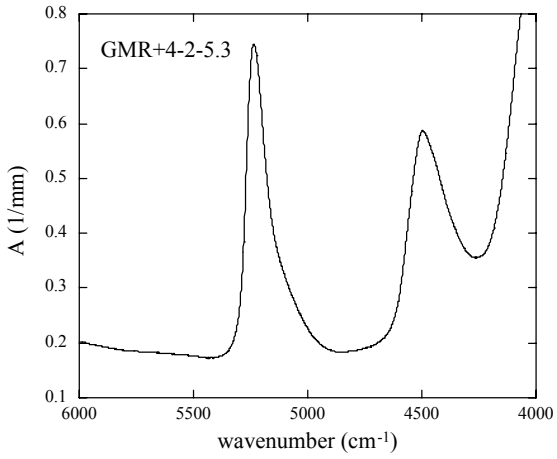
GMR+4-2-5.3
A (1/mm)
wavenumber (cm-1)

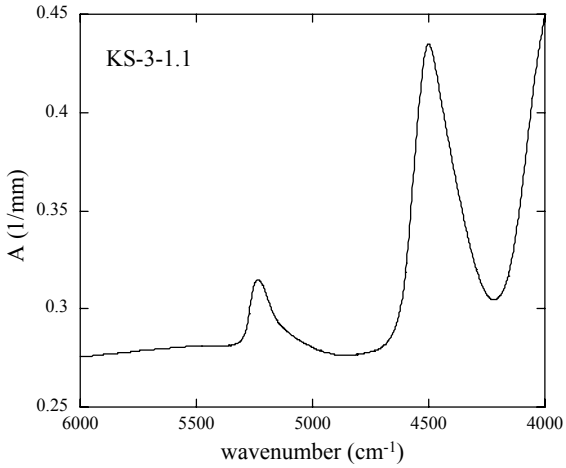
KS-3-1.1
A (1/mm)
wavenumber (cm-1)

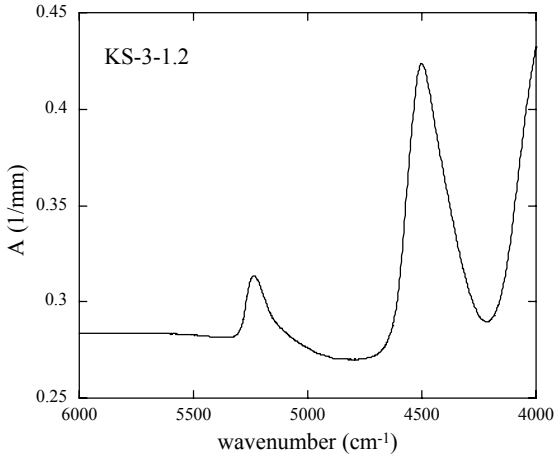
KS-3-1.2
A (1/mm)
wavenumber (cm-1)

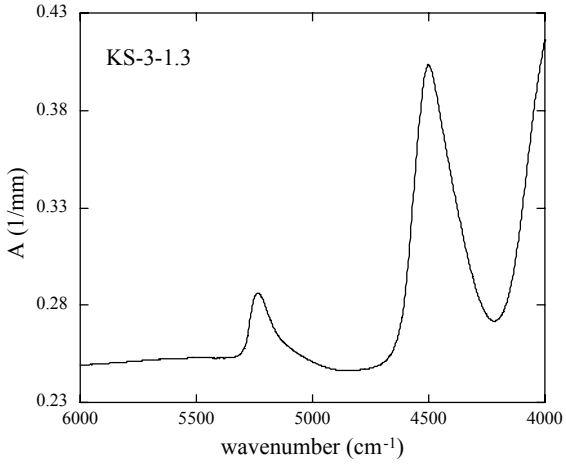
KS-3-1.3
A (1/mm)
wavenumber (cm-1)

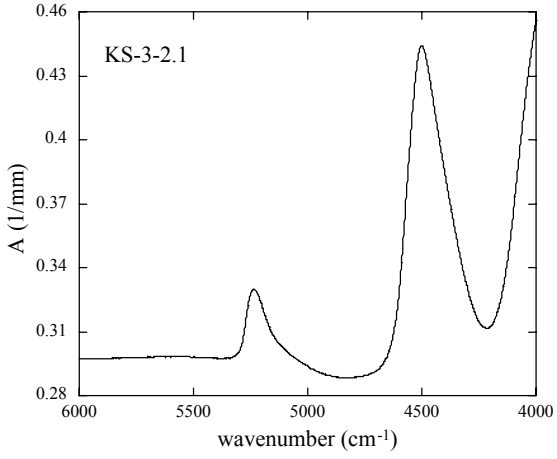
KS-3-2.1
A (1/mm)
wavenumber (cm-1)

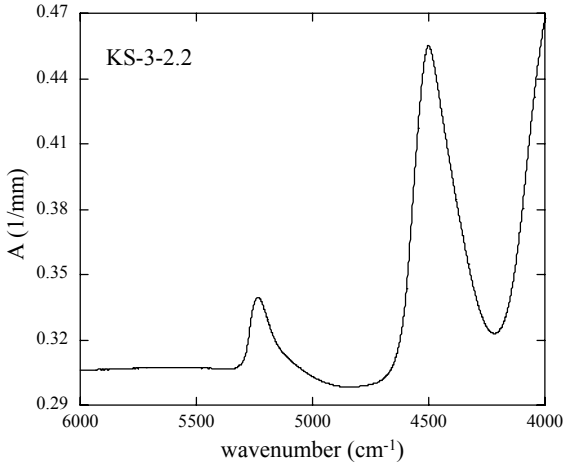
KS-3-2.2
A (1/mm)
wavenumber (cm-1)

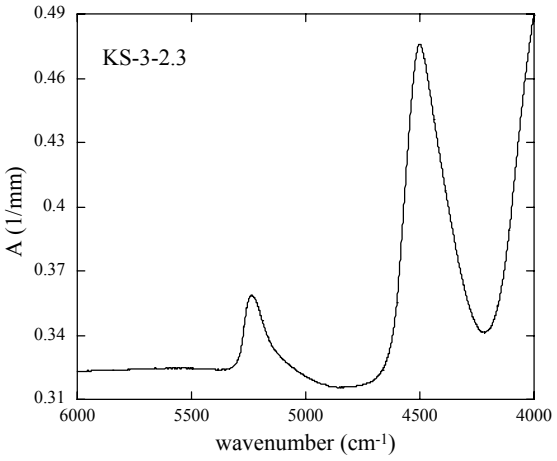
KS-3-2.3
A (1/mm)
wavenumber (cm-1)

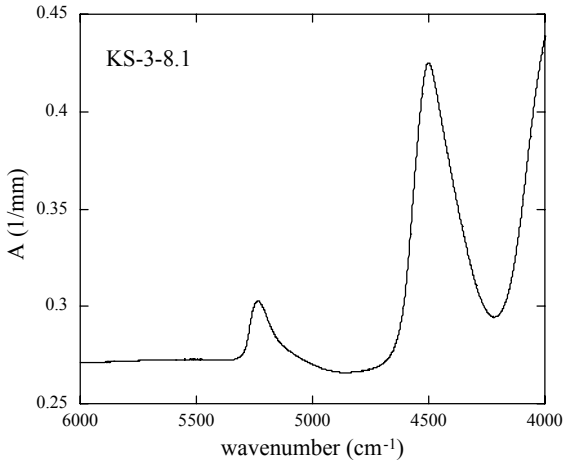
KS-3-8.1
A (1/mm)
wavenumber (cm-1)

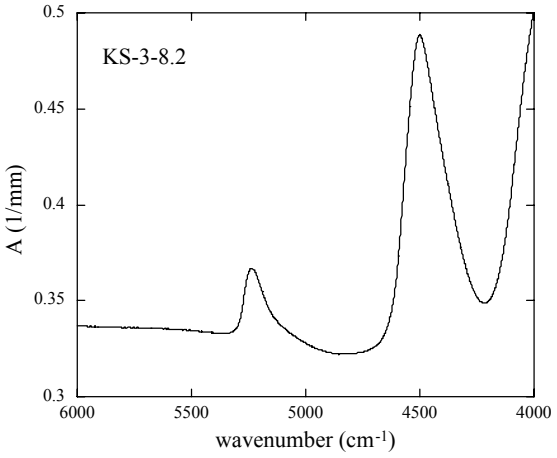
KS-3-8.2
A (1/mm)
wavenumber (cm-1)

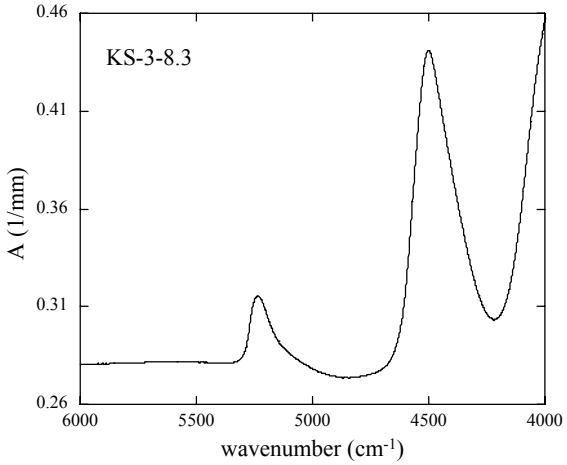
KS-3-8.3
A (1/mm)
wavenumber (cm-1)

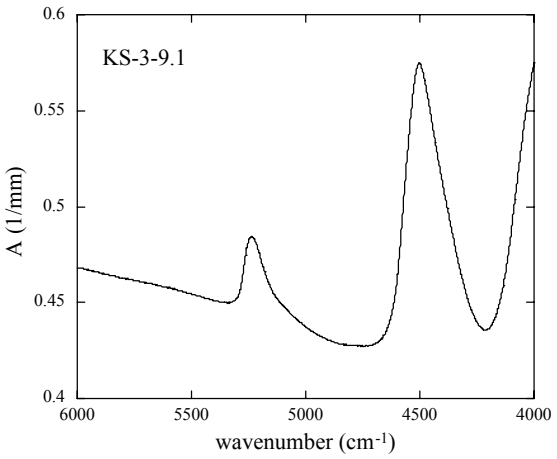
KS-3-9.1
A (1/mm)
wavenumber (cm-1)

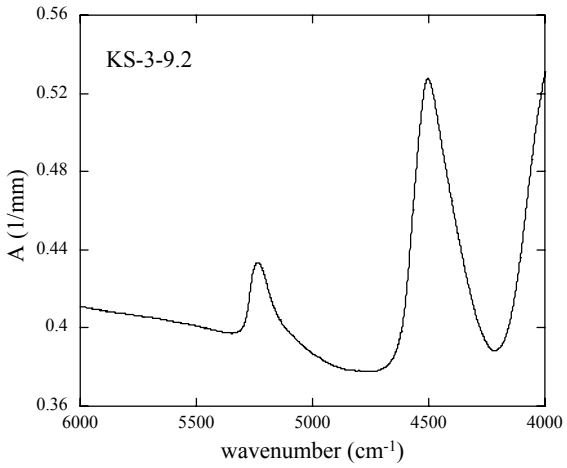
KS-3-9.2
A (1/mm)
wavenumber (cm-1)

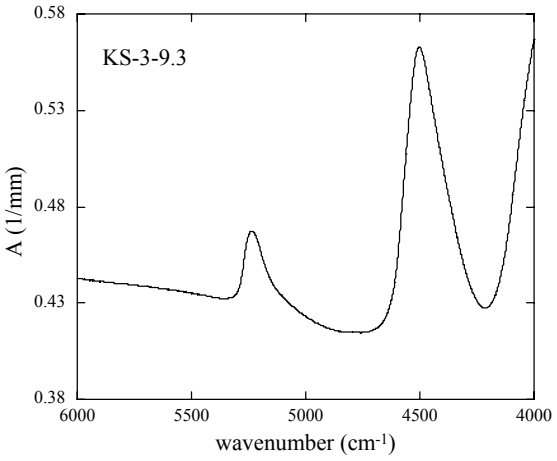
KS-3-9.3
A (1/mm)
wavenumber (cm-1)

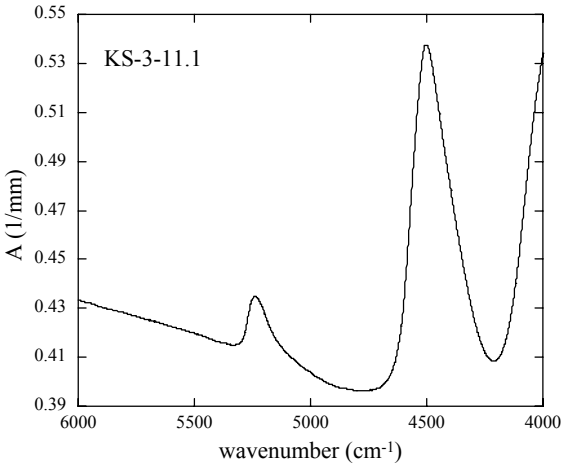
KS-3-11.1
A (1/mm)
wavenumber (cm-1)

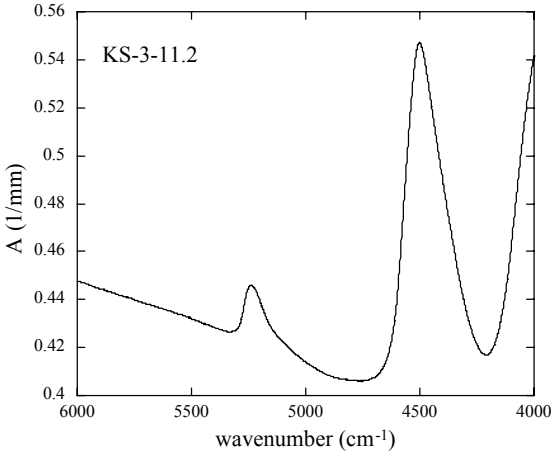
KS-3-11.2
A (1/mm)
wavenumber (cm-1)

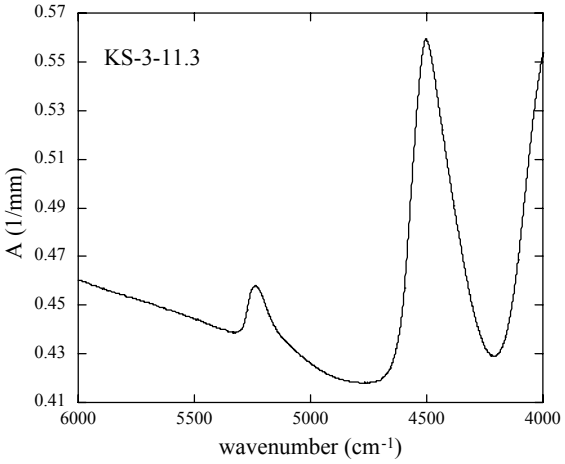
KS-3-11.3
A (1/mm)
wavenumber (cm-1)

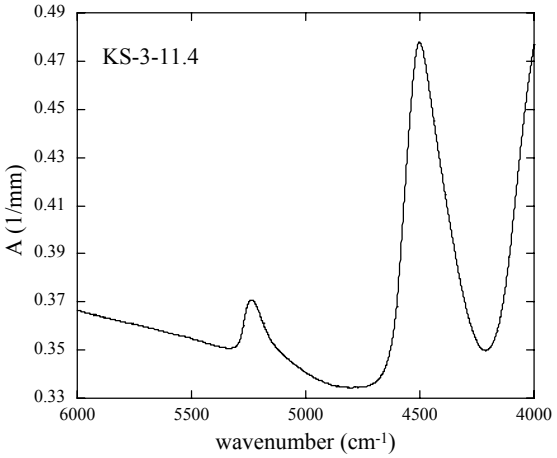
KS-3-11.4
A (1/mm)
wavenumber (cm-1)

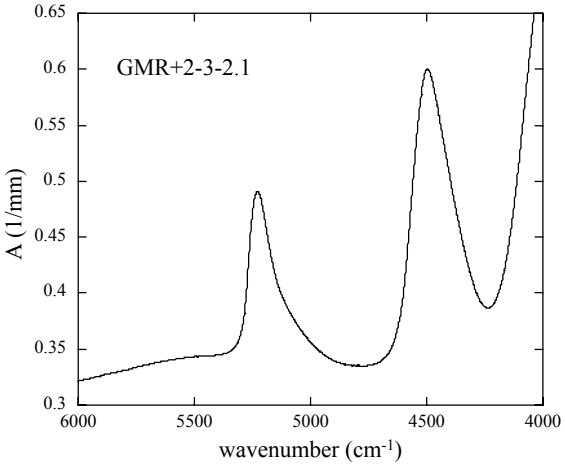
GMR+2-3-2.1
A (1/mm)
wavenumber (cm-1)

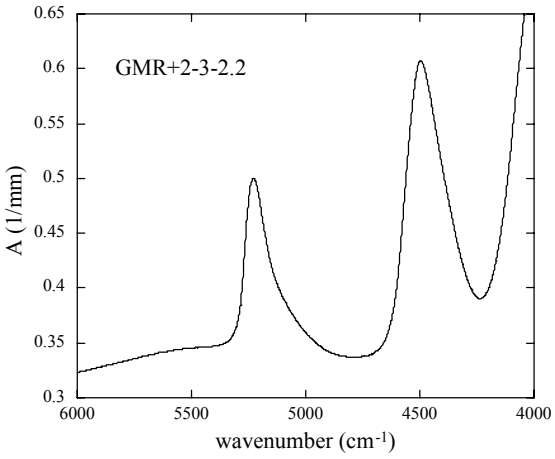
GMR+2-3-2.2
A (1/mm)
wavenumber (cm-1)

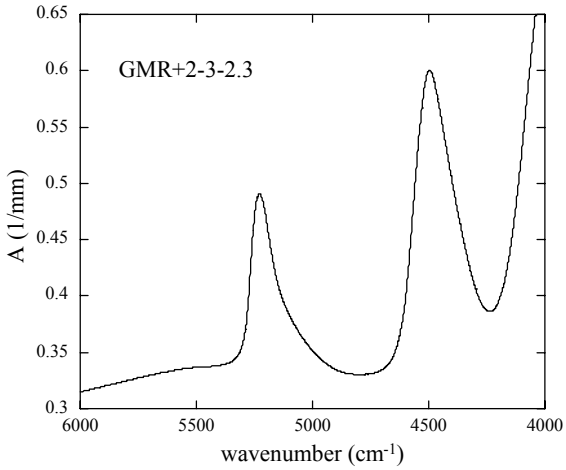
GMR+2-3-2.3
A (1/mm)
wavenumber (cm-1)

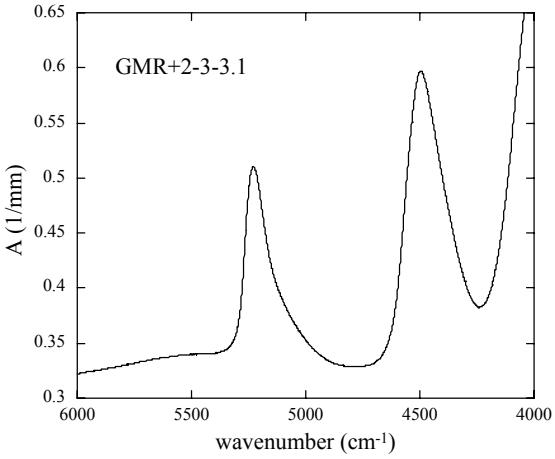
GMR+2-3-3.1
A (1/mm)
wavenumber (cm-1)

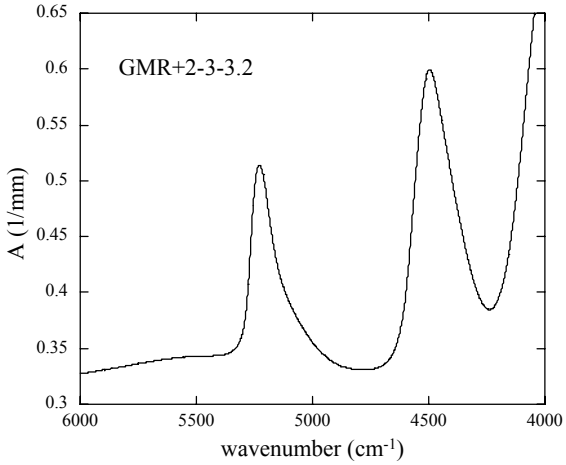
GMR+2-3-3.2
A (1/mm)
wavenumber (cm-1)

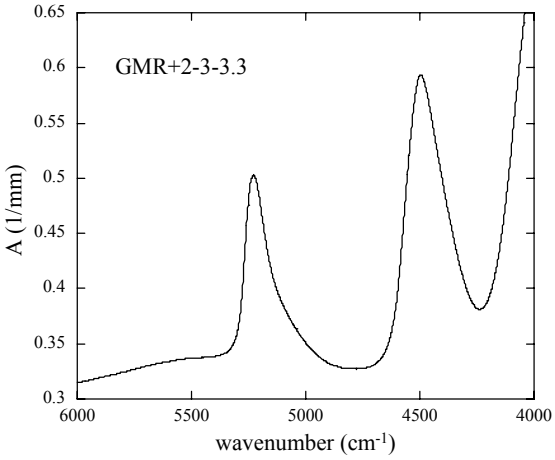
GMR+2-3-3.3
A (1/mm)
wavenumber (cm-1)

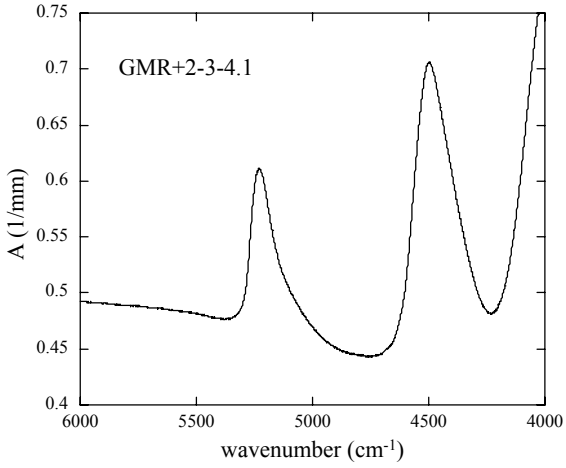
GMR+2-3-4.1
A (1/mm)
wavenumber (cm-1)

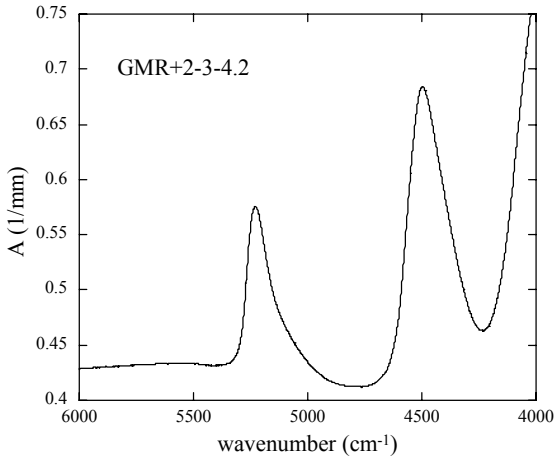
GMR+2-3-4.2
A (1/mm)
wavenumber (cm-1)

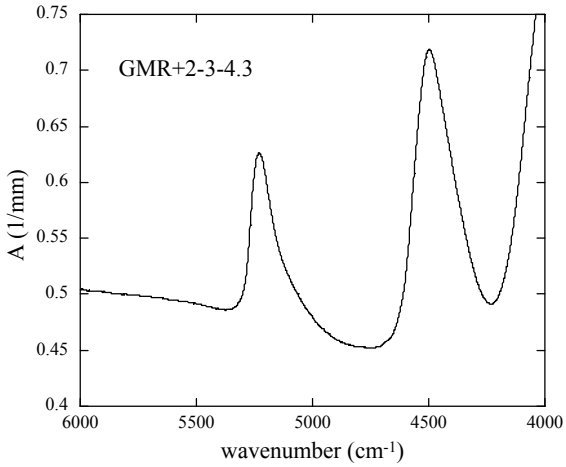
GMR+2-3-4.3
A (1/mm)
wavenumber (cm-1)

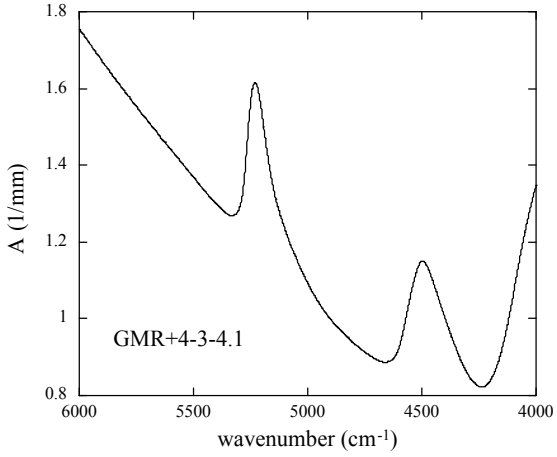
GMR+4-3-4.1
A (1/mm)
wavenumber (cm-1)

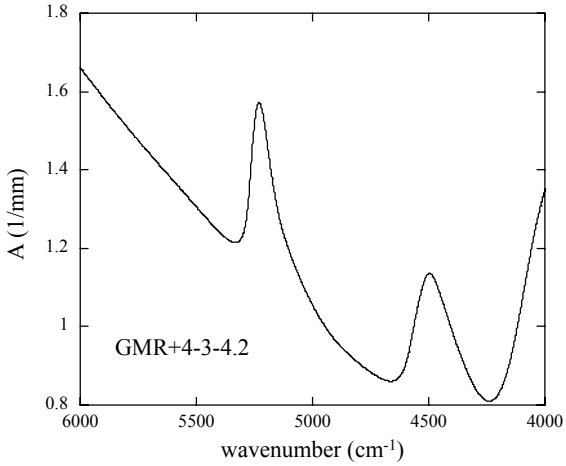
GMR+4-3-4.2
A (1/mm)
wavenumber (cm-1)

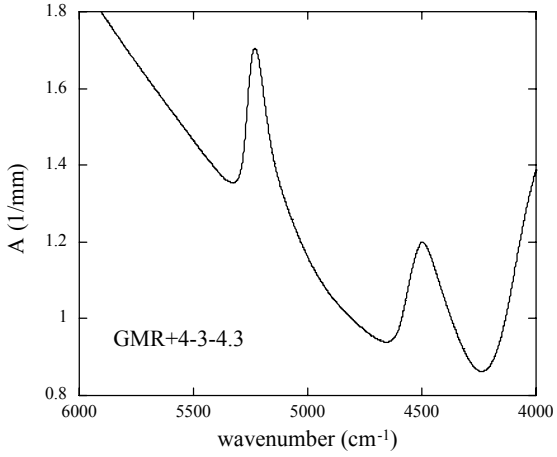
GMR+4-3-4.3
A (1/mm)
wavenumber (cm-1)

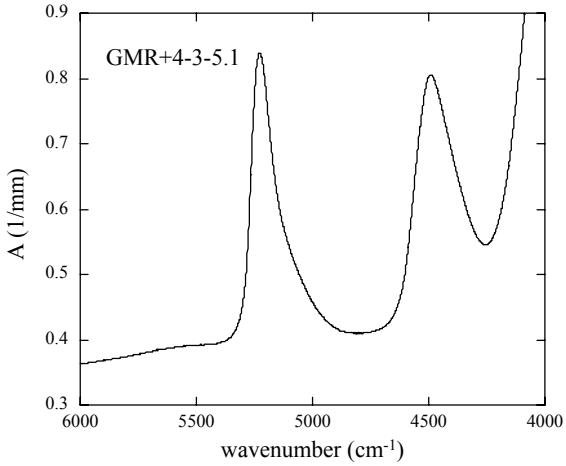
GMR+4-3-5.1
A (1/mm)
wavenumber (cm-1)

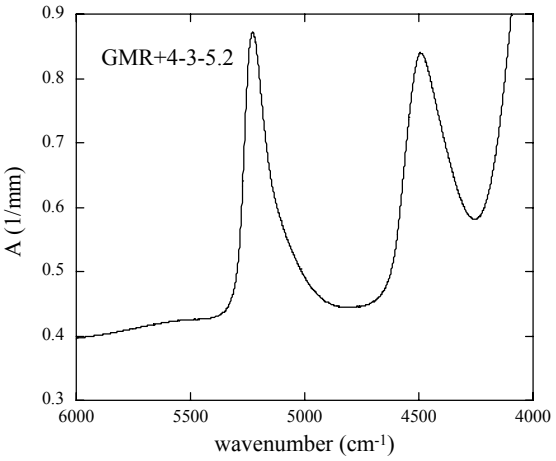
GMR+4-3-5.2
A (1/mm)
wavenumber (cm-1)
0.9
0.8
0.7
0.6
0.5
0.4
0.3
6000
5500
5000
4500
4000

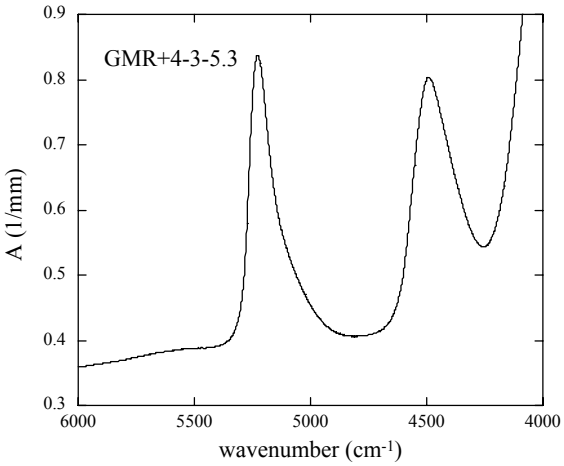
GMR+4-3-5.3
A (1/mm)
wavenumber (cm-1)
0.9
0.8
0.7
0.6
0.5
0.4
0.3
6000
5500
5000
4500
4000

APPENDIX D

DATABASE FOR EASINESS OF CRYSTALLIZATION FOR DIFFERENT MELTS AT DIFFERENT *P-T* CONDITION

Experimental database for easiness of crystallization for different melts at different *P-T* condition has been accumulated at the experimental petrology laboratory, the University of Michigan. The references are listed at the end of the table.

Table D.1 Pressure dependence of easiness of crystallization for different melts at different temperatures.

#	Composition	H_2O_t	*P*	*T*	*t*	*q*	Crystallization*	Ref◊
		wt%	GPa	K	s	K/s		
1	rhyolite	6.53	0.5	613	7200	50	N	4
2	rhyolite	6.53	0.5	613	1260	50	N	4
3	rhyolite	4.6	0.3	623	18000	50	N	13
4	rhyolite	3.89	1	623	261360	50	N	11
5	rhyolite	6.53	0.5	643	300	0.017	N	4
6	rhyolite	5.33	0.5	673	300	0.017	N	4
7	rhyolite	3.89	1	673	46800	50	N	11
8	rhyolite	3.89	2	673	172800	50	N	11
9	rhyolite	5.18	2	673	720000	50	N	12
10	rhyolite	3.71	3	673	259200	50	N	11
11	rhyolite	3.65	0.5	678	300	0.0017	N	4
12	rhyolite	3.65	0.5	678	600	59	N	4
13	rhyolite	3.64	0.5	703	300	0.017	N	4
14	rhyolite	2.63	0.0001	723	600	0.017	N	1
15	rhyolite	3.65	0.5	723	300	1	N	4
16	rhyolite	1.8	1	723	183600	50	N	11
17	rhyolite	3.89	1	723	10800	50	N	11
18	rhyolite	3.89	2	723	14400	50	N	11
19	rhyolite	3.89	3	723	21600	50	N	11
20	rhyolite	3.89	3	723	21600	50	N	11
21	rhyolite	5.27	0.5	733	300	1	N	4
22	rhyolite	2.39	0.0001	735	600	0.000177	N	1

23	rhyolite	6.53	0.5	743	300	50	N	4
24	rhyolite	1.571	0.0001	752	600	0.000177	N	1
25	rhyolite	3.06	0.0001	753	600	0.108	N	1
26	rhyolite	3.65	0.5	753	600	1	N	4
27	rhyolite	5.27	0.5	753	240	50	N	4
28	rhyolite	0.87	0.5	753	1067900	30	N	3
29	rhyolite	3.89	2	753	1260	50	N	11
30	rhyolite	5.1	2	753	172800	50	Y	12
31	rhyolite	0.85	3	763	36000	50	Y	11
32	rhyolite	1.49	0.0001	773	176220	4.27	N	2
33	rhyolite	4.6	0.3	773	300	50	N	13
34	rhyolite	1.8	1	773	600	50	N	11
35	rhyolite	3.89	1	773	600	50	N	11
36	rhyolite	1.8	2	773	86400	50	N	11
37	rhyolite	5.91	2	773	54000	50	Y	12
38	rhyolite	1.8	3	773	172800	50	N	11
39	rhyolite	3.89	3	773	960	50	N	11
40	rhyolite	0.9	4	773	10800	50	Y	11
41	rhyolite	0.9	6.2	773	10800	50	Y	11
42	rhyolite	3	0.0001	783	600	0.55	N	1
43	rhyolite	3.65	0.5	793	300	52	N	4
44	rhyolite	1.77	0.0001	798	26820	12.59	N	2
45	rhyolite	3.71	0.5	803	68520	30	N	3
46	rhyolite	0.809	0.0001	813	600	0.0002	N	1
47	rhyolite	0.8	1	813	187200	54	N	11
48	rhyolite	1.729	0.0001	823	600	0.017	N	1
49	rhyolite	1.824	0.0001	823	600	0.017	N	1
50	rhyolite	1.681	0.0001	823	600	0.125	N	1
51	rhyolite	1.855	0.0001	823	600	0.13	N	1
52	rhyolite	1.879	0.0001	823	600	0.82	N	1
53	rhyolite	1.8	1	823	600	55	N	11
54	rhyolite	1.8	2	823	7200	55	N	11
55	**rhyolite**	**0.9**	**3**	**823**	**176400**	**55**	**N**	**11**
56	**rhyolite**	**0.9**	**3**	**823**	**864000**	**55**	**N**	**11**
57	**rhyolite**	**0.9**	**4**	**823**	**11100**	**55**	**Y**	**11**
58	rhyolite	1.8	3	823	7200	55	N	11
59	rhyolite	1.81	0.0001	824	10800	59	N	2
60	rhyolite	0.186	0.0001	825	3628800	20	N	10
61	rhyolite	7.6	0.5	828	9065	70	N	3
62	rhyolite	0.73	0.5	836	236800	30	N	3
63	rhyolite	0.839	0.0001	843	600	0.002	N	1
64	rhyolite	1.421	0.0001	843	600	0.017	N	1
65	rhyolite	1.433	0.0001	843	600	0.141	N	1
66	rhyolite	0.928	0.0001	847	600	0.017	N	1
67	rhyolite	1.92	0.0001	848	2700	84	N	2
68	rhyolite	1.31	0.0001	848	16800	14.1	N	2
69	rhyolite	1.8	2	853	600	58	N	11
70	rhyolite	1.42	0.0001	863	600	0.762	N	1

71	rhyolite	0.82	0.81	865	252900	30	N	3
72	rhyolite	0.81	0.05	868	167700	30	N	3
73	**rhyolite**	**0.811**	**0.0001**	**872**	**600**	**0.049**	**N**	**1**
74	**rhyolite**	**0.839**	**0.0001**	**873**	**600**	**0.0055**	**N**	**1**
75	**rhyolite**	**0.85**	**0.0001**	**873**	**21600**	**65**	**N**	**11**
76	**rhyolite**	**0.85**	**3**	**873**	**7200**	**60**	**Y**	**11**
77	**rhyolite**	**0.87**	**1**	**873**	**14400**	**60**	**N**	**11**
78	**rhyolite**	**0.88**	**3**	**873**	**2400**	**60**	**N**	**11**
79	**rhyolite**	**0.9**	**2**	**873**	**14400**	**60**	**N**	**11**
80	**rhyolite**	**0.9**	**4**	**873**	**10800**	**60**	**Y**	**11**
81	**rhyolite**	**0.9**	**4**	**873**	**10800**	**60**	**Y**	**11**
82	rhyolite	1.118	0.0001	873	600	0.15	N	1
83	rhyolite	1.155	0.0001	873	600	0.915	N	1
84	rhyolite	1.16	0.0001	873	5760	20	N	2
85	rhyolite	1.39	0.0001	873	3900	20	N	2
86	rhyolite	1.87	0.0001	873	1215	20	N	2
87	rhyolite	2	2	873	600	60	N	11
88	rhyolite	2	3	873	600	60	N	11
89	rhyolite	2.26	2	873	43200	60	N	12
90	rhyolite	2.28	2	873	86400	60	N	12
91	rhyolite	3.61	3	873	60	1	N	13
92	rhyolite	3.96	2	873	14400	60	Y	12
93	rhyolite	5.1	1	873	36000	60	N	12
94	rhyolite	0.79	0.2	874	227760	30	N	3
95	rhyolite	0.892	0.0001	875	600	0.017	N	1
96	rhyolite	0.79	0.5	875	263650	30	N	3
97	rhyolite	0.77	0.0001	876	93160	30	N	3
98	rhyolite	1.86	0.5	878	144300	30	N	3
99	rhyolite	0.802	0.0001	880	600	0.161	N	1
100	rhyolite	0.85	3	883	3600	0.01	Y	13
101	rhyolite	0.831	0.0001	893	600	0.018	N	1
102	rhyolite	0.84	0.0001	893	600	0.018	N	1
103	rhyolite	0.85	3	903	3600	0.01	Y	13
104	rhyolite	0.8	0.0001	923	600	75	N	11
105	rhyolite	0.8	0.0001	923	7200	75	N	11
106	rhyolite	0.84	0.0001	923	2400	75	N	11
107	rhyolite	0.85	1	923	600	65	N	11
108	rhyolite	0.89	2	923	600	65	N	11
109	rhyolite	0.85	3	923	600	3.3	Y	13
110	rhyolite	0.85	3	923	600	0.33	Y	13
111	rhyolite	2.01	1	923	600	0.1	N	13
112	rhyolite	3.82	1	923	120	1	N	13
113	rhyolite	0.513	0.0001	941	600	0.017	N	1
114	rhyolite	0.87	2	953	600	68	N	11
115	rhyolite	7.6	0.5	969	720	30	N	3
116	rhyolite	0.124	0.0001	971	1450800	20	N	10
117	rhyolite	1.37	0.011	973	259200	0.5	N	10
118	rhyolite	2.18	0.0249	973	172800	0.5	N	10

119	rhyolite	3.89	2	973	60	1	N	13
120	rhyolite	3.89	3	973	60	10	N	13
121	**rhyolite**	**0.8**	**0.0001**	**973**	**600**	**50**	**N**	**11**
122	**rhyolite**	**0.82**	**1**	**973**	**480**	**70**	**N**	**11**
123	**rhyolite**	**0.8**	**1**	**973**	**300**	**0.1**	**N**	**13**
124	**rhyolite**	**0.8**	**2**	**973**	**300**	**0.1**	**N**	**13**
125	**rhyolite**	**0.85**	**3**	**973**	**600**	**70**	**Y**	**11**
126	**rhyolite**	**0.82**	**3**	**973**	**300**	**0.1**	**Y**	**13**
127	**rhyolite**	**0.9**	**4**	**973**	**3600**	**70**	**Y**	**11**
128	rhyolite	0.836	0.0001	993	300	12.7	N	6
129	rhyolite	0.9	4	993	600	0.5	Y	13
130	rhyolite	0.805	0.0001	1000	300	20	N	6
131	rhyolite	0.784	0.0001	1003	600	79	N	6
132	rhyolite	0.88	0.0001	1013	60	12.7	N	6
133	rhyolite	0.8	0.0001	1021	300	65	N	6
134	rhyolite	0.116	0.0001	1023	1292400	20	N	10
135	rhyolite	0.68	0.0001	1023	300	17.8	N	6
136	rhyolite	0.766	0.0001	1023	300	84	N	6
137	rhyolite	0.8	3	1023	600	0.333	Y	13
138	rhyolite	0.82	1	1023	120	1	N	13
139	rhyolite	0.82	2	1023	120	1	N	13
140	rhyolite	0.82	3	1023	120	10	N	13
141	rhyolite	0.83	3	1023	120	1	N	13
142	rhyolite	0.84	0.0001	1023	450	130	N	6
143	rhyolite	0.85	3	1023	120	75	N	11
144	rhyolite	0.85	3	1023	120	1	N	13
145	rhyolite	0.855	0.0001	1023	600	174	N	6
146	rhyolite	1.8	2	1023	120	10	N	13
147	rhyolite	1.8	2	1023	120	1	N	13
148	rhyolite	1.8	3	1023	120	10	N	13
149	rhyolite	1.8	3	1023	120	1	N	13
150	rhyolite	1.83	1	1023	120	1	N	13
151	**rhyolite**	**3.89**	**2**	**1023**	**60**	**10**	**N**	**13**
152	**rhyolite**	**3.89**	**3**	**1023**	**60**	**75**	**Y**	**13**
153	rhyolite	0.8	0.0001	1024	600	14	N	6
154	rhyolite	0.7	1	1073	60	10	N	13
155	rhyolite	0.8	1	1073	120	80	N	13
156	rhyolite	0.8	2	1073	120	10	N	13
157	rhyolite	0.82	0.2	1073	300	0.167	N	4
158	rhyolite	0.83	0.1	1073	600	0.167	N	4
159	rhyolite	0.85	2	1073	300	0.167	N	13
160	rhyolite	1.78	0.2	1073	600	80	N	4
161	rhyolite	1.81	1	1073	60	10	N	13
162	rhyolite	1.82	2	1073	60	80	N	13
163	rhyolite	2.41	0.1	1073	600	80	N	4
164	rhyolite	2.5	0.2	1073	600	80	N	4
165	**rhyolite**	**3.89**	**1**	**1073**	**60**	**10**	**N**	**13**
166	**rhyolite**	**3.89**	**1**	**1073**	**60**	**80**	**N**	**13**

167	**rhyolite**	**3.89**	**2**	**1073**	**60**	**80**	**N**	**13**
168	**rhyolite**	**3.89**	**3**	**1073**	**60**	**80**	**Y**	**13**
169	rhyolite	0.9	4	1103	300	4	Y	13
170	rhyolite	0.103	0.0001	1123	219600	20	N	10
171	rhyolite	0.105	0.0001	1123	867600	20	N	10
172	**rhyolite**	**0.77**	**0.0061**	**1123**	**259200**	**0.5**	**N**	**10**
173	**rhyolite**	**0.77**	**2**	**1123**	**120**	**85**	**N**	**13**
174	**rhyolite**	**0.77**	**3**	**1123**	**60**	**85**	**Y**	**13**
175	**rhyolite**	**0.85**	**2**	**1123**	**300**	**85**	**N**	**13**
176	rhyolite	1.1	0.0112	1123	338400	0.5	N	10
177	rhyolite	1.11	0.0114	1123	172800	0.5	N	10
178	**rhyolite**	**1.76**	**0.0253**	**1123**	**176400**	**0.5**	**N**	**10**
179	**rhyolite**	**1.8**	**3**	**1123**	**120**	**85**	**Y**	**13**
180	rhyolite	2.41	0.2	1123	3600	0.67	N	4
181	rhyolite	3.89	3	1123	60	85	Y	13
182	rhyolite	0.106	0.0001	1124	1134000	20	N	10
183	rhyolite	7.6	0.5	1126	240	30	N	3
184	rhyolite	6	0.25	1135	1800	2	N	3
185	rhyolite	7.6	0.5	1173	0	2	N	3
186	rhyolite	7.6	0.5	1173	1800	2	N	3
187	rhyolite	2.3	0.5	1173	7200	1.67	N	5
188	rhyolite	0.225	0.5	1180	36000	30	N	3
189	rhyolite	0.7	0.0061	1268	173160	0.5	N	10
190	rhyolite	0.102	0.0001	1272	1083600	20	N	10
191	rhyolite	0.099	0.0001	1273	691200	20	N	10
192	rhyolite	0.12	0.1	1273	1800	1.67	N	5
193	rhyolite	0.12	0.1	1273	14400	1.67	N	5
194	rhyolite	0.12	0.3	1273	14400	1.67	N	5
195	**rhyolite**	**0.78**	**0.2**	**1273**	**300**	**100**	**N**	**4**
196	**rhyolite**	**0.81**	**0.2**	**1273**	**300**	**6.7**	**N**	**4**
197	**rhyolite**	**0.83**	**0.2**	**1273**	**300**	**0.83**	**N**	**4**
198	**rhyolite**	**0.9**	**4**	**1273**	**120**	**100**	**Y**	**13**
199	**rhyolite**	**0.99**	**0.0114**	**1275**	**88200**	**0.5**	**N**	**10**
200	rhyolite	1.15	0.5	1273	600	0.017	N	4
201	rhyolite	1.15	0.5	1273	600	100	N	4
202	rhyolite	1.55	0.0252	1273	86400	0.5	N	10
203	rhyolite	1.57	0.025	1273	86400	0.5	N	10
204	rhyolite	5	0.5	1273	600	100	N	5
205	rhyolite	5	1	1273	600	100	N	5
206	rhyolite	5	1.5	1273	600	100	N	5
207	rhyolite	0.219	0.5	1298	14400	30	N	3
208	rhyolite	0.9	0.5	1298	14400	1.67	N	5
209	rhyolite	0.24	0.5	1307	5400	1.67	N	5
210	rhyolite	2.2	0.5	1307	5400	1.67	N	5
211	rhyolite	2.2	0.5	1307	5400	1.67	N	5
212	rhyolite	2	0.5	1307	5400	1.67	N	5
213	rhyolite	0.78	0.1	1373	300	100	N	4
214	rhyolite	3.71	2	1373	60	100	N	13

215	rhyolite	5.1	2	1373	624	100	N	12
216	rhyolite	5.1	2	1373	613	100	N	12
217	rhyolite	0.24	0.5	1375	1800	1.67	N	5
218	rhyolite	0.9	0.5	1375	1800	1.67	N	5
219	rhyolite	2.2	0.5	1375	1800	1.67	N	5
220	rhyolite	3.8	0.5	1375	1800	1.67	N	5
221	rhyolite	2	0.5	1375	1800	1.67	N	5
222	rhyolite	0.9	0.5	1471	1200	1.67	N	5
223	rhyolite	2.4	0.5	1471	1200	1.67	N	5
224	rhyolite	4.1	0.5	1471	1200	1.67	N	5
225	rhyolite	0.64	0.0061	1473	144000	0.5	N	10
226	rhyolite	0.89	0.011	1473	86400	0.5	N	10
227	rhyolite	1.44	0.025	1473	79200	0.5	N	10
228	rhyolite	1.47	0.025	1473	82800	0.5	N	10
229	rhyolite	1.48	0.025	1473	86400	0.5	N	10
230	rhyolite	3.61	3	1473	60	100	N	13
231	rhyolite	6.4	0.5	1478	900	2	N	3
232	rhyolite	6	0.25	1488	1200	2	N	3
233	rhyolite	5.1	1	1573	248	100	N	12
234	rhyolite	3.97	2	1573	252	100	N	12
235	rhyolite	2.27	2	1573	587	100	N	12
236	rhyolite	0.9	4.1	1673	120	100	Y	13
237	rhyolite	5.91	2	1773	120	100	N	12
238	rhyolite	0.02	0.5	1873	7200	100	N	13
239	rhyolite	5.17	2	1873	128	100	N	12
240	rhyolite	0.9	4	1873	60	100	Y	13
241	andesite	1.57	1	1523	0	100	N	7
242	andesite	3.2	1	1573	300	100	N	7
243	andesite	1.57	1	1573	300	100	N	7
244	andesite	5.6	1	1573	120	100	N	7
245	andesite	3.5	0.5	1673	90	100	N	7
246	andesite	3.5	1.5	1673	90	100	N	7
247	andesite	2.1	1	1773	60	100	N	7
248	andesite	1.51	1	1773	60	100	N	7
249	andesite	1.59	1	1813	126	100	N	7
250	dacite	2.517	0.0001	753	3000	20	N	8
251	dacite	1.453	0.0001	773	4202	20	N	8
252	dacite	2.513	0.0001	773	1800	20	N	8
253	dacite	2.45	0.1	776	172200	30	N	9
254	dacite	2.354	0.0001	791	270	20	N	8
255	dacite	1.463	0.0001	792	1200	20	N	8
256	dacite	1.453	0.0001	792	2100	20	N	8
257	dacite	2.314	0.0001	810	484	20	N	8
258	dacite	0.74	0.0001	824	1744680	20	N	9
259	dacite	1.425	0.0001	833	600	20	N	8
260	dacite	2.45	0.1	834	689315	30	N	9
261	dacite	1.518	0.0001	845	180	20	N	8
262	dacite	1.525	0.0001	845	180	20	N	8

263	dacite	1.411	0.0001	863	180	20	N	8
264	dacite	2.45	0.1	878	103975	30	N	9
265	dacite	1.45	0.097	881	180900	100	N	9
266	dacite	0.75	0.0975	881	413880	100	N	9
267	dacite	2.45	0.14	881	40878	100	N	9
268	dacite	2.45	0.13	910	19660	100	N	9
269	dacite	0.73	0.099	911	484260	100	N	9
270	dacite	4.7	1	1423	300	100	N	7
271	dacite	4.6	1	1473	300	100	N	7
272	dacite	3.5	0.5	1573	73	100	N	7
273	dacite	2.9	1	1573	480	100	N	7
274	dacite	6.2	0.5	1673	120	100	N	7
275	dacite	6.3	1.5	1673	120	100	N	7
276	dacite	3.1	1	1773	90	100	N	7

*: “N” means no crystallization in the quenched glass and “Y” means significant crystallization. The crystallized samples were classified as failed experiments and were not discussed in the respective papers even though the samples were part of the respective study.

◊: references: 1. Zhang et al. 1997b; 2. Liu and Zhang, 2000; 3. Zhang and Behrens, 2000; 4. Zhang et al., 2000; 5. Behrens and Zhang, 2001; 6. Xu and Zhang, 2002; 7. Behrens et al., 2004; 8. Liu et al., 2004a; 9. Liu et al., 2004b; 10. Liu et al., 2005; 11. Hui et al., in revision; 12. Ni and Zhang, revised; 13. this study.